ASME PTC 19.5-2022
[Revision of ASME PTC 19.5-2004 (R2013)]

Flow Measurement

Performance Test Codes

AN AMERICAN NATIONAL STANDARD

The American Society of Mechanical Engineers

ASME PTC 19.5-2022
[Revision of ASME PTC 19.5-2004 (R2013)]

Flow Measurement

Performance Test Codes

AN AMERICAN NATIONAL STANDARD

The American Society of Mechanical Engineers
Two Park Avenue • New York, NY • 10016 USA

Date of Issuance: September 15, 2023

The next edition of this Code is scheduled for publication in 2027.

This code or standard was developed under procedures accredited as meeting the criteria for American National Standards. The standards committee that approved the code or standard was balanced to ensure that individuals from competent and concerned interests had an opportunity to participate. The proposed code or standard was made available for public review and comment, which provided an opportunity for additional public input from industry, academia, regulatory agencies, and the public-at-large.

ASME does not "approve," "certify," "rate," or "endorse" any item, construction, proprietary device, or activity. ASME does not take any position with respect to the validity of any patent rights asserted in connection with any items mentioned in this document, and does not undertake to insure anyone utilizing a standard against liability for infringement of any applicable letters patent, nor does ASME assume any such liability. Users of a code or standard are expressly advised that determination of the validity of any such patent rights, and the risk of infringement of such rights, is entirely their own responsibility.

Participation by federal agency representatives or persons affiliated with industry is not to be interpreted as government or industry endorsement of this code or standard.

ASME accepts responsibility for only those interpretations of this document issued in accordance with the established ASME procedures and policies, which precludes the issuance of interpretations by individuals.

The endnotes and preamble in this document (if any) are part of this American National Standard.

The American Society of Mechanical Engineers
Two Park Avenue, New York, NY 10016-5990

CONTENTS

Notice xi

Foreword xii

Committee Roster xiv

Correspondence With the PTC Committee xv

Section 1 **Object, Scope, and Uncertainty** 1

1-1 Object 1

1-2 Scope 1

1-3 Uncertainty 1

1-4 References to ASME Standards 1

Section 2 **Definitions, Values, and Descriptions of Terms** 3

2-1 General 3

2-2 Primary Definitions and Systems of Units 3

2-3 Symbols and Dimensions 3

2-4 Thermal Expansion 3

2-5 References 5

Section 3 **Differential Pressure Class Meters** 6

3-1 Nomenclature 6

3-2 General Equation for Mass Flow Through a Differential Pressure Class Meter 6

3-3 Basic Physical Concepts Used in the Derivation of the General Equation for Mass Flow . 6

3-4 Theoretical Flow — Liquid as the Flowing Fluid 8

3-5 Theoretical Flow — Gas or Vapor as the Flowing Fluid 10

3-6 Factors Not Accounted for in Theoretical Mass Flow by Idealized Flow Assumptions . . . 11

3-7 Discharge Coefficient, C, in the Incompressible Fluid Equation 11

3-8 Discharge Coefficient, C, and the Expansion Factor, ε, for Gases 12

3-9 Calculation of Expansion Factor, ε 12

3-10 Determining Discharge Coefficient for Differential Pressure Class Meters 12

3-11 Thermal Expansion/Contraction of Inlet Section and Primary Element 13

3-12 Selection and Recommended Use of Differential Pressure Class Meters 13

3-13 Restrictions of Use 15

3-14 Procedure for Sizing a Differential Pressure Class Meter 15

3-15 Flow Calculation Procedure 17

3-16 Sample Calculation 17

3-17 References 21

Section 4 **Orifice Meters** 23

4-1 Nomenclature 23

4-2 Introduction 23

4-3 Types of Thin-Plate, Square-Edged Orifices 23

4-4 Code Compliance Requirements 23

4-5	Multiple Sets of Differential Pressure Taps	23
4-6	Machining Tolerances, Dimensions, and Markings for Orifice Plate	24
4-7	Machining Tolerances and Dimensions for Differential Pressure Taps	27
4-8	Location of Temperature and Static Pressure Measurements	30
4-9	Empirical Formulations for Discharge Coefficient, C	30
4-10	Limitations and Uncertainty of Eq. (4-9-1) for Discharge Coefficient, C	31
4-11	Uncertainty of Expansion Factor, ε	32
4-12	Unrecoverable Pressure Loss	33
4-13	Calculations of Differential Pressure Class Flow Measurement Systematic Uncertainty	33
4-14	Procedure for Fitting a Calibration Curve and Extrapolation Technique	37
4-15	References	39
Section 5	**Nozzles and Venturis**	40
5-1	Nomenclature	40
5-2	Introduction	40
5-3	Required Proportions of ASME Nozzles	40
5-4	Nozzle Pressure Tap Requirements	46
5-5	Nozzle Installation Requirements	47
5-6	Discharge Coefficient for ASME Nozzles	48
5-7	The ASME Venturi Tube	49
5-8	Venturi Design and Design Variations	51
5-9	Venturi Pressure Taps	52
5-10	Discharge Coefficient of the ASME Venturi	53
5-11	Installation Requirements for the ASME Venturi	53
5-12	Laboratory Calibrations	53
5-13	Uncertainty of Expansion Factor, ε	53
5-14	Unrecoverable Pressure Loss	54
5-15	References	54
Section 6	**Differential Pressure Class Meter Installation and Flow Conditioning Requirements**	55
6-1	Nomenclature	55
6-2	Introduction	55
6-3	Metering Section Requirements	55
6-4	Meter Installation in the Metering Section	56
6-5	Additional Pipe Length Requirements	57
6-6	Flow Conditioners and Installation	62
6-7	Installation of Temperature Sensors	62
6-8	References	64
Section 7	**Sonic Flow Nozzles and Venturis — Critical Flow, Choked Flow Conditions**	65
7-1	Nomenclature	65
7-2	Introduction	65
7-3	Definitions and Description of Terms	70
7-4	Guiding Principles	72
7-5	Instruments and Methods of Measurement	72
7-6	Installation	76
7-7	Pressure and Temperature Measurements	77
7-8	Computation of Results	81

7-9	Flow Uncertainty	86
7-10	Discharge Coefficients	87
7-11	Other Methods and Examples	91
7-12	Special Applications	97
7-13	References	98
Section 8	**Flow Measurement by Velocity Traverse**	101
8-1	Nomenclature	101
8-2	Introduction	101
8-3	Traverse Measurement Locations	103
8-4	Recommended or Required Locations of Measurement Sections	110
8-5	Use and Calibration Requirements for Sensors	111
8-6	Flow Measurement by Pitot Rake	117
8-7	General Requirements	120
8-8	Flow Computation Corrections	120
8-9	Uncertainty Analysis	121
8-10	References	122
Section 9	**Ultrasonic Flowmeters**	123
9-1	Scope	123
9-2	Purpose	123
9-3	Definitions and Symbols	123
9-4	Applications	124
9-5	Flowmeter Description	125
9-6	Performance-Affecting Characteristics	129
9-7	Calibration	139
9-8	Error Sources and Their Reduction	141
Section 10	**Tracer Method for Measuring Water Flow**	145
10-1	Nomenclature	145
10-2	Introduction	145
10-3	Constant Rate Injection Method	145
10-4	Tracer Selection	146
10-5	Mixing Length and Mixing Distance	146
10-6	Procedure	148
10-7	Fluorometric Method of Analysis	149
10-8	Flow Test Setup	150
10-9	Uncertainty	154
10-10	Reference	155
Section 11	**Vortex Shedding Meters**	156
11-1	Nomenclature	156
11-2	Principle of Measurement	156
11-3	Flowmeter Descriptions	157
11-4	Application Considerations	158
11-5	Installation	160
11-6	Operation	161
11-7	Calibration and Uncertainty	161
11-8	References	164

Section 12 **Mechanical Meters** . . . 165
12-1 Nomenclature . . . 165
12-2 Introduction . . . 165
12-3 Turbine Meters . . . 166
12-4 Turbine Meter Signal Transducers and Indicators . . . 166
12-5 Calibration . . . 166
12-6 Recommendations for Use . . . 168
12-7 Piping Installation and Disturbances . . . 170
12-8 Example of Flow Measurement by Turbine Meter With Natural Gas . . . 170
12-9 Random Uncertainty Due to Time Variance of Data . . . 171
12-10 Field Checks . . . 172
12-11 Positive Displacement Meters . . . 172
12-12 References . . . 175
Section 13 **Coriolis Mass Flowmeters** . . . 177
13-1 Definitions and Nomenclature . . . 177
13-2 Introduction . . . 177
13-3 Meter Construction . . . 179
13-4 Calibration and Uncertainty . . . 181
13-5 Application Considerations . . . 188
13-6 Field Uncertainty Examples . . . 190

Mandatory Appendix
I Laboratory Calibration Evaluation and Extrapolation . . . 197

Nonmandatory Appendices
A Pulsating Flow Measurement . . . 204
B Critical Flow Functions for Air by R. C. Johnson . . . 217
C Deviation of Johnson C* Values . . . 218
D Real Gas Correction Factors . . . 219
E Conversion Factors . . . 223
F Thermal Expansion Tables . . . 233
G Historical Definitions of Units of Measurement . . . 242

Figures
3-4-1 Water Leg Correction for Flow Measurement . . . 9
3-12.3-1 Unrecoverable Pressure Loss Versus Beta Ratio . . . 16
4-6-1 Standard Orifice Plate . . . 24
4-6.1-1 Deflection of an Orifice Plate by Differential Pressure . . . 25
4-7-1 Location of Pressure Taps for Orifices With Flange Taps . . . 28
4-7-2 Location of Pressure Taps for Orifices With Corner Taps . . . 29
4-10.1-1 Minimum Reynolds Number for Flange Taps . . . 32
5-3-1 High β Nozzle . . . 41
5-3-2 Low β Nozzle . . . 42
5-3-3 Throat Tap Nozzle for $\beta > 0.44$ . . . 42
5-3-4 Throat Tap Nozzle for $\beta \leq 0.44$ . . . 43

5-3-5 Throat Tap Nozzle End Detail 43
5-3-6 Example Throat Tap Nozzle Flow Section 44
5-3.4-1 ASME Nozzle Required Surface Finish to Produce a Hydraulically Smooth Surface 45
5-3.4-2 Boring in Flow Section Upstream of Nozzle 46
5-5.6-1 Nozzle With Diffusing Cone 48
5-6.2.1-1 Reference Curve for Throat Tap Nozzles 49
5-7-1 Profile of the ASME Venturi 50
6-5.3.1-1 Allowable Diameter Steps for 0.2% Additional Uncertainty 61
6-6.1-1 Flow Conditioner Designs 63
7-2-1 Ideal Mach Number Distribution Along Venturi Length at Typical Subcritical and Sonic Flow Conditions 67
7-2.2-1 Definition of Sonic Flow as the Maximum of the Flow [See Eq. (7-2-1)] 69
7-3.2-1 Schematic Representation of Flow Defects at Venturi Throat 71
7-3.2-2 Schematic Diagram of Sonic Surfaces at the Throat of an Axially Symmetric Sonic Flow Venturi Nozzle 72
7-4-1 Requirements for Maintaining Sonic Flow in Venturi Nozzles 73
7-4-2 Mass Flow Versus Back-Pressure Ratio for a Flow Nozzle Without a Diffuser and a Venturi Nozzle With a Diffuser 73
7-5.3.1-1 Standardized Toroidal Throat Sonic Flow Venturi Nozzle 75
7-5.3.3-1 Standardized Cylindrical Throat Sonic Flow Venturi 76
7-5.3.4-1 ASME Long-Radius Flow Nozzles 77
7-6.2-1 Standardized Inlet Flow Conditioner and Locations for Pressure and Temperature Measurements 78
7-6.3-1 Comparison of the “Continuous Curvature” Inlet With the “Sharp-Lip, Free-Standing” Inlet 78
7-7.1.1-1 Static and Total (Stagnation) Pressure Measurements on a Pipe 79
7-7.1.2-1 Standardized Pressure Tap Geometry Installation 80
7-8.3-1 Generalized Compressibility Chart 83
7-8.6.1-1 Calculation Processes for the Isentropic Path From Inlet to Sonic Throat for a Real Gas Using the Method of Johnson 85
7-10.2-1 Composite Results for Toroidal-Throat Venturi Nozzles 89
7-10.2-2 Mean Line Discharge Coefficient Curves for Toroidal-Throat Venturi Nozzles 90
7-11.1.1-1 Error in Method 3 for Air Based on Sonic Flow Functions When Using Air Property Data 92
7-11.1.4-1 Error in Sonic Flow Function, C^*, for Air Using Method 6 Based on Ideal Gas Theory With Ratio of Specific Heats Corresponding to the Inlet Stagnation State 95
8-3.1-1 Pipe Velocity Measurement Loci 104
8-3.2-1 Duct Velocity Measurement Loci for Gaussian Distribution 109
8-3.2-2 Recommended Number of Measurement Loci for the Equal-Area Method 110
8-5.1-1 Pitot Tubes Not Requiring Calibration 112
8-5.1-2 Pitot Tubes Needing Calibration But Acceptable 113
8-5.1.2-1 Wedge-Type Five-Hole Probe Installation Schematic 114
8-5.1.2-2 Five-Hole Probe Designs 115
8-5.1.2-3 The Fechheimer Probe Installation 116
8-6-1 Insertion Type Pitot Rake 118
8-6-2 Pitot Rake 119
8-6-3 Impact Pressure Tube Rake 120
9-5.1.3-1 Common Acoustic Path Configurations 126

9-5.3.2-1 Wetted Recessed Transducer Configuration . . . 127
9-5.5-1 Acoustic Flow Measuring System Block Diagram . . . 130
9-6.1.1.3-1 Reflective Path Transducer Configuration . . . 131
9-6.1.2.5-1 Recessed Transducer Configuration . . . 133
9-6.1.2.6-1 Protruding Transducer Configuration . . . 133
9-6.1.2.7-1 Flush Transducer Configuration . . . 134
9-6.1.2.9-1 Waveguide Transducer Configuration . . . 135
9-6.2.2-1 Cross-Beam Transducer Configuration . . . 136
9-8.4-1 Laminar (Blue) and Turbulent (Red) Flow Velocity Profiles and 1-, 2-, 3-, and 5-Beam Acoustic Patch Diagrams . . . 143
10-5-1 Schematic Control Volume . . . 147
10-5.1-1 Experimental Results . . . 147
10-7.3-1 Example Calibration Curves . . . 151
10-8.1-1 Tracer Injection Schematic . . . 152
10-8.2-1 Sampling System . . . 153
10-8.3-1 Fluorometer Signal Versus Time . . . 153
11-2-1 Vortex Formation . . . 157
11-5.5-1 Locations of Pressure and Temperature Measurements . . . 161
11-7.1-1 Illustration of a K-Factor Curve . . . 162
12-11-1 Positive Displacement Volumeters . . . 173
12-11.3-1 Method of Interpolation of Positive Displacement Meter Performance From Calibration Data to Other Fluid Viscosity and Operating Conditions . . . 175
13-3.1-1 Typical Mechanical Arrangement . . . 179
13-3.1-2 Oscillating Flow Tubes . . . 180
13-3.2-1 Electronic Transmitter . . . 181
13-4.2.3-1 Typical Calibration Curve With Uncertainty Bands (2σ Limits Shown) . . . 185
13-4.3.2.1-1 Temperature Effect on Zero (2σ Limits Shown) . . . 186
13-4.3.2.2-1 Pressure Effect on Span (2σ Limits Shown) . . . 187
13-5.1.2-1 Pressure Drop Versus Mass Flow . . . 189
I-6.3-1 Regression of Calibration Data With 95% Confidence Limits . . . 202
A-3.1-1 Measured Errors Versus Oscillating Differential Pressure Amplitude Relative to the Steady State Mean . . . 205
A-3.2-1 Fluid-Metering System Block Diagram . . . 207
A-3.6-1 Experimental and Theoretical Pulsation Error . . . 210
A-4.1-1 Semi-Log Plot of Theoretical Meter Pulsation Error Versus Rotor Response Parameter for Sine Wave Flow Fluctuation, D_2 = 0.1, and Pulsation Index, I = 0.1 and 0.2 . . . 211
A-4.5-1 Experimental Meter Pulsation Error Versus Pulsation Index . . . 213
B-1-1 Graph of Critical Flow Functions for Air . . . 217
C-1-1 Graph of Deviation of Critical Flow Functions for Air (Shown in Figure B-1-1) . . . 218
D-1-1 Graph of Correction Factors for Air to Real Gas From Ideal Gas, up to 30 atm . . . 220
D-1-2 Graph of Correction Factors for Air to Real Gas From Ideal Gas, up to 100 atm . . . 221
D-1-3 Graph of Correction Factors for Air to Real Gas From Ideal Gas, up to 300 atm . . . 222

Tables

2-3-1 Symbols Typically Used in Flow Measurement . . . 4
3-1-1 Symbols Specifically Applied in Sections 3 through 6 (in Addition to Symbols in Table 2-3-1) . . . 7

3-2-1 Values of Constants in the General Equation for Various Units 8
3-4-1 Units and Conversion Factor for Water Leg Correction for Flow Measurement 10
3-12.2-1 Uncertainty of Discharge Coefficient, C, (Uncalibrated) and Expansion Factor, ε 14
3-16-1 Natural Gas Analysis 17
4-6.1-1 Recommended Plate Thickness, E, for Stainless Steel Orifice Plate 25
4-13.1-1 Sensitivity Coefficients in the General Equation for Differential Pressure Meters 34
4-13.2.1-1 Example 1 — Systematic Uncertainty Analysis for Given Steam Flow Orifice Metering Run 35
4-13.2.2-1 Example 2 — Systematic Uncertainty Analysis for Given Steam Flow Orifice Metering Run 35
4-13.2.3-1 Example 3 — Systematic Uncertainty Analysis for Given Gas Flow and Meter Tube 36
4-13.4.1-1 Systematic Uncertainty, 0.075% Accuracy Class Differential Pressure Transmitter 38
4-13.4.2-1 Systematic Uncertainty, 0.075% Accuracy Class Static Pressure Transmitter 38
4-13.5-1 Systematic Uncertainty Analysis for Given Gas Flowmetering Run With Laboratory Calibration 38
6-5.1-1 Straight Lengths for Orifice Meters 58
6-5.1-2 Straight Lengths for Nozzles 59
6-5.1-3 Straight Lengths for Classical Venturi 60
6-6.1.1-1 Hole Coordinates for Perforated Plate 64
6-6.2-1 Loss Coefficients for Flow Conditioners 64
7-1-1 Symbols Specifically Applied in Section 7 (in Addition to Symbols in Table 2-3-1) 66
7-10.2-1 Summary of Points Plotted in Figure 7-10.2-1 and Coefficients for Eq. (7-10-2) 88
7-10.3-1 Discharge Coefficients for Cylindrical-Throat Venturi Nozzles 91
7-11.1.1-1 Percent Error in Method 3 Based on Sonic Flow Functions and Air Property Data 92
7-11.1.2.1-1 Sonic Flow Function, C^*_i, and Critical Property Ratios [Ideal Gases and Isentropic Relationships, Eqs. (7-2-7) through (7-2-9)] Versus Type of Ideal Gas 94
8-1-1 Symbols Specifically Applied in Section 8 (in Addition to Symbols in Table 2-3-1) 102
8-3.1-1 Locations and Weighting Factors for Gaussian Method in Pipes 105
8-3.1-2 Locations and Weighting Factors for Chebychev Method in Pipes 105
8-3.1-3 Locations and Weighting Factors for the Log-Linear Method in Pipes 106
8-3.1-4 Locations and Weighting Factors for the Equal-Area Method in Pipes 106
8-3.2-1 Locations and Weighting Factors for the Gaussian Method in Rectangular Ducts 107
8-3.2-2 Locations and Weighting Factors for Chebychev Method in Rectangular Ducts 108
8-3.2-3 Locations and Weighting Factors for the Equal-Area Velocity Method in Rectangular Ducts 109
8-9-1 Sample Uncertainty Estimate 122
9-3.2-1 Symbols Specifically Applied in Section 9 (in Addition to Symbols in Table 2-3-1) 124
10-1-1 Symbols Specifically Applied in Section 10 (in Addition to Symbols in Table 2-3-1) 146
10-7.2-1 Temperature Exponents for Tracer Dyes 149
10-9.2-1 Typical Uncertainties Using a Fluorescent Tracer 154
11-1-1 Symbols Specifically Applied in Section 11 (in Addition to Symbols in Table 2-3-1) 156
11-7.3-1 Recommended Distance From Disturbance for Less Than 0.5% Increase in Uncertainty . 163
11-7.4-1 Vortex Measurement Uncertainty Example 163
11-7.4-2 Vortex Measurement Uncertainty Example With Installation Uncertainty 164
11-7.4-3 Vortex Measurement Uncertainty Example With Vortex Meter, Pressure Sensor, and Temperature Sensor Uncertainties 164
12-1-1 Symbols Specifically Applied in Section 12 (in Addition to Symbols in Table 2-3-1) 165
13-1.2-1 Symbols Specifically Applied in Section 13 (in Addition to Symbols in Table 2-3-1) 178
13-4.2.1.3.1-1 Impact of Meter Tube Gas Velocity on Performance 182

13-4.2.1.3.2-1	Measurement Recommendations for Different Gas Test Pressures	183
13-4.2.2.4-1	Best Practices for Liquid and Gas Testing Data Collection Time	183
13-6.1-1	Example 1 — Analysis of Unheated Natural Gas Applications at Maximum Flow Rate	191
13-6.1-2	Example 1 — Analysis of Unheated Natural Gas Application at Minimum Flow Rate	192
13-6.2-1	Example 2 — Analysis of Heated Natural Gas Applications at Maximum Flow Rate	193
13-6.2-2	Example 2 — Analysis of Heated Natural Gas Applications at Minimum Flow Rate	194
13-6.3-1	Example 3 — Analysis of Liquid Condensate Application With Flowmeter Zeroed	195
13-6.4-1	Example 4 — Analysis of Liquid Condensate Application With Flowmeter Not Zeroed	196
I-1-1	Symbols Used in Mandatory Appendix I (in Addition to Symbols in Table 2-3-1)	197
I-6-1	Calibration Data, Test Data, and Predicted Value for an ASME Throat Tap Nozzle	201
A-3.1-1	Error Threshold Versus Relative Amplitude of ΔP	206
E-1-1	Conversions to SI (Metric) Units	224
E-1-2	Conversion Factors for Pressure (Force/Area)	226
E-1-3	Conversion Factors for Specific Volume (Volume/Mass)	227
E-1-4	Conversion Factors for Specific Enthalpy and Specific Energy (Energy/Mass)	228
E-1-5	Conversion Factors for Specific Entropy, Specific Heat, and Gas Constant [Energy/(Mass × Temperature)]	230
E-1-6	Conversion Factors for Viscosity (Force × Time/Area ~ Mass/Length × Time)	231
E-1-7	Conversion Factors for Kinematic Viscosity (Area/Time)	232
F-1-1	Thermal Expansion Data (SI)	234
F-1-2	Thermal Expansion Data (U.S. Customary)	239

NOTICE

All ASME Performance Test Codes (PTCs) shall adhere to the requirements of ASME PTC 1, General Instructions. It is expected that the Code user is fully cognizant of the requirements of ASME PTC 1 and has read them before applying ASME PTCs.

ASME PTCs provide unbiased test methods for both the equipment supplier and the users of the equipment or systems. The Codes are developed by balanced committees representing all concerned interests and specify procedures, instrumentation, equipment-operating requirements, calculation methods, and uncertainty analysis. Parties to the test can reference an ASME PTC confident that it represents the highest level of accuracy consistent with the best engineering knowledge and standard practice available, taking into account test costs and the value of information obtained from testing. Precision and reliability of test results shall also underlie all considerations in the development of an ASME PTC, consistent with economic considerations as judged appropriate by each technical committee under the jurisdiction of the ASME Board on Standardization and Testing.

When tests are run in accordance with a Code, the test results, without adjustment for uncertainty, yield the best available indication of the actual performance of the tested equipment. Parties to the test shall ensure that the test is objective and transparent. All parties to the test shall be aware of the goals of the test, technical limitations, challenges, and compromises that shall be considered when designing, executing, and reporting a test under the ASME PTC guidelines.

ASME PTCs do not specify means to compare test results to contractual guarantees. Therefore, the parties to a commercial test should agree before starting the test, and preferably before signing the contract, on the method to be used for comparing the test results to the contractual guarantees. It is beyond the scope of any ASME PTC to determine or interpret how such comparisons shall be made.

FOREWORD

The history of this Instruments and Apparatus Supplement began when the American Society of Mechanical Engineers (ASME) organized the Research Committee on Fluid Meters in 1916. This Committee's stated objective was to prepare "a textbook on the theory and use of fluid meters sufficient as a standard reference." The first edition of Part 1 of their report, published in 1924, met that objective. It received immediate approval and was widely referenced by users of fluid meters and educators. The Committee originally planned to issue the report on Fluid Meters in three parts: Part 1, Their Theory and Application, followed by Parts 2, A Description of Meters, and 3, Selection and Installation. However, Part 1 was so well received that second and third editions were needed before the other two parts could be prepared. The second edition of Part 1 was considerably different from the first, although it followed roughly the same format and arrangement; the third edition was very similar to the second. These were published in 1927 and 1930, respectively.

Part 2 of the report was published in 1931 and contained a complete description of the physical characteristics of the meters then being manufactured. Unfortunately, the material in Part 2 rapidly became obsolete and the Committee decided to advise those interested in the descriptions to secure them from the manufacturers, whose literature would necessarily be up to date.

Part 3, published in 1933, gave instructions for correct installation of meters and discussed the effect of incorrect installation. However, Part 3 was also abandoned, in this case because the Committee decided the material in it should be an integral part of the complete report.

The fourth edition of Part 1 was issued in 1937 as a completely new draft. Earlier editions had been criticized because the material as presented was difficult to put to practical use. A change in format and the addition of new material apparently corrected this problem, since this edition went through many printings.

The fifth edition, issued in 1959, followed this successful general format and included material gained in the long interval since the previous edition. The Committee also issued a manual, Flowmeter Computation Handbook, in 1961. The procedures in this publication could be adapted to computer programming.

The format of the sixth edition, published in 1971, differed slightly from that of the fourth and fifth editions. Each section was complete by itself, so altering one section would not affect the preceding or following sections.

The sixth edition, somewhat like the third edition and its Part 3, was divided into two parts. The material on installation and application became both a part of the complete report and a separate publication, ASME Performance Test Code (PTC) 19.5, Flow Measurement. This was in accordance with an agreement made between the Research Committee on Fluid Meters and the Performance Test Code Committee in 1964. Practically all of the material in ASME PTC 19.5 was taken from Fluid Meters, and most of the writers were also members of the Research Committee on Fluid Meters. The two committees decided to combine the material into one publication in such a way that the sections dealing with specifications and instructions could be published separately, which would reduce the work of the committees and the number of separate publications. However, this publication also prompted considerable criticism that the material as presented was difficult to put to practical use.

Consequently, the Board on Performance Test Codes, which is now the PTC Standards Committee under the Board on Standardization and Testing, formed a committee to address these concerns. This committee produced ASME PTC 19.5-2004, Flow Measurement, which included a much broader range of methods of flow measurement than any of its predecessors. Even so, it did not include every method, only those that were judged at the time to meet the requirements and needs of test codes by providing results of the highest level of accuracy consistent with the best engineering knowledge and practice currently available.

ASME PTC 19.5-2022 provides guidance on the proper use of flowmeters including guidance on estimating their measurements' systematic uncertainties. The choice of flow-measurement devices and calibration requirements in any given case depends on the requirements of the PTC referencing this Supplement.

ASME PTC 19.5-2022 includes recommendations from the ASME Board on Standardization Testing Task Groups on ASME equations for fluid flow through a classic ASME venturi, wall tap nozzle, and orifice meter, which reconcile some differences between ASME PTC 19.5 and ASME MFC-3. These recommendations resulted in updates to the discharge coefficients for venturi meters, wall tap nozzles, and orifice meters; updates to the straight-length requirements; and some updates to the systematic uncertainties.

ASME PTC 19.5-2022 has added further guidance and a method for determining the uncertainty of extrapolating the calibration data of some flowmeters. The PTC referencing this Supplement should define the acceptable added uncertainty for extrapolation of the meter's data used in specific applications.

Sections have been added to cover the frequently used Coriolis and ultrasonic flowmeters. A new section on vortex meters, which are used in some performance testing, has also been added. PTC documents typically do not reference the use of electromagnetic flowmeters; the ASME PTC 19.5 Committee recommends the use of ASME MFC-16-2014 for guidance.

This Code is available for public review on a continuing basis. This provides an opportunity for additional input from industry, academia, regulatory agencies, and the public-at-large.

ASME PTC 19.5-2022 was approved by the PTC Standards Committee on April 21, 2021, and was approved as an American National Standard by the American National Standard Institute Board of Standards Review on January 5, 2022.

ASME PTC COMMITTEE
Performance Test Codes

(The following is the roster of the committee at the time of approval of this Code.)

STANDARDS COMMITTEE OFFICERS

S. A. Scavuzzo, *Chair*
T. K. Kirkpatrick, *Vice Chair*
D. Alonzo, *Secretary*

STANDARDS COMMITTEE PERSONNEL

P. G. Albert, Consultant
D. Alonzo, The American Society of Mechanical Engineers
J. M. Burns, Burns Engineering Services, Inc.
A. E. Butler, GE Power and Water
W. C. Campbell, Generating Plant Performance Consultants
J. Gonzalez, Generación SAU
R. E. Henry, Consultant
D. R. Keyser, Survice Engineering
T. K. Kirkpatrick, McHale & Associates, Inc.
M. P. McHale, McHale & Associates, Inc.
J. W. Milton, Chevron, USA
S. P. Nuspl, Consultant
R. Pearce, Kansas City Power and Light
S. A. Scavuzzo, The Babcock & Wilcox Co.
J. A. Silvaggio, Jr., Siemens Demag Delaval Turbomachinery, Inc.
T. L. Toburen, T2E3
W. C. Wood, Consultant
T. C. Heil, *Alternate*, The Babcock & Wilcox Co.
R. P. Allen, *Honorary Member*, Consultant
P. M. McHale, *Honorary Member*, McHale & Associates, Inc.
R. R. Priestley, *Honorary Member*, Consultant
R. E. Sommerlad, *Honorary Member*, Consultant

PTC 19.5 COMMITTEE — FLOW MEASUREMENT

P. G. Albert, *Chair*, Consultant
K. Kenneally, *Vice Chair*, MPR Associates, Inc.
M. Pagano, *Secretary*, The American Society of Mechanical Engineers
A. G. Caswell, Jr., Clean Air Engineering
J. Dwyer, Primary Flow Signal, Inc.
C. J. Erwin, GE Power
J. Foster, Emerson Process Management
A. Hawley, Southwest Research Institute
A. Jackson-Sandfort, Vogt Power International
M. Keilty, Endress + Hauser Flowtec AG
D. R. Keyser, Survice Engineering
S. Korellis, EPRI
D. R. Kuhny, Micro Motion, Inc.
W. R. Murray, Krohne
B. R. Novitsky, U.S. Air Force — AFMETCAL
J. B. Nystrom, Alden Research Lab
F. Saldarriaga, Global Forensic Investigations
P. Stacy, Alden Research Lab
R. Wakeland, Wakeland Engineering, PLLC
K. W. John, *Alternate*, U.S. Air Force — AFMETCAL
C. Wakeland, *Alternate*, Wakeland Engineering, PLLC
A. Banerjee, *Contributing Member*, Lehigh University
R. Jethra, *Contributing Member*, WIKA USA
T. K. Kirkpatrick, *Contributing Member*, McHale & Associates, Inc.

CORRESPONDENCE WITH THE PTC COMMITTEE

General. ASME codes and standards are developed and maintained by committees with the intent to represent the consensus of concerned interests. Users of ASME codes and standards may correspond with the committees to propose revisions or cases, report errata, or request interpretations. Correspondence for this Code should be sent to the staff secretary noted on the committee's web page, accessible at https://go.asme.org/PTCcommittee.

Revisions and Errata. The committee processes revisions to this Code on a periodic basis to incorporate changes that appear necessary or desirable as demonstrated by the experience gained from the application of the Code. Approved revisions will be published in the next edition of the Code.

In addition, the committee may post errata on the committee web page. Errata become effective on the date posted. Users can register on the committee web page to receive e-mail notifications of posted errata.

This Code is always open for comment, and the committee welcomes proposals for revisions. Such proposals should be as specific as possible, citing the paragraph number(s), the proposed wording, and a detailed description of the reasons for the proposal, including any pertinent background information and supporting documentation.

Cases

(a) The most common applications for cases are

(1) to permit early implementation of a revision based on an urgent need

(2) to provide alternative requirements

(3) to allow users to gain experience with alternative or potential additional requirements prior to incorporation directly into the Code

(4) to permit the use of a new material or process

(b) Users are cautioned that not all jurisdictions or owners automatically accept cases. Cases are not to be considered as approving, recommending, certifying, or endorsing any proprietary or specific design, or as limiting in any way the freedom of manufacturers, constructors, or owners to choose any method of design or any form of construction that conforms to the Code.

(c) A proposed case shall be written as a question and reply in the same format as existing cases. The proposal shall also include the following information:

(1) a statement of need and background information

(2) the urgency of the case (e.g., the case concerns a project that is underway or imminent)

(3) the Code and the paragraph, figure, or table number(s)

(4) the edition(s) of the Code to which the proposed case applies

(d) A case is effective for use when the public review process has been completed and it is approved by the cognizant supervisory board. Approved cases are posted on the committee web page.

Interpretations. Upon request, the committee will issue an interpretation of any requirement of this Code. An interpretation can be issued only in response to a request submitted through the online Interpretation Submittal Form at https://go.asme.org/InterpretationRequest. Upon submitting the form, the inquirer will receive an automatic e-mail confirming receipt.

ASME does not act as a consultant for specific engineering problems or for the general application or understanding of the Code requirements. If, based on the information submitted, it is the opinion of the committee that the inquirer should seek assistance, the request will be returned with the recommendation that such assistance be obtained. Inquirers can track the status of their requests at https://go.asme.org/Interpretations.

ASME procedures provide for reconsideration of any interpretation when or if additional information that might affect an interpretation is available. Further, persons aggrieved by an interpretation may appeal to the cognizant ASME committee or subcommittee. ASME does not "approve," "certify," "rate," or "endorse" any item, construction, proprietary device, or activity.

Interpretations are published in the ASME Interpretations Database at https://go.asme.org/Interpretations as they are issued.

Committee Meetings. The PTC Standards Committee regularly holds meetings that are open to the public. Persons wishing to attend any meeting should contact the secretary of the committee. Information on future committee meetings can be found on the committee web page at https://go.asme.org/PTCcommittee.

Section 1
Object, Scope, and Uncertainty

1-1 OBJECT

The purpose of this ASME Performance Test Code (PTC) Supplement is to give instructions and guidance for the accurate determination of flows commonly needed in support of individual PTCs. The choice of flow measurement device and calibration requirement depends on the requirements of the PTC referencing this Supplement. The purpose of the measurement, uncertainty required, and specific application must all be taken into consideration. It is not the intent of this Supplement to supersede the guidance or requirements of any PTC. The intent is to provide a common document that can be referenced by all PTCs.

1-2 SCOPE

This Supplement describes the techniques and methods of flow measurements required or recommended by ASME PTCs. A variety of commonly used flow measurement devices are included to provide details for the different applications referenced by various PTCs. This is a supplementary document that does not supersede the mandatory requirements of any PTC, unless such an agreement has been expressed in writing prior to testing or a PTC requires that specified sections or paragraphs within this Supplement be used.

1-3 UNCERTAINTY

This Supplement provides guidance on potential magnitudes and sources of uncertainty to assist in the derivation of the expected overall systematic uncertainty of a specific flow measurement. This overall systematic uncertainty includes estimated component uncertainties for

(a) flow coefficients for an uncalibrated meter
(b) calibration
(c) extrapolation of a calibrated meter beyond its calibrated range
(d) installation requirements and potential risks for deviations
(e) additional requirements to improve the flow measurement

The uncertainty of any flow measurement depends on the type and design of the instrument; the characteristics of the flow along with flow conditioning upstream and downstream; the pressure, temperature, density, frequency output, and stability of the flow; and the installation of sensing lines for differential-pressure measurements.

The specific uncertainty for each flow measurement can be determined by information in this Supplement; the specific ASME PTC; ASME PTC 19.1; and, in some cases, manufacturer's guidance. The uncertainty values shown in this Supplement are typically systematic values for a component or examples of systematic uncertainties. The reported uncertainty values are at 95% confidence level. The uncertainty values represent plus/minus (±) values unless asymmetrical uncertainty exists, in which case the plus (+) and minus (−) values along with sign will be shown.

1-4 REFERENCES TO ASME STANDARDS

Below is a list of ASME publications referenced in this Code. In all cases, the latest edition shall apply. Specific references to ASME and other publications are included within each section.

ASME B31.1. Power Piping.
ASME B31.3. Process Piping.
ASME MFC-3M. Measurement of Fluid Flow in Pipes Using Orifice, Nozzle, and Venturi.
ASME MFC-7. Measurement of Gas Flow by Means of Critical Flow Venturi Nozzles.
ASME MFC-8M. Fluid Flow in Closed Conduits: Connections for Pressure Signal Transmissions Between Primary and Secondary Devices.
ASME MFC-16. Measurement of Liquid Flow in Closed Conduits with Electromagnetic Flowmeters.

ASME PTC 1. General Instructions.
ASME PTC 2. Definitions and Values.
ASME PTC 6. Steam Turbines.
ASME PTC 11. Fans.
ASME PTC 18. Hydraulic Turbines and Pump-Turbines.
ASME PTC 19.1. Test Uncertainty.
ASME PTC 19.2. Pressure Measurement.
ASME PTC 19.3. Temperature Measurement.

Section 2
Definitions, Values, and Descriptions of Terms

2-1 GENERAL

The equations in this Supplement are written in the primary system of units explained below, except where specifically noted. This is to simplify the text and focus on the physical and scientific principles involved in the measurement of flow. Users should convert particular units into these primary units, calculate the flow, and reconvert the result back into their preferred units. For international use, equations using pounds for force, slugs for mass, feet for length, and seconds for time appear identical to equations using newtons, kilograms, meters, and seconds, respectively. Subsection 2-2 contains primary definitions and systems of units; Nonmandatory Appendix G contains historical definitions of units of measure.

2-2 PRIMARY DEFINITIONS AND SYSTEMS OF UNITS

(a) The force of 1 lb applied to a mass of 1 slug (also known as a geepound) will accelerate said mass at the rate of 1 ft/sec^2.

(b) The force of 1 N applied to a mass of 1 kg will accelerate said mass at the rate of 1 m/s^2.

(c) Equations written in the units described in (a) and (b) will appear identical. Converting measured values to the above primary U.S. Customary units can simplify the expression of test results in metric [Systeme Internationale (SI)] units.

(d) By way of contrast and for clarification, the force of 1 lbf applied to a mass of 1 lbm will accelerate said mass at the rate that is equal to 32.1740486 ft/sec^2. The proportionality constant g_c is equal to 32.1740486 lbm-ft/lbf-sec^2 and is necessary to account for units of length, time, and force. Note that g_c is not the local acceleration of gravity at the test site.

(e) The required source for precise physical values, conversion factors, and definitions is ASME PTC 2.

2-3 SYMBOLS AND DIMENSIONS

Table 2-3-1 describes the symbols typically used in flow measurement. Additional symbols are described in their respective sections.

2-3.1 Common Conversion Factors

See Nonmandatory Appendix E for common conversion factors.

2-4 THERMAL EXPANSION

This subsection deals with piping and primary element materials. In most cases, the piping and primary element diameters are measured at room temperature but are used at the actual temperature of the flowing fluid (assumed to be the same as piping and primary element temperature). It is customary to assume, unless given otherwise, that the dimensional measurement takes place at 20°C (68°F).

2-4.1 Linear Thermal Expansion

The mean coefficient of linear thermal expansion is defined by

$$\alpha = \left(\frac{1}{L_b}\right)\left(\frac{dL}{dT}\right) \tag{2-4-1}$$

where

α = mean coefficient of linear expansion from base temperature, b, to actual temperature, T $(1/T)$

L_b = length at base temperature, b

Table 2-3-1
Symbols Typically Used in Flow Measurement

Symbol	Description	Dimensions [Note (1)]	Units	
			SI	U.S. Customary
A	Area	L^2	mm^2	$in.^2$
C	Discharge coefficient	Dimensionless	Dimensionless	Dimensionless
C	Acoustic velocity, speed of sound	LT^{-1}	m/s	ft/sec
C^*_i	Sonic flow function	Dimensionless	Dimensionless	Dimensionless
c_p	Constant pressure specific heat	$L^2T^{-2}\theta^{-1}$	kJ/(kg·K)	Btu/(lbm·°R)
c_v	Constant volume specific heat	$L^2T^{-2}\theta^{-1}$	kJ/(kg·K)	Btu/(lbm·°R)
d	Diameter, usually of pipe or inlet section of flow element	L	mm	in.
d	Diameter, usually of bore or throat	L	mm	in.
f	Frequency	T^{-1}	Hz	1/sec
G	Mass flux	$ML^{-2}T^{-1}$	$kg/(m^2·s)$	$lbm/(ft^2·sec)$
g_c	Proportionality constant [Note (2)]			
g_L	Local acceleration due to gravity	LT^{-2}	m/s^2	ft/sec^2
h	Specific enthalpy	L^2T^{-2}	kJ/kg	Btu/lbm
L, l	Length or distance	L	mm	in.
MW	Molecular weight	M	kg/kmol	lbm/lbmol
P	Pressure	$ML^{-1}T^{-2}$	Pa	psi [Note (3)], atm
q_v	Volumetric flow rate	L^3T^{-1}	m^3/s, L/s, m^3/h	ft^3/sec, gal/min, ft^3/min
q_m	Mass flow rate	MT^{-1}	kg/s	lbm/sec. lbm/hr
R_u	Universal gas constant	$ML^2T^{-2}\theta^{-1}$	8.314 kJ/(kmol·K)	1,545 ft·lbf /(lbmol·°R)
Re	Reynolds number	Dimensionless	Dimensionless	Dimensionless
S	Sensitivity coefficient	...	...	...
s	Specific entropy	$L^2T^{-2}\theta^{-1}$	kJ/(kg·K)	Btu/(lbm °R)
T	Temperature	θ	°C, K (absolute)	°F, °R (absolute)
t	Time	T	s	sec
u_{rand}	Relative random uncertainty	Dimensionless	%	%
u_{sys}	Relative systematic uncertainty	Dimensionless	%	%
V	Velocity	LT^{-1}	m/s	ft/sec
v	Specific volume	L^3M^{-1}	m^3/kg	ft^3/lbm
Z	Compressibility factor for a gas	Dimensionless	Dimensionless	Dimensionless
α	Linear thermal expansion factor	θ^{-1}	1/°C	1/°F
β	Diameter (beta) ratio, d/D	Dimensionless	Dimensionless	Dimensionless
γ	Ratio of specific heats	Dimensionless	Dimensionless	Dimensionless
Δ	Finite difference operator	Dimensionless	Dimensionless	Dimensionless
δ	Small difference, calculus differential operator	Dimensionless	Dimensionless	Dimensionless
ε	Expansion factor of a flowing compressible fluid	Dimensionless	Dimensionless	Dimensionless
κ	Isentropic exponent, as in the expansion or compression of gas	Dimensionless	Dimensionless	Dimensionless
μ	Absolute viscosity	$ML^{-1}T^{-1}$	kg/(m·s)	lbm/(ft·sec), cP
ν	Kinematic viscosity	L^2T^{-1}	m^2/s	ft^2/sec, cSt
ρ	Density	ML^{-3}	kg/m^3	lbm/ft^3
σ	Standard deviation	...	...	...
Subscripts				
D	Based on pipe or inlet section diameter	...	...	...
d	Based on bore or throat diameter	...	...	...

NOTES:
(1) Dimensions:
L = length
M = mass
T = time

Table 2-3-1
Symbols Typically Used in Flow Measurement (Cont'd)

NOTES: (Cont'd)
θ = thermodynamic temperature
(2) More details on the proportionality constant are located in Section 3.
(3) In the U.S., Customary units — "psia" (lbf/in.^{2}, absolute) or "psig" (lbf/in.^{2}, gauge) — are the most common symbols used for pressure.

The ratio of length at temperature, T, to length at base temperature, b, is given by

$$L_T/L_b = 1 + \alpha(T - b) \tag{2-4-2}$$

where
L_T = length at temperature, T

2-4.2 Tables of Linear Thermal Expansion for Selected Materials

Nonmandatory Appendix F, Table F-1-1 contains SI unit values of L_T/L_b in the mean coefficients of thermal expansion, α and linear thermal expansion, B, which is expressed as $(L_T - L_b)$ per 1 m when L_b is taken to be 1 000 mm (1 m) and L_T is calculated using eq. (2-4-2). Table F-1-2 contains U.S. Customary unit values of the mean coefficients of thermal expansion, α and linear thermal expansion, B, which is expressed as $(L_T - L_b)$ per 100 ft when L_b is taken to be 1 200 in. (100 ft) and L_T is calculated using eq. (2-4-2). The data in Nonmandatory Appendix F is for informational purposes only, and it should not be inferred that materials are suitable for all the temperature ranges shown.

2-5 REFERENCES

Abramowitz, M., and Stegun, I., eds. [1983 (1964)]. Handbook of Mathematical Functions with Formulas, Graphs, and Mathematical Tables. Dover Publications.

ASHRAE Technical Committee on Psychrometrics (1977). ASHRAE Brochure on Psychrometry. American Society of Heating, Refrigerating and Air-Conditioning Engineers.

Avallone, E., and Baumeister, T., eds. (1987). Mark's Standard Handbook for Mechanical Engineers (9th ed.). McGraw-Hill.

Bean, H. S., ed. (1971). Fluid Meters: Their Theory and Application (6th ed.). The American Society of Mechanical Engineers.

Chase, M. W. (1998). NIST–JANAF Thermochemical Tables (4th ed.). American Chemical Society; American Institute of Physics for the National Institute of Standards and Technology.

CRC Report No. 530 (1983). Handbook of Aviation Fuel Properties. Coordinating Research Council.

CTI ATC-105 (2019). Acceptance Test Code for Water Cooling Towers. Cooling Tower Institute.

Eshbach, O., and Sanders, M. (1975). Handbook of Engineering Fundamentals (3rd ed.). John Wiley and Sons.

HEI 118-1984. Standards for Steam Surface Condensers (8th ed.). Heat Exchange Institute.

Kutz, M. (2005). Mechanical Engineers' Handbook (3rd ed.). John Wiley and Sons.

Meyer, C. A. (1993). ASME Steam Tables: Thermodynamic and Transport Properties of Steam (6th ed.). The American Society of Mechanical Engineers.

Miller, R. W. (1996). Flow Measurement Engineering Handbook (3rd ed.). McGraw-Hill.

M. W. Kellogg Company for the Office of Saline Water (1971). Saline Water Conversion Engineering Data Book (2nd ed.). U.S. Department of the Interior.

Oberg, E., Jones, F. D., Horton, H. L., Ryffel, H. H, and McCauley C. J. (2016). Machinery's Handbook (30th ed.). Industrial Press.

Perry, R. H., Chilton, C. H., and Kilpatrick, S. D. (1963). Perry's Chemical Engineers' Handbook (4th ed.). McGraw-Hill.

Stewart, R. B., Jacobsen, R. T., and Penoncello, S. G. (1986). ASHRAE Thermodynamic Properties of Refrigerants. American Society of Heating, Refrigerating and Air-Conditioning Engineers.

Weast, R. C. (1979). CRC Handbook of Chemistry and Physics: A Ready-Reference Book of Chemical and Physical Data (59th ed.). CRC Press.

Section 3
Differential Pressure Class Meters

3-1 NOMENCLATURE

Symbols used in Sections 3 through 6 are included in Tables 2-3-1 and 3-1-1. For any equation that consists of a combination of symbols with units shown in Tables 2-3-1 and 3-1-1, the user must be sure to apply the proper conversion factors.

3-2 GENERAL EQUATION FOR MASS FLOW THROUGH A DIFFERENTIAL PRESSURE CLASS METER

(a) The general equation for mass flow through a differential pressure class meter is as follows:

$$q_m = n\frac{\pi}{4}d^2 C\varepsilon\sqrt{\frac{2\rho(\Delta p)g_c}{1-\beta^4}} \tag{3-2-1}$$

Equation (3-2-1) is applied to flow calculations for all orifices, nozzles, and venturis described in Sections 4 and 5 and is valid for both liquids and gases flowing at subsonic velocity.

(b) Values of the unit conversion constant, n, and the proportionality constant, g_c, for commonly used combinations of units are shown in Table 3-2-1. The first row shows SI units. The second row shows U.S. customary units. The third row shows U.S. Absolute Engineering units, which are less commonly used but, similar to SI units, are derived by setting the proportionality constant equal to unity. Use of other units for any parameter(s) in the general equation is permissible, provided the n factor is correctly determined.

(c) If manometers are used to measure the differential pressure, then the acceleration of gravity, g_L, at the location of use must be taken into consideration, as well as the difference in densities between the upper and lower fluids in the manometer. When manometers are used, $\Delta P = \rho h(g_L/g_c)$, where h is the height of manometer fluid and the density of the manometer fluid is corrected per ASME PTC 19.2.

(d) The development of the general equation follows in subsection 3-3.

3-3 BASIC PHYSICAL CONCEPTS USED IN THE DERIVATION OF THE GENERAL EQUATION FOR MASS FLOW

(a) Introduction. The physical concepts and assumptions used for the derivation of eq. (3-2-1) are well documented. The equation is derived from the principles of conservation of energy and mass between the upstream and downstream taps, identified in the equations as subscripts 1 and 2, respectively. Flow behavior and fluid properties are idealized, and errors introduced by these assumptions are corrected by the discharge coefficient, C, and the expansion factor, ε, for accurate calculation of mass flow.

The discharge coefficient, C, corrects for the idealized theoretical assumptions of flow behavior made in the derivation of the flow equation.

The expansion factor, ε, corrects for the compressibility effects of a gas as it flows between locations 1 and 2.

(b) Energy Equation. Flow through a differential pressure meter is idealized as Newtonian steady state flow, with one-dimensional velocities across the flow areas.

$$\delta q = \delta w + du + Pdv + vdP + \frac{1}{g_c}VdV + \frac{g_L}{g_c}dz \tag{3-3-1}$$

Each of the terms of eq. (3-3-1) must be in consistent units of energy per unit mass.

Table 3-1-1
Symbols Specifically Applied in Sections 3 through 6 (in Addition to Symbols in Table 2-3-1)

Symbol	Description	Dimensions [Note (1)]	Units	
			SI	U.S. Customary
e_c	Eccentricity of meter relative to pipe or inlet section diameter	L	mm	in.
k	Deviation of pipe inside diameter or inlet section diameter	L	μm	μin.
k_l	Flow conditioner loss coefficient	Dimensionless	Dimensionless	Dimensionless
k/D	Relative roughness of pipe	Dimensionless	Dimensionless	Dimensionless
L_1	Ratio of location of a pressure tap to D	...	...	...
l_1, l_2'	Dimension for spacing a pressure tap as measured from its centerline	L	mm	in.
N	Units conversion factor for general equation of flow through a differential pressure class meter	...	...	...
q	Specific heat	L^2T^{-2}	kJ/kg	Btu/lbm
q_{m_c}	Mass flow (compressible)	MT^{-1}	kg/s	lbm/hr
q_{m_i}	Mass flow (incompressible)	MT^{-1}	kg/s	lbm/hr
$q_{m_{tc}}$	Mass flow (theoretically compressible)	MT^{-1}	kg/s	lbm/hr
$q_{m_{ti}}$	Mass flow (theoretically incompressible)	MT^{-1}	kg/s	lbm/hr
r	Ratio of downstream pressure to upstream pressure; P_2/P_1	Dimensionless	Dimensionless	Dimensionless
s'	Distance of the step from the upstream pressure tap	L	mm	in.
U	Total steady state uncertainty	Dimensions of variable	...	...
u	Specific energy	L^2T^{-2}	kJ/kg	Btu/lbm
w	Specific work	L^2T^{-2}	kJ/kg	Btu/lbm
z	Elevation	L	m	ft
α_P	Pipe, inlet section material thermal expansion factor	θ^{-1}	1/°C	1/°F
α_{PE}	Flow element material thermal expansion factor	θ^{-1}	1/°C	1/°F
β	Ratio of bore to pipe or inlet section diameters, d/D	Dimensionless	Dimensionless	Dimensionless
$\Delta\omega$	Unrecoverable pressure loss	$ML^{-1}T^{-2}$	Pa	psi
ε	Expansion correction factor for compressible fluids	Dimensionless	Dimensionless	Dimensionless
τ	Total deflection	L	mm	in.
Subscript	**Description**			
actual	Actual value	...	...	...
meas	Measured	...	...	...
true	True, reference value	...	...	...
1	Upstream pressure tap location, cross section, or conditions	...	...	...
2	Downstream pressure tap location, cross section, or conditions	...	...	...

NOTE: (1) Dimensions:
L = length
M = mass
T = time
θ = thermodynamic temperature

Table 3-2-1
Values of Constants in the General Equation for Various Units

Units	Mass Flow Rate Units, q_m	Meter Geometry Units, d or D	Fluid Density Units, ρ	Differential Pressure Units, ΔP	Value of Constants	
					Proportionality Constant, g_c	Units Conversion Constant, n
SI	kg/sec	m	kg/m^3	Pa	g_c = 1.0 dimensionless	$n = 1.0\left(\frac{kg}{m \cdot s^2 \cdot Pa}\right)^{1/2}$
U.S. Customary	lbm/hr	in.	lbm/ft^3	$lbf/in.^2$	$g_c = 32.1740486 \frac{lbm \cdot ft}{lbf \cdot sec^2}$	$n = 300.0\left(\frac{ft \cdot sec}{in. \cdot hr}\right)$
U.S. Absolute	slugs/sec	ft	$slugs/ft^3$	lbf/ft^2	g_c = 1.0 dimensionless	$n = 1.0\left(\frac{slug \cdot ft}{lbf \cdot sec^2}\right)^{1/2}$

Further idealizations are made by assuming that the flow through a differential pressure meter section is a reversible thermodynamic process in the absence of external work or heat.

$$0 = \frac{dP}{\rho} + \frac{VdV}{g_c} + \frac{g_L}{g_c}dz \tag{3-3-2}$$

The integration of eq. (3-3-2) further depends on whether the fluid is treated as incompressible or compressible.

The elevation term in eq. (3-3-2) and the general eq. (3-3-1) is always zero because the differential pressure is corrected when necessary. In those cases where installation in an inclined pipe is necessary, the elevation change between pressure taps ($z_2 - z_1$) must be considered. The differential pressure is corrected for the difference in elevation of the pressure taps for the fluid within the pipe and the fluid within the sensing lines before the flow is calculated.

(c) Conservation of Mass Equation. Under the assumptions of (b), conservation of mass is written in the form

$$q_m = \rho_1 V_1 A_1 = \rho_2 V_2 A_2 \tag{3-3-3}$$

or

$$V_1 = \frac{\rho_2}{\rho_1}\beta^2 V_2 \tag{3-3-4}$$

in any set of consistent units.

3-4 THEORETICAL FLOW — LIQUID AS THE FLOWING FLUID

(a) For the special case where the flowing fluid is a liquid or incompressible, integrating the energy equation [see eq. (3-3-2)] between the upstream tap and the downstream tap gives Bernoulli's equation.

$$\frac{P_1}{\rho} + \frac{V_1^2}{2g_c} + \frac{g_L}{g_c}z_1 = \frac{P_2}{\rho} + \frac{V_2^2}{2g_c} + \frac{g_L}{g_c}z_2 \tag{3-4-1}$$

(b) Combining eq. (3-4-1) (with elevation term of zero) with eq. (3-3-3) and applying $A_2 = \pi d^2/4$ gives the following theoretical flow:

$$q_m = \frac{\pi}{4}d^2 \frac{1}{\sqrt{1-\beta^4}} \sqrt{2\rho(\Delta P)g_c} \tag{3-4-2}$$

It is important to note that d, D, and β vary with temperature and materials as explained in subsection 3-11.

When a differential pressure meter is installed on a flow element that is located in a vertical or inclined steam or water line, the measurement must be corrected for the difference in sensing line height and the fluid head change. No correction is required for a tap elevation difference if the fluid in the sensing line has the same density as the flowing fluid. Then the fluid in the sensing line compensates for the elevation difference. However, if the taps are at different elevations and the density in the sensing lines is different from that of the flowing fluid, a correction is required for the differences in density and elevation. The correction is shown in Figure 3-4-1. See Table 3-4-1 for units and conversion factors.

Figure 3-4-1
Water Leg Correction for Flow Measurement

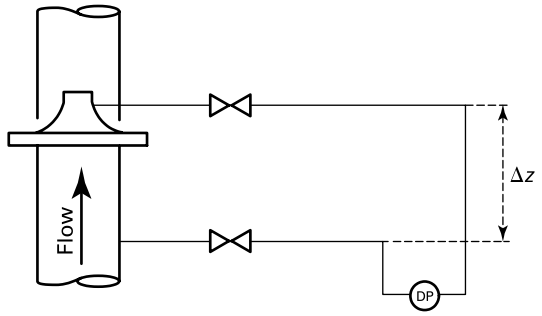

(a) Configuation A [Note (1)]

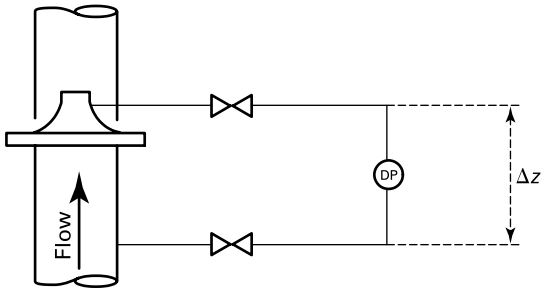

(b) Configuration B [Note (2)]

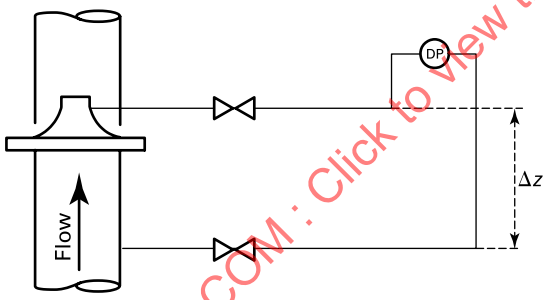

(c) Configuration C [Note (2)]

NOTES:
(1) For measurement of steam or water, Configuration A is the preferred sensing line configuration to facilitate establishment of the water legs and remain confident that the water legs remain established.
(2) For measurement of steam or water, Configurations B and C are not recommended since special precautions must be taken to establish the water legs and be assured the water legs remain established.

Table 3-4-1
Units and Conversion Factor for Water Leg Correction for Flow Measurement

Units	Differential Pressure, ΔP, Units	Fluid Density, ρ, Units	Local Acceleration Due to Gravity, g_L, Units	Differential Elevation, Δz, Units	Conversion Factor: Values of Constants: Proportionality Constant, g_c	Conversion Factor: Values of Constants: Units Conversion Constant, n
SI	Pa	kg/m^3	m/s^2	m	$g_c \equiv 1.0$, dimensionless	$n \equiv 1.0$, dimensionless [Note (1)]
U.S. Customary	$lbf/in.^2$	lbm/ft^3	ft/sec^2	ft	$g_c = 32.1740486 \ \frac{lbm - ft}{lbf - s^2}$	$n \equiv 1/144 \frac{ft^2}{in.}$

GENERAL NOTE: g_L is the local acceleration due to gravity, ft/sec^2 per an acknowledged source, or may be estimated as: $g_L = 32.1740486 \times \{1 - 0.0026373 \times \cos(2 \times \text{deg latitude} \times \pi/180) + 0.0000059 \times [\cos^2(2 \times \text{deg latitude} \times \pi/180)]\} - 0.000003086 \times$ feet elevation or for SI, $g_L = m/sec^2 = 9.80616 \times \{1 - 0.0026373 \times \cos(2 \times \text{deg latitude} \times \pi/180) + 0.0000059 \times [\cos^2(2 \times \text{deg latitude} \times \pi/180)]\} - 0.000003086 \times$ meters elevation

NOTE: (1) $N \equiv kg\text{-}m/s^2$ and $Pa \equiv N/m^2$. Therefore, $Pa \equiv kg/m\text{-}s^2$

For upward flow (see Figure 3-4-1)

$$\Delta P_{true} = \Delta P_{meas} + n(\rho_{amb} - \rho_{pipe})(g_L/g_c)\Delta z \tag{3-4-3}$$

For downward flow

$$\Delta P_{true} = \Delta P_{meas} - n(\rho_{amb} - \rho_{pipe})(g_L/g_c)\Delta z \tag{3-4-4}$$

where

ρ_{amb} = the density of the fluid in the uninsulated sensing line at Δz
ρ_{pipe} = the density of the flowing fluid

CAUTION: Do not install the upper sensing line against a steam or water line that is located inside the insulation and extends down to where the lower sensing line protrudes from the insulation in order to avoid making the differential pressure correction. The fluid in the sensing line within the pipe insulation is not always at the same density as the fluid in the pipe, so a significant error can be introduced.

(c) Equation (3-4-2) is equivalent to eq. (3-2-1) before correction factors and unit conversions are applied. It is the theoretical incompressible flow equation for the flow of fluids through differential pressure meters.

3-5 THEORETICAL FLOW — GAS OR VAPOR AS THE FLOWING FLUID

(a) Assuming an ideal gas in an isentropic process

$$r = \frac{P_2}{P_1} = \left[\frac{\rho_2}{\rho_1}\right]^{\kappa} = \left[\frac{T_2}{T_1}\right]^{\frac{\kappa}{\kappa-1}} \tag{3-5-1}$$

(b) Integrating the energy equation [see eq. (3-3-2)] for these conditions

$$0 = \frac{\kappa}{\kappa - 1}\left[\frac{P_2}{\rho_2} - \frac{P_1}{\rho_1}\right]^{\kappa} + \left[\frac{V_2^2 - V_1^2}{2g_c}\right]^{\frac{\kappa}{\kappa-1}} \tag{3-5-2}$$

(c) Substituting eq. (3-3-4) to eliminate V_1, substituting eq. (3-5-1), and implementing conservation of mass

$$q_{m_{tc}} = \left(\frac{\pi}{4}d^2\right)\rho_2\left|\left(\frac{2g_c\kappa}{\kappa - 1}\right)\left(\frac{P_1}{\rho_1}\right)\left(\frac{1 - r^{\frac{\kappa-1}{\kappa}}}{1 - \beta^4 r^{\frac{2}{\kappa}}}\right)\right|^{0.5} \tag{3-5-3}$$

(d) Equation (3-5-3) can be modified using $P_1 = \Delta P/(1 - r)$ and again by substituting eq. (3-5-1), and is written

$$q_{m_{tc}} = \frac{\pi}{4} d^2 \frac{\sqrt{2\rho(\Delta P) g_c}}{\sqrt{1-\beta^4}} \times \left[r^{2/\kappa} \left(\frac{\kappa}{\kappa - 1} \right) \left(\frac{1 - r^{\frac{\kappa-1}{\kappa}}}{1 - r} \right) \right] \left(\frac{1 - \beta^4}{1 - \beta^4 r^{2/\kappa}} \right)^{0.5} \quad (3\text{-}5\text{-}4)$$

(e) Equation (3-5-4) is equivalent to eq. (3-5-1) before correction factors and unit conversions are applied and modified by the term in brackets. The bracketed term is the derived value of ε_1, the expansion correction factor for the pressure being sensed at the upstream pressure tap, for nozzles and venturis.

(f) The compressibility effects of flow through an orifice include sudden radial expansion. Straightforward derivation of the values for ε used for orifices cannot be developed with the basic principles of this paragraph. The equation for ε used for orifices is discussed in subsection 3-9.

(g) Equation (3-5-4) is the theoretical compressible equation for subsonic flow of ideal, compressible fluids through flow nozzles and venturis.

3-6 FACTORS NOT ACCOUNTED FOR IN THEORETICAL MASS FLOW BY IDEALIZED FLOW ASSUMPTIONS

The major reasons that $q_{m_{ti}}$ and $q_{m_{tc}}$ must be corrected by the discharge coefficient to achieve accurate measurement are as follows:

(a) The minimum cross section of the flow stream (location of minimum pressure) may not coincide with the bore or throat area. This is particularly true for orifices.

(b) P_2 varies with pressure-tap location. The correction to actual flow depends on pressure tap location.

(c) All static pressure taps exhibit an error in static pressure measurement.

(d) Velocity profiles are not uniform.

(e) No flow is frictionless or reversible.

3-7 DISCHARGE COEFFICIENT, *C*, IN THE INCOMPRESSIBLE FLUID EQUATION

(a) To correct errors introduced by the idealized flow assumptions in the incompressible fluid equation, the discharge coefficient, C, is introduced and defined as

$$C = \frac{q_{m_i}}{q_{m_{ti}}} \quad (3\text{-}7\text{-}1)$$

In most cases, when the differential pressure meters are calibrated to determine C over a range of flows, water is used and the static weight/time technique is used to determine q_{m_i}. Depending on the required uncertainty, however, flow calibration may be performed using a second calibrated flowmeter (secondary flow standard). When a Performance Test Code uncertainty requirement permits, flow calibration may also be performed using gas as the flowing fluid. The introduction of the gas expansion factor may render this type of calibration less accurate. In any case, a series of q_{m_i} versus ΔP data is obtained during calibration, and, with $q_{m_{ti}}$ defined by the hydraulic equation [eq. (3-4-2)], C can be written as follows:

$$C = \frac{q_{m_i}}{\frac{\pi}{4} d^2 \frac{1}{\sqrt{1-\beta^4}} \sqrt{2\rho(\Delta P) g_c}} \quad (3\text{-}7\text{-}2)$$

(b) For geometrically similar meters, C is a function of bore or pipe Reynolds number (Re) only and can be derived from dimensional analysis. Calibration data of geometrically similar meters are extremely repeatable, provided the meters are manufactured and installed in strict accordance with Sections 4, 5, and 6, including dimensions, tolerances, and required straight length and/or flow-conditioning.

(c) Because the discharge coefficient is a function of bore or throat Re only, a water calibration of a given differential pressure device is applicable for any measured fluid without loss of accuracy. This includes gases, provided the corrections detailed in subsections 3-8 and 3-9 are made. Similarly, a differential pressure device that has been calibrated with gas can be used to measure liquid.

3-8 DISCHARGE COEFFICIENT, C, AND THE EXPANSION FACTOR, ε, FOR GASES

For gases, the flow equation is further modified by the expansion correction factor, ϵ, to account for the effects of compressibility. For a given flowmeter calibrated using liquid

$$\varepsilon = \frac{q_{m_c}}{q_{m_i}} = \frac{q_{m_c}}{\frac{\pi}{4} d^2 C \frac{1}{\sqrt{1-\beta^4}} \sqrt{2\rho(\Delta P) g_C}} \tag{3-8-1}$$

A water calibration to determine C versus Re for a differential pressure meter can therefore be used to measure flow of a gas.

3-9 CALCULATION OF EXPANSION FACTOR, ε

(a) The expansion factor for nozzles and venturi tubes, with density determined at the upstream pressure tap, has been derived [see eq. (3-5-4)].

$$\varepsilon_1 = \left[r^{2/\kappa} \left(\frac{\kappa}{\kappa - 1} \right) \left(\frac{1 - r^{\frac{\kappa-1}{\kappa}}}{1 - r} \right) \left(\frac{1 - \beta^4}{1 - \beta^4 r^{\frac{2}{\kappa}}} \right) \right]^{0.5} \tag{3-9-1}$$

Equation (3-9-1) is valid for any gas or vapor for which κ is known.

(b) For orifices, abrupt radial as well as axial expansions take place, and the analytical derivation of eq. (3-9-1) is invalid. Based on the data, the static pressure measurement is obtained on the upstream side of the orifice, then

$$\varepsilon_1 = 1 - (0.351 + 0.256\beta^4 + 0.93\beta^8) \left[1 - \left(\frac{P_2}{P_1} \right)^{\frac{1}{\kappa}} \right] \tag{3-9-2}$$

(c) Equation (3-9-2) has been validated experimentally for air, natural gas, and steam only. However, it may also be used for any gas or vapor for which κ is known.

(d) Equations (3-9-1) and (3-9-2) are valid only for cases where $P_2/P_1 \geq 0.8$. To avoid Mach number effects, differential pressure meters must not be sized for compressible fluids such that the pressure ratio is lower than 0.8.

(e) Temperature is measured downstream of the meter to avoid disturbing the flow profile. Static pressure is usually measured at the upstream tap. Temperature at the upstream tap, T_1, can be calculated using eq. (3-5-1) and the relationship $\Delta P = P_1 - P_2$. In most cases, T_1 may be assumed equal to the downstream tap, T_2. Rigorous calculation should be performed if uncertainties introduced by this assumption are larger than the uncertainties introduced by the measurement of P_2, T_2, and ΔP, which is very rare.

(f) When the general equation is used for incompressible or liquid flows, $\varepsilon \equiv 1.0$.

3-10 DETERMINING DISCHARGE COEFFICIENT FOR DIFFERENTIAL PRESSURE CLASS METERS

(a) It follows from subsections 3-7 through 3-9 that, for each type of differential pressure meter specified herein

$$C = C(\text{Re},\ \beta,\ D) \tag{3-10-1}$$

The relationships of C versus Re are available for each type of meter described in Sections 4 and 5 over the range of specified sizes and Reynolds numbers. These are based on the repeatable results of thousands of hydraulic laboratory calibrations of differential pressure meters of like type and size. Sections 4 and 5 give the empirical C versus Re relationship, along with the concomitant uncertainty of C, for each type of differential pressure meter.

(b) Some PTC tests may allow the use of the empirical formulations for discharge coefficient for certain measurements when uncertainty requirements are met. For some critical test measurements, the test code may require a laboratory calibration of a specified differential pressure meter to determine the specific C versus Re relationship for that meter to meet uncertainty requirements. Laboratory calibration serves as a check that the meter was fabricated correctly and the specified laboratory-determined calibration curve of C versus Re reduces the uncertainty of C.

(c) When a differential pressure meter is calibrated in a meter testing laboratory to determine the C versus Re relationship for that specific meter, the entire flow-metering section must be tested. This includes the upstream and downstream piping, manufactured such that the metering section meets the straight length and other dimensional requirements of Section 6. Without the upstream and downstream piping, the calibration is only for the primary element. A positive,

mechanical alignment method shall be in place to replicate the precise position of the metering primary element within the assembly when it was calibrated. The flowmetering section must remain free from dirt and moisture for shipping and storage. Whenever possible, the flow section should be shipped as one piece, not disassembled for shipping or installation.

3-11 THERMAL EXPANSION/CONTRACTION OF INLET SECTION AND PRIMARY ELEMENT

(a) In actual flow conditions, both d and D change from the measured values in the factory or laboratory because of thermal expansion or contraction. This occurs when the flowing fluid is at a temperature different from that at which the primary element and the inlet section were measured.

$$d_{\text{actual}} = d_{\text{meas}} + \alpha_{PE} d_{\text{meas}} (T - T_{\text{meas}}) \tag{3-11-1}$$

$$D_{\text{actual}} = D_{\text{meas}} + \alpha_{P} D_{\text{meas}} (T - T_{\text{meas}}) \tag{3-11-2}$$

$$\beta_{\text{actual}} = \frac{d_{\text{actual}}}{D_{\text{actual}}} \tag{3-11-3}$$

(b) The actual values of d, D, and β are used to calculate q_m to account for thermal expansion or contraction. It is assumed that the flow element and inlet section are at the same temperature as the flowing fluid. Either T_1 or T_2 may be used.

(c) For uncalibrated devices, 20°C (68°F) may be assumed if T_{meas} is unknown. For calibrated devices, T_{meas} is the fluid temperature of the calibration liquid if the calibration data were not corrected to standard temperature.

3-12 SELECTION AND RECOMMENDED USE OF DIFFERENTIAL PRESSURE CLASS METERS

The major considerations when selecting a differential pressure class meter are outlined herein.

3-12.1 Beta, Pipe Size, and Reynolds Number

Each meter described in Sections 4 and 5 has limiting values for β, pipe size, and Reynolds number. In selecting and sizing a meter, care must be taken to stay within these limits. For example, if the chosen value of differential pressure for the design or expected flow in the sizing of an orifice results in a calculated β that exceeds the prescribed limits, it might be necessary to use a flow nozzle or venturi. Both devices have a higher capacity for the same size. Discharge coefficients for nozzles and venturi-metering runs are in the order of 1.0 compared to typical discharge coefficients of orifices in the order of 0.6.

In some cases, when the flow section diameter is different from that of the adjacent process pipe, pipe expanders or reducers can be used at the ends of the flow section. This is permissible provided the flow section, both upstream and downstream of the primary element, is of adequate length as prescribed in Section 6.

3-12.2 Uncertainty

The systematic uncertainty of the empirical formulation of the discharge coefficient and the expansion factor in the general equation is given for each device in Sections 4 and 5 only if it is manufactured, installed, and used as specified herein. The results are summarized in Table 3-12.2-1 for uncalibrated meters. Detailed calculation of overall uncertainty in flow measurement by differential pressure meters is discussed in Section 4. The uncertainty of the discharge coefficient is usually by far the most significant component of flow-measuring uncertainty, assuming that process and differential pressure instrumentation are satisfactory.

Qualified meter testing laboratories can achieve uncertainties of less than 0.10% for water calibrations and of 0.25% for gas calibrations. Consult the laboratory to obtain the value of the actual uncertainty. Accreditation to a standard such as ISO/IEC 17025 should be used to assess laboratory qualifications and uncertainty.

Differential-producing flowmeters have an inherent discharge coefficient that can be determined by calibration to reduce the meter's uncertainty. In addition, the total measurement uncertainty of the flow through a meter includes the uncertainty of fluid density, pressure, temperature, and differential-pressure as well as of the secondary instrumentation required to measure these values (see Section 4).

During calibration, the flows should encompass the actual operating conditions (often, this is the Reynolds number range) of the meter, and the caveats of para. 3-10(c) should be met. Laboratory calibrations, by practice, often provide ideal installation conditions during the meter calibration.

Table 3-12.2-1
Uncertainty of Discharge Coefficient, C, (Uncalibrated) and Expansion Factor, ε

	Limiting Values				
Flow Element	**Re_D, Re_d [Note (1)]**	**β**	**D, d, mm (in.) [Note (2)]**	**Uncertainty of Discharge Coefficient, C**	**Uncertainty of Expansion Factor, ε**
Flange tap orifice	$Re_D \geq 5\,000$ or $Re_D \geq 170\beta^2 D$ (D, mm) [$Re_D \geq 4\,318\beta^2 D$ (D, in.)] [Note (3)]	$0.2 \leq \beta \leq 0.6$ $0.6 \leq \beta \leq 0.70$ [Note (4)]	50 (2) $\leq D \leq$ 1 000 (40) $d \geq$ 12.5 (0.5) [Note (5)]	0.5%: $0.2 \leq \beta \leq 0.6$ $(1.667\beta - 0.5)$%: $0.6 \leq \beta \leq 0.70$	$3.5\frac{\Delta P}{\kappa P_1}$%
Corner tap orifice	$Re_D \geq 5\,000$: $0.2 \leq \beta \leq 0.56$ $Re_D \geq 16\,000\beta^2$: $\beta > 0.56$ [Note (3)]	$0.2 \leq \beta \leq 0.6$ $0.6 \leq \beta \leq 0.70$ [Note (4)]	50 (2) $\leq D \leq$ 1 000 (40) $d \geq$ 12.5 (0.5) [Note (5)]	0.5%: $0.2 \leq \beta \leq 0.6$ $(1.667\beta - 0.5)$%: $0.6 \leq \beta \leq 0.70$	$3.5\frac{\Delta P}{\kappa P_1}$%
Wall tap flow nozzle, low β	$10\,000 \leq Re_d \leq 20\,000\,000$	Low β: $0.2 \leq \beta \leq 0.5$	$D <$ 100 (4)	2%	$2\frac{\Delta P}{P_1}$%
Wall tap flow nozzle, high β	$10\,000 \leq Re_d \leq 20\,000\,000$	High β: $0.45 \leq \beta \leq 0.8$	$D <$ 100 (4)	2%	$2\frac{\Delta P}{P_1}$%
Wall tap flow nozzle, low β	$10\,000 \leq Re_d \leq 20\,000\,000$	Low β: $0.2 \leq \beta \leq 0.5$	100 (4) $\leq D \leq$ 1 300 (50)	1%	$2\frac{\Delta P}{P_1}$%
Wall tap flow nozzle, high β	$10\,000 \leq Re_d \leq 20\,000\,000$	High β: $0.45 \leq \beta \leq 0.8$	100 (4) $\leq D \leq$ 1 300 (50)	1%	$2\frac{\Delta P}{P_1}$%
Throat tap flow nozzle, low β	$Re_d \geq 1\,000\,000$	$0.25 \leq \beta \leq 0.5$	100 (4) $\leq D \leq$ 600 (24)	0.7%	$2\frac{\Delta P}{P_1}$%
Machined venturi	$200\,000 \leq Re_d \leq 17\,000\,000$	$0.3 \leq \beta \leq 0.75$	50 (2) $\leq D \leq$ 1 200 (48)	1%	$(4 + 100\beta^8)\frac{\Delta P}{P_1}$%
Fabricated venturi	$200\,000 \leq Re_d \leq 17\,000\,000$	$0.3 \leq \beta \leq 0.75$	100 (2) $\leq D \leq$ 1 200 (48)	1.5%	$(4 + 100\beta^8)\frac{\Delta P}{P_1}$%

NOTES:
(1) Re_D is Reynolds number based on the inlet (pipe) diameter, and Re_d is Reynolds number based on the bore (throat) diameter.
(2) D is the inlet diameter in millimeters (inches), d is the bore (throat) diameter in millimeters (inches).
(3) For the orifice with flange taps, the greater of $Re_D \geq 5\,000$ and $Re_D \geq 170\beta^2 D$ (D, mm) [$Re_D \geq 4318\beta^2 D$ (D, in.)] is the lower limit.
(4) For the orifice, where $\beta > 0.5$ and $Re_D < 10\,000$, then 0.5% must be added to the uncertainties of C shown in this table.
(5) For the orifice, if $D <$ 71.12 mm (2.8 in.), then the following must be added to the uncertainties of C shown in this table:

$0.9(0.75 - \beta)\left(2.8 - \frac{D}{25.4}\right)$% if D is in millimeters or 0.9 (0.75 − β) (2.8 − D)% if D is in inches.

Actual site installation, however, may not provide ideal pipe conditions. As such, additional uncertainty due to "installation effect" shall be considered and combined with the laboratory uncertainty when estimating the total uncertainty of the meter performance once installed for use. If the operating conditions of the meter cannot be achieved during the laboratory calibration, means of extrapolating the calibration results shall be agreed upon by all parties involved in the test. See Mandatory Appendix I for recommended methods of extrapolation.

3-12.3 Unrecoverable Pressure Loss

The unrecoverable pressure loss caused by the primary element is significantly less for venturi tubes or throat tap-flow nozzles with a diffuser section than for wall tap nozzles or orifice metering runs because of the diffuser section. Orifices have the highest unrecoverable pressure loss relative to devices of the same β and inlet diameter. For comparison, the unrecoverable pressure loss versus beta ratio is shown in Figure 3-12.3-1. The equations to calculate these losses for each device are given in Sections 4 and 5.

3-12.4 Specified Installations

To meet the uncertainties listed in Table 3-12.2-1, the meter must be installed in accordance with the requirements of Section 6. Orientation of the differential pressure taps should also be considered.

3-13 RESTRICTIONS OF USE

The following restrictions must be met for proper use of these meters:

(a) The flowmeter, flow section, pressure taps, and connecting tubing must be manufactured, installed, and used in strict accordance with the specifications herein.

(b) The pipe must be flowing full.

(c) The flow must be steady or changing very slowly as a function of time. Pulsations in the flow must be small compared with the total flow rate. The frequency of collecting data must cover several periods of unsteady flow. Refer to Nonmandatory Appendix A on pulsating flow.

(d) If the fluid does not remain in a single phase while passing through the meter, or if it has two phases when entering the meter, then it is beyond the scope of differential class meters in this Supplement.

(e) If the fluid contains suspended particles, such as sand, flow measurement is beyond the scope of differential class meters in this Supplement.

(f) Gas flows must remain subsonic throughout the measuring section.

3-14 PROCEDURE FOR SIZING A DIFFERENTIAL PRESSURE CLASS METER

(a) When differential pressure class meters are being considered, they are sized to suit the user's needs. The adjacent pipe diameter of the metering run and the fluid conditions over the expected flow range are usually known.

(b) One method of sizing the meter is to assume that the inlet section diameter, D, of the metering run will be the same as that of the adjacent pipe and to select a differential pressure to correspond to the maximum expected flow. All terms in eq. (3-2-1) are known except C and d. Equation (3-2-1) may be used to solve for d. The equation may be solved by iteration or successive approximations or any other way that may produce similar results.

(c) It may be preferable to specify the size of the meter, such as that corresponding to a β of 0.6 for an orifice metering run (e.g., to optimize accuracy while minimizing pressure loss). All terms in eq. (3-2-1) are then known except for differential pressure, which should be calculated by the user at maximum expected flow to ensure that the pressure ratio is within limits. To minimize errors associated with water legs, zero setting, and differential pressure measurement, the meter should be sized for a minimum differential pressure of 0.025 MPa [3.61 psi or 100 in. H_2O (68°F)] at the performance test conditions.

(d) The user must be careful when sizing a differential pressure class meter to ensure that the calculated β, d, and Reynolds number are within the specified ranges for each meter, as described in Sections 4 and 5. If any limitations are exceeded, then either a different size of the same meter type (d, D, or both) must be used or a different type of differential pressure class meter should be evaluated for the application. The recommended straight lengths in Section 6 should be considered when sizing the meter.

Figure 3-12.3-1
Unrecoverable Pressure Loss Versus Beta Ratio

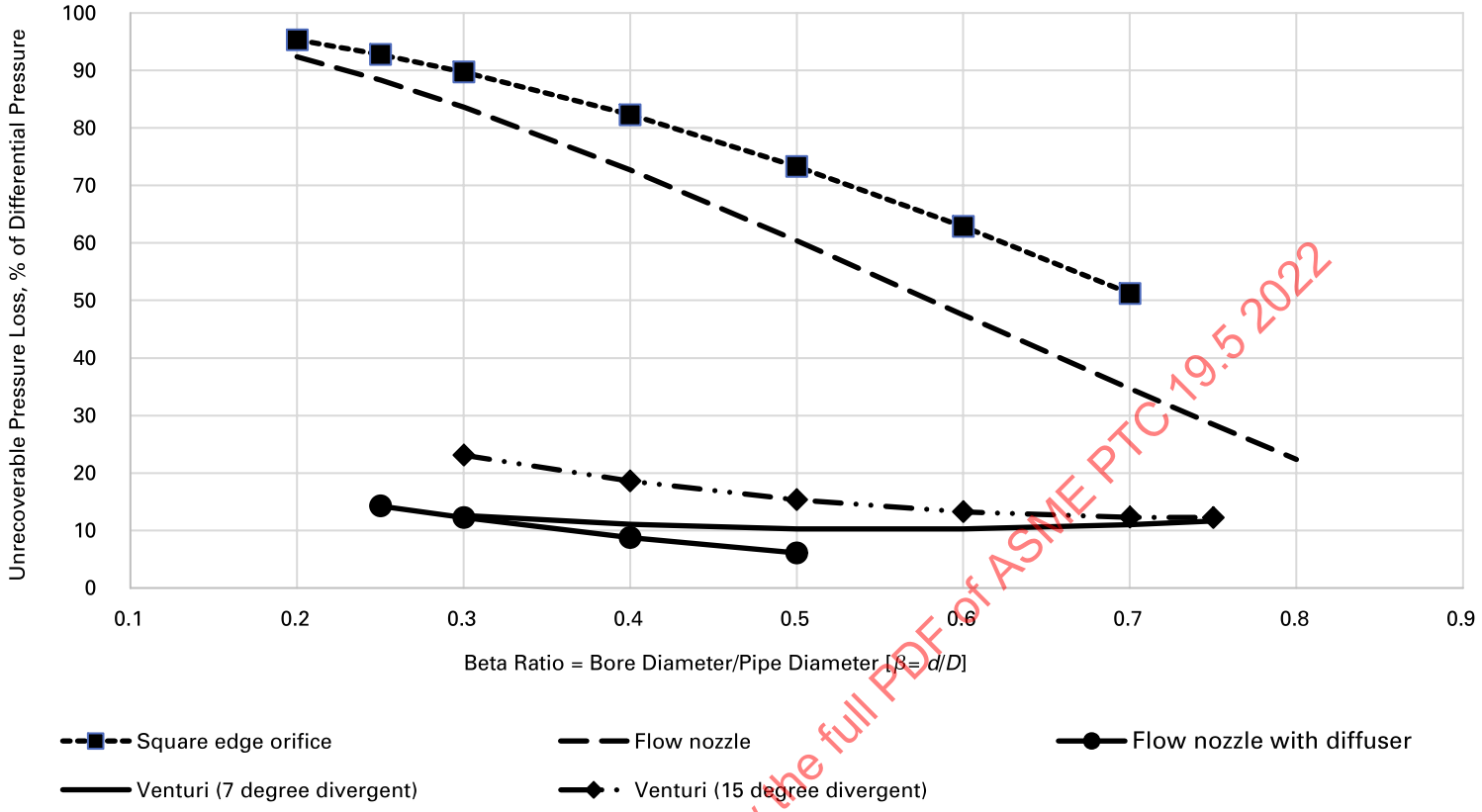

3-15 FLOW CALCULATION PROCEDURE

(a) Equation (3-2-1) is used for all differential pressure class meters and is valid for both liquid and subsonic gas flow measurement.

(b) For gas flows, ε_1 is given by eq. (3-9-1) for flow nozzles and venturi tubes and eq. (3-9-2) for orifice plates. For liquid flows, $\varepsilon_1 \equiv 1.0$.

(c) Per subsection 3-11, d and D are corrected to the fluid temperature of the measurement.

(d) The applicable fluid density is determined from pressure and temperature measurements and, if the fluid is a mixture, such as natural gas, analysis of the constituents. Determine fluid viscosity to calculate the Reynolds number. See Section 2 for references on such properties.

(e) All quantities in the general eq. (3-2-1), except the discharge coefficient, C, are known once (b) through (d) have been completed. Because C depends on Reynolds number, which itself depends on flow, eq. (3-2-1) can be solved by iterative methods.

(f) If the iteration method is used, this process is continued until the difference between successive calculated flows is less than 2% of the estimated uncertainty of the measurement. For example, if the estimated uncertainty is 1.0%, the successive iterations must be within 0.02% of each other.

3-16 SAMPLE CALCULATION

A sample calculation of flow through an orifice metering section, which is not calibrated in a meter testing and given the appropriate process measurements and fluid constituent analysis, is shown for natural gas. The expected systematic component of uncertainty in the flow measurement is 0.7%.

All fluid properties, materials properties, and procedures for calculation of fluid properties of mixtures are taken from the references in this Section and in Section 2.

This example uses the successive iteration method to solve for flow.

(a) Orifice Data

D_{meas} = 202.72 mm (7.981 in.)
d_{meas} = 120.75 mm (4.754 in.)
T_{meas} = 20°C (68°F)
Taps: flange type
Orifice material: 316 stainless steel
Flange material: carbon steel
Static pressure at the upstream side of the plate: 2.01914 MPa (292.85 psia)
Temperature at the downstream side of the plate: 11.978°C (53.56°F)
Differential pressure: 9.7257 kPa (1.4106 psi)
For natural gas analysis, see Table 3-16-1.

Table 3-16-1
Natural Gas Analysis

Constituents	Mole Percent, %	Molar Mass
Nitrogen	0.6563	28.0134
Carbon dioxide	0.7696	44.0100
Methane	96.0333	16.0430
Ethane	1.9658	30.0430
Propane	0.3283	44.0970
N-butane	0.0700	58.1230
Isobutane	0.0700	58.1230
N-pentane	0.0300	72.1500
Isopentane	0.0400	72.1500
N-hexane	0.0367	86.1770
	100.00	Molecular weight = 16.828 kg/kmol

(b) Temperature at the Upstream Side. Temperature at the upstream side of the orifice can usually be assumed to be equal to the temperature at the downstream side without significant loss of accuracy. For an orifice, an isenthalpic expansion is a better representation of the thermodynamic process than an isentropic process, which would be more appropriate for a flow nozzle. Assuming a pressure recovery of about 40%, [ΔP to downstream thermowell is equivalent to (1 − 0.4)(9.7257 kPa) = 5.835 kPa], the downstream pressure is 2.0133 MPa (292.00 psia) and the enthalpy is 831.75 kJ/kg (357.59 Btu/lbm) for the natural gas mixture at the downstream temperature of 11.978°C (53.56°F). The upstream temperature determined at this same enthalpy at 2.01914 MPa (292.85 psia) is 12.006°C (53.61°F). The estimated temperature difference is insignificant at 0.01% on an absolute basis. The downstream temperature will therefore be used as the upstream temperature for the remainder of this example.

(c) Fluid Properties. These properties are obtained from the constituent analysis using NIST REFPROP at 11.978°C (53.56°F), 11.978°C (292.85 psia).

ρ = 14.98889 kg/m^3 (0.935726 lbm/ft^3)
μ = 1.1002 E−05 Pa·s [7.393 E−06 lbm/(ft-sec)]
κ = 1.3708

(d) Thermal Expansion Coefficients of Materials. At the temperature of the flowing fluid
α_{PE} = 15.231 E−06 mm/mm-°C (8.4589 E−06 in./in.-°F)
α_P = 11.454 E−06 mm/mm-°C (6.3726 E−06 in./in.-°F)

(e) Calculation of d, D, and β.

(1) From eq. (3-11-1),

$$d_{actual} = d_{meas} + \alpha_{PE} d_{meas}(T - T_{meas})$$

(SI Units)

$$d_{actual} = 120.75 + (15.231\,E{-}06)(120.75)(11.978 - 20) = 120.7353\ mm \quad (3\text{-}16\text{-}1)$$

(U.S. Customary Units)

$$d_{actual} = 4.754 + (8.4589\,E{-}06)(4.754)(53.56 - 68) = 4.7534\ in.$$

(2) From eq. (3-11-2),

$$D_{actual} = D_{meas} + \alpha_P D_{meas}(T - T_{meas})$$

(SI Units)

$$D_{actual} = 202.72 + (11.454\,E{-}06)(202.72)(11.978 - 20) = 202.7\ mm \quad (3\text{-}16\text{-}2)$$

(U.S. Customary Units)

$$D_{actual} = 7.981 + (6.3726\,E{-}06)(7.981)(53.56 - 68) = 7.9803\ in.$$

(3) From eq. (3-11-3),

$$\beta_{actual} = d_{actual}/D_{actual}$$

(SI Units)

$$\beta_{actual} = 120.7353/202.7 = 0.59564 \quad (3\text{-}16\text{-}3)$$

(U.S. Customary Units)

$$\beta_{actual} = 4.7534/7.9803 = 0.59564$$

Note that at flowing temperatures close to 20ºC (68°F), the diameters are fundamentally unchanged when corrected to flowing temperature. Correction for geometry changes of higher temperature flows, such as for steam, can be far more significant.

(f) Expansion Factor. From eq. (3-9-2),

$$\varepsilon_1 = 1 - (0.351 + 0.256\beta^4 + 0.93\beta^8)\left[1 - \left(\frac{P_2}{P_1}\right)^{\frac{1}{\kappa}}\right]$$

(SI Units)

$$\varepsilon_1 = 1 - \left[0.351 + 0.256(0.59564)^4 + 0.93(0.59564)^8\right] \times \left[1 - \left(\frac{2.01914 - 9.7257\ \text{E}-03}{2.01914}\right)^{\frac{1}{1.3708}}\right] \quad (3\text{-}16\text{-}4)$$

$$\varepsilon_1 = 0.99860$$

(U.S. Customary Units)

$$\varepsilon_1 = 1 - \left[0.351 + 0.256(0.59564)^4 + 0.93(0.59564)^8\right] \times \left[1 - \left(\frac{292.85 - 1.4106}{292.85}\right)^{\frac{1}{1.3708}}\right]$$

$$\varepsilon_1 = 0.99860$$

(g) Iterations. All terms in the general eq. (3-2-1) are now known except for the discharge coefficient. It is solved for iteratively. Equation (3-2-1) is repeated for convenience.

$$q_m = n\frac{\pi}{4}d^2 C\varepsilon\sqrt{\frac{2\rho(\Delta P)g_c}{1-\beta^4}}$$

(SI Units)

$$q_m = 1.0\frac{\pi}{4}(120.7353\,\text{E}-3)^2 C\,(0.99860) \times \frac{2(14.98889)(9.7257\,\text{E}+03)(1.0)}{1-(0.59564)^4} \quad (3\text{-}16\text{-}5)$$

$$q_m = 6.602723C$$

(U.S. Customary Units)

$$q_m = 300.0\frac{\pi}{4}(4.7534)^2 C\,(0.99860) \times \sqrt{\frac{2(0.935726)(1.4106)(32.1740486)}{1-(0.59564)^4}}$$

$$q_m = 52{,}404C$$

(1) Iteration 1. For the first iteration, assume $C = 0.60000$.

(SI Units)

$$q_m(\text{iteration 1}) = (6.602723)(0.60000) \quad (3\text{-}16\text{-}6)$$

$$q_m = 3.961634\ \text{kg/s}$$

(U.S. Customary Units)

$$q_m(\text{iteration 1}) = (52{,}404)(0.6)$$

$$q_m = 31{,}442\ \text{lbm/hr}$$

When D is in millimeters, the Reynolds number equation must be multiplied by 1/1,000 to convert D to meters as shown below.

(SI Units)

$$Re_D = \frac{\rho V}{\mu}\frac{D}{1\,000} = \frac{4\,000 q_m}{\mu \pi D} \tag{3-16-7}$$

When D is in inches, the Reynolds number equation must be multiplied by 1/12 to convert D to feet as shown below.

(U.S. Customary Units)

$$Re_D = \frac{\rho V}{\mu}\frac{D}{12} = \frac{q_m}{75 \mu \pi D}$$

From eqs. (3-16-2), (3-16-5), (3-16-6), and (3-16-7),

(SI Units)

$$\begin{aligned} Re_D(\text{iteration 1}) &= \frac{4\,000(3.961634)}{(1.1002\,\text{E}{-}05)\pi(202.7)} \\ &= 2\,261\,830 \end{aligned} \tag{3-16-8}$$

(U.S. Customary Units)

$$\begin{aligned} Re_D(\text{iteration 1}) &= \frac{31{,}442}{75(7.393\,\text{E}{-}06)\pi(7.9803)} \\ &= 2{,}261{,}830 \end{aligned}$$

(2) Iteration 2. Discharge coefficient is a function of metering geometry and Reynolds number. Equation (4-9-1) is applicable and is given for convenience. (See Section 4 for empirical equations for discharge coefficients for orifice meters.)

(SI Units)

$$\begin{aligned} C = {} & 0.5961 + 0.0261\beta^2 - 0.216\beta^8 + 0.000521\left(\frac{10^6\beta}{\text{Re}_D}\right)^{0.7} + \left[0.0188 + 0.0063\left(\frac{19\,000\beta}{\text{Re}_D}\right)^{0.8}\right]\beta^{3.5}\left(\frac{10^6}{\text{Re}_D}\right)^{0.3} \\ & + \left[0.043 + 0.080e^{-10\left(\frac{25.4}{D}\right)} - 0.123e^{-7\left(\frac{25.4}{D}\right)}\right]\left[1 - 0.11\left(\frac{19\,000\beta}{\text{Re}_D}\right)^{0.8}\right] \\ & \times \frac{\beta^4}{1-\beta^4} - 0.031\left\{\frac{2\left(\frac{25.4}{D}\right)}{(1-\beta)} - 0.8\left[\frac{2\left(\frac{25.4}{D}\right)}{(1-\beta)}\right]^{1.1}\right\}\beta^{1.3} \end{aligned} \tag{3-16-9}$$

(U.S. Customary Units)

$$\begin{aligned} C = {} & 0.5961 + 0.0261\beta^2 - 0.216\beta^8 + 0.000521\left(\frac{10^6\beta}{\text{Re}_D}\right)^{0.7} + \left[0.0188 + 0.0063\left(\frac{19{,}000\beta}{\text{Re}_D}\right)^{0.8}\right]\beta^{3.5}\left(\frac{10^6}{\text{Re}_D}\right)^{0.3} \\ & + \left(0.043 + 0.080e^{-10\left(\frac{1}{D}\right)} - 0.123e^{-7\left(\frac{1}{D}\right)}\right) \times \left[1 - 0.11\left(\frac{19{,}000\beta}{\text{Re}_D}\right)^{0.8}\right]\frac{\beta^4}{1-\beta^4} \\ & - 0.031\left\{\frac{2\left(\frac{1}{D}\right)}{(1-\beta)} - 0.8\left[\frac{2\left(\frac{1}{D}\right)}{(1-\beta)}\right]^{1.1}\right\}\beta^{1.3} \end{aligned}$$

From eqs. (3-16-2), (3-16-3), (3-16-7), (3-16-8), and (3-16-9), C is calculated for iteration 2.

$$C(\text{iteration 2}) = 0.60434$$

Note that the difference [(0.60434 – 0.60000)/0.60000] is equal to 0.72%. By the criteria of para. 3-15(f), this is far too large and another iteration is clearly required.

With uncertainty requirements in the flow of 0.5%, convergence must be within 2% of 0.5%, or within 0.01%.

From eq. (3-16-5), the corresponding flow to C (iteration 2) is

(SI Units)

$$\begin{aligned} q_m(\text{iteration 2}) &= 6.602723C \\ &= (6.602723)(0.60434) \\ &= 3.990300\ \text{kg/s} \end{aligned} \tag{3-16-10}$$

(U.S. Customary Units)

$$\begin{aligned} q_m(\text{iteration 2}) &= 52{,}404\ \text{C} = (52\,404)(0.60434) \\ &= 31{,}670\ \text{lbm/hr} \end{aligned}$$

From eq. (3-16-7), the corresponding Reynolds number is

(SI Units)

$$\begin{aligned} \text{Re}_D(\text{iteration 2}) &= \frac{4\,000(3.990\,300)}{(1.1002\,\text{E}{-}05)\pi(202.7)} \\ &= 2\,278\,200 \end{aligned} \tag{3-16-11}$$

(U.S. Customary Units)

$$\text{Re}_D(\text{iteration 3}) = \frac{31{,}670}{75(7.393)10^{-6}\pi(7.9803)} = 2{,}278{,}200$$

NOTE: See also eq. (3-16-8)

(3) From the values of q_m and Re_D calculated from eqs. (3-16-9) through (3-16-11), C is calculated as

$$C\ (\text{iteration 3}) = 0.60433$$

The discharge coefficient, and therefore the mass flow, have converged within the 0.01% criterion based on the difference calculation |(0.60433 – 0.60434)/0.60434| equal to 0.0017%. Thus, the calculated flow is 3.990300 kg/s (31,670 lbm/hr).

(h) Notes on Sample Calculation. In the sample calculation, eq. (3-16-9) shows that the discharge coefficient is a very weak function of Reynolds number, which is why so few iterations are required for convergence.

3-17 REFERENCES

ASTM D 1945-96E1. Standard Test Method for Analysis of Natural Gas by Gas Chromatography. American Society for Testing and Materials.

ASTM D 3588. Standard Practice for Calculating Heat Value, Compressibility Factor, and Relative Density of Gaseous Fuels. American Society for Testing and Materials.

ASME MFC-3M–2004 (R2017). Measurement of Fluid Flow in Pipes Using Orifice, Nozzle, and Venturi. The American Society of Mechanical Engineers.

ASME MFC-3Ma–2007. Addenda to ASME MFC-3M–2004, Measurement of Fluid Flow in Pipes Using Orifice, Nozzle, and Venturi. The American Society of Mechanical Engineers.

Bean, H. S., ed. (1971). Fluid Meters: Their Theory and Application (6th ed.) The American Society of Mechanical Engineers.

Benedict, R. P. (1980). Fundamentals of Pipe Flow. John Wiley and Sons.

Benedict, R. P. (1977). Fundamentals of Temperature, Pressure, and Flow Measurements (2nd ed.). John Wiley and Sons.

ISO 5167-1:1991. Measurement of fluid flow by means of pressure differential devices — Part 1: Orifice plates, nozzles, and Venturi tubes inserted in circular cross-section conduits running full. International Organization for Standardization.

ISO 5167-1/AMD1:1998. Measurement of fluid flow by means of pressure differential devices — Part 1: Orifice plates, nozzles, and Venturi tubes inserted in circular cross-section conduits running full —Amendment 1. International Organization for Standardization.

ISO/IEC 17025:2017. General requirements for the competence of testing and calibration laboratories. International Organization for Standardization.

Lemmon, E., Huber, M., and McLinden, M. (2013). NIST Standard Reference Database 23: Reference Fluid Thermodynamic and Transport Properties-REFPROP, Version 9.1, Nat'l Std. Ref. Data Series. National Institute of Standards and Technology.

Sabersky, R. H., Acosta, A. J., and Hauptmann, E. G. (1971). Fluid Flow, a First Course in Fluid Mechanics (2nd ed.). Macmillan.

Shapiro, A. H. (1953). The Dynamics and Thermodynamics of Compressible Fluid Flow. Ronald Press.

Starling, K. E., and AGA Transmission Measurement Committee (1985). Compressibility and Supercompressibility for Natural Gas and Other Hydrocarbon Gases: A. G. A. Transmission Committee Report No. 8. American Gas Association.

Section 4
Orifice Meters

4-1 NOMENCLATURE

Symbols used in this Section are included in Tables 2-3-1 and 3-1-1.

4-2 INTRODUCTION

This type of differential pressure class meter consists of a flat plate that is thin relative to the diameter of the flow section. The diameter, d, in the general equation for mass flow [see eq. (3-2-1)] has been bored through it precisely and the upstream edges of the meter that are exposed to flow must be sharp. The primary element is, therefore, referred to as a thin-plate, square-edged orifice.

4-3 TYPES OF THIN-PLATE, SQUARE-EDGED ORIFICES

Thin-plate, square-edged orifices are classified based on the locations of their differential pressure taps.

Two types of tap geometries are recommended by this Supplement for orifice meters used in ASME performance tests

(a) flange taps

(b) corner taps

Pressure tap locations for flange taps are given by the measured distance from the centerline of the upstream pressure tap to the upstream face A and from the centerline of the downstream pressure tap to the downstream face B of the orifice plate (see Figure 4-7-1). The thickness of the gaskets or other sealing material is included in the given dimension.

In a corner tap arrangement, the pressure holes open in the corner are formed by the pipe wall, the face of the flanges, or by the orifice plate and carrier ring (see Figure 4-7-2).

4-4 CODE COMPLIANCE REQUIREMENTS

Thin-plate, square-edged orifice metering runs must be manufactured and installed in accordance with this subsection and Section 6 to be in compliance with this Supplement. Flow measurement accuracy is affected by

(a) thermal expansion and pressure-induced distortion affecting orifice geometry

(b) orifice plate dimensions and construction

(c) orifice bore concentricity to the pipe

(d) location of temperature and static pressure measurements

(e) Reynolds number limitations

(f) pressure tap construction and geometry

(g) metering section requirements

(h) additional straight pipe length requirements and/or conditioner installation

This Section addresses (a) through (f). Compliance requirements for (g) and (h) are discussed in Section 6.

4-5 MULTIPLE SETS OF DIFFERENTIAL PRESSURE TAPS

At least two sets of differential pressure taps separated by 90 deg or 180 deg are required. When installed horizontally, the connecting tubing must meet the recommended slope as indicated in ASME MFC-8M. Care should be taken that the pressure taps do not become plugged; therefore, no tap should be located at the bottom. When measuring liquids, taps oriented vertically downward are more susceptible to being plugged by debris. Taps oriented vertically upward are susceptible to gas collection, introducing error in pressure measurement. Upward oriented taps are not preferred but may be used. Using multiple sets of taps may help to indicate orifice degradation caused by use, debris, or other irregularities.

Figure 4-6-1
Standard Orifice Plate

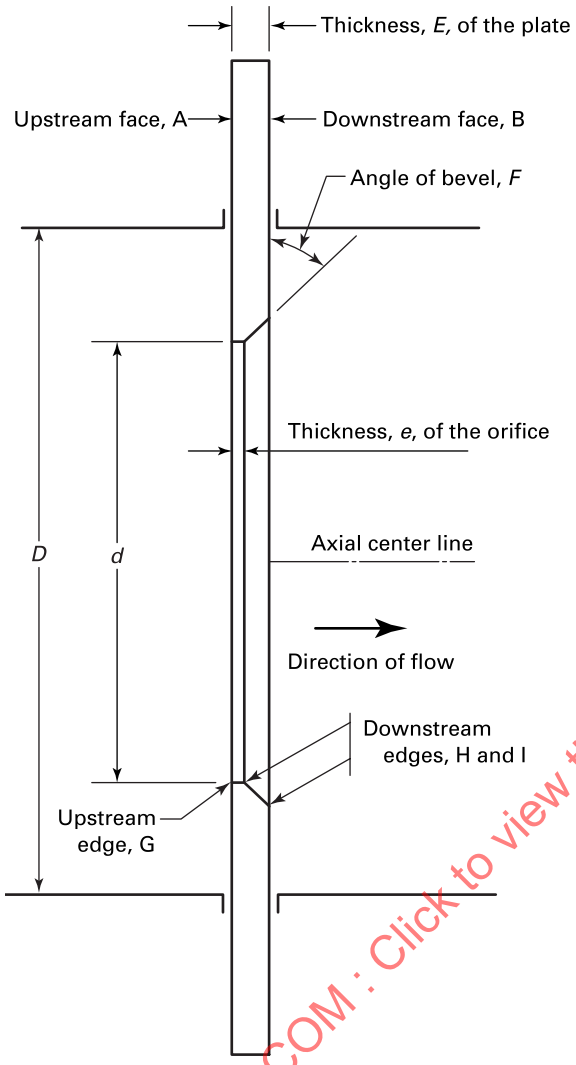

Two sets of differential pressure taps are required to achieve the lowest desired uncertainty. Differential pressure is measured at each set of taps. The flow calculation is done separately for each pair and averaged. If the meter is flow calibrated, then the discharge coefficient should be derived for each tap set and used in the flow calculation. Investigation is needed if the results differ from each tap set calculation by more than 0.2%.

4-6 MACHINING TOLERANCES, DIMENSIONS, AND MARKINGS FOR ORIFICE PLATE

Unless otherwise noted, all symbols for machining tolerances, dimensions, and markings for orifice plates in paras. 4-6.1 through 4-6.8 correspond to those in Figure 4-6-1.

4-6.1 Deflection and the Required Thickness, *E*, of Orifice Plate

Deflection of the orifice plate during flowing conditions is unavoidable (see Figure 4-6.1-1). The orifice thickness, E, shall be sufficient such that the total deflection, τ, is less than $0.01(D - d)/2$ (assuming the plate was perfectly flat with zero differential pressure applied). Table 4-6.1-1 provides the recommended thicknesses for nominal pipe sizes up to DN 600 (NPS 24) when the orifice plate is mounted with orifice flanges. Deflection calculations should be performed if the differential pressure, temperature, or orifice installation deviates from the conditions stated in the notes of Table 4-6.1-1.

Figure 4-6.1-1
Deflection of an Orifice Plate by Differential Pressure

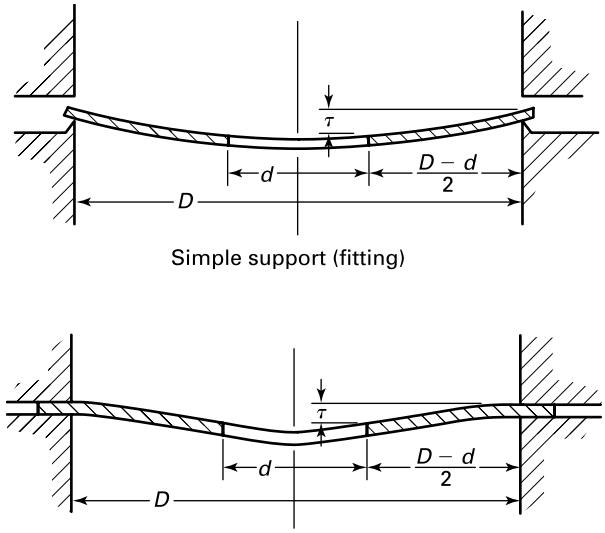

Table 4-6.1-1
Recommended Plate Thickness, *E*, for Stainless Steel Orifice Plate

Pipe Diameter	Nominal Plate Thickness, mm (in.)
DN ≤ 150 (NPS ≤ 6)	3.18 (0.125)
150 < DN ≤ 300 (6 < NPS ≤ 12)	6.35 (0.250)
300 < DN ≤ 500 (12 < NPS ≤ 20)	9.53 (0.375)
500 < DN ≤ 600 (20 < NPS ≤ 24)	12.7 (0.500)

GENERAL NOTES:
(a) The additional requirements of paras. 4-6.1 and 4-6.2 must be met.
(b) Nominal plate thicknesses are shown in millimeters (inches).
(c) Nominal plate thicknesses are shown in increments of 3.175 mm (0.125 in.), which are typical values.
(d) This Table is provided as a guideline for standard plate thicknesses when used with orifice flanges only. Orifice plates installed in orifice fittings or ring type joint (RTJ) holders may require thicker orifice plates for the same conditions.
(e) Thicknesses shown are based on a maximum differential pressure of 248 kPa (36 psi) at temperatures not exceeding 65.5°C (150°F).

The thickness, E, of the plate shall not exceed $0.05D$ except when 50 mm ≤ D ≤ 64 mm (2 in. ≤ D ≤ 2.5 in.), in which case an E value up to 3.18 mm (0.125 in.) is typically acceptable. The values of E measured at any point of the plate shall not differ by more than $0.001D$.

4-6.2 Upstream Face, *A*

With zero differential pressure applied, the plate upstream face, A, must be flat within $0.005(D - d)/2$. The orifice plate mounting shall have no significant distorting effect on the plate. Refer to para. 4-6.1 for additional requirements.

(a) The upstream face, A, within a circle whose diameter is not less than D and is concentric with the bore, must meet the following roughness criteria:

(1) for d ≤ 127 mm (5.0 in.), maximum roughness = 1.27 μm (50 μin.)

(2) for d > 127 mm (5.0 in.), maximum roughness is the lesser of $10^{-5}d$ and 2.54 μm (100 μin.)

(b) The orifice plate should include a tab that projects beyond the flanges. This tab or the perimeter of the plate itself, if feasible, shall be permanently marked on the upstream side with the following information:

(1) the measured bore diameter to four decimal places

(2) the measured upstream diameter to three decimal places if it is from the same supplier as the orifice plate

(3) the instrument or orifice identifying number

It is also suggested, but not mandatory, that the tab be marked with the plate thickness, E, and angle of bevel, even if that is zero.

4-6.3 Downstream Face, *B*

The downstream face, B, does not have to be machined to the same tolerances as the upstream face. The surface roughness of this face may be twice the value stated for the upstream face in para. 4-6.2. Imperfections smaller than 6 mm (0.25 in.) long and 0.5 mm (0.020 in.) deep are allowed on the downstream face; however, these imperfections shall not encroach on the edges H and I. Flatness and roughness can be judged acceptable by visual and tactile inspection.

4-6.4 Thickness, *e*, of the Orifice

The length of the cylindrical bore of the orifice, e, measured normal to the plane of the inlet face must be between $0.005D$ and $0.02D$. Any values of e measured around the bore shall not differ by more than $0.001D$. The inside surface of the orifice bore shall have no defects such as grooves, ridges, pits, or lumps visible to the naked eye.

4-6.5 Plate Thickness, *E*, and Bevel

If the thickness, E, of the orifice plate is greater than the thickness, e, of the orifice, then the downstream side shall be beveled. The beveled surface has the same smoothness requirements as the upstream side of the orifice plate A. The angle of bevel F shall be 45 deg ± 15 deg. If a bevel is required, its minimum dimension, $E - e$, measured along the axis of the bore shall not be less than 0.2 mm (0.008 in.).

4-6.6 Edges G, H, and I

The upstream edge, G, and downstream edges, H and I, must be completely free of any burrs, nicks, wire edges, or other manufacturing deficiencies detectable by visual or tactile inspection. The upstream edge, G, must be sharp. It is defined as sharp if the radius of the edge is not greater than $0.0004d$.

Visual inspection of the edge, G, of orifices of $d \geq 25$ mm (1 in.) is sufficient to check edge sharpness compliance. If the edge does not appear to reflect a beam of light when viewed by the naked eye, the sharpness requirements are met. If there is any doubt, the edge radius must be measured.

For orifices of $d < 25$ mm (1 in.), the edge radius should be measured. The edge radius can be measured by the lead foil impression method, casting method, or paper recording roughness method.

The downstream edges, H and I, do not have the same rigorous requirements as the upstream edge. This is because they are in the separated flow region. Small defects should be undetectable by the naked eye.

4-6.7 Orifice Diameter, *d*

The diameter shall be such that $0.20 \leq \beta \leq 0.70$ and it shall be greater than or equal to 12.5 mm (0.5 in.). The orifice diameter should be sized to achieve a differential pressure of at least 0.025 MPa [3.61 psi or 100 in. H_2O (68°F)] at the test condition. The manufactured diameter is reported as the mean of four measured diameters spaced at approximately 45 deg. More diametrical measurements can be specified but must be spaced in approximately equal radial angles to each other. Caution must be exercised to avoid damaging the inlet edge G while measuring the diameter.

No measured diameter shall differ by more than 0.05% from the mean diameter.

4-6.8 Eccentricity and Alignment of Orifice in Metering Section

The concentricity of the orifice with respect to the upstream and downstream pipes, or eccentricity, is defined as the perpendicular distance between the center of the orifice bore and the centerline of the metering section's bore. For line sizes greater than 100 mm (4 in.), such eccentricity must not exceed $0.0025D/(0.1 + 2.3\beta^4)$. In smaller line sizes, the eccentricity must not exceed 0.8 mm (0.03 in.) toward the taps, or 1.5% of D away from the taps.

An orifice plate must be perpendicular to the centerline of the metering run within 1 deg.

The manufacturing and installation requirements to comply with the above requirements are addressed further in Section 6.

4-6.9 Orifice Drain Hole

Orifice plates for use in horizontal pipes are sometimes made with drain holes. The drain hole is located flush with the bottom of the pipe when measuring gaseous fluids or flush with the top of the pipe when measuring liquids.

Orifice meters used for performance testing shall not have drain holes through the face of the orifice connecting the upstream and downstream parts of the metering section.

4-7 MACHINING TOLERANCES AND DIMENSIONS FOR DIFFERENTIAL PRESSURE TAPS

Unless otherwise noted, all symbols for machining tolerances and dimensions, and markings for differential pressure taps in paras. 4-7.1 and 4-7.2 correspond to those in Figure 4-7-1.

Unless otherwise noted, all symbols for machining tolerances and dimensions and markings for differential pressure taps in para. 4-7.3 correspond to those in Figure 4-7-2.

4-7.1 Flange Taps — Shape, Diameter, and Angular Position

The centerline of the flange taps must meet the pipe centerline and be at right angles to it within 3 deg. At the point of breakthrough, the hole must be circular.

The edges must be flush with the internal surface of the pipe wall and be as sharp as can be reasonably manufactured. Because it is critical to eliminate burrs or wire edges at the inner edge, rounding is permitted but it should be minimized. The radius caused by rounding must not exceed $0.06\phi a$, where ϕa is the diameter of the individual tap holes in Figure 4-7-1.

Visually, no irregularities shall appear inside the connecting hole. This applies both to the edges of the hole where the hole meets D in the pipe, flange, or fitting and to the edges of the hole within $2.5\phi a$ from D.

Upstream and downstream tap holes must be the same diameter. The recommended size of the tap holes is 13 mm (0.50 in.) for pipe diameters greater than or equal to 100 mm (4 in.). The recommended tap diameters for 50 mm (2 in.) and 76 mm (3 in.) nominal pipe diameters are 6 mm (0.25 in.) and 9.5 mm (0.375 in.), respectively.

The pressure tap holes must be circular and cylindrical for a length of at least 2.5 times the internal diameter of the tap, measured from the inner wall of the pipe or flange.

Elevation differences of taps and tubing installation can negatively affect the measurement of the differential pressure; therefore, caution is advised concerning correct calculations. Also, if the metering run is installed downstream of a bend or a tee, the taps should be installed so that their axes are perpendicular to the plane of the bend or tee.

4-7.2 Flange Taps Orifice Metering Runs — Spacing of Taps

The spacing (ℓ_1 or ℓ_2') of a pressure tap is the distance between the centerline of the pressure tap and the plane of the specified face of the orifice plate. The spacing of the pressure tap is shown in Figure 4-7-1. When installing the pressure taps, consider the thickness of the gaskets and/or sealing materials being used.

The center of the tap for P_1 is $\ell_1 = 25.4$ mm (1.00 in.) measured from the upstream face A of the orifice plate. The center of the tap for P_2 is $\ell_2' = 25.4$ mm (1.00 in.) measured from the downstream face B of the orifice plate. Manufacturing tolerances for flange tap locations are shown in Figure 4-7-1.

4-7.3 Corner Tap Orifice Metering Runs

(a) The spacing between the centerlines of the taps and the respective faces of the plate is equal to half the tap diameter or half the annular slot width, so that the edges break through the wall flush with the faces of the plate.

(b) The taps may be either single taps or annular slots. Both types of taps can be located in either the pipe or its flanges or carrier rings, as shown in Figure 4-7-2.

(c) The diameter, ϕa, of single taps or the width, a, of annular slots are given below. The minimum diameter is determined in practice by the likelihood of accidental obstruction by air bubbles or built-up debris.

In (1) and (2), a represents the width of the annular slot of the carrier ring and ϕa represents the diameter of the individual tap.

(1) For clean fluids and gases

(-a) $\beta \le 0.65$, $0.005D \le (a \text{ or } \phi a) \le 0.03D$

(-b) $\beta > 0.65$, $0.01D \le (a \text{ or } \phi a) \le 0.02D$

(2) For any values of β

(-a) for clean fluids, 1 mm (0.04 in.) $\le (a \text{ or } \phi a) \le$ 10 mm (0.4 in.)

(-b) for gases with annular chambers, 1 mm (0.04 in.) $\le a \le$ 10 mm (0.4 in)

(-c) for gases and liquefied gases with single taps, 4 mm (0.16 in.) $\le \phi a \le$ 10 mm (0.40 in.)

Figure 4-7-1
Location of Pressure Taps for Orifices With Flange Taps

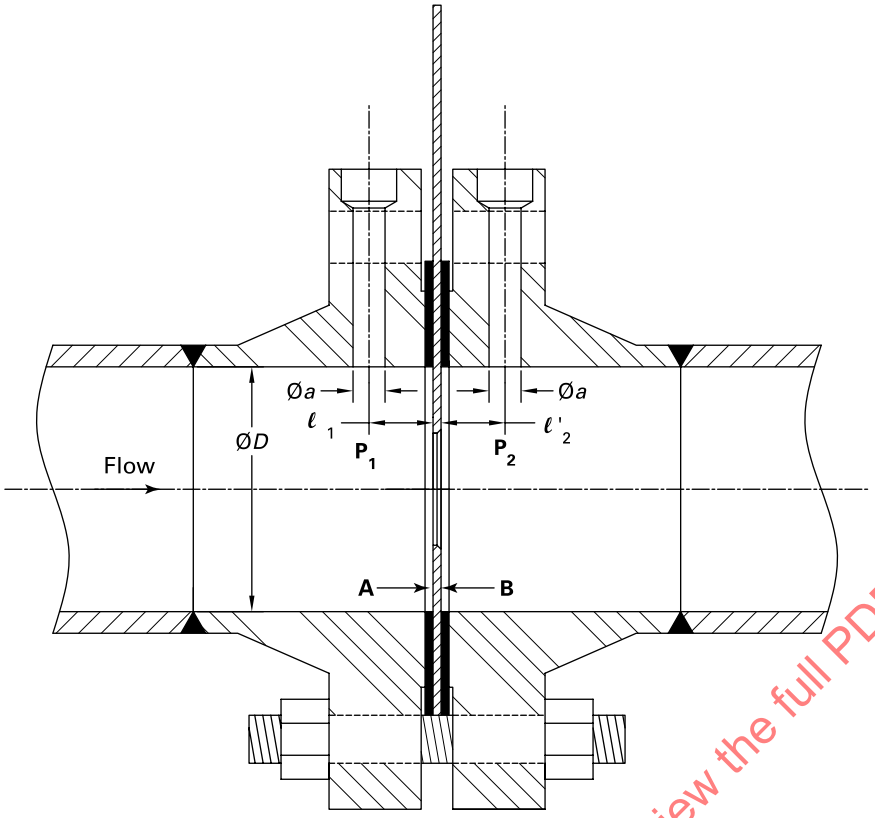

LEGEND:
- $Øa$ = diameter of individual tap holes
- A = upstream side of orifice plate
- B = downstream side of orifice plate
- $ΦD$ = inlet diameter
- ℓ_1 = location of upstream tap hole
- ℓ'_2 = location of downstream tap hole
- P_1 = high pressure sensing point
- P_2 = low pressure sensing point

GENERAL NOTE: The location of the differential pressure taps must be in accordance with the following tolerances:

$\ell_1 = \ell'_2$ = 25.4 mm ± 0.5 mm (1.00 in. ± 0.02 in.) for $\beta > 0.6$ and $D < 150$ mm (6 in.)
= 25.4 mm ± 1 mm (1.00 in. ± 0.04 in.) for $\beta < 0.6$
= 25.4 mm ± 1 mm (1.00 in. ± 0.04 in.) for $\beta > 0.6$ and 150 mm ≤ D ≤ 1 000 mm (6 in. ≤ D ≤ 40 in.)

Figure 4-7-2
Location of Pressure Taps for Orifices With Corner Taps

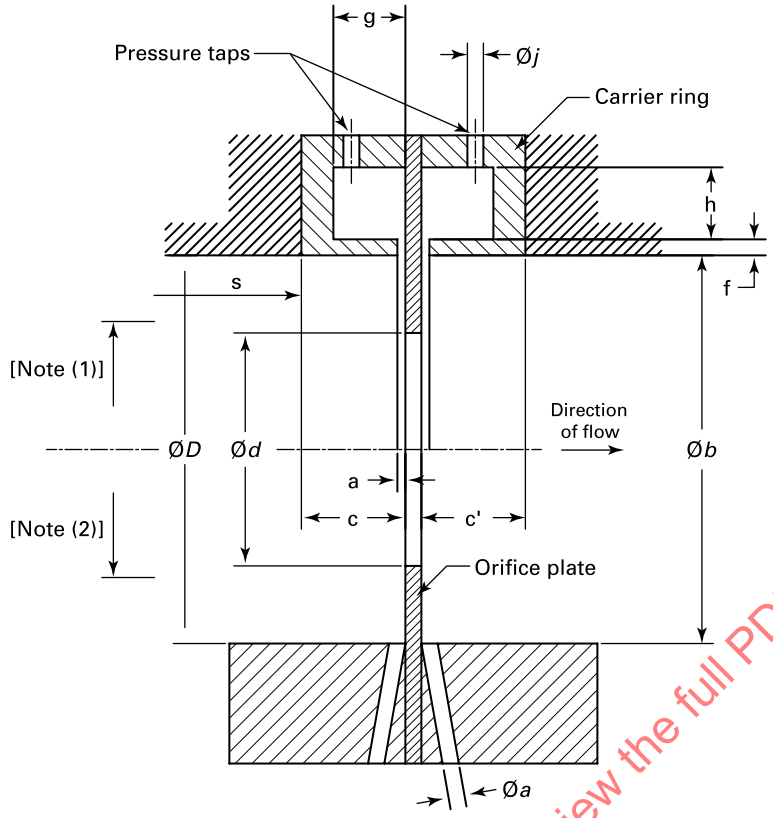

LEGEND:

a	=	width of annular slot
$Øa$	=	diameter of individual tap holes
$Φb$	=	inside diameter of carrier ring
c	=	length of upstream rig
c'	=	length of downstream ring
f	=	slot depth
g	=	annular chamber dimensions
h	=	annular chamber dimensions
s	=	distance from upstream step to carrier ring
$Øj$	=	diameter of pressure tap in carrier ring

NOTES:
(1) Carrier ring with annular slot.
(2) Individual taps.

(d) The annular slots should break through the inside wall of the pipe over the entire perimeter with no break in continuity. If this is not possible, each annular chamber shall connect with the inside of the pipe by at least four openings, the axes of which are at equal angles to one another and the individual opening area of each being at least 12 mm^2 (0.019 $in.^2$).

(e) Multiple pressure tap sets should be located symmetrically about a vertical or horizontal center line. The individual upstream and downstream pressure taps, constituting a tap set, should be in line with each other and shall have the same diameter.

(f) The inside diameter, b, of the carrier rings must be equal to or greater than the diameter, D, of the inlet section to ensure that the carrier rings do not protrude into the pipe. The inside diameter must not be greater than $1.04D$.

(g) The following restrictions are placed on the geometry of the pressure taps for corner tap orifice metering runs:

(1) $D \le b \le 1.04D$

(2) $c \le 0.5D$

(3) $c' \le 0.5D$

(4) $f \ge 2a$

(5) area $gh \ge fa/2$

(h) All surfaces of the ring that can be in contact with the measured fluid shall be clean and have a well-machined finish. The surface finish shall meet the pipe roughness requirements.

(i) The pressure taps connecting the annular chambers to the secondary device are pipe-wall taps, circular at the point of breakthrough and with diameter j between 4 mm and 10 mm (0.16 in. and 0.4 in.).

(j) The upstream and downstream carrier rings are not necessarily symmetrical to each other, but they shall both comply with the specifications herein.

(k) The diameter, D, of the inlet section used for the calculation of the diameter ratio is to be measured and must be the arithmetic mean of measurements made in at least four equally separated diameters in the plane of the upstream tap. If a carrier ring is used, then the mean diameter of the carrier ring, b, must be used in the calculation. This also applies to the length requirement so that the length, s, is to be taken from the upstream edge of the recess formed by the carrier ring.

4-8 LOCATION OF TEMPERATURE AND STATIC PRESSURE MEASUREMENTS

The general equation for mass flow [see eq. (3-2-1)] was developed to calculate the velocity at the throat of the device. Thus, temperature and static pressure measurements for density and viscosity determination are preferably determined at the upstream side of the orifice. However, temperature measurement upstream can interfere with the flow pattern and introduce errors. Thermometer wells with diameters less than $0.03D$ should be located a minimum of $5D$ upstream of the orifice face A. If they must be located within $3D$, an additional uncertainty of ±0.5% must be added. If possible, it is preferred to locate the thermometer a minimum of $5D$ downstream of the orifice face B. (See Figure 4-7-1.)

For a gas or vapor, with the requirement that $P_2/P_1 \ge 0.80$, or for a liquid, it is acceptable to assume that $T_1 = T_2$ without any loss of accuracy. This can be confirmed by assuming isentropic expansion of the fluid across the orifice and using the measured differential and static pressures, taking note that there is some pressure recovery.

The static pressure of the fluid is measured in the radial plane of the upstream pressure tap. This can be done using a separate pressure tap or by tee-in connection with the differential pressure measurement line. Care must be taken to avoid introducing errors when connecting static pressure measurement in common with a differential pressure measurement. In the case of corner tap orifices, static pressure can be measured by means of carrier ring taps.

4-9 EMPIRICAL FORMULATIONS FOR DISCHARGE COEFFICIENT, *C*

The discharge coefficient of an orifice metering section accounts for the variability of geometry, the effect of the boundary layer, and the effect of velocity profile. The recommended equation covers the two recommended tap geometries, corner, and flange taps as follows:

$$C = 0.5961 + 0.0261\beta^2 - 0.216\beta^8 + 0.000521 \times \left(\frac{10^6\beta}{\mathrm{Re}_D}\right)^{0.7} + (0.0188 + 0.0063A) \times \beta^{3.5}\left(\frac{10^6}{\mathrm{Re}_D}\right)^{0.3} + (0.043 + 0.080e^{-10L_1} - 0.123e^{-7L_1}) \times (1 - 0.11A)\frac{\beta^4}{1-\beta^4} - 0.031(M_2' - 0.8M_2'^{1.1})\beta^{1.3} \quad (4\text{-}9\text{-}1)$$

When D < 71.12 mm (2.8 in.), the following term shall be added:

(SI Units)

$$+0.011(0.75-\beta)\left(2.8-\frac{D}{25.4}\right)$$

(U.S. Customary Units)

$$+0.011(0.75-\beta)(2.8-D)$$

where

L_1 = ℓ_1/D = quotient of the distance of the upstream tap from the upstream face of the plate and the inlet section diameter
Re_D = pipe Reynolds number
β = d/D = diameter ratio

$$A=\left(\frac{19,000\beta}{\mathrm{Re}_D}\right)^{0.8}$$

$$M'_2=\frac{2L'_2}{1-\beta}$$

where

L'_2 = ℓ'_2/D = quotient of the distance of the downstream tap from the downstream face of the plate, ℓ'_2, and the inlet section diameter, D (L'_2 denotes the reference of the downstream spacing from the downstream face, while L_2 would denote the reference of the downstream spacing from the upstream face)

The values of L_1 and L'_2 used in this equation when the dimensions are in accordance with the requirements of para. 4-7.3 and Figure 4-7-2 for corner taps and para. 4-7-2 and Figure 4-7-1 for flange taps are as follows:

(a) for corner taps

$$L_1=L'_2=0$$

(b) for flange taps

(1) for D, mm: $L_1=L'_2={}^{25.4}/_{D}$

(2) for D, in.: $L_1=L'_2={}^{1}/_{D}$

Equation 4-9-1 is valid only for the tap arrangements defined and specified above. It is not permitted to enter into the equation pairs of L_1 and L'_2 that do not equal the values of one of the specified tapping dimensions.

4-10 LIMITATIONS AND UNCERTAINTY OF EQ. (4-9-1) FOR DISCHARGE COEFFICIENT, *C*

4-10.1 Limits of Use

The limits of use for eq. (4-9-1) are as follows:

(a) $d \geq 12.5$ mm (0.5 in.)
(b) 50 mm (2.0 in.) $\leq D \leq$ 1 000 mm (40 in.)
(c) $0.20 \leq \beta \leq 0.70$
(d) $\mathrm{Re}_D \geq 5\,000$ for $0.2 \leq \beta \leq 0.56$ (for corner)
(e) $\mathrm{Re}_D \geq 16\,000\beta^2$ for $\beta > 0.56$ (for corner)
(f) $\mathrm{Re}_D \geq 5\,000$ and $\mathrm{Re}_D \geq 170\beta^2 D$ (mm) (flange taps), whichever is greater
(g) $\mathrm{Re}_D \geq 5\,000$ and $\mathrm{Re}_D \geq 4318\beta^2 D$ (in.) (flange taps), whichever is greater

See Figure 4-10.1-1 for the minimum Reynolds number for flange tops.

4-10.2 Uncertainties of the Discharge Coefficient of Uncalibrated Orifice Sections

For both flange and corner tapping, when β, Re_D, D, and k/D are assumed to be known without error, the relative uncertainty of the value of the discharge coefficient, C, is equal to

(a) 0.5% for $0.2 \leq \beta \leq 0.6$

Figure 4-10.1-1
Minimum Reynolds Number for Flange Taps

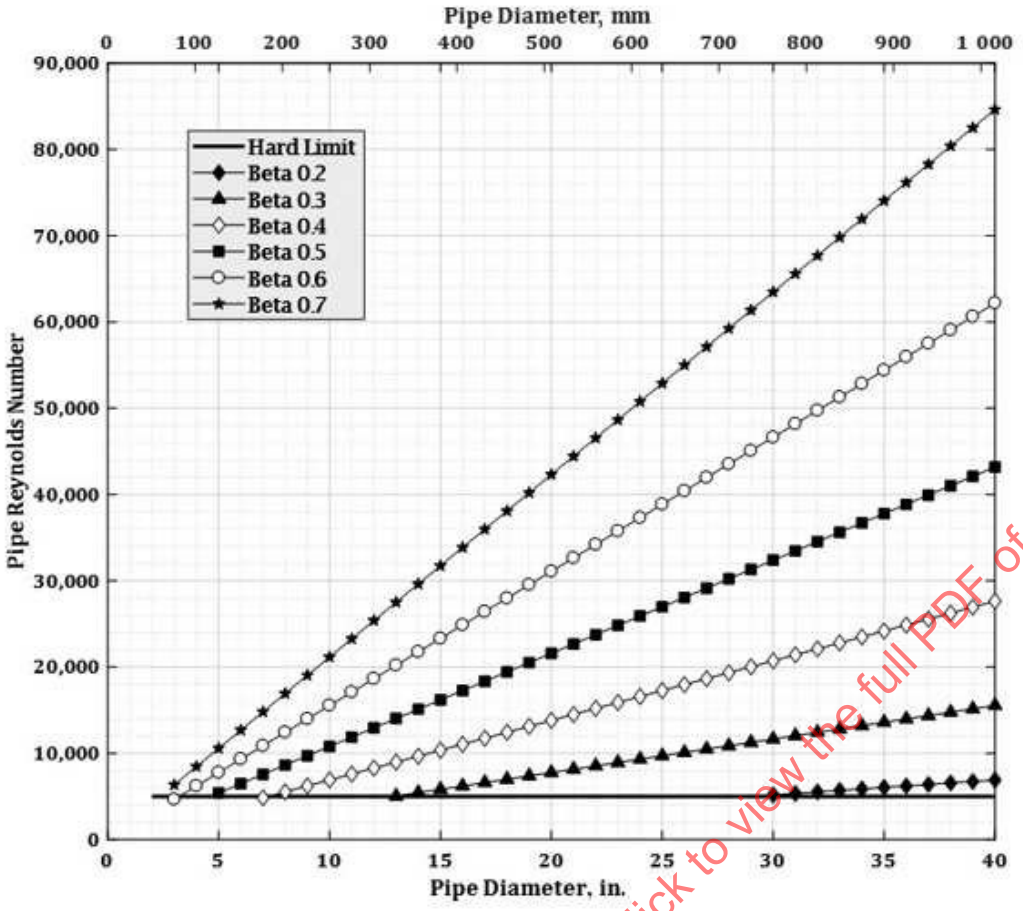

(b) $(1.667\beta - 0.5)\%$ for $0.6 < \beta \le 0.70$

Where D < 71.12 mm (2.8 in.), the following relative uncertainty shall be added to the values in (a) and (b):

(SI Units)

$$0.9(0.75 - \beta)\left(2.8 - \frac{D}{25.4}\right)\%$$

(U.S. Customary Units)

$$0.9(0.75 - \beta)(2.8 - D)\%$$

Where $\beta > 0.5$ and $\mathrm{Re}_D < 10\,000$, 0.5% shall be added to the values in (a) and (b):.

Flow measurements in performance testing may require the orifice metering sections to be calibrated to achieve the desired measurement uncertainty. The method of evaluating the laboratory calibration data to estimate the coefficient uncertainty is presented in Mandatory Appendix I.

4-11 UNCERTAINTY OF EXPANSION FACTOR, ε

When β, $\frac{\Delta P}{P_1}$, and κ are assumed to be known without error, the relative uncertainty, %, of the value of the expansion factor, ε, for orifice meters is equal to $3.5\frac{\Delta P}{\kappa P_1}\%$.

4-12 UNRECOVERABLE PRESSURE LOSS

The unrecoverable pressure loss, $\Delta\omega$, is related to the pressure drop across the orifice, ΔP, by

$$\Delta\omega = \frac{\sqrt{1-\beta^4(1-C^2)} - C\beta^2}{\sqrt{1-\beta^4(1-C^2)} + C\beta^2}\Delta P$$

with $\Delta\omega$ and ΔP in the same units.

4-13 CALCULATIONS OF DIFFERENTIAL PRESSURE CLASS FLOW MEASUREMENT SYSTEMATIC UNCERTAINTY

4-13.1 Derivation

This uncertainty analysis of differential pressure class flow measurement is valid if the calculations of mass flow are performed and the metering sections and orifices are manufactured and installed strictly in accordance with this Supplement. Deviation from this Supplement in manufacture, installation, calculations, or any other requirement adversely affects uncertainty.

Sample calculations shown are for orifice metering sections.

Steam and gas are the chosen fluids for sample calculation of uncertainty because all terms are then used in the fundamental flow equation [see eq. (4-13-1)], which is repeated below for the user's convenience. Water or incompressible flow measurement uncertainty would be calculated similarly but without the expansion factor term.

$$q_m = n\frac{\pi}{4}d^2C\varepsilon\sqrt{\frac{2\rho(\Delta P)g_c}{1-\beta^4}} \tag{4-13-1}$$

Defining B as the systematic uncertainty in the units of measure of its subscripted variable

$$B_{q_m} = \left[\left(\frac{\partial q_m}{\partial C}B_C\right)^2 + \left(\frac{\partial q_m}{\partial \varepsilon}B_\varepsilon\right)^2 + \left(\frac{\partial q_m}{\partial D}B_D\right)^2 + \left(\frac{\partial q_m}{\partial d}B_d\right)^2 + \left(\frac{\partial q_m}{\partial \Delta P}B_{\Delta P}\right)^2 + \left(\frac{\partial q_m}{\partial \rho}B_\rho\right)^2\right]^{0.5} \tag{4-13-2}$$

After differentiation, dividing by q_m to get fractional units, and algebra

$$\frac{B_{q_m}}{q_m} = \left[\left(\frac{B_C}{C}\right)^2 + \left(\frac{B_\varepsilon}{\varepsilon}\right)^2 + \left(\frac{2\beta 4}{1-\beta 4}\right)\left(\frac{B_D}{D}\right)^2 + \left(\frac{2}{1-\beta 4}\right)\left(\frac{B_d}{d}\right)^2 + \left(\frac{B_{\Delta P}}{2\Delta P}\right)^2 + \left(\frac{B_\rho}{2\rho}\right)^2\right]^{0.5} \tag{4-13-3}$$

Uncertainty as a percentage is then equal to $100 \times \dfrac{U_{q_m}}{q_m}$

The square root of the coefficient of each term in eq. (4-13-3) is the sensitivity coefficient, S, of the particular variable, X. The sensitivity coefficients from eq. (4-13-3) are summarized in Table 4-13.1-1.

4-13.2 Uncertainty Calculation — General

The uncertainties of instrumentation for measurement of the fluid conditions and orifice differential pressure are used herein and in paras. 4-13.2.1 through 4-13.5.

There are no additional uncertainty considerations in completely steady-state conditions using eq. (4-13-3) for uncertainty analysis if the parameters on the right side of eq. (4-13-1) are independent. Although they are not entirely independent, the unaccounted-for cross products are completely insignificant, as shown herein.

The discharge coefficient, C, is a function of Reynolds number, which is calculated based on temperature, pressure, and constituent analysis of a gas mixture (for density and viscosity calculations). At high Reynolds numbers ($Re_D > 100{,}000$), a change in the Reynolds number of 25% results in a change in the discharge coefficient of less than 0.1%. Therefore, with a typical uncertainty in the Reynolds number due to viscosity and velocity estimates, the uncertainty in the discharge coefficient due to Reynolds number errors is considerably less than the uncalibrated orifice meter uncertainty.

The expansion factor, ϵ, also depends on pressure and differential pressure. Equation (3-9-2) is used to calculate the expansion factor for orifice meters.

Table 4-13.1-1
Sensitivity Coefficients in the General Equation for Differential Pressure Meters

Term in General Flow Rate [See Eq. (3-2-1)]	Sensitivity Coefficient
C	1.00
ϵ	1.00
D	$2\beta^4/(1 - \beta^4)$
d	$2/(1 - \beta^4)$
ΔP	0.50
ρ	0.50

$$\varepsilon_1 = 1 - (0.351 + 0.256\beta^4 + 0.93\beta^8)\left[1 - \left(\frac{P_2}{P_1}\right)^{\frac{1}{\kappa}}\right]$$

The uncertainty of the empirical formulation of ε_1 in the calculations is greater than the uncertainty in ε_1 due to process measurement error. As an example, consider a metering section with a beta ratio of 0.6 and a measured differential pressure of 0.037 MPa (5.4 psi) for a compressible fluid with a specific heat ratio of 1.3 at a pressure of 2.068 MPa (300 psi). The uncertainty in ε_1 is calculated from subsection 4-11 to be 0.048% at typical instrument uncertainties of 0.2%.

Three examples of uncertainty calculations are given in paras. 4-13.2.1 through 4-13.2.3; two are for steam mass flow and one is for natural gas fuel mass flow. Note that these examples only include the systematic uncertainties and do not consider random uncertainties. A post-test uncertainty analysis would have to include random uncertainties caused by data fluctuations per ASME PTC 19.1. See para. 4-13.3.

4-13.2.1 Example 1: Uncertainty of Typical Steam Flow Measurement, Orifice Metering Run for $\beta \le 0.6$. Orifice geometry and design flow conditions for a typical steam flow measurement are as follows (see Table 4-13.2.1-1):

D = 254.51 mm (10.02 in.)
d = 124.49 mm (4.9012 in.)
β = 0.4891
differential pressure = 124.42 kPa (18.046 psi)
steam pressure = 1 930 kPa (280 psia)
steam temperature = 221°C (430°F)
κ = 1.3

4-13.2.2 Example 2: Uncertainty of Typical Steam Flow Measurement, Orifice Metering Run for $\beta > 0.6$. Steam flow orifice geometry and flow conditions are as follows (see Table 4-13.2.2-1):

D = 304.8 mm (12.00 in.)
d = 213.36 mm (8.400 in.)
β = 0.7000
differential pressure = 54.020 kPa (7.835 psi)
steam pressure = 448.2 kPa (65 psia)
steam temperature = 182.22°C (360°F)
κ = 1.3

Table 4-13.2.1-1
Example 1 — Systematic Uncertainty Analysis for Given Steam Flow Orifice Metering Run

Parameter, X	Parameter Total Uncertainty, $\left(\frac{B_X}{X}\right)$	Sensitivity Factor on Flow Measurement, S	$\left(\frac{B_X}{X}\right)(S)$
Discharge coefficient, C	0.5%	1.00	0.5%
Expansion factor, ϵ	$3.5\frac{\Delta P}{\kappa P_1} = 3.5\frac{124.42}{1.3(1930)} = 0.17\%$	1.00	0.17%
Pipe diameter, D	0.2%	$\frac{2\beta^4}{1-\beta^4} = \frac{2(0.4891)^4}{1-(0.4891)^4} = 0.121$	0.0242%
Orifice diameter, d	±0.05%	$\frac{2}{1-\beta^4} = \frac{2}{1-(0.4891)^4} = 2.121$	0.106%
Differential pressure, ΔP	±0.25%	0.50	0.125%
Density, ρ	±0.27% [Note (1)]	0.50	0.135%
		Systematic uncertainty at 95% confidence level, root sum square	**0.57% [Note (2)]**

NOTES:
(1) The uncertainty for ρ has been determined from the parameter total uncertainty for differential pressure, $B_{\Delta P}/\Delta P = 0.25\%$, and the uncertainty for temperature, $B_T = 0.3°C$ (0.5°F).
(2) The systematic uncertainty is determined using eq. (4-13-3) after $\left(\frac{B_X}{X}\right)(S)$ is determined for each parameter.

Table 4-13.2.2-1
Example 2 — Systematic Uncertainty Analysis for Given Steam Flow Orifice Metering Run

Parameter, X	Parameter Total Uncertainty, $\left(\frac{B_X}{X}\right)$	Sensitivity Factor on Flow Measurement, S	$\left(\frac{B_X}{X}\right)(S)$
Discharge coefficient, C	0.67%	1.00	0.67%
Expansion factor, ϵ	$3.5\frac{\Delta P}{\kappa P_1} = 3.5\frac{54.020}{1.3(448.2)} = 0.32\%$	1.00	0.32%
Pipe diameter, D	0.2%	$\frac{2\beta^4}{1-\beta^4} = \frac{2(0.7000)^4}{1-(0.7000)^4} = 0.632$	0.126%
Orifice diameter, d	0.05%	$\frac{2}{1-\beta^4} = \frac{2}{1-(0.7000)^4} = 2.632$	0.132%
Differential pressure, ΔP	0.25%	0.50	0.125%
Density, ρ	0.27% [Note (1)]	0.50	0.135%
		Systematic uncertainty at 95% confidence level, root sum square	**0.79% [Note (2)]**

NOTES:
(1) The uncertainty for ρ has been determined from the parameter total uncertainty for differential pressure, $B_{\Delta P}/\Delta P = 0.25\%$, and the uncertainty for temperature, $B_T = 0.3°C$ (0.5°F).
(2) The systematic uncertainty is determined using eq. (4-13-3) after $\left(\frac{B_X}{X}\right)(S)$ is determined for each parameter.

4-13.2.3 Example 3: Uncertainty of Typical Fuel Gas Flow Measurement, Orifice Metering Run for $\beta < 0.6$. Fuel flow orifice geometry and flow conditions for a typical fuel gas flow measurement are as follows (see Table 4-13.2.3-1):

D = 202.72 mm (7.9810 in.)
d = 118.96 mm (4.6834 in.)
β = 0.5868
differential pressure = 29.19 kPa (4.234 psi)
gas pressure = 2 586 kPa (375 psia)
gas temperature = 15.56°C (60°F)
κ = 1.3

4-13.3 Random Uncertainty Due to Data Fluctuations

The post-test uncertainty analysis must consider fluctuation of actual data. The differences in degrees of freedom of the data should be considered in calculation of the random component of uncertainty. The analyses in this Section just consider systematic uncertainties at 95% confidence level.

During a test run, the random standard uncertainty must be determined, multiplied by the Student's t value (typically 2 for a test run), and combined with the systematic uncertainty by root sum square to determine the expanded uncertainty (the overall measurement uncertainty at 95% confidence level).

Examples of complete uncertainty analyses, including random uncertainty from fluctuation in data, are given in ASME PTC 19.1, which is referenced for details of post-test uncertainty analysis requirements.

4-13.4 Instrumentation Uncertainties for the Determination of Flow Measurement Systematic Uncertainties

Paragraphs 4-13.4.1 through 4-13.4.3 summarize the reasons for selecting individual instrumentation uncertainties for determining flow measurement systematic uncertainties. Many differential pressure and static pressure instruments' specifications and calibrations define percent uncertainties (accuracy class) as a function of span and not reading. Therefore, in these cases, the uncertainty values must be multiplied by the instrument span divided by the instrument reading to determine the uncertainty as a percent of reading for use in the uncertainty analysis. In the following examples, the readings are assumed to be the full span of the instrument to simplify the calculations.

Table 4-13.2.3-1
Example 3 — Systematic Uncertainty Analysis for Given Gas Flow and Meter Tube

Parameter, X	Parameter Total Uncertainty, $\left(\frac{B_X}{X}\right)$	Sensitivity Factor on Flow Measurement, S	$\left(\frac{B_X}{X}\right)(S)$
Discharge coefficient, C	0.5%	1.00	0.5%
Expansion factor, ε	$3.5\frac{\Delta P}{\kappa P_1} = 3.5\frac{29.19}{1.3(2585)} = 0.030\%$	1.00	0.030%
Pipe diameter, D	0.2%	$\frac{2\beta^4}{1-\beta^4} = \frac{2(0.5868)^4}{1-(0.5868)^4} = 0.269$	0.054%
Orifice diameter, d	0.05%	$\frac{2}{1-\beta^4} = \frac{2}{1-(0.7000)^4} = 2.269$	0.113%
Differential pressure, ΔP	0.25%	0.50	0.125%
Density, ρ	0.34% [Note (1)]	0.50	0.17%
		Systematic uncertainty at 95% confidence level, root sum square	**0.56% [Note (2)]**

NOTES:
(1) The uncertainty for ρ is determined from the root sum square of the parameter total uncertainty for density, B_ρ/ρ, (for perfect analysis) and the constitute analysis uncertainty. For perfect gas analysis, the parameter total uncertainty for differential pressure, $B_{\Delta P}/\Delta P = 0.25\%$, and the uncertainty for temperature, U_T = 0.3°C (0.5°F). The constitute analysis uncertainty is equal to 0.2%.
(2) The systematic uncertainty is determined using eq. (4-13-3) after $\left(\frac{B_X}{X}\right)(S)$ is determined for each parameter.

4-13.4.1 Differential Pressure. Differential pressure transmitters installed specifically for test purposes are assumed to be of the 0.075% accuracy class. For this calculation, it is assumed that transmitters are selected for a specific application so that their range does not affect uncertainty. It is also assumed that local ambient temperature is 26.7°C (80°F) and that there is insignificant water leg error.

Additional instrument uncertainties are caused by

(a) static pressure effects

(b) ambient temperature effects

(c) vibration effects

Other small error sources can be power supply effects or radio frequency interference (RFI) effects and are considered zero. Each manufacturer documents the influence of these effects on its instrumentation. Typical values and differential pressure systematic uncertainty at steady state conditions are given in Table 4-13.4.1-1. With the above assumptions, 0.23% represents the instrument systematic uncertainty in steady state. To be conservative, 0.25% is used for the uncertainty of differential pressure in the uncertainty calculations in this Section.

4-13.4.2 Static Pressure. Making the same assumptions as for the differential pressure measurement, static pressure systematic uncertainty at steady state conditions is estimated, for a 0.075% class gage pressure transmitter, in Table 4-13.4.2-1. With the above assumptions, 0.21% represents the instrument systematic uncertainty in steady state. To be conservative, ±0.25% is used for the systematic uncertainty of static pressure in the uncertainty calculations in this Section.

4-13.4.3 Temperature. Several options exist to determine temperature to within 0.3°C (0.5°F) (assuming no temperature stratification). For example, resistance temperature detectors typically have digital accuracies of 0.2°C (0.3°F) in broad temperature ranges. Combined with data acquisition uncertainty and other effects, 0.3°C (0.5°F) maximum uncertainty is achievable and can be improved with applied laboratory calibrations.

4-13.5 Uncertainty of Typical Gas Fuel Flow Measurement for a Laboratory-Calibrated Orifice Metering Section

Table 4-13.5-1 calculates the systematic uncertainty of the natural gas flow measurement example in Table 4-13.2.3-1, with the metering section laboratory-calibrated at the test Reynolds number range. The overall measurement uncertainty is then significantly reduced.

To ensure the laboratory uncertainty is maintained, several precautions are necessary. A positive mechanical alignment method shall be in place to replicate the precise position of the orifice element within the flow section assembly when it was calibrated. The flowmeter section must remain dirt and moisture free for shipping and storage. Whenever possible, it is preferred to ship the flow section as one piece and not disassembled for shipping or installation. However, inspection of the orifice is permitted with no impact to the calibration when a positive mechanical alignment method is part of the design.

The laboratory-derived discharge coefficient uncertainty of the water-calibrated orifice metering section is 0.25% and is applicable to gas testing when used in the calibrated Reynolds number range. Laboratory-calibrated uncertainty of the discharge coefficient uncertainty of an orifice metering section may be as low as 0.15%. Extrapolation of laboratory calibration data may increase the uncertainty of the resulting discharge coefficient (see Mandatory Appendix I).

As shown in subsection 4-11, the uncertainty in the compressibility effects is proportional to the ratio of differential pressure and static pressure or the velocity of the fluid. This is reasonable because, as Mach number increases, compressibility effects also increase, as does the resulting uncertainty. The uncertainty in the discharge coefficient is treated separately from the uncertainty due to compressibility effects. The pipe and orifice diameter uncertainties are revised to 0% because the uncertainties of the diameters are included in the uncertainty of the discharge coefficient as determined by the flow calibration. A flow calculation must include a correction for the thermal expansion of the diameters due to the difference in the temperature of the fluid being measured versus the fluid temperature during calibration. The uncertainty for this correction is assumed to be negligible in this uncertainty calculation.

4-14 PROCEDURE FOR FITTING A CALIBRATION CURVE AND EXTRAPOLATION TECHNIQUE

The method for fitting a calibration curve and extrapolating the calibration beyond the highest Reynolds number that the orifice metering run was calibrated is described in Mandatory Appendix I.

Table 4-13.4.1-1
Systematic Uncertainty, 0.075% Accuracy Class Differential Pressure Transmitter

Parameter	Sensitivity, %/%	Instrument Systematic Uncertainty, %	Sensitivity × Uncertainty, %
Calibration	1.0	0.075	0.075
Static pressure	1.0	0.1	0.1
Temperature effect	1.0	0.15	0.15
Vibration	1.0	0.1	0.1
Repeatability	1.0	0.05	0.05
Data acquisition system	1.0	0.04	0.04
Root sum square	...	...	0.23

Table 4-13.4.2-1
Systematic Uncertainty, 0.075% Accuracy Class Static Pressure Transmitter

Parameter	Sensitivity, %/%	Systematic, %	Sensitivity × Uncertainty, %
Calibration	1.0	0.075	0.075
Temperature effect	1.0	0.15	0.15
Vibration	1.0	0.1	0.1
Repeatability	1.0	0.05	0.05
Data acquisition system	1.0	0.04	0.04
Barometric pressure	0.05	0.1	0.0
Root sum square	...	...	0.21

Table 4-13.5-1
Systematic Uncertainty Analysis for Given Gas flowmetering Run With Laboratory Calibration

Parameter, X	Parameter Total Uncertainty, $\left(\frac{B_X}{X}\right)$	Sensitivity Factor on Flow Measurement, S	$\left(\frac{B_X}{X}\right)(S)$
Discharge coefficient, C	0.25% [Note (1)]	1.00	0.25%
Expansion factor, ε	$3.5\frac{\Delta P}{\kappa P_1} = 3.5\frac{29.19}{1.3(258)} = 0.030\%$	1.00	0.030%
Inlet section diameter, D	...	...	0% [Note (2)]
Orifice diameter, d	...	...	0% [Note (2)]
Differential pressure, ΔP	0.25%	0.50	0.125%
Density, ρ	0.34% [Note (3)]	0.50	0.17%
		Systematic uncertainty at 95% confidence level, root sum square	**0.33% [Notes (4), (5)]**

NOTES:
(1) This value of the discharge coefficient uncertainty was determined from a laboratory calibration in conjunction with Mandatory Appendix I.
(2) Any errors in measurement of D and d are compensated by the calibrated discharge coefficient.
(3) The uncertainty for ρ is determined from the root sum square of the parameter total uncertainty for density B_ρ/ρ (for perfect gas analysis) and the constitute analysis uncertainty. For perfect gas analysis, the parameter total uncertainty for differential pressure, $B_{\Delta P}/\Delta P = 0.25$ % and the uncertainty for temperature, B_T = 0.3ºC (0.5ºF). The constitute analysis uncertainty is equal to 0.2%.
(4) The laboratory-calibrated orifice section has an uncertainty of 0.33% for fuel gas flow, reduced from 0.56% if the empirical formulation for the discharge coefficient is used.
(5) The systematic uncertainty is determined using eq. (4-13-3) after $\left(\frac{B_X}{X}\right)(S)$ is determined for each parameter.

4-15 REFERENCES

ASME MFC-3M–2004 (R2017). Measurement of Fluid Flow in Pipes Using Orifice, Nozzle, and Venturi. The American Society of Mechanical Engineers.

ASME MFC-3Ma–2007. Addenda to ASME MFC-3M–2004, Measurement of Fluid Flow in Pipes Using Orifice, Nozzle, and Venturi. The American Society of Mechanical Engineers.

ASME MFC-8M–2001 (R2016). Fluid Flow in Closed Conduits: Connections for Pressure Signal Transmissions Between Primary and Secondary Devices. The American Society of Mechanical Engineers.

Bean, H. S., ed. (1971). Fluid Meters: Their Theory and Application (6th ed.). The American Society of Mechanical Engineers.

ISO 5167-2:2003. Measurement of fluid flow by means of pressure differential devices inserted in circular-cross section conduits running full — Part 2: Orifice plates. International Organization for Standardization.

Reader-Harris, M. J., and Sattary, J. A. (1990). "The orifice plate discharge coefficient equation." Flow Measurement and Instrumentation, 1(2) (Jan.), 67–76. https://doi.org/10.1016/0955-5986(90)90031-2.

Reader-Harris, M. J., Sattary, J. A., and Spearman, E. P. (1995). "The orifice plate discharge coefficient equation — further work." Flow Measurement and Instrumentation, 6(2) (Apr.), 101–114. https://doi.org/10.1016/0955-5986(94)00001-O.

Section 5
Nozzles and Venturis

5-1 NOMENCLATURE

Symbols used in Section 5 are included in Tables 2-3-1 and 3-1-1.

5-2 INTRODUCTION

This Section shall be used with Section 3, which describes the theory of operation necessary for proper flow measurement, and Section 6, which provides guidance and requirements for the installation of these primary elements into a flow section that then comprises the flowmeter.

The primary element types described in this Section include three types of nozzles and one type of venturi.

(a) ASME low β ratio nozzles ($0.2 \le \beta \le 0.5$)
(b) ASME high β ratio nozzles ($0.45 \le \beta \le 0.8$)
(c) ASME throat tap nozzles ($0.25 \le \beta \le 0.5$)
(d) ASME (classical Herschel) venturi ($0.30 \le \beta \le 0.75$)

These meters have extensive histories that include calibration data, field experience, and use in Performance Test Code work. Other nozzles and flow tubes may be used by agreement if equivalent care is taken in their fabrication and installation and if they are calibrated in a laboratory in conformance with applicable requirements provided in this Section.

5-3 REQUIRED PROPORTIONS OF ASME NOZZLES

Dimensions specifically shown in Figures 5-3-1 through 5-3-5 are required for each of the three types of ASME nozzles with respect to the throat and pipe inside diameter.

(a) high β nozzle
(b) low β nozzle
(c) throat tap nozzle for $\beta > 0.44$
(d) throat tap nozzle for $\beta \le 0.44$

NOTE: Throat tap nozzles for ASME PTC 6-2004 applications are subject to the additional requirements of that code.

The ASME throat tap primary element and other components of the flow section are shown in Figure 5-3-6. The throat tap nozzle flow section consists of the primary element, the diffusing section if used, the flow conditioner, and the upstream and downstream lengths. Figure 5-3-6 illustrates additional installation and flow conditioning requirements for ASME PTC 6 applications. See Section 6 for installation and flow conditioning requirements.

5-3.1 Entrance Section

All ASME flow nozzles have the shape of a quarter ellipse in the entrance section. The values of the major axis and the minor axis of the ellipse are shown in Figures 5-3-1 through 5-3-4 for each type of flow nozzle. The major centerline of the ellipse shall be parallel to the centerline of the nozzle within 0.1%. The ellipse shall terminate at a point no greater than D regardless of the value of the minor axis.

5-3.2 Throat Section

The throat section shall have a diameter, d, and a length as shown in Figures 5-3-1 through 5-3-4. The measured value of d shall be the average of four equally spaced radial measurements of the throat diameter taken in each of three equally spaced planes along the length of the throat section, covering at least three-quarters of the throat length for a total of 12 diametric measurements. No diameter shall differ by more than 0.05% from the average diameter, d. Under no circumstances shall the throat diameter increase toward the nozzle exit. A decrease in diameter toward the exit end is acceptable if it is within the 0.05% variation allowed from the average diameter.

5-3.3 Exit End Section

The exit end section is shown in detail in Figure 5-3-5 and applies to all ASME nozzle designs.

5-3.4 General Requirements for ASME Flow Nozzles

The distance from the pipe inside diameter to the outside diameter of the nozzle throat shall be greater than or equal to 3 mm (0.125 in.) for wall tap nozzles.

The thickness, t, shall be sufficient to prevent distortion of the nozzle throat from the stresses of machining, installation, or conditions of use.

The surface of the inner face of the nozzle shall be machined smooth and, if necessary, polished to achieve a maximum roughness as determined from the ratio of required surface finish to throat diameter, d (this ratio is shown on the vertical axis of Figure 5-3.4-1), and no greater than 0.8 μm (32 μin.). The exit end must not have rounding or burrs.

Boring in the section upstream of the nozzle is shown in Figure 5-3.4-2.

The downstream (outside) face of the nozzle shall be cylindrical and machined smooth or otherwise constructed so as to eliminate any pockets or pits that might retain debris or matter that may be in the fluid.

ASME flow nozzles may be made from any material that does not wear easily and remains dimensionally stable with known thermal expansion properties.

Section 6 defines the requirements of the metering section in which the nozzle is assembled. Specifics are given for lengths, centering, and fabrication requirements.

Figure 5-3-1
High β Nozzle

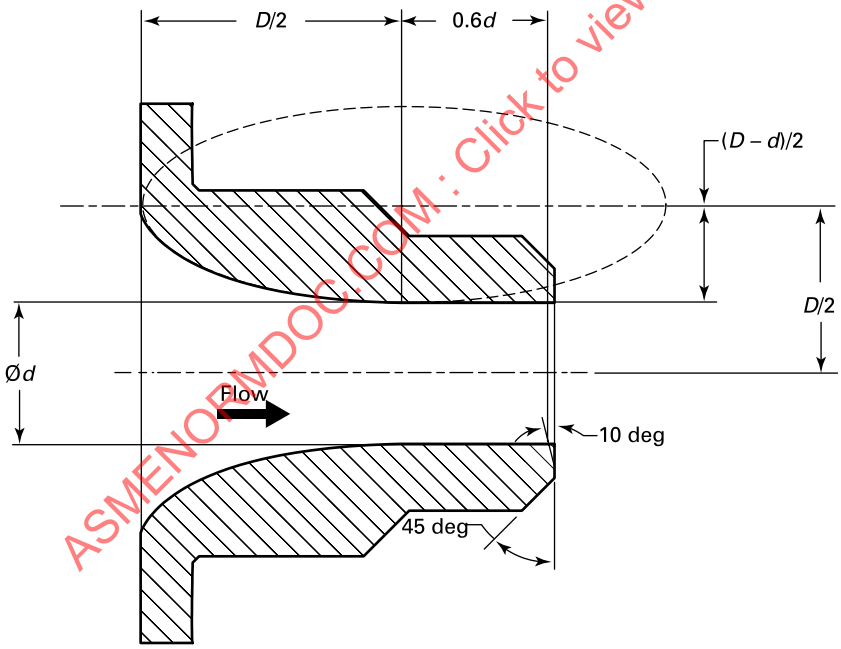

Figure 5-3-2
Low β Nozzle

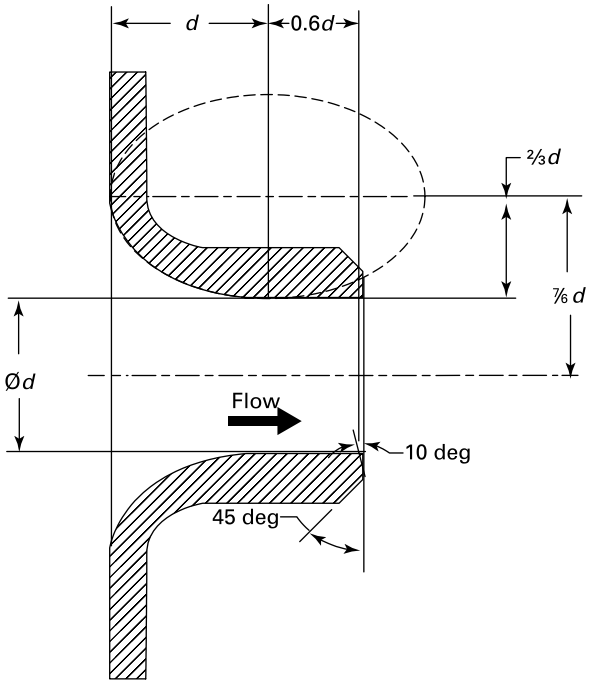

Figure 5-3-3
Throat Tap Nozzle for β > 0.44

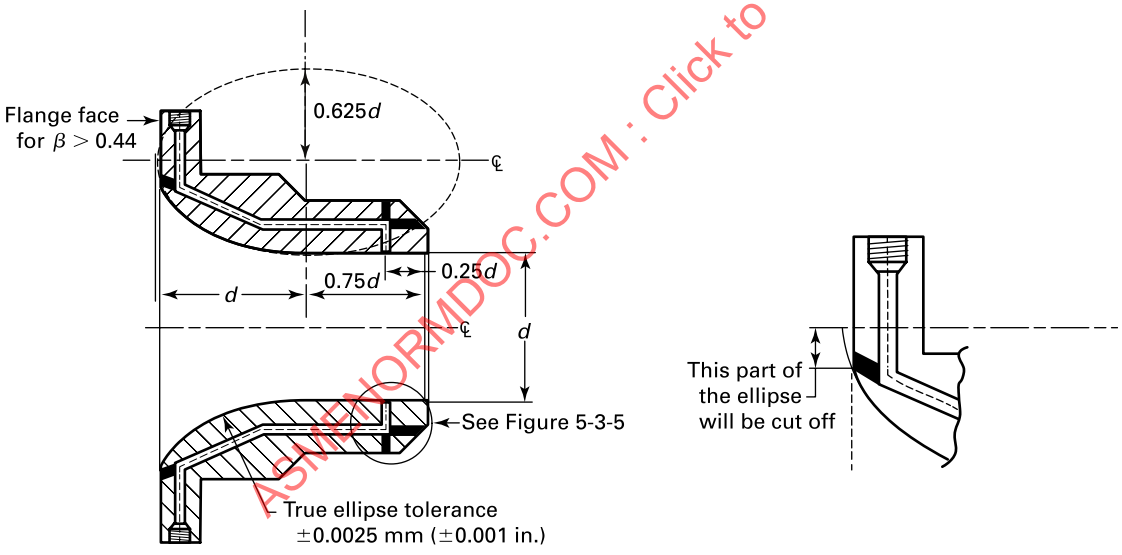

Figure 5-3-4
Throat Tap Nozzle for $\beta \leq 0.44$

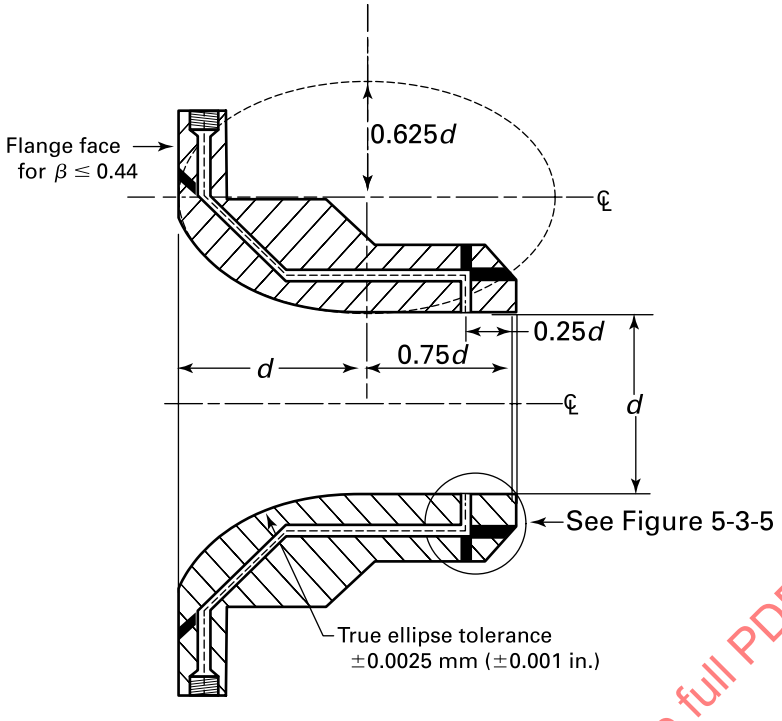

Figure 5-3-5
Throat Tap Nozzle End Detail

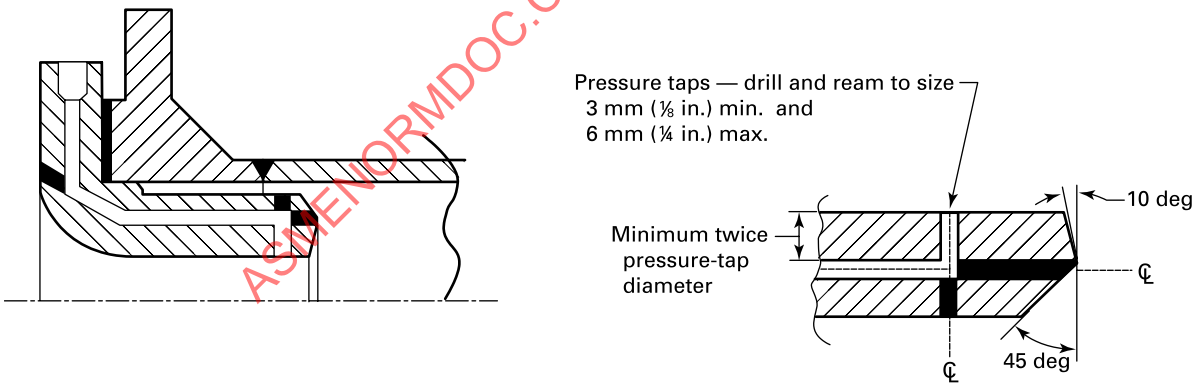

Figure 5-3-6
Example Throat Tap Nozzle Flow Section

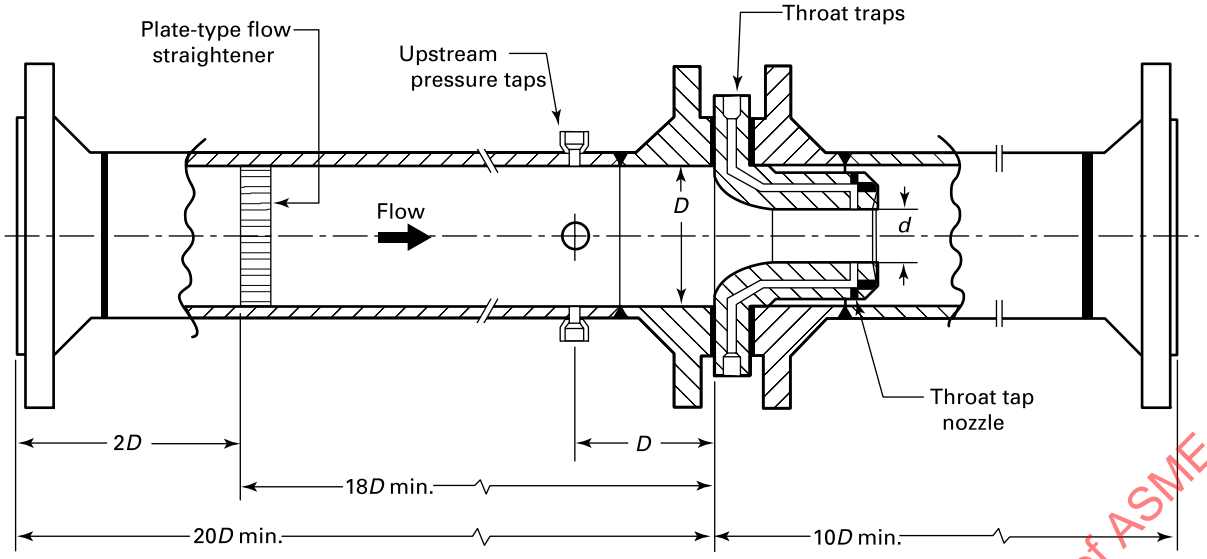

GENERAL NOTE: No obstruction, such as thermocouple wells, backing rings, etc., are permitted.

Figure 5-3.4-1
ASME Nozzle Required Surface Finish to Produce a Hydraulically Smooth Surface

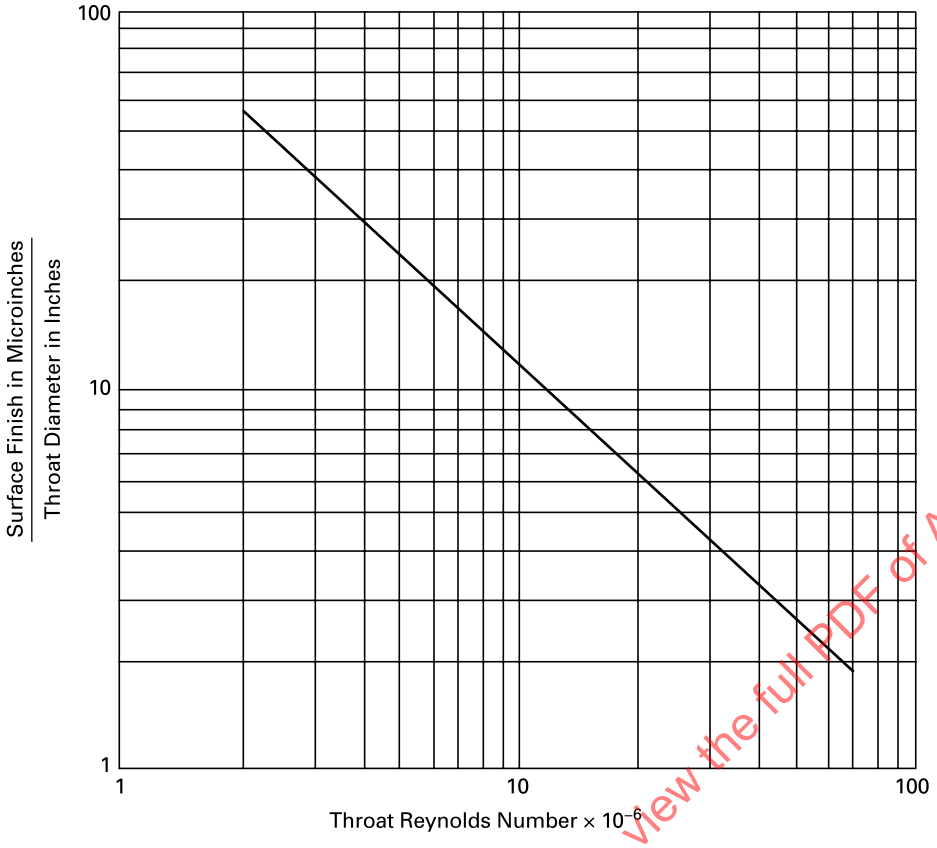

GENERAL NOTE: The vertical axis of this graph can be relabeled $\frac{\text{surface finish } (\mu\text{m})}{\text{throat diameter (m)}}$ to determine the surface finish in micrometers when the throat diameter is in meters.

Figure 5-3.4-2
Boring in Flow Section Upstream of Nozzle

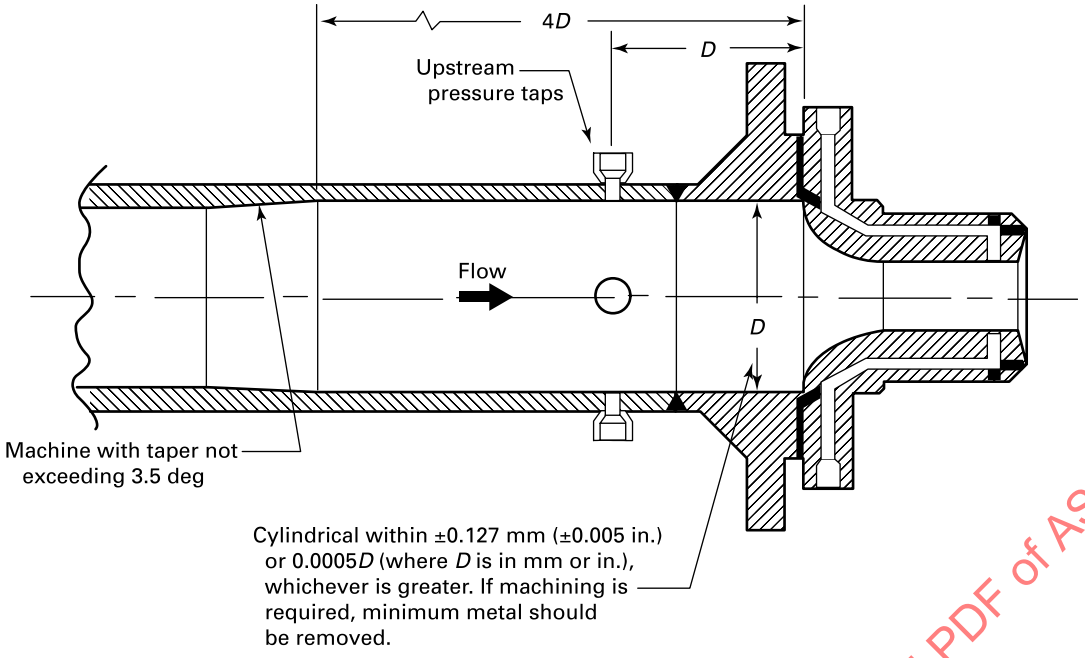

5-4 NOZZLE PRESSURE TAP REQUIREMENTS

The upstream tap shall be located in the pipe wall at a distance, D, ($+0.2D$, $-0.1D$) from the plane of the inlet face of the nozzle. Nozzles without throat taps shall use wall taps located at $0.5D$ ($\pm 0.01D$) downstream of the plane of the inlet face of the nozzle. Under some installation geometries, this specification places the tap downstream of the nozzle exit plane and that is not permitted. Under no circumstances may any part of the downstream tap be located downstream of the nozzle exit.

A minimum of two differential pressure tap sets separated by 90 deg or 180 deg are required. When installed horizontally, the connecting tubing must meet the recommended slope. Care should be taken that the pressure taps do not become plugged; therefore, no tap should be located at the bottom. Taps oriented vertically downward are more susceptible to being plugged by debris. Taps oriented vertically upward are susceptible to gas collection, introducing error in pressure measurement when measuring liquids. Upward oriented taps are not preferred but may be used. Using multiple sets of taps may help to indicate nozzle degradation caused by use, debris, or other irregularities.

Two sets of differential pressure taps are required to achieve the lowest desired uncertainty. Differential pressure is measured at each set of taps. The flow calculation is done separately for each pair and averaged. If the meter is flow calibrated, then the discharge coefficient should be derived for each tap set and used in the flow calculation. Investigation is needed if the results differ from each tap set calculation by more than 0.2%.

5-4.1 Wall Tap Nozzles

The upstream and downstream taps for wall tap nozzles shall have the same diameter.

For high and low β wall tap nozzles, the diameter of pressure taps shall be less than $0.13D$ and less than 13 mm (0.5 in.). No restriction is placed on the minimum diameter, which is determined in practice by the need to prevent blockage and to give satisfactory dynamic performance.

The pressure taps shall be circular and cylindrical over a length of at least 2.5 times the internal diameter of the tap, measured from the inner wall of the pipeline.

5-4.2 Throat Tap Nozzles

The throat tap nozzle shall be manufactured with four throat taps located 90 deg apart. The throat pressure taps shall be between 3 mm (0.125 in.) and 6 mm (0.25 in.) in diameter and at least 2 diameters deep. They shall be machined perpendicular to the bore surface, have sharp corners, and be free from nicks, burrs, scratches, or wire edges. The surface finish shall be as described in para. 5-3.4 and shall be free from ripples, scratches, and burrs. The pressure taps shall be drilled and reamed before performing the final boring and polishing of the throat section. A plug shall be pressed into the hole and removed after this final finishing of the throat. Use of a plug is required to ensure proper machining of a sharp burr-free tap hole edge. Any slight burr shall be removed. Additional details for throat tap nozzles are provided in ASME PTC 6.

5-5 NOZZLE INSTALLATION REQUIREMENTS

In cases where the flow section does not include all elements described in paras. 5-5.1 through 5-5.7, additional uncertainty shall be included for the effects of the installation, including velocity distributions and upstream and downstream piping (e.g., relative roughness and misalignment of the pipe centerlines).

5-5.1 Flanged Installation

ASME nozzles are designed to be installed between raised face pipe flanges. Nozzles may also be used with other styles of flanges if such use does not interfere with the flow.

5-5.2 Installation Without Flanges

ASME nozzles may also be installed directly in pipe by welding or pinning the nozzle to the pipe inside diameter. If such a method is used, care should be taken to ensure against any protrusions into the flow upstream or downstream of the nozzle.

5-5.3 Centering

The nozzle shall be manufactured using either a shoulder or pins. See Section 6 for specific centering requirements.

5-5.4 Straight Lengths

The upstream and downstream straight length requirements to meet the uncalibrated discharge coefficient uncertainties are specified in Section 6. Straight length requirements for ASME PTC 6-2004 calibrated throat tap nozzles are found in that code and shown in Figure 5-3-6.

5-5.5 Flow Conditioners

One of the appropriate flow conditioners discussed in Section 6 should be used for achieving the best repeatability between laboratory calibration and field test installations.

5-5.6 Diffusers

A diffuser section may be added to the exit of a throat tap nozzle to reduce the amount of unrecoverable pressure loss, but the throat shall be extended by $d/2$. It shall be properly installed (see example in Figure 5-5.6-1). Note that for a two-piece nozzle and diffuser assembly, a step transition of $1.013d$ to $1.017d$ is required as shown in Figure 5-5.6-1 to avoid any protrusion of the diffuser section into the throat flow stream. The flow nozzle shall be calibrated and used with the diffuser always attached.

5-5.7 Assembly

Subsection 6-4 defines requirements for primary element installation including alignment and centering. Whenever possible, it is preferred to ship the flow section as one piece and not disassembled for shipping or installation.

Figure 5-5.6-1
Nozzle With Diffusing Cone

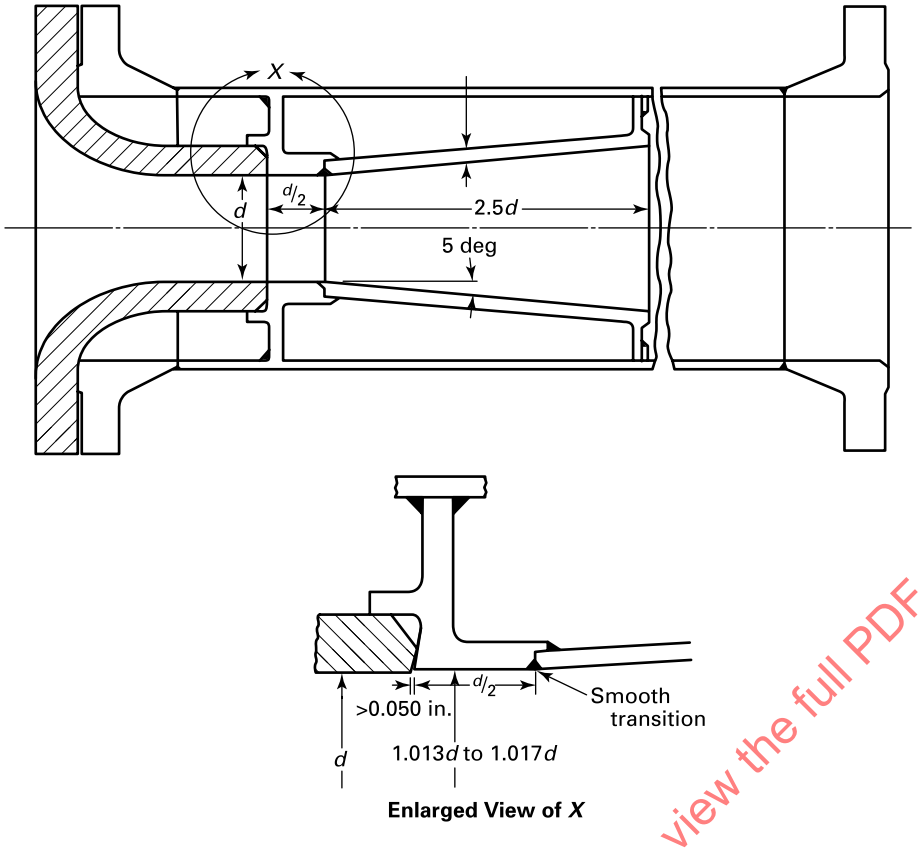

5-6 DISCHARGE COEFFICIENT FOR ASME NOZZLES

5-6.1 High β and Low β Nozzles

5-6.1.1 Equation for the Discharge Coefficient. The discharge coefficient, C, for both high β and low β nozzles with wall taps is given by

$$C = 0.9965 - 0.00653\left(\frac{1{,}000{,}000}{Re_d}\right)^{0.5} \tag{5-6-1}$$

where

Re_d = throat Reynolds number

Equation (5-6-1) is limited to 50 mm (2 in.) ≤ D ≤ 630 mm (25 in.) and for 10,000 ≤ Re_d ≤ 20,000,000.

The discharge coefficient equation covers the laminar, transition, and turbulent Reynolds number ranges. The transition region is influenced by factors such as roughness, turbulence intensity, and upstream conditions affecting the transition between laminar and turbulent boundary layers. Typically, transition occurs between throat Reynolds numbers of approximately 500,000 and 2,000,000.

5-6.1.2 Uncertainty of the Discharge Coefficient for Uncalibrated Flow Sections. When the nozzle is made and installed in accordance with ASME PTC 19.5, the uncertainty of the discharge coefficient in eq. (5-6-1) for uncalibrated flow sections is ±1% for wall tap nozzles with D ≥ 100 mm (4 in.) and ±2% with D < 100 mm (4 in.).

Figure 5-6.2.1-1
Reference Curve for Throat Tap Nozzles

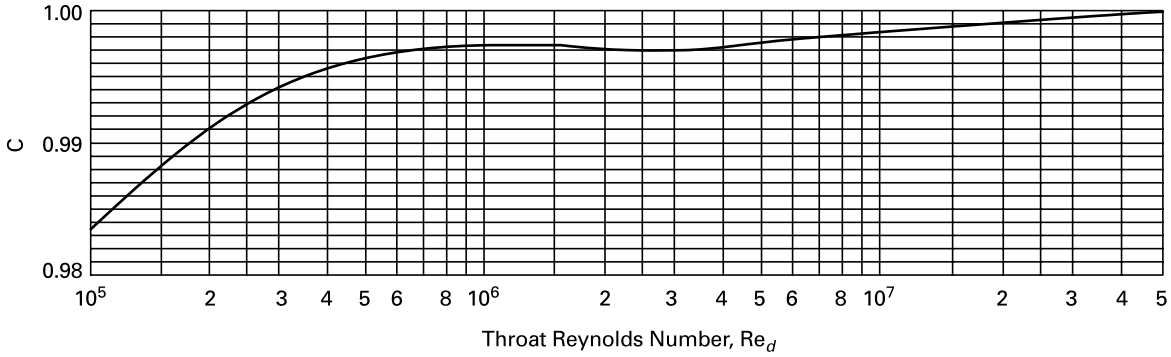

5-6.2 Throat Tap Nozzles

5-6.2.1 Reference Curve and Equation for the Discharge Coefficient. The reference curve for throat tap nozzles is shown in Figure 5-6.2.1-1 and was derived from a detailed boundary layer analysis and corroborated later by a study yielding the expression given in eq. (5-6-2) (see ASME PTC 6). The equation is limited to throat Reynolds numbers greater than or equal to 1,000,000. The reference curve is shown for throat Reynolds numbers greater than or equal to 100,000.

The curve illustrates a laminar flow regime for throat Reynolds numbers less than 1,000,000. In practice, laminar flow may occur up to Reynolds numbers of about 500,000. The laminar boundary layer usually begins to transition to include a partly turbulent boundary layer at Reynolds numbers between 500,000 and 800,000. The fully turbulent boundary layer regime generally occurs with Reynolds numbers between 1,000,000 and 3,500,000.

A study using flat-plate boundary layer development yielded the following equation, which closely agrees with Figure 5-6.2.1-1 for Reynolds numbers greater than 1,000,000 (See ASME PTC 6-2004):

$$C = 1.0054 - 0.185\mathrm{Re}_d^{-0.2}\left(1 - \frac{361{,}239}{\mathrm{Re}_d}\right)^{0.8} \tag{5-6-2}$$

Equation (5-6-2) is limited to throat Reynolds numbers greater than or equal to 1,000,000.

5-6.2.2 Uncertainty of the Discharge Coefficient for Uncalibrated Flow Sections. Throat tap nozzles are typically calibrated. However, when the nozzles are made and installed in accordance with this Supplement and the additional requirements for ASME PTC 6-2004 throat tap nozzles, the uncertainty of the discharge coefficient in eq. (5-6-2) for uncalibrated flow sections is ±0.7% for throat Reynolds numbers greater than or equal to 1,000,000.

For throat Reynolds numbers less than 1,000,000, the reference curve may be used (see Figure 5-6.2.1-1), but the uncertainty is larger than the value in the preceding paragraph. For applications with throat Reynolds numbers less than 1,000,000 that require a defined uncertainty, a calibration is needed at the applicable range of Reynolds numbers to determine the discharge coefficient (see subsection 5-12).

5-7 THE ASME VENTURI TUBE

The venturi tube combines a cylindrical inlet section, a convergent section, a cylindrical throat, and a divergent section into a single unit. Suitable pressure taps are provided for observing the difference in pressures between the inlet and the throat.

The proportions of a venturi tube used for metering liquids or gases are substantially the same as those adopted in 1887 by its inventor, Clemens Herschel. The required form of construction is shown in Figure 5-7-1. Starting at the upstream end, the first portion is a cylindrical inlet that matches the upstream inside diameter of the pipe. This section shall be carefully manufactured to meet the requirements of para. 5-8.1 and Section 6. The inlet has pressure taps and its diameter is accurately measured. The inlet static pressure shall be measured with a minimum of two pressure taps, evenly spaced around the inlet section, measured independently. Four taps may be used if desired.

Figure 5-7-1
Profile of the ASME Venturi

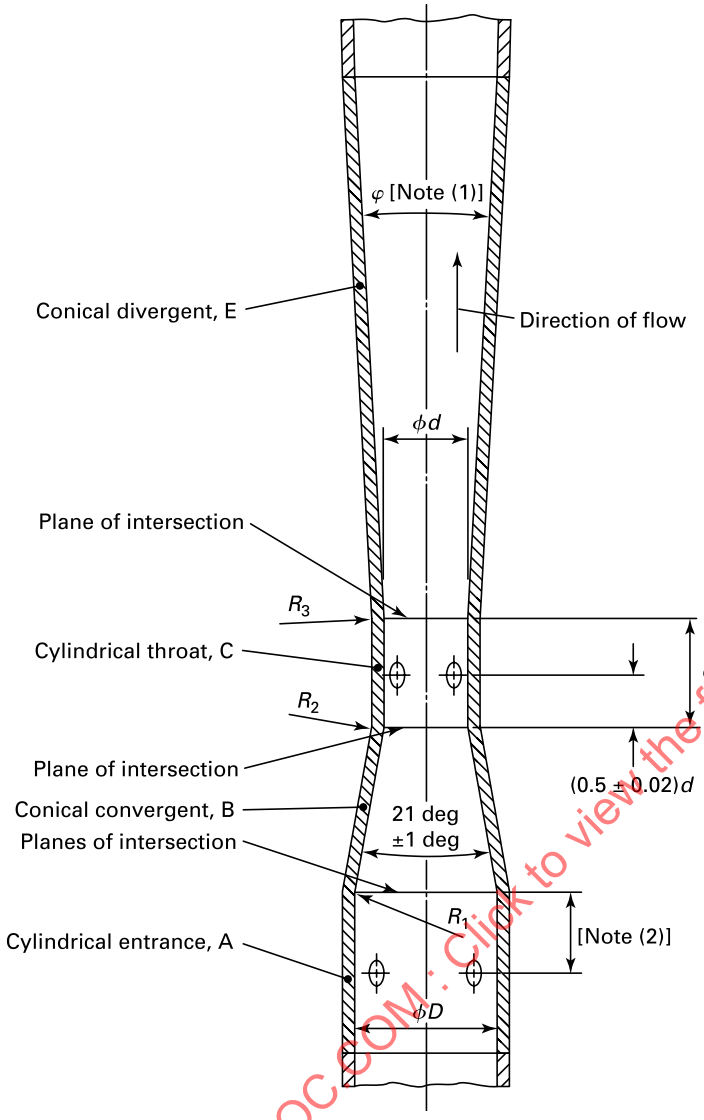

NOTES:
(1) 7 deg ≤ ϕ ≤ 15 deg
(2) Specific pressure tap requirements are provided in subsection 5-9.

Following the inlet cylinder is the convergent cone that has an included angle of 21 deg. The entrance cone leads to the short cylindrical throat that is accurately machined or fabricated. The pressure taps in the throat measure static pressure in the throat.

The end of the throat leads into the exit or diffuser cone, which has an included or total angle between 7 deg and 15 deg. Various designs, materials, and methods of manufacture are used for venturi tubes.

There are two types of ASME venturi tubes for ASME PTC 19.5 applications

(a) machined convergent section

(b) fabricated (also known as a "rough welded") convergent section

"As-cast" convergent sections are not suitable for ASME PTC 19.5 applications. ASME PTC 19.5 requirements apply to both machined and fabricated types unless otherwise stated.

5-8 VENTURI DESIGN AND DESIGN VARIATIONS

The diameter of the throat of the venturi should be such that $0.30 \le \beta \le 0.75$. The angle of the diverging cone does not influence the discharge coefficient.

5-8.1 Entrance Section

The entrance section shall have a length equal to or greater than its inside diameter, D. Upstream pipe sections may be needed to satisfy the straight length requirements of Section 6. The inside diameter of the entrance section shall not vary from the matching pipe inside diameter by more than $0.01D$ and it shall be concentric with the matching upstream pipe when examined visually. The inside diameter of the entrance section shall be measured in the plane of the pressure taps at a minimum of four equally spaced (approximately 45 deg) measurements passing through the centerline of the section. These measurements shall be made so that at least one measurement is taken at or near each pressure tap. No inside diameter measurement shall vary from the average of these measurements by more than ±0.3%.

5-8.2 Convergent Section

The convergent section shall be conical with an included angle of 21 deg ± 1 deg. The profile of the convergent section may be checked with a straight template and shall not deviate from the template by more than $0.005D$.

5-8.3 Throat

The throat inside diameter, d, shall be cylindrical to within 0.1% of the average inside diameter. The throat shall be parallel with the centerline of the venturi tube assembly. The length of the throat shall be equal to $d \pm 0.03d$.

The inside diameter, d, shall be measured in the plane of the pressure taps at four equally spaced radial measurements passing through the centerline of the throat. The location of these measurements may be made beginning at any point on the internal circumference as long as at least one measurement is taken at or near each pressure tap. No inside diameter measurement shall vary from the average of these measurements by more than 0.1%.

5-8.4 Divergent Section

The divergent section shall be conical and shall have an included angle between 7 deg and 15 deg. An angle of 7 deg produces minimum unrecoverable pressure loss. The smallest diameter of the divergent section shall be not less than the inside diameter, d. There shall be no protrusion, step, or shoulder impeding the flow from the throat. The larger end of the divergent section shall have an inside diameter, D, and shall terminate at the matching pipe or component inside diameter D unless truncated as allowed by agreement. When furnishing venturi tubes without flanged ends, the venturi may be supplied with an exit cylinder section attached to the divergent section to accommodate installation to the matching downstream pipe.

A venturi tube may be shortened by up to 35% of the divergent section length by truncation. A venturi tube is truncated when the outlet diameter of the divergent section is less than the matching pipe or component inside diameter, D. Such truncation may increase the unrecoverable pressure loss.

5-8.5 Roughness

If the ASME venturi has a machined convergent section, then the entrance, convergent, and throat sections should have a hydraulically smooth surface finish. This is determined from the ratio of surface finish to throat diameter, d (as shown on the vertical axis of Figure 5-3.4-1), and the surface finish shall always be less than 2.54 μm (100 μin.). Machining or surface polishing is acceptable.

If the ASME venturi has a fabricated convergent section, then the entrance and convergent sections shall have a surface finish less than 6.4 μm (250 μin.). The throat section shall have a surface finish less than 2.54 μm (100 μin.). These venturis are welded or otherwise fabricated with a higher allowable roughness for the entrance and convergent sections than the throat section.

5-8.6 Materials

Venturi tubes shall be manufactured from a material that does not wear excessively and remains dimensionally stable in continued use.

5-8.7 Manufacture

The surface finish of the throat section is critical to proper flow measurement. The throat surface should be protected by one of the following methods:

(a) After it is joined to the convergent section, the throat section is machined or otherwise verified to be of sufficient smoothness.

(b) The throat section is of sufficient length to allow for the manufacture of the radius, R_2, and a portion of the convergent angle, so that the joining of the convergent section to the throat shall be at a diameter greater than d (see Figure 5-7-1).

(c) In joining the convergent and divergent sections to the throat, the sections shall be centered with the throat. There shall be no steps between the inside diameters of the two parts.

5-8.8 Characteristics of a Machined Convergent Section

For a machined convergent section, the radius of curvature R_1 shall be $0.25D$ maximum, and the radii of curvature for R_2 and R_3 shall be $0.25d$ maximum. The length of the cylindrical part between the end of the radius R_2 and the beginning of the radius R_3 shall be no less than $0.89d$ (see Figure 5-7-1).

5-8.9 Characteristics of a Fabricated Convergent Section

For a fabricated convergent section, there shall be no curvature for R_1, R_2, and R_3 other than that resulting from welding (see Figure 5-7-1).

5-9 VENTURI PRESSURE TAPS

5-9.1 Number of Taps

A minimum of two upstream and two throat taps shall be provided. Although two taps are required, four upstream and four throat taps are recommended. Tap sets should be individually instrumented for flow measurement. Other pressure tap requirements in subsection 5-4 also apply.

5-9.2 Tap Location

Upstream taps shall be located on the entrance section at a distance of $0.5D$ ($\pm 0.05D$) upstream of the convergent section. Throat taps shall be located at $0.5d$ ($\pm 0.02d$) downstream of the end of the convergent section. Both upstream and throat taps shall be spaced equally (i.e., 180 deg or 90 deg apart).

5-9.3 Tap Hole Edge

The edge of each pressure tap hole shall be square, sharp, and free from burrs or nicks at the inner surface.

5-9.4 Tap Length

The pressure tap hole shall be circular and cylindrical for a length at least 2.5 times the diameter of the hole measured from the inside surface of the venturi.

5-9.5 Tap Size

The tap hole should be between 4 mm (0.15 in.) and 10 mm (0.4 in.) inclusive, but not greater than $0.1D$ for upstream taps and $0.13d$ for throat taps. Pressure taps should be as small as possible, but the possibility of tap hole plugging by contamination should also be considered.

5-9.6 Pressure Taps With Annular Chambers.

The area of the free cross section of the annular chamber of the pressure taps shall be greater than or equal to half the total area of the tap holes connecting the chamber to the pipe. See Section 6 for straight length requirements.

5-10 DISCHARGE COEFFICIENT OF THE ASME VENTURI

5-10.1 Equation for the Discharge Coefficient

The discharge coefficient, C, for the ASME venturi is given by

$$C = 1.0054 - \frac{0.185}{\mathrm{Re}_d^{0.2}} \tag{5-10-1}$$

where

Re_d = throat Reynolds number

Equation (5-10-1) is limited to $200{,}000 \le \mathrm{Re}_d \le 17{,}000{,}000$.

For a machined convergent section, the discharge coefficient is limited to 50 mm (2 in.) $\le D \le$ 1 200 mm (48 in.). For a fabricated convergent section, eq. (5-10-1) is limited to 100 mm (4 in.) $\le D \le$ 1 200 mm (48 in.).

The discharge coefficient equation covers the laminar, transition, and turbulent Reynolds number regimes. Additional discussion of these boundary layers is provided in para. 5-6.2. Equation (5-10-1) is a modified form of the throat tap correlation given by eq. (5-6-2) and is applicable for the extended Reynolds number range shown herein.

5-10.2 Uncertainty of Discharge Coefficient for Uncalibrated Flow Sections

When the venturi is made and installed in accordance with this Supplement, the uncertainty of the discharge coefficient in eq. (5-10-1) for uncalibrated flow sections is ±1.0% for a machined convergent section and ±1.5% for a fabricated convergent section.

5-11 INSTALLATION REQUIREMENTS FOR THE ASME VENTURI

5-11.1 Installation Requirements

See subsections 6-4 and 6-5 for installation and straight length requirements.

5-11.1.1 Roughness of Upstream Pipe. See subsection 6-3 for upstream pipe roughness requirements.

5-11.1.2 Alignment of the ASME Venturi. The offset between the centerlines of the upstream pipe and the venturi shall be less than $0.005D$ and shall be aligned with the upstream piping to within 1 deg.

5-12 LABORATORY CALIBRATIONS

Calibration requirements and the Reynolds number extrapolation methodology suitable for nozzles and venturis are provided in Mandatory Appendix I.

The uncertainty of a calibrated flow section shall be determined applying the methods in ASME PTC 19.1 to both the laboratory facilities and the calibration data. Achievable best estimates of calibration uncertainties for flow facilities are

(a) 0.1% for water calibrations
(b) 0.1% for hydrocarbon liquids and viscous fluids
(c) 0.25% for well-known gases

5-13 UNCERTAINTY OF EXPANSION FACTOR, ε

When β and $\Delta P/P_1$ are assumed to be known without error, the relative uncertainty, %, of the value of the expansion factor, ε, shall be calculated as shown herein.

(a) For the ASME nozzles, the relative uncertainty is calculated using eq. (5-13-1).

$$\text{uncertainty of } \varepsilon = 2\left(\frac{\Delta P}{P_1}\right)\% \tag{5-13-1}$$

(b) For the ASME venturi, the relative uncertainty is calculated using eq. (5-13-2).

$$\text{uncertainty of } \varepsilon = \left(4 + 100\beta^8\right)\left(\frac{\Delta P}{P_1}\right)\% \tag{5-13-2}$$

with ΔP and P_1 in the same units.

5-14 UNRECOVERABLE PRESSURE LOSS

5-14.1 ASME Nozzles Without a Diffusing Section

The unrecoverable pressure loss, $\Delta\omega$, is related to the measured pressure drop across the nozzle, ΔP, by

$$\Delta\omega = \frac{\sqrt{1 - \beta^4\left(1 - C^2\right)} - C\beta^2}{\sqrt{1 - \beta^4\left(1 - C^2\right)} + C\beta^2}\Delta P \tag{5-14-1}$$

with $\Delta\omega$ and ΔP in the same units.

5-14.2 ASME Nozzles With a Diffusing Section

Specific designs may have lower losses, but a reasonable estimate of the unrecoverable pressure loss, $\Delta\omega$, as related to the measured pressure drop across the nozzle, ΔP, is given by

$$\Delta\omega = \left(0.274 - 0.626\beta + 0.40\beta^2\right)\Delta P \tag{5-14-2}$$

with $\Delta\omega$ and ΔP in the same units.

5-14.3 ASME Venturis

The unrecoverable pressure loss, $\Delta\omega$, is related to the measured pressure drop across the venturi, ΔP, by the following equations for divergent sections without truncation:

(a) For a 7 deg exit cone

$$\Delta\omega = \left(0.218 - 0.42\beta + 0.38\beta^2\right)\Delta P \tag{5-14-3}$$

(b) For a 15 deg exit cone

$$\Delta\omega = \left(0.436 - 0.86\beta + 0.59\beta^2\right)\Delta P \tag{5-14-4}$$

with $\Delta\omega$ and ΔP in the same units.

5-15 REFERENCES

ASME PTC 6–2004. Steam Turbines. The American Society of Mechanical Engineers.
ASME MFC-3M–2004. Measurement of Fluid Flow in Pipes Using Orifice, Nozzle, and Venturi. The American Society of Mechanical Engineers.
ASME MFC-3Ma–2007. Addenda to ASME MFC-3M–2004, Measurement of Fluid Flow in Pipes Using Orifice. Nozzle, and Venturi. The American Society of Mechanical Engineers.
Miller, R. W. (1996). Flow Measurement Engineering Handbook (3rd ed.). McGraw-Hill.

Section 6
Differential Pressure Class Meter Installation and Flow Conditioning Requirements

6-1 NOMENCLATURE

Symbols used in Section 6 are included in Tables 2-3-1 and 3-1-1.

6-2 INTRODUCTION

The optimum location for a primary element (e.g., orifice, nozzle, or venturi) is where the flow conditions immediately upstream approximate those of a fully developed profile free from swirl. Empirical discharge coefficients are based on data from laboratories that approximate such a condition.

A fully developed, turbulent velocity profile describes a flow condition that is constant with distance along the pipe-length. The velocity profile is axially symmetric, changing slowly across the central area of the conduit. It then changes more rapidly toward the wall, where it eventually goes to zero velocity at the conduit surface. Superimposed on this time-average profile is isotropic turbulence. The difference between this profile and the uniform profile assumed in one-dimensional theory gives rise to the published calibration coefficients for various classes of flowmeters. Flow calibration laboratories make every effort to approximate this velocity profile by using flow conditioners and sufficient lengths of straight pipe. However, this velocity profile is rarely found in the plant where a performance test is conducted.

Up to 50 straight pipe diameters are required for viscous effects to produce a fully developed profile. Meanwhile, fittings of all types disturb the velocity distribution. Whenever flow goes around a bend, higher velocities are found downstream outside of the bend and angular momentum is imparted to the flow, skewing the velocity profile. When two such bends are found close to each other and out of plane, a helical streamline pattern called swirl may be generated. Swirl degrades the accuracy of differential pressure meters. Significant straight pipe, greater than 50 pipe diameters, is required for the fluid viscosity to affect the decay of angular momentum and to redistribute the velocity profile.

Subsection 6-3 describes the specially fabricated piping adjacent to the primary element; together, these comprise the metering section. Additional straight pipe lengths are required to achieve the uncertainty levels in Sections 3, 4, and 5. These lengths are dependent on the type of upstream fitting and are described in subsection 6-5. If sufficient straight pipe length is unavailable to achieve the requisite uncertainty for the metering section, the use of a flow conditioner is recommended (see subsection 6-6). Various conditioner designs are effective in removing swirl or redistributing the axial velocity profile, and some do both. The tradeoff comes in how much unrecoverable pressure loss can be tolerated. Calibration of the metering section may be required to achieve the lowest possible uncertainty. For differential pressure meter calibration, see para. 3-10(c).

6-2.1 Recommended Practice

When the temperature of the fluid is above or below ambient such that the difference in temperature may affect the fluid properties, thermal insulation of the entire meter section may be advisable.

6-3 METERING SECTION REQUIREMENTS

The metering section is composed of specially fabricated pipe sections $4D$ upstream and $2D$ downstream of the primary element. The normal methods of fabricating piping and components are not satisfactory for accurate flow measurement. The requirements set forth in para. 6-3.1 must be followed, and no deviations are permitted. In the design stages, the installation drawing shall be checked for clarity and precision of fabrication instructions. After fabrication, inspection shall be performed to ensure that all requirements are met, and documentation shall be created to record when the necessary corrections have been made. Measurements shall be made as required by para. 6-5.3. Additional straight lengths of standard piping are required both upstream and downstream of the primary element to achieve the uncertainty values defined for three differential producing meters (orifice, nozzle, or venturi) when a flow conditioner is not included.

These are given in Tables 6-5.1-1 through 6-5.1-3. Metering section lengths with a flow conditioner are discussed in subsection 6-6. Temperature-measuring connections may be required under certain conditions and are specified in subsection 6-7.

6-3.1 Fabrication of the Metering Section Pipe

The following shall be considered when fabricating the metering section pipe:

(a) Boring or honing may be necessary to secure the required degree of surface smoothness and circularity in the metering section, defined as $4D$ preceding the inlet and $2D$ following the outlet of the primary element. The surface roughness shall not be greater than 8.89 μm (350 μin.). The pipe shall be cylindrical in shape such that no diameter departs from the average diameter, D, by more than 0.3%. The internal surface of the required additional run of pipe immediately preceding and following the metering section shall be straight and free from mill scale, pits or holes, reamer scores or rifling, bumps, and other irregularities. The $4D$ inlet section shall be faired into upstream pipe at an included angle of less than 30 deg when the upstream pipe diameter is smaller. The depth of material removed shall be the minimum required to obtain the desired condition, and all finishing operations shall be done after welding of flanges and pressure connections. Flanges, when used, shall be constructed and attached to the pipe so that there is no recess greater than 6 mm (0.25 in.) between the primary element and the flange face, measured parallel to the axis of the pipe. For meters with divergent section, the downstream pipe section does not need to meet the stringent requirements for smoothness and circularity.

(b) Grooves, scoring, pits, raised ridges resulting from seams, distortion caused by welding, offsets, backing rings, and similar irregularities, regardless of size, that change the inside diameter at such points by more than $0.001D$ shall not be permitted. When required, the roughness may be corrected by filling in, grinding, or filing off to obtain smoothness.

(c) Control should be effected by valves located downstream of the primary element. Isolating valves located upstream at distances greater than or equal to those recommended in Tables 6-5.1-1 through 6-5.1-3 shall be full-port gate- or ball-type valves and shall be fully open.

(d) Suitable drains or blow offs should be provided on the underside of the pipe on the inlet and outlet sides of the primary element when steam is measured in a horizontal pipe. If the pressures are measured through annular chambers, there should be drains in these chambers. In installations other than horizontal, the pipe adjacent to the primary element should be drained at the point of minimum elevation. The valves or cocks used on these drains should close tightly.

(e) Vents should be located on the upper side of the horizontal pipe to eliminate any entrapped gas when an incompressible fluid is measured. In installations other than horizontal, the piping system should be vented at the highest point.

6-4 METER INSTALLATION IN THE METERING SECTION

6-4.1 Alignment

The angular alignment of the primary element centerline with the metering section centerline (both upstream and downstream pipe sections) shall be less than 1 deg. In the case of an orifice plate, this requirement may be met by checking that the plate is perpendicular to the pipe centerline, also ensuring that the bore is perpendicular to the plate.

6-4.2 Centering

The primary element shall be centered with eccentricity defined as the distance between the throat centerline and the pipe centerline. The acceptable eccentricity, e_c, to achieve the uncalibrated meter coefficients defined in individual sections is different for each differential meter type. For orifice meters and wall tap nozzles, the eccentricity limits apply to both upstream and downstream pipe sections. For throat tap nozzles and meters with a divergent section, the eccentricity requirement is not applicable to the downstream pipe section.

6-4.2.1 Nozzles. For nozzles, the acceptable eccentricity is defined by

$$e_c \leq \frac{0.005}{0.1 + 2.3\beta^4} D \tag{6-4-1}$$

6-4.2.2 Orifice Meters. For orifice meters, the acceptable eccentricity is defined differently in directions perpendicular and parallel to the axis of any pressure tap. For the perpendicular direction, the eccentricity shall be less than that defined by eq. (6-4-1). For the parallel direction, the eccentricity shall be less than one-half that defined by eq. (6-4-1). If one or more taps have an eccentricity in the parallel direction between ½ and 1 times eq. (6-4-1), the meter may be used but the uncertainty must be increased by 0.3%. If the eccentricity in either the parallel or perpendicular direction for any tap exceeds those defined by eq. (6-4-1), the additional uncertainty cannot be defined.

6-4.2.3 Venturi Meters. For venturi meters, the acceptable eccentricity is defined as $0.005D$.

6-5 ADDITIONAL PIPE LENGTH REQUIREMENTS

6-5.1 Pipe Length

The metering section shall be fitted between two sections of straight cylindrical pipe of constant cross-sectional area in which there is no obstruction or branch connection (whether there is flow into or out of such connections during measurement). The required minimum straight lengths of pipe vary according to fitting type, the type of primary element, and the diameter ratio, β. Table 6-5.1-1 (for orifices), Table 6-5.1-2 (for nozzles), and Table 6-5.1-3 (for venturi meters) include the upstream and downstream total straight lengths required in pipe diameters for two cases. Case A is the systematic uncertainty of the discharge coefficient as stated in each section for uncalibrated meters (no additional discharge coefficient uncertainty), and case B requires that a systematic uncertainty of 0.5% be added arithmetically.

The lengths listed in Tables 6-5.1-1 through 6-5.1-3 include the required specially fabricated pieces of the metering section ($4D$ upstream and $2D$ downstream). It is not practical to show every possible installation; each must be considered on its own merits. For β values between those listed in Tables 6-5.1-1 through 6-5.1-3, a linear interpolation may be applied with rounding to the larger whole number. The values given in these tables were obtained experimentally with sufficient straight lengths of pipe upstream of each kind of fitting to assume that the flow upstream of the disturbance was fully developed and swirl free.

For lengths exceeding case A in Tables 6-5.1-1 through 6-5.1-3, the systematic uncertainties of the uncalibrated discharge coefficient defined in Sections 3, 4, and 5 or a laboratory calibration uncertainty may be used. For lengths between columns A and B in these tables, a systematic uncertainty of 0.5% must be added arithmetically to the uncalibrated discharge coefficient uncertainty or laboratory calibration uncertainty. For a length shorter than those given in Column B, the uncertainty that should be added is undetermined but is most likely greater than 0.5%. In such instances, it is good practice to calibrate the meter in the piping arrangement of the installation. When the piping of the installation is replicated in the laboratory calibration, the systematic uncertainty of the discharge coefficient or a laboratory calibration may be used. For a symmetrical abrupt area reduction, a straight length of $30D$ is required for no additional uncertainty, and $15D$ is required for 0.5% additional uncertainty for all meter types.

6-5.2 Cases Not Covered

For installations not covered explicitly or where the piping configuration and fittings are not known at the time of design, the worst case shall be used (the maximum lengths of straight pipe). When more than one type of piping configuration is found upstream of the metering section, each one may have some effect, because it is not always the first fitting configuration upstream that governs. If there is less than the recommended straight pipe between any two configurations (labeled S) shown on the relevant schedules in Tables 6-5.1-1 through 6-5.1-3, then the metering section shall be fabricated in accordance with the maximum lengths specified on the applicable schedules. Better yet, a calibration should be performed in accordance with Mandatory Appendix I.

If several fittings (other than 90 deg bends) are placed in series upstream from the primary element, the following rule shall be applied: between the closest fitting to the primary element and the primary element itself, there shall be a straight length as specified for the fitting and for the actual value of β. Also, between this fitting and the preceding one, there shall be a straight length equal to one-half of the value given for the second upstream fitting as specified for a β value equal to 0.7, no matter what the actual value of β may be. This requirement does not apply when that fitting is an abrupt symmetrical reduction covered in para. 6-5.1.

When the primary element is installed in a pipe leading from an upstream open space or large vessel, either directly or through any fitting, the total length of pipe between the open space and the primary element shall never be less than $30D$.

6-5.3 Pipe Diameter Requirements

6-5.3.1 Upstream Pipe Measurement. The pipe is considered straight when it appears so by visual inspection. The $4D$ inlet section shall be measured on four or more diameters in the plane of the inlet pressure tap to compute the diameter, D, of the primary element. Measurements shall be made on four or more diameters in two additional cross sections distributed approximately equally for a distance of $2D$ upstream. The values of all such upstream diameters shall agree within 0.3%.

To assure no additional uncertainty is incurred, the pipe between $4D$ and $10D$ upstream shall have a diameter within ±0.3% of the diameter, D, determined in the $4D$ inlet section. Moreover, any step caused by misalignment of pipe sections must not exceed 0.3% of D at any point on the internal circumference of the pipe. Mating flanges, if any, require the bores to be matched and the flanges aligned on installation. Dowels or self-centering gaskets can be used.

Table 6-5.1-1
Straight Lengths for Orifice Meters

	On Upstream (Inlet) Side of the Primary Element																Downstream (Outlet) Side	
	Single 90 deg Bend or Tee (Flow From One Branch Only) [Note (1)]		Two or More 90 deg Bends in Same Plane, $30D \geq S > 10D$ [Note (1)]		Two or More 90 deg Bends in Same Plane, $S \leq 10D$ [Note (1)]		Two 90 deg Bends in Perpendicular Planes $S < 5D$ [Note (1)]		Two 90 deg Bends in Perpendicular Planes, $30D \geq S > 5D$ [Note (1)]		Concentric Reducer ($2D$ to D Over a Length of $1.5D$ to $3D$)		Concentric Expander ($0.5D$ to D Over a Length of D to $2D$)		Full-port Gate or Ball Valve Fully Open		All Fittings in This Table	
β	A	B	A	B	A	B	A	B	A	B	A	B	A	B	A	B	A	B	A	B
0.2	10	6	14	7	14	7	34	17	19	18	5	No Data [Note (2)]	6	No Data [Note (2)]	12	6	4	2
0.3	10	6	16	8	16	8	34	17	44	18	5	No Data [Note (2)]	9	8	12	6	5	2.5
0.4	16	7	18	9	18	9	50	25	44	18	5	No Data [Note (2)]	12	8	12	6	6	3
0.5	22	9	20	10	22	10	75	34	44	18	8	5	20	9	12	6	6	3
0.6	42	13	30	18	42	18	65	25	44	20	9	5	26	11	14	7	7	3.5
0.67	44	20	44	18	44	20	60	18	44	20	12	6	28	14	18	9	7	3.5
0.75	44	20	44	18	44	22	75	18	44	20	22	11	36	18	24	12	8	4

GENERAL NOTES:

(a) S is distance measured from the downstream end of curved portion of upstream bend to the upstream end of the curved portion of the downstream bend.

(b) All straight lengths are expressed as multiples of diameter, D. The pipe relative roughness shall not exceed that of a smooth, commercially available pipe approximately $k/D < 10^{-3}$.

(c) Straight lengths required to meet the systematic uncertainties of the discharge coefficient delineated herein are given in Column A. Straight lengths between the values in Column A and the values in Column B require a systematic uncertainty of 0.5% be added arithmetically to the uncertainties as presented herein for each meter. No estimate of the uncertainty is possible if the straight length is shorter than the required lengths shown in Column B.

NOTES:

(1) The radius of curvature of the bend shall be equal to or greater than $1.5D$. Lengths are measured from the end of the curvature of the bend.

(2) Data are not available for shorter lengths, which could be used to give the required straight lengths for 0.5% added uncertainty.

Table 6-5.1-2
Straight Lengths for Nozzles

	On Upstream (Inlet) Side of the Primary Element												Downstream (Outlet) Side	
	Single 90 deg Bend or Tee (Flow From One Branch Only) [Note (1)]		Two or More 90 deg Bends in Same Plane [Note (1)]		Two or More 90 deg Bends in Different Planes [Note (1)]		Reducer (2D to D Over a Length of 1.5D to 3D)		Expander (0.5D to D Over a Length of D to 2D)		Full-port Gate or Ball Valve Fully Open		All Fittings in This Table	
β	A	B	A	B	A	B	A	B	A	B	A	B	A	B
0.2	10	6	14	7	34	17	5	No Data [Note (2)]	16	8	12	6	4	2
0.3	10	6	16	8	34	17	5	No Data [Note (2)]	16	8	12	6	5	2.5
0.4	14	7	18	9	36	18	5	No Data [Note (2)]	16	8	12	6	6	3
0.5	14	9	20	10	40	20	6	5	18	9	12	6	6	3
0.6	18	9	26	13	48	24	9	5	22	11	14	7	7	3.5
0.75	36	18	42	21	70	35	22	11	38	19	24	12	8	4

GENERAL NOTES:

(a) S is distance measured from the downstream end of curved portion of upstream bend to the upstream end of the curved portion of the downstream bend.

(b) All straight lengths are expressed as multiples of diameter, D. The pipe relative roughness shall not exceed that of a smooth, commercially available pipe approximately $k/D < 10^{-3}$.

(c) Straight lengths required to meet the systematic uncertainties of the discharge coefficient delineated herein are given in Column A. Straight lengths between the values in Column A and the values in Column B require a systematic uncertainty of 0.5% be added arithmetically to the uncertainties as presented herein for each meter. No estimate of the uncertainty is possible if the straight length is shorter than the required lengths shown in Column B.

NOTES:

(1) The radius of curvature of the bend shall be equal to or greater than 1.5D. Lengths are measured from the end of the curvature of the bend.

(2) Data are not available for shorter lengths, which could be used to give the required straight lengths for 0.5% added uncertainty.

Table 6-5.1-3
Straight Lengths for Classical Venturi

	On Upstream (Inlet) Side of the Primary Element									
	Single 90 deg Bend [Note (1)]		Two 90 deg Bends in Same or Different Plane [Note (1)]		Reducer (3D to D Over a Length of 3.5D)		Expander (0.75D to D Over a Length of D)		Full-port Gate or Ball Valve Fully Open	
β	A	B	A	B	A	B	A	B	A	B
0.3	8	3	8	3	2.5	No Data [Note (2)]	2.5	No Data [Note (2)]	2.5	No Data [Note (2)]
0.4	8	3	8	3	2.5	No Data [Note (2)]	2.5	No Data [Note (2)]	2.5	No Data [Note (2)]
0.5	9	3	10	3	5.5	2.5	2.5	No Data [Note (2)]	3.5	2.5
0.6	10	3	10	3	8.5	2.5	3.5	2.5	4.5	2.5
0.7	14	3	18	3	10.5	2.5	5.5	3.5	5.5	3.5
0.75	16	8	22	8	11.5	3.5	6.5	4.5	6.5	3.5

GENERAL NOTES:
(a) All straight lengths are expressed as multiples of diameter, D. The pipe relative roughness shall not exceed that of a smooth, commercially available pipe approximately $k/D < 10^{-3}$.
(b) Straight lengths required to meet the systematic uncertainties of the discharge coefficient delineated herein are given in Column A. Straight lengths between the values in Column A and the values in Column B require a systematic uncertainty of 0.5% be added arithmetically to the uncertainties as presented herein for each meter. No estimate of the uncertainty is possible if the straight length is shorter than the required lengths shown in Column B.

NOTES:
(1) The radius of curvature of the bend shall be equal to or greater than 1D. Lengths are measured from the end of the curvature of the bend.
(2) Data are not available for shorter lengths, which could be used to give the required straight lengths for 0.5% added uncertainty.

Beyond 10D, no additional uncertainty in the discharge coefficient is incurred provided that the upstream pipe diameter is smaller than D by not greater than 2% of the mean value, D, determined in the 4D inlet section. If the pipe diameter beyond 10D upstream is greater than that downstream of it, the permitted diameter and allowable difference is increased from 2% to 6% of D. Any misalignment causing a step in the mated piping is required to meet the limits. These limits require no additional uncertainty.

If the above limits are exceeded, a systematic uncertainty of 0.2% shall be added arithmetically to the systematic uncertainty of the uncalibrated or laboratory discharge coefficient if the diameter step meets the following criteria:

$$\frac{\Delta D}{D} \leq 0.002\frac{\left(\frac{s'}{D} + 0.4\right)}{0.1 + 2.3\beta^4} \tag{6-5-1}$$

$$\frac{\Delta D}{D} \leq 0.05 \tag{6-5-2}$$

where
s' = distance of the step from the upstream pressure tap or, if a carrier ring is used, from the upstream edge of the recess formed by the carrier ring

For beta ratios less than 0.43, eq. (6-5-1) is not applicable. The diameter step requirements are illustrated in Figure 6-5.3.1-1, which was generated by applying eq. (6-5-1) for $\beta = 0.50$, $\beta = 0.55$, and $\beta = 0.65$, and by applying eq. (6-5-2).

6-5.3.2 Downstream Pipe Measurement. Measurements of the diameter of the outlet section shall be made 1D downstream of the outlet plane of a primary element without a divergent section. For orifice meters and wall tap nozzles, the 2D downstream pipe must meet the same requirements as the upstream 4D pipe. Beyond 2D, the downstream pipe diameter shall not differ by more than 3% for the minimum distance defined in the appropriate straight length tables.

For meters with throat taps with or without divergent sections, the diameter shall be within 90% of the upstream diameter.

Figure 6-5.3.1-1
Allowable Diameter Steps for 0.2% Additional Uncertainty

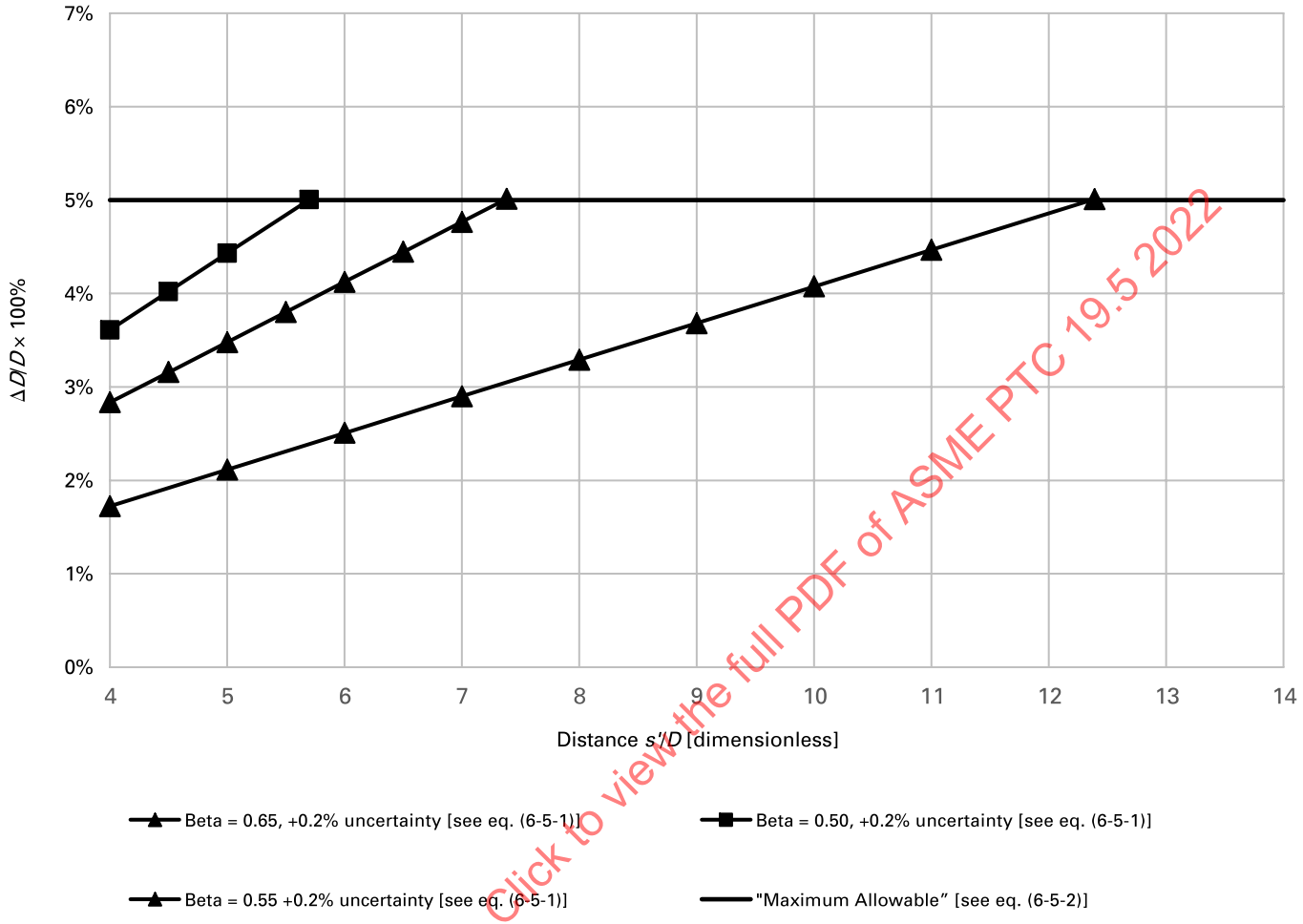

6-6 FLOW CONDITIONERS AND INSTALLATION

If the requirements for straight pipe cannot be met or the upstream piping configuration is more complicated than any of those listed in Tables 6-5.1-1 through 6-5.1-3, then the use of a flow conditioner is recommended to achieve the uncalibrated meter uncertainty. A minimum of 2D of straight pipe upstream of the flow conditioner is required and 18D straight pipe is required from the upstream end of the conditioner to the inlet of the primary element.

6-6.1 Flow Conditioner Design

The recommended designs of flow conditioners are shown in Figure 6-6.1-1. For removing both swirl and smoothing the velocity profile, the flow conditioner types in illustrations (a) and (b) are preferred. The tubular conditioner consists of multiple parallel tubes fixed together and held rigidly in the pipe. It is important in this case that the various tubes are parallel with each other and with the pipe axis. If this requirement is not met, the straightener itself might introduce disturbances into the flow. There shall be 19 to 52 tubes with a length of at least 2D; for example, 44 tubes are shown in Figure 6-6.1-1, illustration (a). The tubes shall be joined in a bundle and installed tangent to the pipe wall.

ASME MFC-3M contains specific design guidelines and dimensional requirements for flow conditioners.

6-6.1.1 Perforated Plate Conditioner. This conditioner uses a low-pressure drop perforated plate with a nonuniform hole distribution. The geometry of the design is shown in Figure 6-6.1-1, illustration (b), and hole coordinates are specified in Table 6-6.1.1-1. The specified thickness may be accomplished with a plate (see Figure 6-6.1-1) or a plate used in conjunction with tubes (not shown). Economic and manufacturing considerations determine which type is used. This plate and tube type are typically used for larger pipe sizes. The design and hole coordinates are identical for both types, plate or plate and tubes. The upstream side of the holes shall be beveled in all cases. The upstream plane of the flow straightener is located 18D upstream of the test flow nozzle inlet.

Other types of flow straighteners may be used if the ability to remove swirl and distortion from the upstream flow has been demonstrated. ASME MFC-3M includes specific guidelines for compliance testing of flow conditioners.

6-6.2 Flow Conditioner Loss

Typical unrecoverable pressure loss is given as

$$\Delta P = k_1 \rho \frac{V^2}{2} \tag{6-6-1}$$

The loss coefficient, k_1, is shown in Table 6-6.2-1 for various conditioner types.

6-7 INSTALLATION OF TEMPERATURE SENSORS

This paragraph specifies the installation of thermometers in the metering section. For a more thorough description and recommendations for accurate temperature measurement, see ASME PTC 19.3.

Thermometer wells with a diameter less than 0.03D require 5D pipe length before the meter for no additional uncertainty and a minimum of 3D for an additional uncertainty of 0.5%. Larger diameter wells (diameters up to 0.13D) require 20D and 10D upstream pipe length. If a flow conditioner is used, the preferable location is 2D upstream of the conditioner. Downstream, they may not be placed closer than 5 pipe diameters to the exit of the primary element.

When peened thermocouples are installed, they cause no interference with the flow. Thermocouples can be peened into the walls of piping and pressure vessels only when the wall thickness is greater than twice their hole depth.

Figure 6-6.1-1
Flow Conditioner Designs

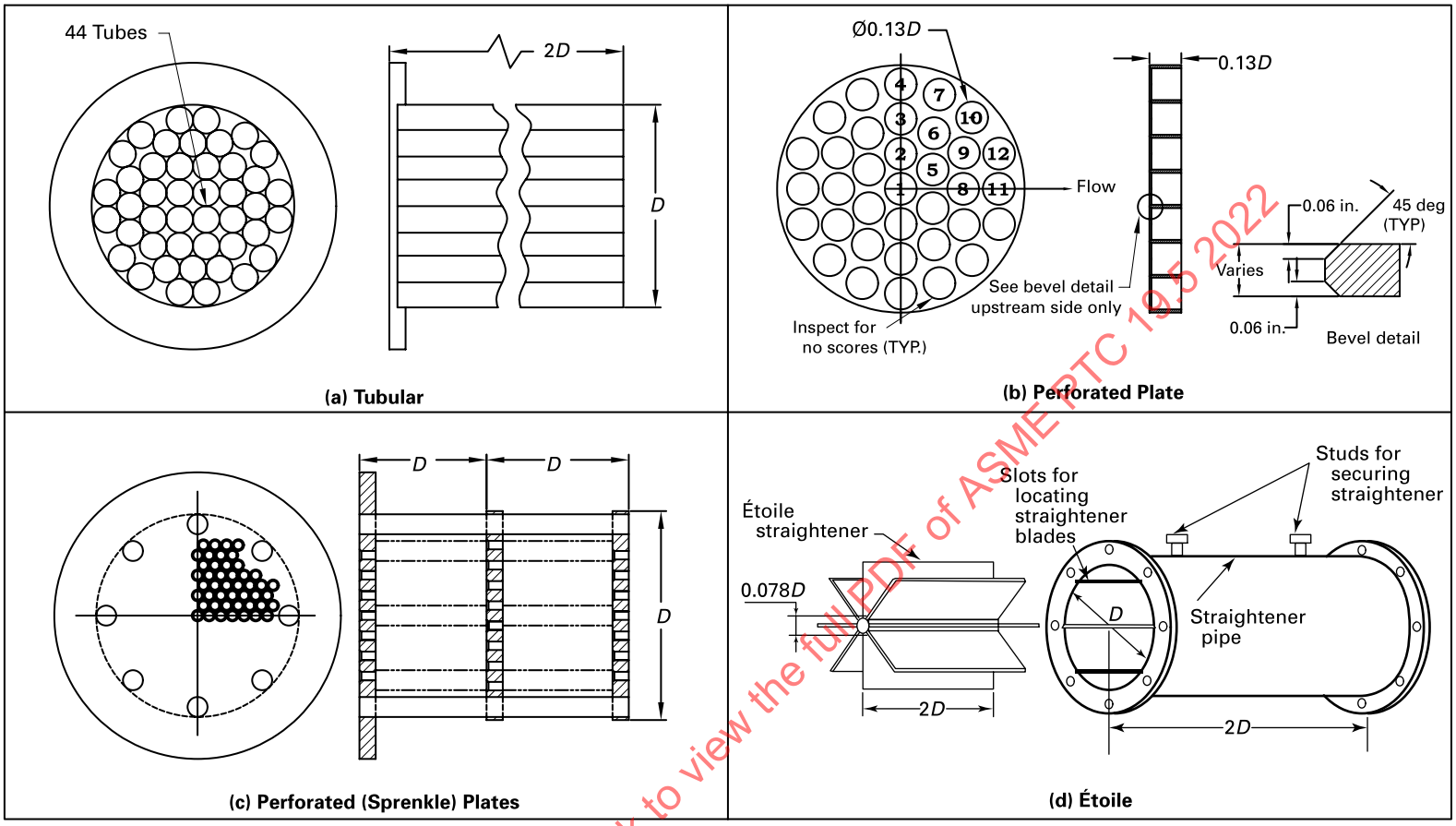

Table 6-6.1.1-1
Hole Coordinates for Perforated Plate

No.	X-axis	Y-axis
1	0	0
2	0	0.142*D*
3	0	0.283*D*
4	0	0.423*D*
5	0.129*D*	0.078*D*
6	0.134*D*	0.225*D*
7	0.156*D*	0.381*D*
8	0.252*D*	0
9	0.255*D*	0.146*D*
10	0.288*D*	0.288*D*
11	0.396*D*	0
12	0.397*D*	0.143*D*

GENERAL NOTE: D = pipe inside diameter.

Table 6-6.2-1
Loss Coefficients for Flow Conditioners

Flow Conditioner Type	k_1
Tubular (41 tubes)	8
Tubular (19 tubes)	5
Perforated (Sprenkle) plates	11
Etoile	1

6-8 REFERENCES

ASME MFC-3M–2004. Measurement of Fluid Flow in Pipes Using Orifice, Nozzle, and Venturi. The American Society of Mechanical Engineers.

ASME MFC-3Ma–2007. Addenda to ASME MFC-3M–2004, Measurement of Fluid Flow in Pipes Using Orifice, Nozzle, and Venturi. The American Society of Mechanical Engineers.

Bean, H. S., ed. (1971). Fluid Meters: Their Theory and Application (6th ed.). The American Society of Mechanical Engineers.

Kinghorn, F. C., McHugh, A., and Dyet, W. D. (1991). "The use of étoile flow straighteners with orifice plates in swirling flow." Flow Measurement and Instrumentation, 2(3) (July), 162–168.

Lewis, E. L., ed., and Naval Boiler and Turbine Lab, Philadelphia, PA. (1965). Instrument Standards (12th ed.). Defense Technical Information Center.

Miller, R. W. (1996). Flow Measurement Engineering Handbook (3rd ed.). McGraw-Hill.

Section 7
Sonic Flow Nozzles and Venturis — Critical Flow, Choked Flow Conditions

7-1 NOMENCLATURE

Symbols used in Section 7 are included in Tables 2-3-1 and 7-1-1. For any equation that consists of a combination of symbols with units shown in Tables 2-3-1 and 7-1-1, the user must be sure to apply the proper conversion factors.

7-2 INTRODUCTION

In 1839, Saint-Venant and Wantzel used the works of Bernoulli and Venturi to develop a general equation for the discharge of fluids from apertures, by which a sonic-flow limit could be inferred. The phenomenon that the mass rate of flow of a gas through a nozzle reaches a maximum that is directly proportional to the inlet pressure was observed by Weisbach in 1866 and again by Fleigner in 1874. The sonic flow nozzle has been used as a reference meter, as a transfer standard, as a control for regulating the flow of a gas, and as a propulsion engine.

The sonic flowmeter may be classed with variable-head meters in that it requires a constriction in the conduit, inlet pressure, and temperature measurements as well as knowledge of thermodynamic properties for the calculation of the mass flow of gases and vapors. The feature that distinguishes sonic flow nozzles and venturis from subsonic head meters is that the fluid stream is accelerated to sonic velocity at the throat.

Sonic flow exists when the mass flow is the maximum possible for the existing upstream conditions. When sonic flow is established, the flow is referred to as being choked. This is because the flow cannot be regulated by adjustments in valves located downstream of the constriction, as can be done with subsonic flowmeters. Thus, when sonic flow is established, the mass flow is controlled by the inlet conditions to the sonic flow device and is independent or nearly independent (depending on the wall contour and ratio between inlet/outlet pressure) of the downstream pressure.

Sonic flow nozzles and venturis operate at an average throat velocity that closely approximates the local sonic velocity, which is the sonic flow condition (ASME MFC-7-2016). Sonic velocity is assumed in the plane of the throat in the one-dimensional flow model used to determine theoretical flow.

Figure 7-2-1 shows a venturi nozzle designed for sonic flow measurements (Smith and Matz, 1962) and includes a comparison of the Mach number distribution through the venturi during subsonic and sonic flow operation. The average throat Mach number cannot exceed a nominal value of 1.0 in any sonic flow device. References in the literature to supersonic nozzles indicate that the velocities downstream of the throat are supersonic.

7-2.1 Advantages and Disadvantages of Sonic Flowmeters

All sonic flowmeters have certain characteristics in common. Because the mass flow is determined solely by the state of the fluid stream at the inlet to the nozzle, there is no need for a differential pressure measurement to calculate the flow as in subsonic variable-head devices. Thus, two measurements instead of three are required, eliminating the need for a throat pressure tap. The proportional relationship between the mass flow and the inlet stagnation pressure at constant temperature, which is indicated in eq. (7-8-9) for ideal gases and eq. (7-8-11) for real gases, is an advantage over the square root relationship between the flow and the differential pressure measurement, which is indicated in eq. (3-2-1) in a subsonic variable-head meter. The linear relationship permits approximately 3 times the range of flow measurements compared to the square root relationship for equal instrument ranges for the pressure and differential pressure measurements.

The greater range of the sonic flowmeter does not come without a penalty. At fixed downstream conditions, the total pressure loss across the sonic flowmeter is approximately proportional to the flow. These losses are caused by fluid friction losses from turbulence (vortices) and losses across shock waves in addition to boundary layer losses. Therefore, the pumping power required increases in proportion to the flow range covered. This is not a characteristic of subsonic flow devices as these have comparatively small total pressure losses.

Table 7-1-1
Symbols Specifically Applied in Section 7 (in Addition to Symbols in Table 2-3-1)

Symbol	Description	Dimensions [Note (1)]	Units	
			SI	U.S. Customary
L, l	Length or distance	L	mm	in.
A	Cross-sectional area of flow	L^2	m^2	ft^2
c	Speed of sound	LT^{-1}	m/s	ft/sec
C^*_i	Ideal gas sonic flow function	Dimensionless	Dimensionless	Dimensionless
C^*_R	Real gas sonic flow function	Dimensionless	Dimensionless	Dimensionless
C^*_{Ri}	Isentropic real gas sonic flow function	Dimensionless	Dimensionless	Dimensionless
d	Diameter of sonic flowmeter throat	L	mm	in.
e	Error	Dimensions of variable	...	...
M	Mach number	Dimensionless	Dimensionless	Dimensionless
P^*	Absolute static pressure at the sonic flowmeter throat	$ML^{-1}T^{-2}$	Pa	psi, atm
P_0	Absolute stagnation pressure of the fluid at the sonic flowmeter inlet	$ML^{-1}T^{-2}$	Pa	psi, atm
P_1	Absolute static pressure of the fluid upstream of the sonic flowmeter	$ML^{-1}T^{-2}$	Pa	psi, atm
P_2	Absolute static pressure of the fluid at the sonic flowmeter exit (downstream)	$ML^{-1}T^{-2}$	Pa	psi, atm
r	Radius	L	mm	in.
r_t	Radius of flowmeter throat	L	mm	in.
r_c	Radius of curvature of sonic flowmeter inlet	L	mm	in.
R	Individual gas constant	$ML^2T^{-2}\theta^{-1}$	kJ/(kg·K)	ft·lbf /(lbm·°R)
Re_d	Sonic flowmeter throat Reynolds number	Dimensionless	Dimensionless	Dimensionless
R_f	Recovery factor	Dimensionless	Dimensionless	Dimensionless
s	Specific entropy of the fluid	$L^2T^{-2}\theta^{-1}$	kJ/(kg·K)	Btu/(lbm °R)
T_p	Absolute temperature of flowing stream sensed by probe	θ	K	°R
T^*	Absolute static temperature of the fluid at the sonic flowmeter throat	θ	K	°R
T_0	Absolute stagnation pressure of the fluid at the sonic flowmeter inlet	θ	K	°R
T_1	Absolute static temperature of the fluid at the sonic flowmeter inlet	$ML^{-1}T^{-2}$	Pa	psi
V	Velocity of fluid	LT^{-1}	m/s	ft/sec
V^*	Velocity of fluid at throat equal to sonic velocity	LT^{-1}	m/s	ft/sec
v	Specific volume of fluid	L^3/M	m^3/kg	ft^3/lbm
Z	Compressibility factor	Dimensionless	Dimensionless	Dimensionless
γ	Ratio of specific heats	Dimensionless	Dimensionless	Dimensionless
ρ	Density of the fluid	ML^{-3}	kg/m^3	lbm/ft^3
Superscripts				
*	Sonic property, value at the sonic flowmeter throat inlet			
Subscripts				
0	Stagnation property			
1	Property at upstream conditions			
2	Property at sonic flowmeter exit (downstream)			
i	Ideal property			
R	Reduced property			
r	Ratio			

NOTE: (1) Dimensions:
L = length
M = mass
T = time
θ = thermodynamic temperature

Figure 7-2-1
Ideal Mach Number Distribution Along Venturi Length at Typical Subcritical and Sonic Flow Conditions

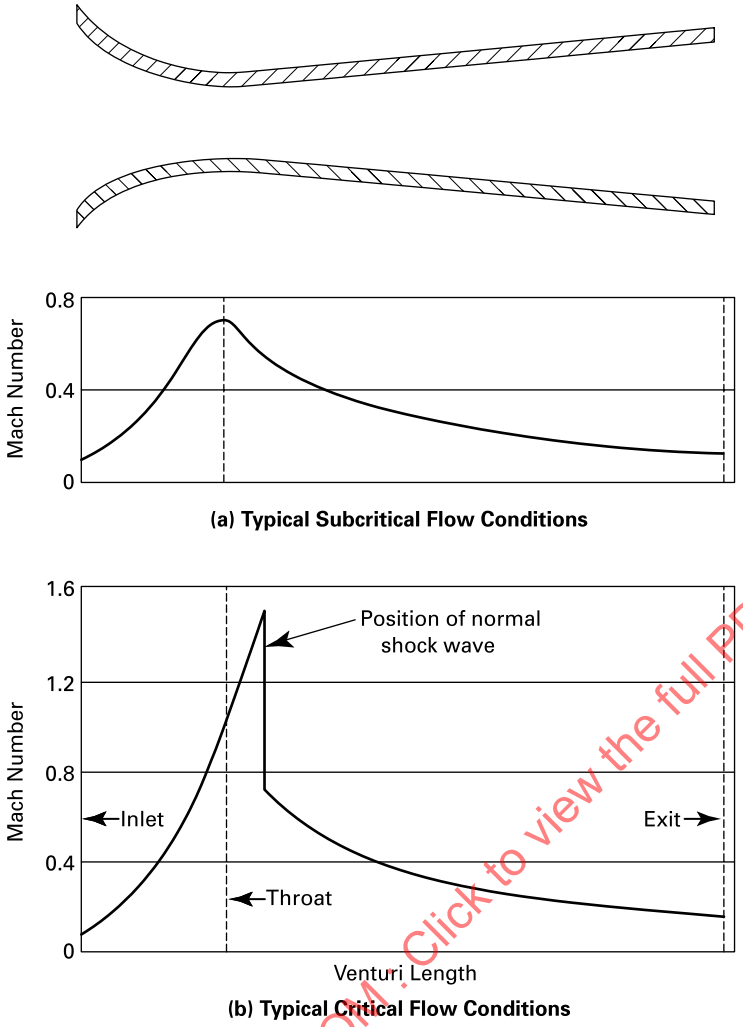

(a) Typical Subcritical Flow Conditions

(b) Typical Critical Flow Conditions

GENERAL NOTE: Figure from Smith and Matz, 1962.

A related disadvantage of the sonic flowmeter is the acoustical disturbance created in the downstream fluid. At the high end of the flow range, with low downstream pressure, the exit velocities can be in the high supersonic range. The resulting shock waves cause acoustical noise and turbulence, which may affect apparatus performance and downstream measurements in some applications. Special attention must be paid to this potential problem in calibration activities.

The fact that the flow is both measured and controlled by the inlet conditions to a sonic flowmeter may be an advantage or a disadvantage, depending on the application. In calibration applications, this feature can be an advantage. However, in most industrial applications, it is a disadvantage. Subsonic devices will measure the fluid flow in a conduit without greatly affecting the flow, because the total pressure loss over the flow range from frictional effects is low. This is not true for sonic flow nozzles and venturis.

Sonic flowmeters are relatively unaffected by disturbances in the inlet fluid stream, other than swirl, compared to their subsonic counterparts. Flow measurement errors caused by pulsation and nonstandard inlet velocity profiles are at least an order of magnitude smaller for sonic flowmeters than for subsonic variable-head flowmeters. This is because of two factors. First, the acceleration of the stream to sonic velocity mitigates (washes out) the inlet disturbances before they reach the throat. Second, the inlet pressure measurement is affected far less by these disturbances, by a factor of 15 (Smith and Matz, 1962), compared with the differential pressure measurement required by subsonic devices.

The relatively large pressure drop from the inlet to the throat of the sonic flowmeter, as required to reach sonic velocity, results in a correspondingly large variation in the fluid properties. Compared with subsonic devices, this requires more accurate fluid properties and more sophisticated calculation methods in some operating regimes to realize the sonic flowmeter's potential for high accuracy. Alternatively, it would be necessary to accept a larger uncertainty, as was done for the expansion factors of variable-head flowmeters at the highest throat velocities (Bean, 1971). Fortunately, these limitations were largely overcome by fluid property research and the development of rigorous electronic computations. Highly accurate data have long been available for steam and, more recently, for several gases.

The Mach number is fixed at every location from the inlet to the throat, where it is nominally equal to Mach 1, in a sonic flowmeter. Therefore, the discharge coefficient is only a function of the throat Reynolds number. Because the Mach number varies with the flow in a subsonic variable-head flowmeter, the discharge coefficient is a function of both the Mach number and the Reynolds number. Consequently, the predicted discharge coefficients of sonic flowmeters can have substantially lower uncertainties than their subsonic counterparts (Arnberg and Ishibashi, 2001a).

The stability and accuracy of sonic flow devices make them particularly well suited for use as transfer standards. Studies by Varner (1970) and Stevens (1986) obtained stability and accuracy of sonic flow devices by restricting the operation of the sonic flow venturi nozzles to the Reynolds number range below the point at which boundary layer transition from laminar to turbulent would occur.

7-2.2 Historical Development of Concepts

G. A. Goodenough, professor of thermodynamics at the University of Illinois, presented the principles of compressible flow for an ideal gas in *Principles of Thermodynamics* (1920). The equation for the flow of a gas from a plenum at state 1 through a short tube to a pressure, P_2, downstream of the tube was given in a similar way to

$$q_m = A\sqrt{2g_C\frac{\gamma}{\gamma-1}\frac{P_1}{v_1}\left[\left(\frac{P_2}{P_1}\right)^{\frac{2}{\gamma}} - \left(\frac{P_2}{P_1}\right)^{\frac{\gamma+1}{\gamma}}\right]} \tag{7-2-1}$$

where

A = the area of the cross section
v_1 = the volume per unit mass at state 1

Figure 7-2.2-1 shows a plot of the mass flow versus the downstream pressure. The downstream pressure is reduced from an initial value equal to the inlet pressure (100), indicated as point A, down to zero at point C. The first derivative of the mass flow function, eq. (7-2-1), versus the downstream pressure is equal to zero at the sonic flow point, indicated as point B, which is the maximum of the curve.

The downstream pressure at which the flow reached a maximum value is called the sonic pressure, and the sonic pressure ratio is derived as follows:

$$\frac{P_2}{P_1} = \left(\frac{2}{\gamma+1}\right)^{\gamma/(\gamma-1)} \tag{7-2-2}$$

Because sonic velocity is reached at the throat, this maximum flow condition has been referred to as sonic flow in thermodynamics, gas dynamics, and the early literature.

In the 1930s, gas dynamic scholars recognized the advantage of using the Mach number as a parameter and the isentropic stagnation properties in compressible flow analyses (Shapiro, 1954). Throughout this Section, a subscript of "0" denotes stagnation properties and a superscript of "*" denotes properties at sonic conditions. The isentropic flow functions for ideal gases, with constant ratio of specific heats, are given in eqs. (7-2-3) through (7-2-6).

$$\frac{P}{P_0} = \left(1 + \frac{\gamma-1}{2}M^2\right)^{-\gamma/(\gamma-1)} \tag{7-2-3}$$

$$\frac{\rho}{\rho_0} = \left(1 + \frac{\gamma-1}{2}M^2\right)^{-1/(\gamma-1)} \tag{7-2-4}$$

Figure 7-2.2-1
Definition of Sonic Flow as the Maximum of the Flow [See Eq. (7-2-1)]

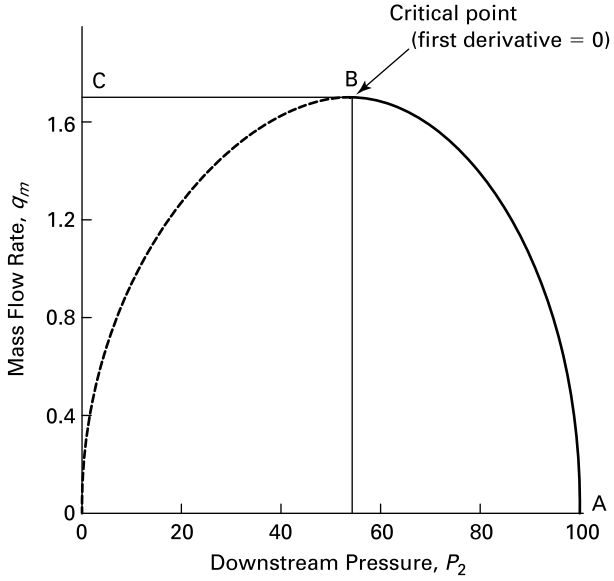

$$\frac{T}{T_0} = \left(1 + \frac{\gamma - 1}{2} M^2\right)^{-1} \tag{7-2-5}$$

$$\frac{A}{A^*} = \frac{1}{M}\left[\left(\frac{2}{\gamma + 1}\right)\left(1 + \frac{\gamma - 1}{2} M^2\right)\right]^{(\gamma+1)/2(\gamma-1)} \tag{7-2-6}$$

Sonic flow eqs. (7-2-3) through (7-2-6) are shown in eqs. (7-2-7) through (7-2-9).

$$\frac{T^*}{T_0} = \frac{2}{\gamma + 1} \tag{7-2-7}$$

$$\frac{P^*}{P_0} = \left(\frac{2}{\gamma + 1}\right)^{\gamma/(\gamma-1)} \tag{7-2-8}$$

$$\frac{\rho^*}{\rho_0} = \left(\frac{2}{\gamma + 1}\right)^{1/(\gamma-1)} \tag{7-2-9}$$

The relationships in eqs. (7-2-3) through (7-2-9) became widely used in fluid metering, gas turbines, rockets, aeronautics, and other technical fields.

7-2.3 General Considerations

The speed of sound is reached at the throat in sonic flowmeters, and this characteristic has led to the following names:
(a) sonic flow nozzle, venturi, or venturi nozzle
(b) critical flow nozzle, venturi, or venturi nozzle
(c) sonic flow orifice (rounded but abrupt inlet contour without a diffuser section)
(d) supersonic nozzle (converging-diverging contour with supersonic velocities)
(e) laval nozzle (converging-diverging contour, named after the pioneer de Laval)

7-3 DEFINITIONS AND DESCRIPTION OF TERMS

7-3.1 Definitions

Terms used to discuss sonic flow are defined herein.

beta ratio: the ratio of the throat diameter of the nozzle to the inlet pipe diameter.

mass flow defect: the difference between the actual mass flow and the theoretical mass flow based on the assumptions made in calculating the theoretical value. This is the sum of the velocity defect (caused by the average velocity at the throat being less than the speed of sound) and the density defect (caused by the average density differing from the value calculated from the assumption of one-dimensional isentropic flow).

sonic flow mass flux: mass flow per unit area perpendicular to the flow.

sonic surface: the location in a fluid stream where the velocity has reached the local speed of sound. This is an imaginary surface with a parabolic or spherical shape near the throat of an axially symmetric sonic flow nozzle or venturi.

7-3.2 General

The theoretical basis for sonic flow calculations follows the theory for subsonic variable-head flowmeters. Sonic flow theory is based on the following assumptions:

(a) The chemical composition of the flowing fluid does not change. (This excludes chemical reactions and elevated temperatures where dissociation of molecules becomes significant.)

(b) The flowing fluid is in a state of thermodynamic equilibrium, such that the equations of state that relate the thermodynamic properties are valid. (This excludes nonequilibrium or metastable states whose properties are time functions.)

(c) The fluid stream is in steady state, i.e., the thermodynamic properties remain constant with time at each point or location in the stream. (This excludes inlet temperature gradients and variations with time because of inadequate upstream mixing.)

(d) The fluid stream is in steady flow. The mass flow is constant through each cross-sectional surface normal to the axis of the fluid stream. (This excludes transient and pulsating flows.)

(e) The flow process from the inlet to the meter throat is reversible (frictionless). The actual flow deviates from this assumption in that the boundary layer is not frictionless. The discharge coefficient provides a correction for this deviation.

(f) The fluid flow is one-dimensional, such that the velocity and thermodynamic properties vary only along the axis of the meter from the inlet to the throat. Conversely, the velocity of the stream and all of the thermodynamic properties are invariant in planes normal to the axis of the meter. (Deviations of the actual flow from this assumption because of the existence of two-dimensional flow are corrected by the discharge coefficient.)

(g) The flowing fluid is a homogeneous compressible fluid, such that each thermodynamic state is totally defined by two independent properties. Examples of fluids that meet these conditions adequately for engineering calculations are as follows:

(1) pure substances in the gaseous phase (e.g., helium, argon, oxygen, nitrogen, carbon dioxide, steam, and other chemically homogeneous gases)

(2) gaseous mixtures that may be treated as pure substances, (e.g., air, intimate mixtures of air, and other gases with water vapor)

(3) intimate mixtures of two or more phases that are finely and uniformly dispersed such that they behave as if they were homogeneous (e.g., a high-quality mixture of saturated water vapor and fine droplets of saturated liquid or similar mixtures of multiple phases that are in thermodynamic equilibrium)

(h) The flow is adiabatic (without heat transfer). This can be especially significant in small meters where the surface area of the meter walls is large relative to the cross-sectional flow area of the fluid stream. It is important that the wall temperature of the meter be close to the temperature of the flowing fluid to reduce heat transfer to an insignificant level.

The frictionless requirement of (e) along with the adiabatic requirement of (h) make the process isentropic.

In accordance with (b), equilibrium is assumed for the thermodynamic states of the fluid in all derivations of theoretical flow. Some nonequilibrium exists immediately following all changes of state since small but finite time is required to reach equilibrium. The theory of equilibrium thermodynamics assumes an idealized quasi-equilibrium process to eliminate any time dependence of the thermodynamic states. Sonic flow devices are more apt to encounter significant nonequilibrium states than subsonic fluid meters because of the higher throat velocities. This is particularly true for very small nozzle sizes.

Venturi designs that have continuous wall curvature from the inlet through the throat provide no time for an equilibrium state to be reached, because the fluid expands continuously through the throat. Designs that have a cylindrical section prior to the sonic flow point provide time for equilibrium to be established. It is unlikely that a significant increase in uncertainty results from nonequilibrium states in most sonic flow applications. However, this possibility should be considered when using fluids with complex molecules that might have relatively long relaxation times, such as carbon dioxide.

As noted parenthetically in the list of assumptions, the actual fluid flow process usually deviates from the theoretical assumptions in only two respects. First, the velocity and fluid properties vary in the radial direction in addition to the axial direction of the meter, making the actual flow pattern two-dimensional instead of one-dimensional, as required by (f). (All sonic flowmeters considered herein have an axially symmetric geometry such that two dimensions define the actual flow condition.) Second, there is significant viscous friction in the boundary layer, making the real flow process irreversible, instead of frictionless (isentropic) flow as required by (e).

Figure 7-3.2-1 shows how these two deviations from the assumptions reduce the actual mass flow below the theoretical value. The radial distribution of mass density, because of centrifugal force effects, increases the actual flow above the theoretical value. This is more than compensated for by the radial distribution of Mach number, which is below the theoretical sonic velocity (i.e., below Mach 1). The sum of these two effects provides the mass flow defect in the inviscid potential flow regime. The viscous friction in the boundary layer provides the second mass flow defect. The mass flow defects are the amounts that each of these effects reduces the actual flow below the flow that would result from the theoretical model defined by the assumptions.

The discharge coefficient is relied upon to compensate for these two deviations of the actual flow from the theoretical model. The sum of the mass flow defects is equal to one minus the discharge coefficient ($1 - C$). Throat Reynolds number is used to correlate the discharge coefficient. (Theoretical solutions indicate that the discharge coefficient is a weak function of the specific heat ratio, in addition to the throat Reynolds number, but this effect is usually ignored and accepted as scatter in experimental results.) The precision with which this correlation can be realized depends on how closely the assumptions are met. Every deviation of the actual flow from the theoretical model, other than the two for which the Reynolds number can correct, will cause loss of accuracy in the flow measurement. This is especially true with greater differences between calibration and application conditions.

A schematic diagram of flow profiles at the venturi throat is shown in Figure 7-3.2-2, indicating the sonic surface to be a paraboloid of different proportions at different Reynolds numbers.

Figure 7-3.2-1
Schematic Representation of Flow Defects at Venturi Throat

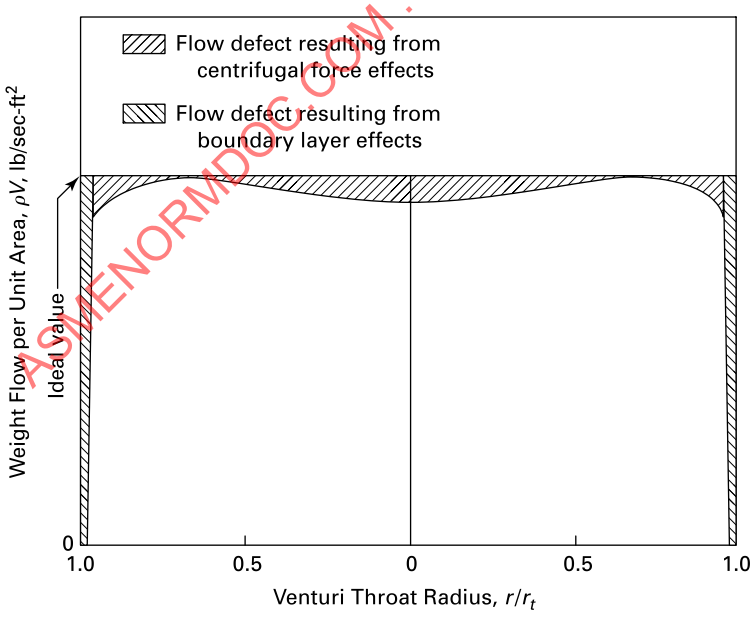

GENERAL NOTE: Figure adapted from Smith and Matz, 1962.

Figure 7-3.2-2
Schematic Diagram of Sonic Surfaces at the Throat of an Axially Symmetric Sonic Flow Venturi Nozzle

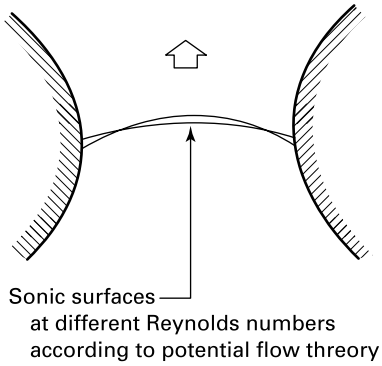

GENERAL NOTE: Figure from Thompson and Arena, 1975.

7-4 GUIDING PRINCIPLES

It is necessary to have a downstream pressure at or below the value required to maintain sonic velocity at the throat of a sonic flowmeter. Monitoring downstream pressure is therefore necessary to ensure that this requirement is met. Choking pressure ratio is defined as the minimum ratio of the inlet stagnation pressure to the downstream static pressure required for sonic flow. The operating conditions must meet or exceed the choking pressure ratio of the meter for operation under sonic flow theory. Conversely, unchoked back-pressure ratio is defined as the ratio of the downstream static pressure to the inlet stagnation pressure at which the velocity at the throat becomes subsonic. The operating conditions must provide back-pressure ratios lower than unchoked back-pressure ratio. Figure 7-4-1 gives maximum back-pressure ratios for sonic flow venturi nozzles (ASME MFC-7–2016).

The design of the diffuser, the fluid density, and other fluid properties all affect the unchoked characteristics of venturi nozzles. A good diffuser design increases the efficiency with which the kinetic energy of the sonic jet is converted to flow work, resulting in a higher exit static pressure.

The back-pressure ratio requirements given in Figure 7-4-1 are based on standardized designs for sonic flow venturi nozzles at Reynolds numbers greater than 2.0×10^5. For venturi nozzles operated from a Reynolds number of 5.0×10^4 to 2×10^5, a minimum back pressure ratio equal to the sonic pressure ratio is recommended. For operation below a Reynolds number of 5.0×10^4, a ratio of 0.30 should be maintained.

It is sometimes necessary to operate in both subsonic and sonic flow regimes. A compromise must then be made in selecting a flowmeter's design. A sonic flow venturi nozzle must have a throat pressure tap added for operation in the subsonic regime. Because there is no performance data for subsonic operation, it must then be calibrated. It may be preferable to select a subsonic meter for which a discharge coefficient equation is available, such as the ASME low-β throat tap flow nozzle, which will also perform reasonably well in the sonic flow regime (Aschenbrenner, 1983). Providing a diffuser section downstream of the throat, as shown in Figure 7-2-1, increases the unchoked back-pressure ratio, as indicated in Figure 7-4-2.

7-5 INSTRUMENTS AND METHODS OF MEASUREMENT

7-5.1 General

The main feature of a sonic or venturi nozzle design is the variation in the cross-sectional flow area in the axial direction from the inlet pipe or plenum to the discharge pipe or plenum (i.e., the meter contour). The contour and possibly the surface roughness determine the essential features (i.e., the discharge coefficient and choking pressure ratio over the operating range). Related features include inlet flow conditioning, the locations and details of the inlet temperature probe(s), the inlet pressure tap(s), and the location of an exit pressure tap for the measurement of the back pressure on the meter.

Figure 7-4-1
Requirements for Maintaining Sonic Flow in Venturi Nozzles

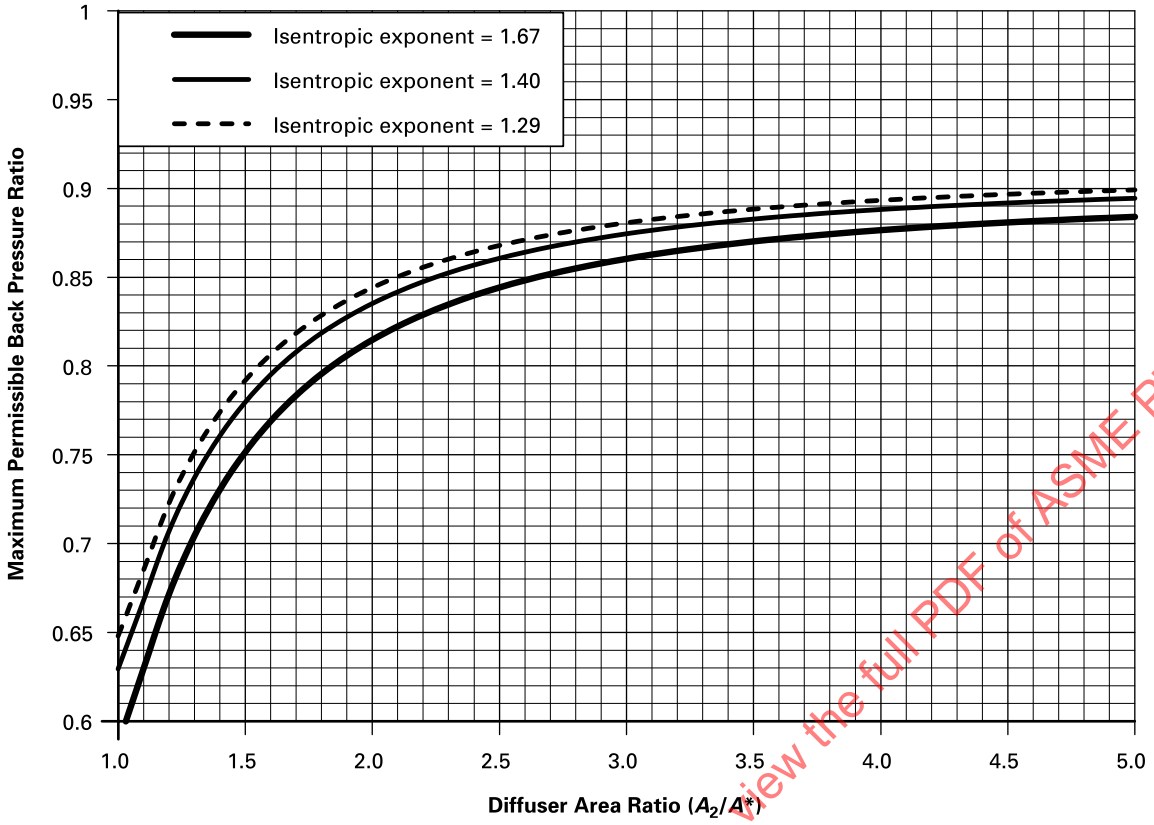

GENERAL NOTE: Figure 7-4-1 applies only for throat Reynolds numbers greater than 2×10^5.

Figure 7-4-2
Mass Flow Versus Back-Pressure Ratio for a Flow Nozzle Without a Diffuser and a Venturi Nozzle With a Diffuser

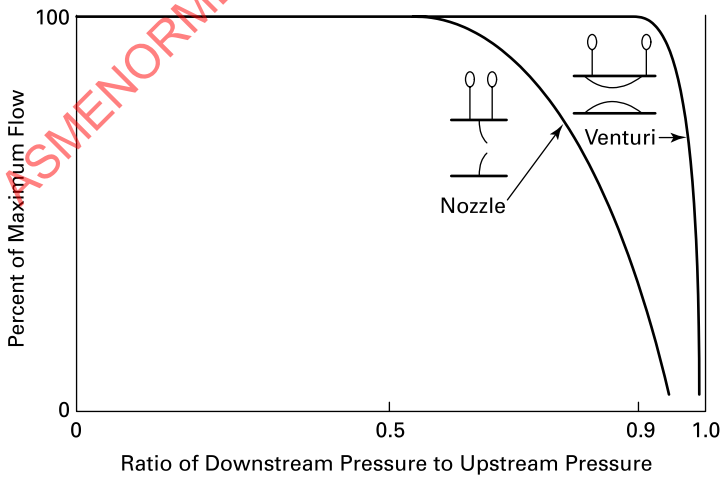

The flow-metering characteristics are mainly determined by the inlet contour. The portion diverging to a location slightly beyond the throat may slightly affect the performance of some meters in some operating regimes because of effects on the throat boundary layer and on the shape of the sonic surface. These possible effects have not been documented. The exit section, primarily the angle and length of the diffuser, determines the efficiency of the diffusion process.

Meter designs are most commonly described in terms of the shape of the walls confining the fluid stream in a longitudinal-section view. Thus, "a circular-arc inlet" refers to the wall shape of the inlet portion of the meter hardware. Similarly, the inlet of an ASME flow nozzle is described as a quadrant of an ellipse. An alternative description gives the full three-dimensional shape. Thus, a circular-arc inlet revolved about the axis of the meter forms a torus, hence "a toroidal throat venturi nozzle" is an alternative description for a nozzle with a circular-arc inlet. ASME MFC-7–2016 uses the term "toroidal throat critical flow venturi."

The discharge coefficient versus Reynolds number relationship and the choking pressure ratio characteristics must be determined for each meter design. Extensive testing is required to obtain a high accuracy over a large Reynolds number range. High confidence in the absolute accuracy of the discharge coefficient can only be obtained by comparing the results of tests that use different primary measurement methods. This would be facilitated by limiting the number of designs studied, which in turn would be encouraged by standards with small tolerances. The tolerances of the present standards (ASME MFC-7–2016 and ISO 9300:2005) are large enough to cause substantial differences in discharge coefficients and thus necessitate a larger uncertainty in the mean calibration curve than might otherwise be required.

7-5.2 Design Criteria

7-5.2.1 Repeatability. It is futile in most applications to attempt to obtain an accuracy of flow measurement higher than the repeatability of the meter. Random uncertainties can be reduced by repetition and averaging, but those that are not truly random cannot be reduced in this manner. Repeatability in boundary layer transition regimes is poor because of the complexity of the mechanisms that trigger the transition. Therefore, it is desirable to develop meter configurations that have minimal changes in their discharge coefficients during transition.

7-5.2.2 Inlet Contour. The inlet contour to the location where sonic velocity is reached should preferably produce a thin boundary layer. This would minimize the change in the discharge coefficient during transition, thereby minimizing loss of accuracy because of non-repeatability in this regime. A thin boundary layer also contributes to a high discharge coefficient, because of a low boundary layer mass flow defect (see Figure 7-3.2-1). This is desirable because it indicates that the actual flow is close to the theoretical model, such that little empirical correction is required of the discharge coefficient. This in turn adds to the confidence with which the discharge coefficient versus Reynolds number correlation can be relied upon to maintain accuracy. This is especially important when there are large differences between calibration and application flow conditions (i.e., the range of states and gases over which the correlation can be applied with tolerable loss of accuracy).

The circular-arc inlet with no cylindrical throat section produces a thin boundary layer. The radius of curvature of the approach section is important in determining the mass flow defect (see Figure 7-3.2-1) and thus the value of the discharge coefficient. The variation of the discharge coefficient as a function of the inlet radius was calculated by Stratford for laminar and turbulent boundary layers versus Reynolds number (Stratford, 1964). The circular-arc nozzle with an inlet radius equal to twice the throat diameter is close to optimum for producing a high discharge coefficient. This is because an inlet radius of twice the throat diameter nearly optimizes the combination of boundary layer thickness and two-dimensional (centrifugal force) flow effects.

7-5.3 Standardized Flow Nozzle and Venturi Designs

7-5.3.1 Toroidal Throat Venturi Nozzle. A toroidal throat venturi nozzle design known in the United States as the modified Smith/Matz venturi nozzle has been adopted by international standards organizations (ASME MFC-7–2016 and ISO 9300:2005). The modification was to the inlet radius of curvature, r_c, which was originally 1.816 times the throat diameter, d, or 1.816d, (Smith and Matz, 1962) and was changed to 2.0d ± 0.2d in the standards. This design is shown in Figure 7-5.3.1-1.

One advantage of the toroidal throat sonic flow venturi is that the continuous inlet curvature passing through the throat lends itself to analysis for the determination of theoretical discharge coefficients.

The design avoids the boundary layer buildup that occurs in a cylindrical section, with its near-zero pressure gradient, and the related problems of transonic shock, flow separation, and boundary layer pressure gradient reversal.

Figure 7-5.3.1-1
Standardized Toroidal Throat Sonic Flow Venturi Nozzle

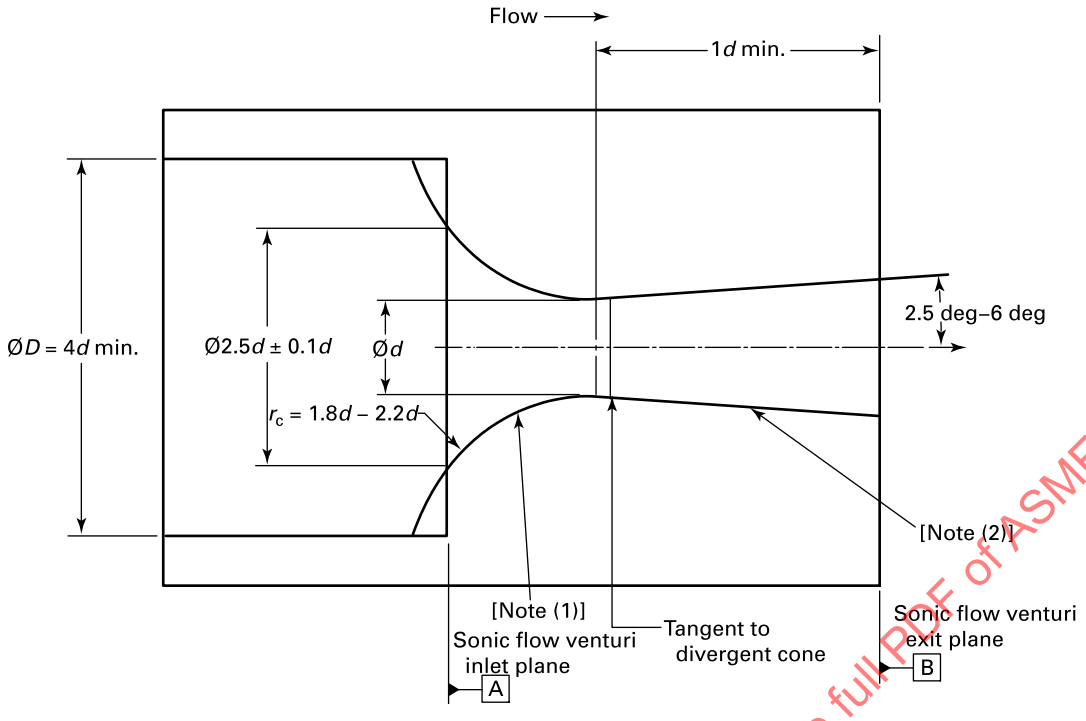

GENERAL NOTE: When it is not practical to manufacture sonic flow venturis to the surface finish and curvature specifications herein, sonic flow venturi performance shall be shown through calibration.

NOTES:
(1) In this region, the surface shall not exceed $15 \times 10^{-6}d$ arithmetic average roughness, and the contour shall not deviate from toroidal form by more than $0.001d$.
(2) In this region, the surface shall not exceed $10^{-4}d$ arithmetic average roughness.

7-5.3.2 High-Precision Venturi Nozzles. Until recently, sonic flow venturi nozzles have been machined using traditional methods and polished to obtain smooth inlets. Funaki and Ishibashi (2008) present extensive results on boundary layer transition. The venturi nozzles were machined to ultra-high precision and accuracy, with mirror finishes obtained without polishing. This was necessary to prevent the data scatter (charged to normal manufacturing tolerances) from obscuring the performance characteristics being studied. They show the data scatter to be greatly reduced, and boundary layer transition starting from throat Reynolds numbers as low as 0.85×10^6 and as high as 1.3×10^6. The transition starts at 1.85×10^6 for venturi nozzles with an inlet radius of curvature equal to the throat diameter ($r_c = 1.0d$), and the same for $r_c = 1.5d$.

In terms of accuracy, high-precision venturi nozzles have discharge coefficients about 0.1% higher than those of traditional manufacture (+0.08% and +0.11% at Reynolds numbers of 1.0×10^6 and 1.0×10^6, respectively) in the laminar boundary layer range.

7-5.3.3 Cylindrical Throat Venturi Nozzle. A sonic venturi with a cylindrical throat section may have manufacturing and metrological advantages over the toroidal throat venturi, especially in small sizes. It is essential that the cylindrical throat not have a taper that could cause the throat to occur at a location other than the exit or, even less desirable, a sonic flow location that oscillates between the inlet and the exit. This venturi design has been accepted as a sonic flow standard (ASME MFC-7–2016 and ISO 9300:2005) and is shown in Figure 7-5.3.3-1.

The cylindrical throat design offers some advantages, primarily in ease of manufacture, but is inferior to the toroidal throat design from a fluid mechanics point of view. First, the inlet radius is more abrupt in that it is equal to the throat diameter instead of twice the throat diameter. This produces larger centrifugal forces, resulting in a larger radial density gradient, compared with the toroidal throat design. Second, the flow discontinuity at the juncture of the inlet curvature and the beginning of the cylindrical throat poses the risk of flow separation, especially following the small inlet radius of curvature. Third, the cylindrical section causes the boundary layer to become thicker than the toroidal throat design. These effects combine to reduce the discharge coefficient, which is an undesirable feature for any flowmeter.

Figure 7-5.3.3-1
Standardized Cylindrical Throat Sonic Flow Venturi

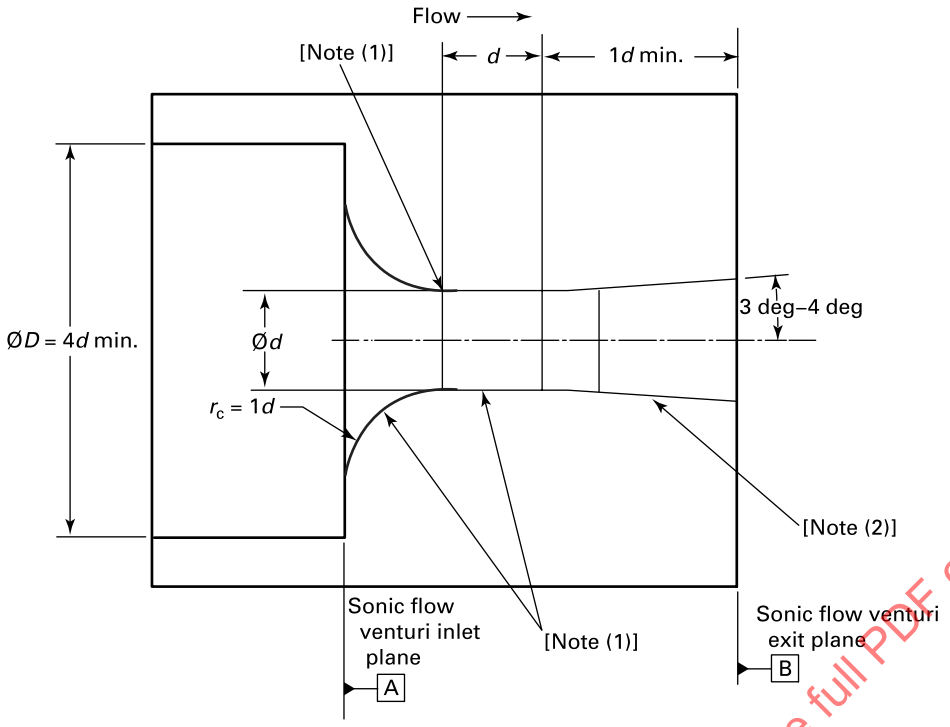

GENERAL NOTE: When it is not practical to manufacture sonic flow venturis to the surface finish and curvature specifications herein, sonic flow venturi performance shall be shown through calibration.

NOTES:
(1) In this region, the surface shall not exceed 15 × 10−6*d* arithmetic average roughness, and the contour shall not deviate from toroidal and cylindrical form by more than 0.001*d*.
(2) In this region, the surface shall not exceed 10−4*d* arithmetic average roughness.
(3) See ASME MFC-7 for the transition region between the convergent section and throat of the sonic flow venturi.

7-5.3.4 ASME Low-β Flow Nozzles. Figure 7-5.3.4-1 shows two standardized ASME nozzles that were designed for subsonic application and offer possibilities for combined subsonic and sonic operation. The high-β ratio design [see Figure 7-5.3.4-1, illustration (a)] is not recommended for use as a sonic flow nozzle because of the high inlet Mach number (a maximum β ratio of 0.25 is recommended). However, it can be used with appropriate correction for the inlet pressure and temperature measurements, with some sacrifice in accuracy. Figure 7-5.3.4-1, illustration (b) shows an ASME low-β ratio flow nozzle with throat pressure taps, which is recommended for combined subsonic and sonic flow operation (see Section 5 for details and dimensions of the ASME flow nozzles).

7-6 INSTALLATION

7-6.1 General

The sonic flowmeter is relatively insensitive to disturbances in the inlet flow stream compared to some flowmeters (Sparks, 1966 and Brennan et al., 1989). This is largely because sonic flowmeters avoid the phase lag and square root errors present in subsonic meters that rely on a differential pressure measurement. Tests on sonic flowmeters found little error from severe pulsations when using an average inlet pressure obtained by a throttled gage line (Kastner, Williams, and Snowden, 1964). This is a major advantage because pulsations are difficult to remove from the fluid stream.

Inlet flow conditioning to establish a standardized velocity profile, which is essential for subsonic flowmeters, is not so important for sonic nozzles and venturis. The inlet profile will have a slight effect on the conversion of the inlet static pressure measurement to average inlet stagnation pressure.

Swirl may cause errors in sonic flowmeters, although no data was found to quantify this effect. Swirl should be removed from the fluid stream by means of an inlet flow straightener.

Figure 7-5.3.4-1
ASME Long-Radius Flow Nozzles

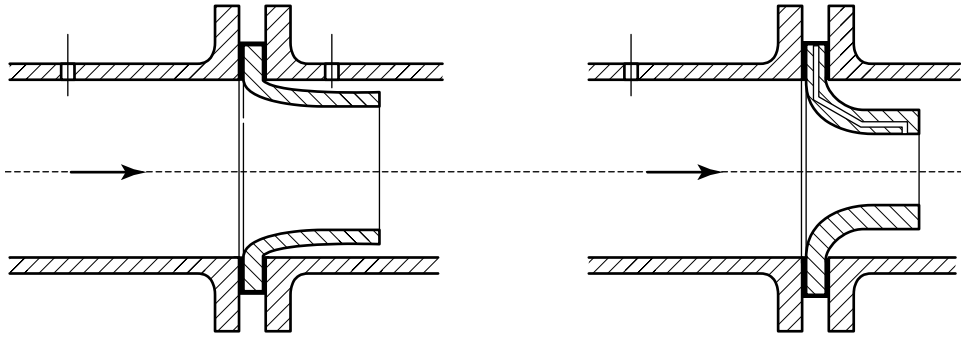

(a) High Beta, β (b) Low Beta, β

7-6.2 Standardized Inlet Flow Conditioner

Inlet flow conditioning methods have been standardized as shown in Figure 7-6.2-1. Details of the inlet flow conditioner are specified in Section 6 of this Supplement, and also in ASME and ISO standards (ASME MFC-7–2016 and ISO 9300:2005)

7-6.3 Inlet Configurations for Sonic Venturi Nozzles

ASME MFC-7-2016 and ISO 9300:2005 permit a range of inlet configurations, as shown in Figure 7-5.3.1-1. The most commonly used inlet configuration is the bulk-head installation shown in Figures 7-5.3.3-1 and 7-5.3.4-1. Figure 7-6.3-1 shows the continuous curvature inlet used by Stevens (1986) compared with the sharp-lip, free-standing inlet used by Smith and Matz (1962).

The sensitivity of three designs of sonic flow venturi nozzles to initial boundary layer thickness, as affected by the inlet configuration, was studied analytically (Brown, Hamilton, and Kwok, 1985). Included in the study were the effects of inlet flow nonuniformity, separation, and the location of the boundary layer transition point. The differences in sensitivities of the three designs for these effects were found to be small. A slight advantage was seen for the free-standing inlet with the toroidal throat venturi nozzle of the Smith and Matz design.

The loose specification on the inlet configuration in the ASME and ISO standards is based on the assumption that the permitted variations in the inlets do not affect the performance significantly. However, as more precise venturi nozzles are manufactured and calibrated by increasingly accurate methods, the differences in their discharge coefficients cast doubt on this assumption. Previously, these differences were attributed entirely to calibration errors. It is probable that tighter specifications will be needed in the standards before lower uncertainties in the universal curve can be obtained. Presently, the lowest uncertainties are obtained by calibrating each configuration of venturi nozzle.

7-7 PRESSURE AND TEMPERATURE MEASUREMENTS

7-7.1 Pressure Measurements

7-7.1.1 Beta Ratio. Beta is the ratio of the throat diameter of the nozzle to the inlet pipe diameter. This ratio is important for mass flow measurements using sonic flow or venturi nozzles because the inlet pressure measurement uses inlet pipe wall pressure tap(s) to measure the static pressure. This method follows the established practice for subsonic nozzles instead of using impact probes, which would involve more complexity and cause disturbances in the inlet stream.

Figure 7-7.1.1-1 illustrates the difference between the static pressure measurements, or the pressure measured with a relative velocity of zero between the point on the pipe wall and the fluid, and the total (stagnation) pressure, or the pressure measured at a point in the flow field in which the flow is brought to rest with respect to the measuring instrument.

Equation (7-7-1) illustrates the correlation between reference (or static) and total pressure shown in Figure 7-7.1.1-1.

$$P_T = P_{\text{static}} + \rho V^2/2 \tag{7-7-1}$$

Figure 7-6.2-1
Standardized Inlet Flow Conditioner and Locations for Pressure and Temperature Measurements

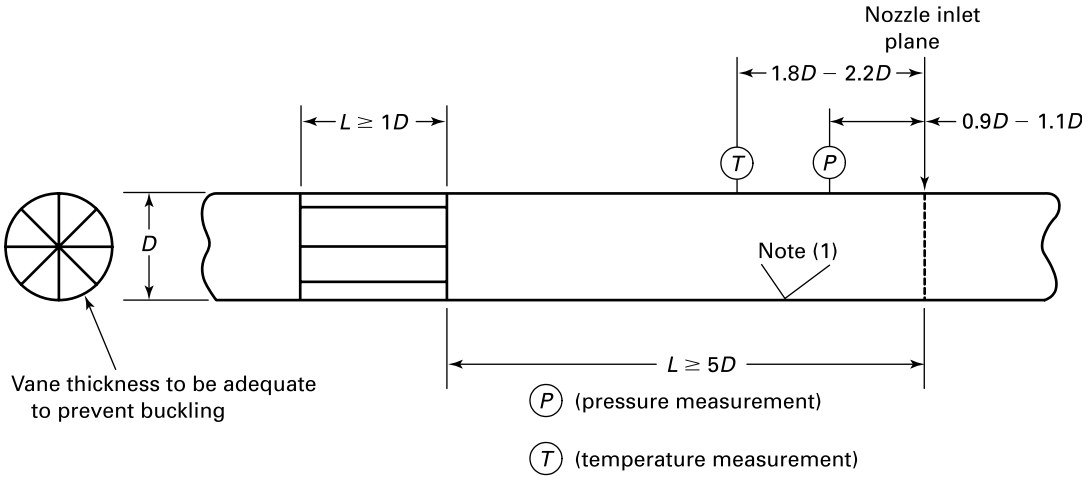

Figure 7-6.3-1
Comparison of the "Continuous Curvature" Inlet With the "Sharp-Lip, Free-Standing" Inlet

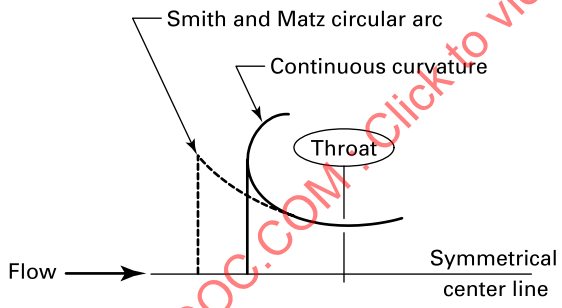

GENERAL NOTE: From Smith and Matz, 1962.

Figure 7-7.1.1-1
Static and Total (Stagnation) Pressure Measurements on a Pipe

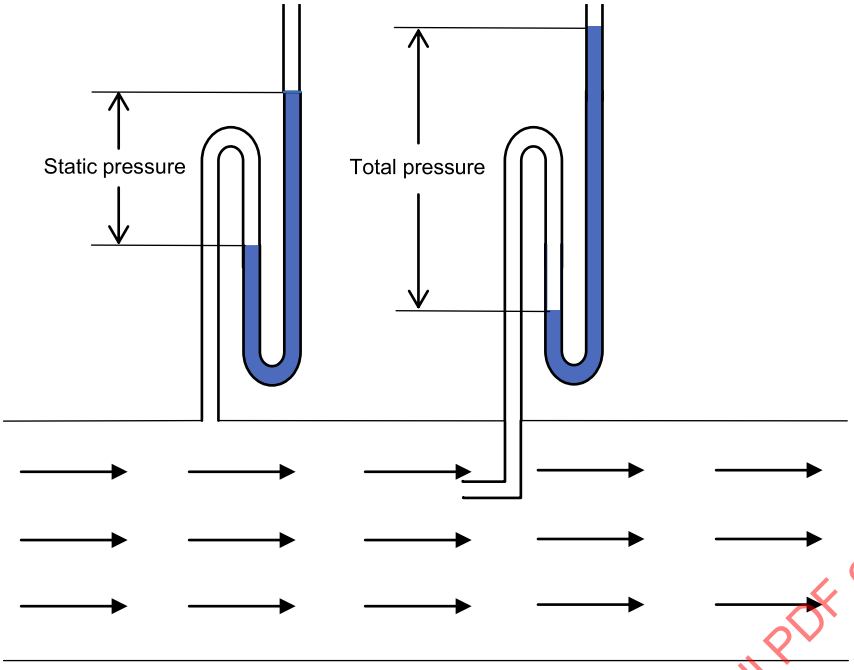

The conversion from static to stagnation pressure is accomplished by isentropic relationships based on one-dimensional flow of an ideal gas. This contains error from the fact that the flow is not one-dimensional. The velocity profile in the inlet section at the location of the wall tap(s) results in a corresponding stagnation pressure profile. The discrepancy caused by this deviation from one-dimensional flow is acceptably small if the correction from static to stagnation pressure is sufficiently small. This is the case when the beta ratio is less than 0.25, which is required in the ISO standard (ISO 9300:2005).

NOTE: In eq. (7-7-1), the real gas sonic flow function is a function of the inlet stagnation pressure and temperature. In an installation having a beta ratio less than 0.25, static conditions can be measured, and the correction may be ignored for all applications except those requiring the lowest uncertainty.

The velocity profile of a properly conditioned inlet stream will vary in a predictable manner with the Reynolds number. Consequently, the error in converting from static to stagnation pressure under ideal conditions is incorporated into the discharge coefficient versus Reynolds number relationship.

When the standardized limit on the β value of 0.25 is not practical because of limitations on the size of the inlet pipe, a compromise is necessary between higher β values and some loss of accuracy in converting from measured inlet static pressure and the average inlet stagnation pressure. At a β of 0.25, the correction from static to stagnation pressure is less than 0.1%, and the uncertainty in this correction because of two-dimensional effects is estimated to be on the order of 0.01%, depending on the Reynolds number. For other β values, the correction can be calculated from the isentropic relationships in eqs. (7-2-1) through (7-2-4) and a similar judgment made as to the possible uncertainty in the correction.

7-7.1.2 Pressure Taps. Pressure tap geometry has been standardized, as shown in Figure 7-7.1.2-1, and the details are specified in ASME MFC-7–2016 and ISO 9300:2005.

7-7.1.3 Pressure Tap Corrections. Pressure tap corrections are not considered necessary for sonic flowmeter installations with beta ratios less than 0.25, in accordance with ISO 9300:2005.

7-7.1.4 Downstream Pressure Measurement. The pressure downstream of the meter must be measured to ensure sonic operation. The standardized location is within 0.5 conduit diameters of the exit plane of the venturi nozzle. ASME MFC-7–2016 permits other locations with corresponding precautions on the use of the choking pressure ratio requirements given in Figure 7-3-1.

Figure 7-7.1.2-1
Standardized Pressure Tap Geometry Installation

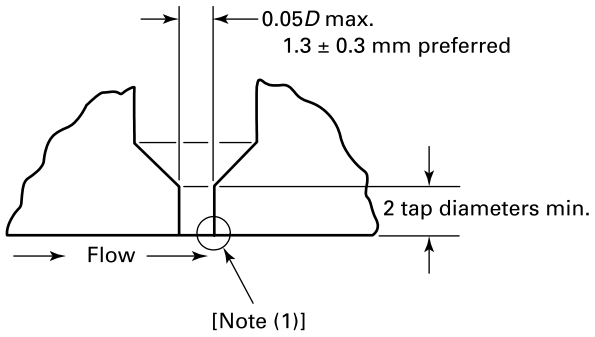

NOTE: (1) Flush, burr-free, and square or lightly rounded to a radius not exceeding 0.1 diameters of the pressure tap.

7-7.1.5 Temperature Measurement. ASME PTC 19.3 shall be followed for temperature measurement. The temperature sensed in a flowing stream by a bare temperature probe, T_p, which does not stagnate the fluid stream, measures a value between the static and stagnation temperature. The correction to stagnation temperature is a function of two quantities.

(a) The first quantity is the recovery factor, as follows:

$$R_f = (T_p - T)/(T_0 - T) \tag{7-7-2}$$

The solution for T_0 from eq. (7-7-2) is as follows:

$$T_0 = T_p/[(T/T_0)(1 - R_f) + R_f] \tag{7-7-3}$$

The value of the recovery factor varies with the shape of the probe, the Reynolds number, and the Mach number of the stream. An approximate value for the recovery factor is 0.85, which is sufficiently accurate when the inlet Mach number is low (e.g., when the β ratio is less than 0.25). Additional details are given in ISO 9300:2005.

(b) The second quantity is the ratio of the static to stagnation temperature (T/T_0) that appears in eq. (7-7-3). This can be calculated from the isentropic relationship in eqs. (7-2-3) through (7-2-6). Alternatively, it can be found from isentropic flow tables that appear in most textbooks on thermodynamics, gas dynamics, or aerodynamics, and in gas property tables (Shapiro, 1954 and Keenan and Kaye, 1948).

7-7.1.5.1 Example.

Flowing fluid = air
Inlet Mach number, Ma = 0.04
Probe temperature, T_p = 289.9 K (520°R)
Recovery factor, R_f = 0.85
T/T_0 = 0.99968
β ratio = 0.2628
From eq. (7-7-3)

(SI Units)

$$T_0 = 289.9/0.999952 = 288.99\ \text{K}$$

(U.S. Customary Units)

$$T_0 = 520/0.999952 = 520.02^\circ\text{R}$$

Note that β in this example slightly exceeded the recommended maximum of 0.25, and the correction to stagnation temperature was still only +0.004%, which would correspond to 0.002% in flow measurement. A few percentage points difference in the recovery factor would not have had a significant effect.

At β values significantly higher than the recommended value of 0.25, the correction becomes larger. In Example 1, if the β ratio were changed to 0.4144, the stagnation temperature would be 288.978 K (520.16°R), for a correction of +0.03%. Considering the square root relationship between the mass flow and absolute temperature, this amounts to a correction of +0.015% in the mass flow. The static to stagnation pressure correction for this same case is 1.007 or +0.7%, and the mass flow would also be corrected +0.7%. The ASME long-radius, high beta ratio flow nozzle [see Figure 7-5.3.4-1, illustration (a)] allows beta ratios as high as 0.8. At a β of 0.8, the temperature correction would be 0.294 K (0.53°R) or +0.5%, for a correction of +0.25% in the mass flow measurement. The pressure correction would be 1.122, for a correction of +12.2% in both the pressure and the mass flow. Because this correction is based on one-dimensional isentropic flow theory for an ideal gas, the error in this correction could be on the order of 1%. This, in addition to uncertainty in the discharge coefficient, is a reason this design is not recommended for sonic flow measurements.

The above examples show that the correction from static to stagnation pressure has about 48 times as much effect on the mass flow measurement as the correction from the bare probe temperature measurement to stagnation temperature.

7-8 COMPUTATION OF RESULTS

7-8.1 Basic Theoretical Relationships

Basic equations and relationships derive from the eight assumptions given in para. 7-3.2 as follows:

(a) Continuity Equation. Conservation of mass for one-dimensional flow, which is applicable to each area of the fluid stream perpendicular to the axis of the meter, is given by

$$q_m = \rho A V \tag{7-8-1}$$

(b) Steady Flow Energy Equation. Conservation of energy, the first law of thermodynamics, applied from the inlet stagnation state to the sonic state at the throat, is given by

$$V^{*2}/2 = h_0 - h^* \tag{7-8-2}$$

(c) Equations of State. Equations of state establish relationships among thermodynamic properties: pressure, temperature, density, compressibility factor, enthalpy, specific heats, ratio of specific heats, and entropy. The relationships depend on the fluid model (i.e., ideal gas, real gas, or vapor).

(d) Isentropic Relationships

$$s_0 = s^* \tag{7-8-3}$$

(e) Local Speed of Sound. Equations for the local speed of sound depend on the fluid model and state properties. The equation for an ideal gas is simple, while the equation for a real gas is complex.

Several equations and methods are available for determining the theoretical sonic flow. Not all the methods are applicable to all compositions of gases and vapors in all operating regimes because of limitations in the availability and accuracy of thermodynamic property data and other factors. The choice of a method is governed by the property data available, the flow measurement accuracy required, and the degree of complexity that is acceptable in the computation for the particular application. Each of these considerations is treated in some detail for each of the equations and methods as they are presented. There are also online databases, including the NIST Standard Reference Database 23: Reference Fluid Thermodynamic and Transport Properties Database-REFPROP, Version 9.1 (Lemmon, Huber, and McLinden, 2013), that can be used to calculate thermophysical properties. A list of references for sonic flow functions is given in ASME MFC-7-2016. Two methods that are recommended are presented in para. 7-8.6, and the remaining methods are presented in subsection 7-11.

7-8.2 Classifications for Theoretical Mass Flow

The methods for determining the theoretical mass flow are grouped into three classifications as described herein.

7-8.2.1 Closed Form Solutions. The simplest theoretical sonic flow equation is for an ideal gas with the specific heats idealized as constants. This equation has sufficient accuracy in many real gas applications over restricted operating regimes, primarily with regard to pressure limitations.

Approximate methods are given for some improvement in accuracy over broader operating regimes for real gases compared to the ideal gas mode. These methods use the compressibility factor, Z, correction to the equation of state. Also, ratios of specific heats are obtained in various ways to approximate the isentropic exponent during expansion from the inlet to the throat of the nozzle or venturi.

7-8.2.2 Iterative Methods Using Gas or Vapor Property Tables. Tables of thermodynamic properties can be used to calculate the flow for various assumed states at the throat of the nozzle. The sonic flow state is then determined where the flow reaches a maximum. Tables of thermodynamic properties have been compiled for many substances for their vapor regimes. Gas tables assume the ideal gas equation of state to be valid but permit the variation of specific heats with temperature to be taken into account.

7-8.2.3 Iterative Methods Using Complex State Equations. The best accuracy over broad operating regimes using real gases and vapors can be obtained by using complex computerized procedures and equations of state described by Johnson (1964). Results from these calculations for air are given in Nonmandatory Appendix C. Sullivan (1989) used more accurate equations of state that were later published by Jacobsen (1991), the results of which are used as the basis for calculating the uncertainties in the other methods. Nonmandatory Appendix C gives the deviations of the Johnson results from those of Sullivan.

7-8.3 Method for Determining the Deviation from Ideal Gas State

The extent of deviation of the compressibility factor, Z, from unity is an indication of how nonideally a gas is behaving in a particular state. This must be known to select a method for determining the sonic flow function to achieve the desired accuracy. Pressure-temperature-density data are correlated by the compressibility factor as follows:

$$Z = P/(\rho RT) \tag{7-8-4}$$

The compressibility factor, Z, is a function of the state of the gas. The real gas equation of state includes the compressibility factor and is correct, subject only to the error in the compressibility factor. Compressibility factors are determined from experimental data, aided by statistical mechanics, and tabulated for each gas composition (et al., 1955).

It is important that the same ideal gas constant, R, be used with the compressibility factors as was used in compiling the compressibility factor tables and charts. Most compressibility factor data are based on the universal gas constant (see para. 7-8.4). Inconsistent use of gas constants with compressibility factors will result in additional error.

In the absence of data for a gas, an estimate of the compressibility factor can be obtained from generalized charts. These charts correlate the compressibility factor by reduced pressures (P/P^*) and reduced temperatures (T/T^*). The reduced properties normalize the data using the sonic point properties (P^*, T^*) based on the principle of corresponding states.

Use the following steps to obtain an estimate of the compressibility factor for a given state (P, T) of a specified gas:

(a) Obtain the sonic point pressure P^* and temperature T^* from sonic property tables available in thermodynamics textbooks.

(b) Calculate the reduced properties for the given state using P/P^* and T/T^*.

(c) The compressibility factor can be found in a chart, such as that shown in Figure 7-8.3-1 for air, using the reduced properties for parameters.

(d) The universal gas constant is used as a basis for correlating the compressibility factors, Z, for real gases (et al., 1955).

7-8.4 Ideal Gas Relationships

The assumption is made that the fluid is an ideal gas for which the equation of state by definition is

$$P = \rho(R_u/M)T \tag{7-8-5}$$

where

M = molecular mass

R_u = universal gas constant; 8.314 kJ/(kmole·K) [1,545 ft·lbf/(lbmole °R)]

In addition to assuming an ideal gas, the further assumption is made that the specific heat values are constant, such that the ratios of specific heats are constant. The isentropic functions given in eqs. (7-2-6) through (7-2-9) are then applicable.

$$P^*/P_0 = (T^*/T_0)^{\gamma/(\gamma-1)} = (\rho^*/\rho_0)^{\gamma} \tag{7-8-6}$$

The speed of sound at the throat for an ideal gas is as follows:

$$c = (\gamma^* R^* T^*)^{0.5} \tag{7-8-7}$$

With the assumption that the ratio of specific heats is constant ($\gamma^* = \gamma_0 = \gamma$), the ideal gas sonic flow function is

Figure 7-8.3-1
Generalized Compressibility Chart

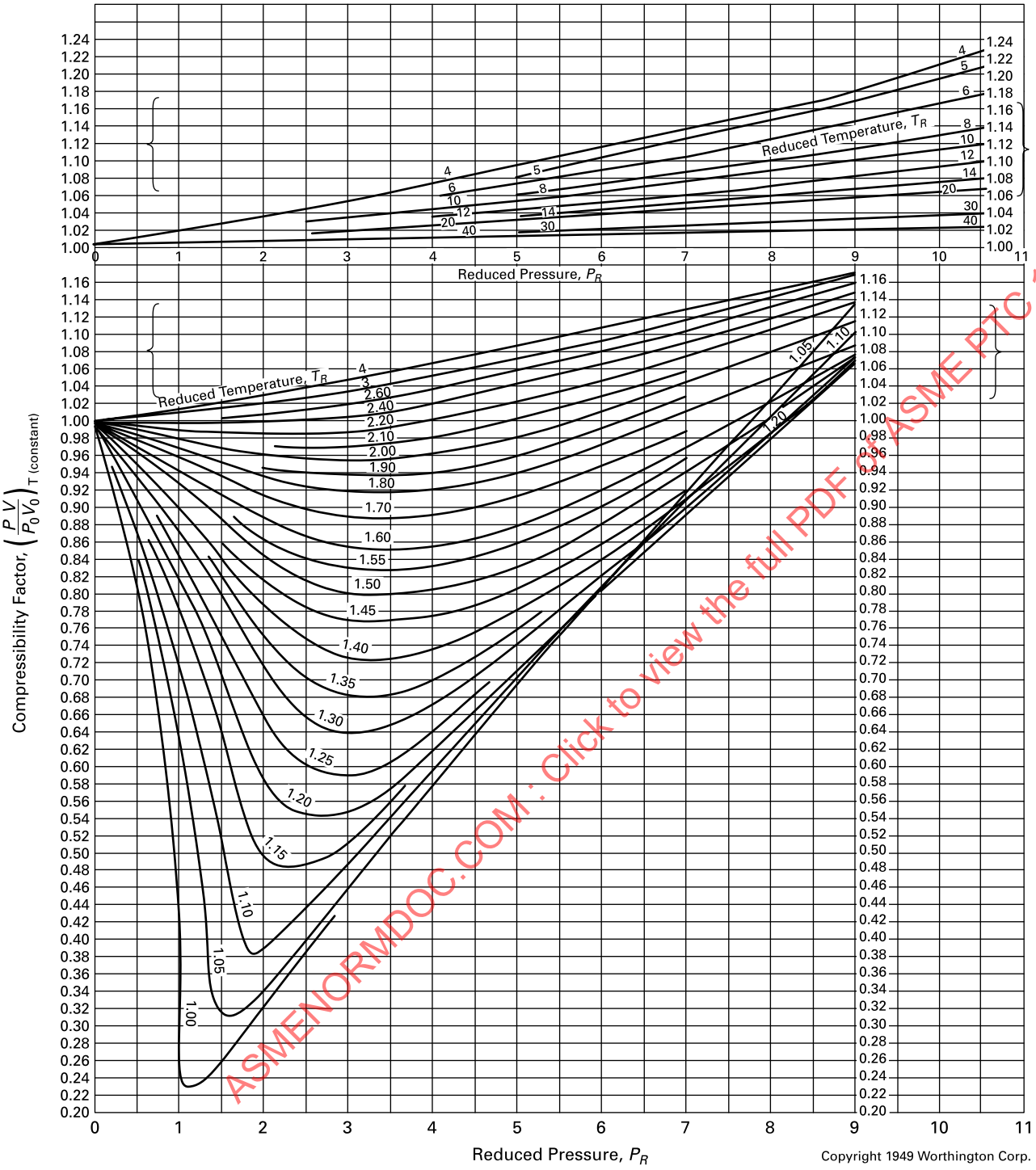

Figure 7-8.3-1
Generalized Compressibility Chart (Cont'd)

GENERAL NOTE: Compressibility factor for gases:
P_R = reduced pressure = P/P^*
T_R = reduced temperature = T/T^*

$$\left(\frac{PV}{P_0V_0}\right)_{T(\text{constant})} = 1 \text{ for ideal gases}$$

P, P^*, T, and T^* are in absolute units.

NOTE: (1) In this range, at reduced temperature approximately equal to 4, the compressibility factor reaches a maximum and then decreases with an increase in reduced temperature values; to avoid confusion in reading, the reduced temperature lines greater than 4 are offset on an identical scale.

$$C_i^* = \sqrt{\gamma\left(\frac{2}{\gamma+1}\right)^{(\gamma+1)/(\gamma-1)}} \tag{7-8-8}$$

The corresponding theoretical flow for an ideal gas with constant specific heats is then

$$q_{mi} = \frac{A^*C_i^*P_0}{\sqrt{(R_u/M)T_0}} \tag{7-8-9}$$

Some methods for calculating the ideal gas sonic flow function, C^*_i, are given in subsection 7-11.

7-8.5 Real Gas Relationships

Sullivan (1981) gives a historical review of theoretical isentropic flow models for real gases. The real gas equation of state is as follows:

$$P = \rho ZRT \tag{7-8-10}$$

The most elementary correction of the ideal gas sonic flow equation for real gas effects is to add the compressibility factor correction to the ideal gas constant [i.e., substituting ZR for the gas constant, R, in eq. (7-8-9)] as follows:

$$C^*_{Ri} = \frac{C_i^*}{Z^{0.5}} \tag{7-8-11}$$

The theoretical equation for the mass flow of a real gas can be calculated from the following:

$$q_{mR} = \frac{P_0A^*C_i^*}{(ZRT_0)^{0.5}} \tag{7-8-12}$$

Two methods for calculating the ideal gas sonic flow function, C^*_i, are given in para. 7-8.6 and the remaining methods are presented in subsection 7-11.

7-8.6 Real Gases, Using Complex Property Equations

7-8.6.1 Method 1: Real Gases, Virial Equation of State. Johnson (1964) published rigorous solutions and extensive tables of sonic flow functions based on real gas properties. Sullivan (1989) added refinements to Johnson's method. These are complex solutions that must have the equations of state programmed for practical evaluation by the iterative procedures they entail.

Two requirements must be met in Method 1 to solve the sonic flow process from the plenum to the throat of the sonic nozzle. First, the plenum and throat entropies must be equal. Second, the throat velocity must be equal to the speed of sound. The processes followed during the calculations to proceed from the plenum to the throat are as shown in Figure 7-8.6.1-1.

Equations for the change of entropy during these processes are as follows:

(a) For the isothermal processes,

$$(s_1 - s_2) = - ZR\ln(P_1/P_0) \tag{7-8-13}$$

$$(s^* - s_2) = - ZR\ln(P^*/P_2) \tag{7-8-14}$$

(b) For the constant pressure process,

$$(s_2 - s_1) = - c_p\ln(T_2/T_1) \tag{7-8-15}$$

(c) For the entropy to be equal at the plenum and throat, the following must be true:

$$(s_1 - s_0) + (s_2 - s_1) + (s^* - s_2) = (s^* - s_0) = 0 \tag{7-8-16}$$

The equations for the entropy changes must be expressed in differential forms to account for the variation of the compressibility factor and specific heat at constant pressure. The variation of specific heat with temperature is taken into account when integrating along the zero-pressure path. (The gas is ideal at zero pressure, where the most accurate data for the specific heat at constant pressure are available.) The compressibility factor must be known and its variation taken into account along the two isothermal processes.

The throat state is calculated by iteration to satisfy the first requirement that the throat and plenum entropies are equal [see eq. (7-8-16)].

To meet the second requirement, the throat velocity and the local speed of sound at the throat must be calculated and iteration continued until the state is found where they are equal. The velocity at the throat is calculated from the energy equation, using the enthalpy decrease from the plenum to the throat. This is determined by integration along the three processes shown in Figure 7-8.6.1-1. The speed of sound is a function of the state at the throat, for which eq. (7-8-17) is used.

$$\begin{aligned} c^2 &= \left(\frac{\delta P}{\delta \rho}\right)_S \\ &= RT\left[Z + \rho\left(\frac{\delta Z}{\delta \rho}\right)_T + \frac{\left[Z + T\left(\frac{\delta Z}{\delta T}\right)_\rho\right]^2}{\frac{c_{P_0}}{R} - 1 - T\left(\frac{\delta}{\delta T}\left\{\int_0^\rho \left[Z - 1 + T\left(\frac{\delta Z}{\delta T}\right)_\rho\right]\frac{d\rho}{\rho}\right\}\right)_\rho}\right] \end{aligned} \tag{7-8-17}$$

The theoretical sonic state at the throat has been determined when both the isentropic and the sonic velocity requirements have been met.

A graph of sonic flow functions for air (Johnson, 1965) is given in Nonmandatory Appendix B.

Figure 7-8.6.1-1
Calculation Processes for the Isentropic Path From Inlet to Sonic Throat for a Real Gas Using the Method of Johnson

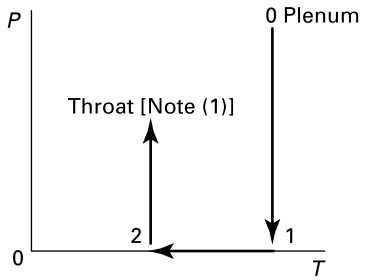

GENERAL NOTE: Adapted from Johnson, 1964.

NOTE: (1) At sonic conditions.

The uncertainty in the sonic flow functions for air (Johnson, 1965) based on results from Sullivan (Sullivan, 1989) is given in Nonmandatory Appendix C. It is seen that the largest discrepancy is 0.4% at the inlet stagnation state corresponding to the highest pressure (100 atm) and lowest temperature (400°R). Below 25 atm, the two methods agree to within 0.02% at temperatures from 400°R to 700°R.

An approximate graphical method for obtaining sonic flow functions for air is given in Nonmandatory Appendix D. The correction factors provided by the graphs convert the ideal gas sonic flow function for air (0.6847315) to real gas values (Sullivan, 1989). The graphs extend to a pressure of 300 atm and cover temperatures from 400°R to 700°R.

7-8.6.2 Method 2: Real Gases, Table Lookup or Curve Fitting to the Results of Method 1. When accurate solutions have been obtained for a gas over the operating range of interest, it may be preferable to use these results rather than recalculate using Methods 1 through 6. Depending on the application, either table interpolation or curve fitting could be used. Both provide close to the maximum available accuracy without the complexity of repeating the calculations. Equations that fit the surface of sonic flow function versus pressure and temperature may be obtained with good accuracy over limited ranges.

7-9 FLOW UNCERTAINTY

7-9.1 Uncertainty in Sonic Flow Function Calculations

Accuracy considerations are complicated by two fundamentals. First, all measurements contain errors. Second, the absolute accuracy of a measurement is never known. Procedures are well established for calculating the propagation of errors to determine the uncertainty in the result. One of the standardized practices should be used (e.g., ASME PTC 19.1), but the basis for applying these procedures is the estimated uncertainty in each error source. The mathematical rigor of the propagation calculations can give the false impression that the uncertainty in the result has been precisely determined. A practical indication of uncertainty is obtained by comparing the results from different methods. The amount of discrepancy often does more to indicate the level of accuracy and confidence that can be placed in the results than formalized uncertainty analyses based on estimates. For this reason, comparisons of results from different flow measurement methods should be made whenever possible.

Convenience and accuracy may both be important in obtaining a flow measurement. A sophisticated data reduction procedure that provides better accuracy might be essential in some cases but, for practical reasons, not desirable in others. One of several components in an uncertainty analysis is the error in the sonic flow function. A trade-off may be made between a more rigorously accurate calculation and a more convenient simplified calculation that could contain a larger bias. Arnberg and Seidl (2000) give errors and corrections that take real gas properties into account for sonic flow functions for air calculated in several ways using ideal gas theory.

7-9.2 Calibration Methods and Uncertainty Estimates for Discharge Coefficients

7-9.2.1 General. Discharge coefficients are determined experimentally and analytically. Experimentally determined discharge coefficients are subdivided into primary and secondary measurements. Secondary measurements are performed with the test meter in series with one or more sonic flowmeters, which have been previously calibrated by primary methods, in parallel. Many primary methods have been developed. Uncertainty estimates using standardized procedures are performed on the primary methods; however, confidence in the absolute accuracy of the primary methods can only be obtained by consistency in the results from the different methods.

7-9.2.1.1 Experimentally Determined Discharge Coefficients. The accurate measurement of mass flow of gas is more difficult than for a liquid. Since liquid calibrations cannot be applied to sonic flow measurements with accuracy, it has been necessary to develop several primary methods for measuring the mass flow of gases. Probe traverses, volume displacement (bell prover), change of state in a calibrated volume, and bulk mass flow measurements (gravimetric methods) have all been used.

7-9.2.1.2 Analytically Determined Discharge Coefficients. Analytically determined discharge coefficients use boundary layer theory and potential flow theory to calculate the deviations of the actual flow from the ideal one-dimensional inviscid flow model. Stratford (1964), Hall (1962), and Ishibashi and Takamoto (1999) provided analytical discharge coefficients for sonic flow nozzles. Smith and Matz (1962) used theory and internal flow measurements to obtain discharge coefficients for sonic flow venturi nozzles.

7-10 DISCHARGE COEFFICIENTS

7-10.1 Method of Correlation of Discharge Coefficients

The discharge coefficient corrects for the deviation of the actual mass flow from the theoretical value. The throat Reynolds number correlates the discharge coefficients for sonic flowmeters. For axially symmetric flowmeter designs, all flow sections are circular in cross section, such that the throat Reynolds number is given by the following:

$$\mathrm{Re}_d = \frac{4q_m}{\pi d\mu} \tag{7-10-1}$$

The absolute viscosity, μ, is determined at the inlet stagnation temperature.

Theoretical solutions for the discharge coefficients of toroidal throat venturi nozzles indicate the discharge coefficient is a weak function of the ratio of specific heats in addition to the Reynolds number. This fact will cause some scatter when the data includes gases with different ratios of specific heat (Arnberg, Britton, and Seidl, 1974).

7-10.2 Discharge Coefficients for Toroidal Throat

For gases with a fixed ratio of specific heats, the analytical solutions indicate that the discharge coefficients can be correlated in the laminar boundary layer range by the following equation:

$$C = a - b\mathrm{Re}_d^{-0.5} \tag{7-10-2}$$

The same form of equation applies in the turbulent boundary layer range with the Reynolds number exponent changed from −0.5 to −0.2. Table 7-10.2-1 summarizes the results from approximately 690 measurements on 95 venturi nozzles compiled from 13 sources (Arnberg and Ishibashi, 2001a and Arnberg and Ishibashi, 2001b). Ten of these were secondary measurements and 680 were primary measurements of various types. Some of these measurements were averaged to reduce random error resulting in 143 points to be plotted. Added to these measured average points were 26 analytical points (Stratford, 1964): 11 for laminar boundary layer and 15 for turbulent. The total 169 points are shown in Figure 7-10.2-1. The scatter in the data is caused by the manufacturing tolerances allowed in the standards, measurement errors, and, most importantly, boundary layer transition. An uncertainty range of 0.3% (2σ or random) is shown. The universal curve is represented by the following:

$$C = 0.9959 - 2.72\mathrm{Re}_d^{-0.5} \tag{7-10-3}$$

Lower uncertainties can be obtained by manufacturing venturi nozzles to closer tolerances than specified by the standards. When the flow range is limited (2.00 E+05 < Re_d < 1.2 E+06) and falls within the laminar boundary layer regime, a particular design of venturi nozzle can be calibrated to an uncertainty as low as 0.07% (systematic + random) (Shapiro, 1954). This uncertainty can be reduced statistically to 0.05% by placing several venturi nozzles in parallel.

High-precision venturi nozzles manufactured by super accurate lathes have performance characteristics that are highly repeatable. The first three references listed in Table 7-10.2-1 used high-performance venturi nozzles. Equation (7-10-4) fits the data from this source, which covers a flow range of (2.1 E+04 < Re_d < 1.4 E+06). At the lower Reynolds numbers, the estimated uncertainty is ±0.2%, which decreases to ±0.1% (systematic + random) at the higher Reynolds numbers.

$$C = 0.9985 - 3.396\mathrm{Re}_d^{-0.5} \tag{7-10-4}$$

The mean curve for the composite data in Figure 7-10.2-1 is fitted by eq. (7-10-3) and is named “the universal curve” (UC). This equation and name were adopted by ISO 9300 as an International Standard in 2005. It is a “universal curve” because it may be used with all toroidal throat venturi nozzles manufactured to ASME MFC-7–2016 or ISO ISO 9300:2005. The UC has the advantage of simplicity and covers Reynolds numbers through laminar, transition, and turbulent boundary layer ranges. This simplicity is obtained by allowing a relatively large tolerance of 0.3% on the discharge coefficient. As seen in Figure 7-10.2-1, all of the data points that fall outside of this band are in the Reynolds number range of 1.0×10^6 to 1.0×10^7, which is where transition is taking place from laminar to turbulent boundary layers.

Figure 7-10.2-2 compares several mean line discharge coefficient curves for toroidal throat venturi nozzles. The boundary layer transition for two sets of high-precision venturi nozzles is also shown. Whereas the transition curves occur at different Reynolds numbers, in both cases they proceed from the mean curve for high-precision venturi nozzles at laminar flow, eq. (7-10-4), to the universal curve, eq. (7-10-3).

Table 7-10.2-1
Summary of Points Plotted in Figure 7-10.2-1 and Coefficients for Eq. (7-10-2)

Reference	*a*	*b*	Re_d, Min.	Re_d, Max.	Nozzles	Diameter, mm	Avg. Pts.
Ishibashi and Takamoto (1998)	0.9985	3.412	2.40 E+04	8.50 E+04	23	3.4~19	23
Ishibashi et al. (1998)	...	...	2.10 E+04	1.70 E+05	5	6.7–13.41	10
Takamoto et al. (1994); Ishibashi and Takamoto (1999)	...	...	4.30 E+04	1.40 E+06	2	6.7 & 19	12
Wendt and von Lavante (2000)	0.9982	3.448	5.00 E+04	1.30 E+05	3	5~10	12
Karnik et al. (1996)	...	...	1.00 E+07	2.40 E+07	2	10, 23.3	2
Stevens (1986)	0.9975	3.901	2.00 E+05	1.20 E+06	14	7.9	21
Smith and Matz (1962), Beale (1999)	...	...	4.00 E+05	5.00 E+06	1	143	7
Olsen (1972)	...	...	8.68 E+05	3.37 E+06	1	25	6
Arnberg, Britton, and Seidle (1974)	0.9974	3.306	4.00 E+04	2.50 E+06	16	3.8~35	18
Anonymous (1986)	...	...	1.60 E+06	3.20 E+07	10	25~59	10
Brain and McDonald (1977)	...	...	3.70 E+05	7.20 E+05	1	5~17	3
Brain and Reid (1978)	...	...	1.50 E+06	1.17 E+07	5	5~17	10
Brain and Reid (1981)	...	...	1.07 E+06	1.07 E+07	12	4.5~34.9	9
Stratford (1964), laminar	0.9984	3.032	1.00 E+05	2.00 E+06	$C_d = a - b\mathrm{Re}_d^{-1/2}$		11
Stratford (1964), turbulent	0.9984	0.0693	5.00 E+05	1.00 E+07	$C_d = a - b\mathrm{Re}_d^{-1/5}$		15

Figure 7-10.2-1
Composite Results for Toroidal-Throat Venturi Nozzles

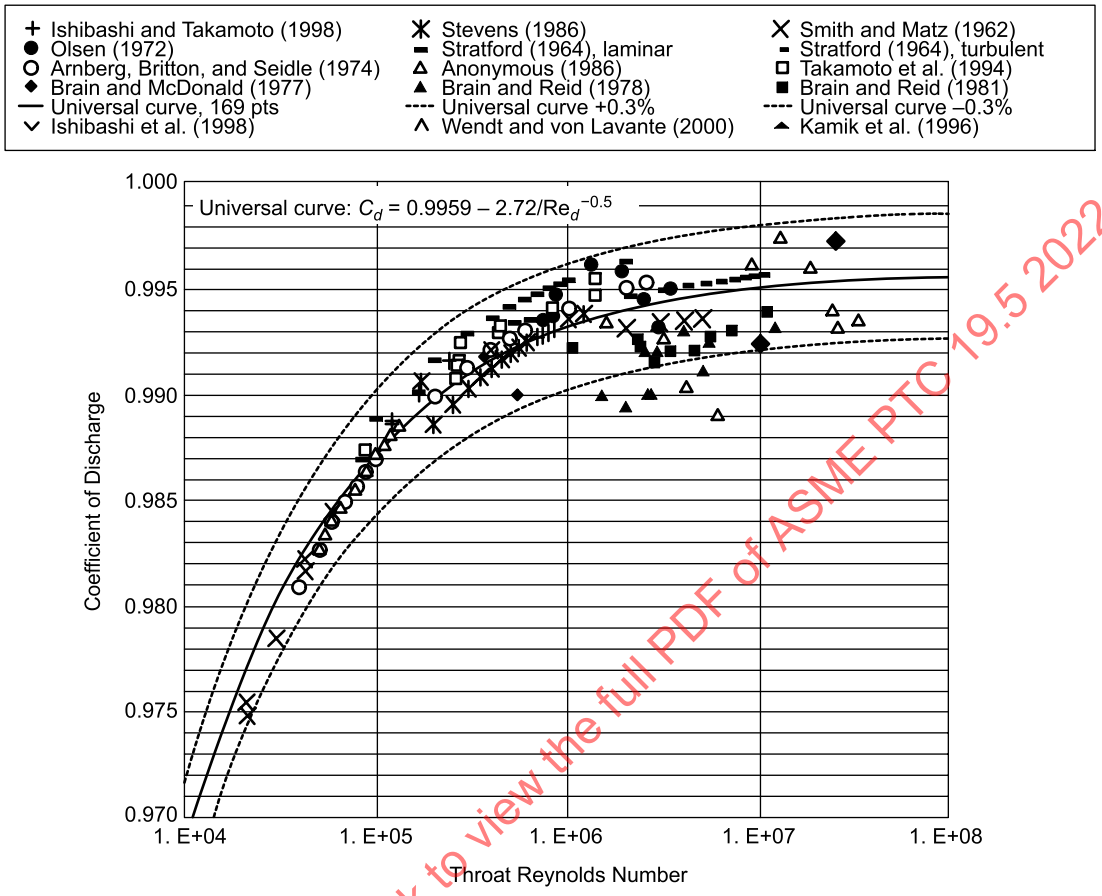

Figure 7-10.2-2
Mean Line Discharge Coefficient Curves for Toroidal-Throat Venturi Nozzles

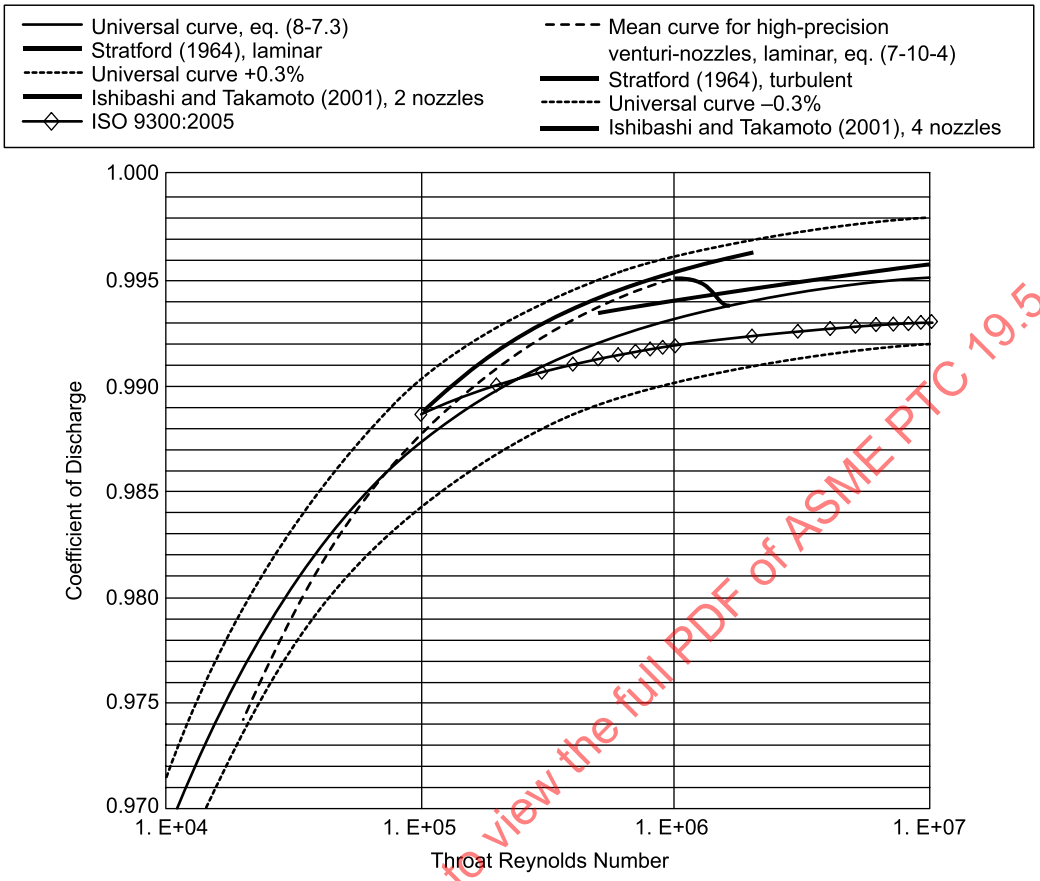

7-10.3 Discharge Coefficients for Cylindrical Throat Venturi Nozzles

The discharge coefficients for the cylindrical throat venturi nozzle are given in Table 7-10.3-1 (ASME MFC-7–2016 and ISO 9300:2005).

The discharge coefficient of the cylindrical throat venturi nozzle has a smaller change in the discharge coefficient (see Table 7-10.3-1) during boundary layer transition than the toroidal throat venturi nozzle. However, this comes at the expense of a thicker throat boundary layer with a correspondingly lower discharge coefficient, as indicated by the following comparison at a throat Reynolds Number of 1.0×10^7:

(a) for cylindrical throat, C = 0.9914 (see Table 7-10.3-1)

(b) for toroidal throat, C = 0.9952 (see Figure 7-10.2-2)

The discharge coefficient for the toroidal throat venturi nozzle is 0.38% higher than the discharge coefficient for the cylindrical throat venturi nozzle. This is discussed further in para. 7-5.3.

7-10.4 Discharge Coefficients for ASME Low-β Throat Tap Flow Nozzles (Arnberg and Ishibashi, 2001b)

Compared to the sonic flow nozzle, which has only one operating parameter, the subsonic flow nozzle has two parameters, the throat Reynolds number and the throat Mach number. Error in the theory and/or real gas properties may have caused the discharge coefficient to exceed 1.0 at the highest Reynolds numbers. Excluding this data, all the results fall within a 1% band.

Where operation in both the subsonic and sonic regimes is required, the ASME low-β throat tap flow nozzle is recommended because of the availability of calibration data for both regimes. It is noted that the downstream pressure must be maintained at a lower value to have sonic flow with the ASME flow nozzle because of the absence of a diffuser (see Figure 7-4-2).

Table 7-10.3-1
Discharge Coefficients for Cylindrical-Throat Venturi Nozzles

Reynolds Number, Re_d	Discharge Coefficient, C
3.5×10^5	0.9887
5×10^5	0.9887
2×10^6	0.9887
3×10^6	0.9890
5×10^6	0.9901
7×10^6	0.9907
1×10^7	0.9914
2×10^7	0.9925

7-10.5 Boundary Layers and Discharge Coefficients

In Figure 7-10.2-2, the curve from Ishibashi and Takamoto (2001) shows the boundary layer transition starting at 1.0×10^6. Figures 11 and 12 of Ishibashi (2003) show boundary layer transition taking place over the Reynolds number range from 1.0×10^6 to 1.5×10^6. The discharge coefficient decreased from 0.995 to 0.9935 from a laminar to a turbulent boundary layer. Varner's nozzles were over 13 times larger than the largest of Isibashi's nozzles. This large difference in size may have influenced the start of the boundary layer transition because of the longer inlet contour. Boundary layer transition in ASME standard nozzles used subsonically, investigated and reported by Murdock and Keyser (1991a and 1991b), manifest the same characteristic shapes and magnitude of effects over the same range of Reynolds number, thereby affecting the discharge coefficient as discussed herein (see Section 5). Ishibashi et al. (2005) report test results for more than 50 sonic flow venturi nozzles at over 250 test conditions, all in the laminar boundary layer range. The standard deviation for the data was 0.04%.

Figure 7-10.2-2 shows the transition from laminar to turbulent boundary layer for two sets of data started at Reynolds numbers of 0.9×10^6 and 1.3×10^6 and completed at about 1.5×10^6. The discharge coefficient decreased from about 0.995 to 0.9935 during transition. These data indicate an added uncertainty in the boundary layer transition range of about 0.15%.

A new equation to take advantage of the lower uncertainty available from more accurate equations applicable specifically to the laminar and turbulent ranges, and to pass through the transition range, is needed.

Funaki and Ishibashi (2008) propose a new UC based on the hyperbolic tangent.

It requires four parameters that are obtained from the equations for the laminar boundary layer range, turbulent boundary layer range, and the transition range (for which the UC is used). The new UC follows the data through the boundary layer transition range. The uncertainty is reduced to below 0.1%, except in the transition range, where uncertainties as to the start of the boundary layer transition increase the uncertainty to about 0.2%. The new UC joins the curve for the turbulent boundary layer range, following the boundary layer transition region.

7-11 OTHER METHODS AND EXAMPLES

7-11.1 Traditional and Useful Methods for the Computation of Flow

The methods in paras. 7-11.1.1 through 7-11.1.5 have been used in the past and, when applied in accordance with the assumptions and conditions specified with each method, can provide sufficient accuracy for the required results. In general, these are direct, simpler, and easier to use. These are also useful for an initial estimate of the flow during the test-design phase of performance testing and to check the reasonableness of the calculated results from the more complex methods. These are listed in priority order of recommendation.

7-11.1.1 Method 3: Real Gas Approximation Using the Ideal Gas Sonic Flow Function Corrected by the Compressibility Factor. This method uses eqs. (7-8-8) and (7-8-11) to obtain an approximation for the real gas sonic flow function. The compressibility factor and ratio of specific heats used in the solution correspond to the inlet stagnation state.

The error in the real gas sonic flow function for air using Method 3, based on Sullivan (1989), is shown in Figure 7-11.1.1-1 (Sullivan, 1981). Table 7-11.1.1-1 gives errors in Method 3 based on sonic flow functions from Johnson (1965).

At an inlet temperature of 263.9 K (475°R) and a pressure of 80 atm, the error from Figure 7-11.1.1-1 is 1.18% compared with 1.67% from Table 7-11.1.1-1. Since Johnson and Sullivan used nearly identical calculation methods, the difference of 0.49% in the results is attributed to discrepancies between the property data of Hilsenrath et al. (1955) and Jacobsen (1991).

Figure 7-11.1.1-1
Error in Method 3 for Air Based on Sonic Flow Functions When Using Air Property Data

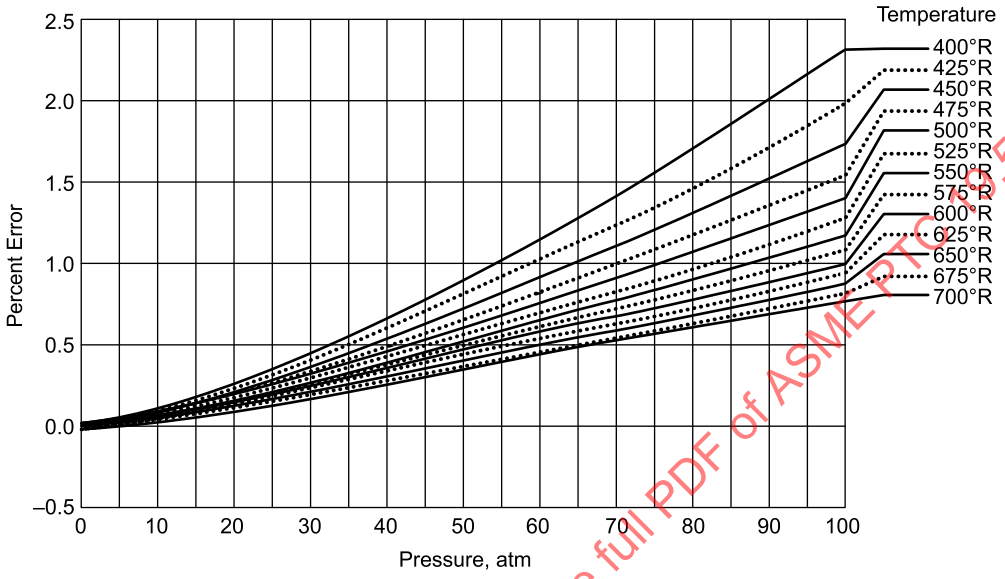

GENERAL NOTES:
(a) Error in real gas sonic flow function for air is based on ideal gas sonic flow function, inlet ratio of specific heats γ_0, and inlet compressibility factor, Z_0.
(b) Sonic flow functions for air are from Sullivan (1989) and air property data are from Jacobsen (1991) and Sullivan (1981).

Table 7-11.1.1-1
Percent Error in Method 3 Based on Sonic Flow Functions and Air Property Data

	Inlet Stagnation Pressure, atm				
Temperature, °R	5	10	20	40	80
475	+0.17	+0.33	+0.65	+ 1.18	+ 1.67
500	+0.13	+0.25	+0.50	+0.91	+1.23
550	+0.06	+0.15	+0.30	+0.52	+0.60
600	+0.03	+0.08	+0.15	+0.26	+0.18
700	−0.03	−0.04	−0.03	−0.09	−0.31

GENERAL NOTE: Sonic flow functions from Johnson (1965) and air property data from Hilsenrath et al. (1955).

7-11.1.2 Method 4: Real Gases and Vapors, Thermodynamic Property Tables. This method is applicable to real gases and vapors for which thermodynamic property tables are available. These tables contain properties such as entropy, enthalpy, and mass density (more commonly the reciprocal, specific volume) as functions of two variables, usually the pressure and temperature. The accuracy of the result using this method is very sensitive to the accuracy and resolution of the property tables.

The gas tables give properties as a function of temperature and are applicable only at low pressures, where deviations from ideal gas properties are small. The thermodynamic property tables account for real gas effects by taking both temperature and pressure into account. With two independent variables instead of one, interpolation of the tables becomes more complex. When the thermodynamic properties have been computerized, the iterative calculations are much easier to perform. Solutions are shown using a table lookup of properties. The same method would apply using computerized properties.

The difference between Method 1 in para. 7-8.6.1 and Method 4 stems from the type of property data used. Method 4 uses the enthalpy and entropy values correlated by researchers in compiling the thermodynamic property tables. Method 1 uses the more fundamental correlation of specific enthalpy and entropy values correlated by researchers in compiling the thermodynamic property tables. Specific heat at constant pressure and compressibility factor or, alternatively, the equations of state are the basis for determining the compressibility factors. A brief summary of the method used by Johnson (1964) is given in para. 7-8.6.1.

7-11.1.2.1 Example. This example uses thermodynamic property tables and linear interpolation between quantities in the tables. This method is not the most accurate, but it is useful because thermodynamic property tables are widely available for many substances.

The gas used is steam and the gas property data is obtained from Keenan and Keys (1959).

For this example, a plenum state is selected where the steam is a nonideal gas (a vapor). This is indicated by a large change in enthalpy at constant temperature, indicating the properties change significantly with pressure as well as temperature.

Inlet stagnation state:

Pressure, P_0 = 6.8948 kPa (1,000 psia)
Temperature, T_0 = 371.1°C (700°F) or 644.25 K (1,160°R)
Enthalpy, h_0 = 3 082.65 kJ/kg (1,325.3 Btu/lbm)
Entropy, s_0 = 6.33923 kJ/(kg·K) [1.5141 Btu/(lbm·°R)]

An iterative solution establishes the throat state. An even temperature from the table is chosen for the first guess.
T^* = 315.6°C (600°F) or 588.88 K (1,060°R)
s^* = s_0 = 6.33923 kJ/(kg · K) [1.5141 Btu/(lbm·°R)]

The following values are found from the tables at this state:
h^* = 2 984.03 kJ/kg (1,282.9 Btu/lbm)
v^* = 0.0516 m^3/kg (0.827 ft^3/lbm)

The throat velocity, V^*, and mass flow per unit area, G^*, are as follows:

(SI Units)

$$\begin{aligned} V^* &= [2g_c(h_0 - h^*)]^{0.5} \\ &= [(2)(1)(1\,000)(3\,082.65 - 2\,984.03)]^{0.5} \\ &= 444.117 \text{ m/s} \end{aligned}$$

(U.S. Customary Units)

$$V^* = [2g_c(h_0 - h^*)]^{0.5} = [(2)(32.174)(778.26)(1{,}325.3 - 1{,}282.9)]^{0.5} = 1{,}457.2 \text{ ft/sec}$$

(SI Units)

$$G^* = V^*/v^* = 444.117/0.0516 = 8\,607 \text{ kg/(s·m}^2\text{)}$$

(U.S. Customary Units)

$$G^* = V^*/\nu^* = 1{,}457.2/0.8205 = 1{,}776\,\text{lbm}/(\text{sec}\cdot\text{ft}^2)$$

Iteration is continued to find the maximum flow, which is the sonic flow point.

The throat temperature and entropy fixed the sonic flow state. Thus, interpolation from the tables gives the state at the throat as

P^* = 3.7694 MPa (546.7 psia)
s^* = 6.33923 kJ/(kg·K) [1.5141 Btu/(lbm·°R)]
T^* = 287.8°C (550°F)

Although not expected to be very accurate, an ideal gas estimate for the throat temperature for a triatomic gas is made using the critical temperature ratio from Table 7-11.1.2.1-1 as follows:

(SI Units)

$$T^*_i = T_0(T^*/T_0) = (644.25)(0.85714) = 552.21\,\text{K}\,(279.06°\text{C})$$

(U.S. Customary Units)

$$T^*_i = T_0(T^*/T_0) = (1,\ 160)(0.85714) = 994.3°\text{R}\,(534.6°\text{F})$$

In spite of the nonideal gas states over this flow process, the ideal gas estimate of the throat temperature would have provided a useful guide for the first estimate, thus reducing the number of iterations required. The real gas theoretical (isentropic) mass flow at a throat temperature of 287.8°C (550°F), corresponding to the sonic flow point, was found to be q_{mR}/A = 8939.7 kJ/(s·m^2) [1,831 lbm/(sec·ft^2)].

The discrepancy between the result from this example and the result from Johnson (1964) is 0.36%. Note that the steam tables were first published in 1936 from a different database than Johnson's value, which was primarily based on Hilsenrath et al. (1955). Presumably, the later property data are the most accurate (see para. 7-11.1.3).

7-11.1.3 Method 5: Ideal Gas, Ratio of Specific Heats Assumed Constant. Regarding eq. (7-8-8), note that for an ideal gas with a constant ratio of specific heats, the sonic flow function, C^*_i, depends only on the composition of the gas (i.e., it is a constant for each gas composition). Whereas no gas is ideal, all gases approach the ideal state at low pressure and most gases behave in a more idealized manner with increasing temperature. In many applications, the simplicity of the flow calculation using eq. (7-8-8) is a desirable feature and may provide a practical approach, assuming the error that is incurred is tolerable.

Values of the sonic flow function from eq. (7-8-8) and the critical property ratios from eqs. (7-2-7) through (7-2-9) are given in Table 7-11.1.2.1-1 for monatomic gases (3 deg of freedom), diatomic gases (5 deg of freedom), and triatomic gases (6 deg of freedom).

The sonic flow functions, C^*_i, given in Table 7-11.1.2.1-1 are quite accurate for monatomic gases because their specific heats are nearly constant.

The constant sonic flow function for a diatomic gas from eqs. (7-2-7) through (7-2-9) can be corrected to the real gas value for air by means of correction factors given in Nonmandatory Appendix D (Arnberg and Seidl, 2000).

Table 7-11.1.2.1-1
Sonic Flow Function, C^*_i, and Critical Property Ratios [Ideal Gases and Isentropic Relationships, Eqs. (7-2-7) Through (7-2-9)] Versus Type of Ideal Gas

Type of Gas	Ratio of Specific Heats	Sonic Flow Function, C^*_i	Critical Temperature Ratio	Critical Pressure Ratio	Critical Density Ratio
Monatomic	$5/3$ = 1.6667	0.72618	0.75000	0.48714	0.64953
Diatomic	$7/5$ = 1.4	0.68473	0.83333	0.52828	0.63393
Triatomic	$8/6$ = 1.333	0.67322	0.85714	0.53977	0.62944

The following ideal gas relationships show that the ratio of specific heats is related to the specific heat at constant pressure and the gas constant:

$$R = c_p - c_v \tag{7-11-1}$$

Ratio of specific heats:

$$\gamma = c_p / c_v \tag{7-11-2}$$

Gamma function:

$$\frac{\gamma - 1}{\gamma} = \frac{R}{c_p} = \frac{\overline{R}}{\overline{c}_p} \tag{7-11-3}$$

Consequently, the sonic flow function, C^*_i, will vary for any particular ideal gas as the specific heat at constant pressure varies. This imposes restrictions on the operating states and/or flow measurement accuracy obtainable from Method 3, Method 5, and Method 6, which is introduced in para. 7-11.1.4, wherein the variation of specific heats is not taken into account.

7-11.1.4 Method 6: Ideal Gas, Ratio of Specific Heats at Inlet Stagnation State. The easiest way to partially compensate for changes in specific heats is to use the ratio of specific heats corresponding to the inlet stagnation state, instead of a fixed value for each gas, as in Method 5. The error in Method 6 is shown in Figure 7-11.1.4-1.

Figure 7-11.1.4-1
Error in Sonic Flow Function, C^*_i, for Air Using Method 6 Based on Ideal Gas Theory With Ratio of Specific Heats Corresponding to the Inlet Stagnation State

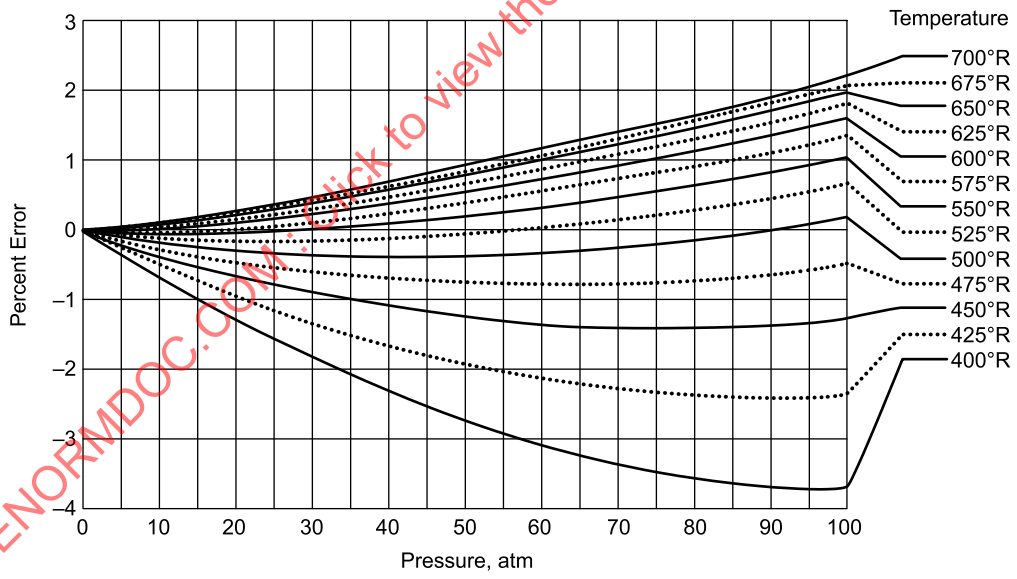

GENERAL NOTES:
(a) Error in ideal gas critical flow function for air, based on inlet ratio of specific heats, γ_0.
(b) From Arnberg and Seidl, 2000.

7-11.1.4.1 Example.

Gas = air
Inlet stagnation pressure, P_0 = 100 atm
Inlet stagnation temperature, T_0 = 287.8°C (550°R)
Real gas (Sullivan, 1989), C^*_R = 0.7083
Real gas (Hilsenrath et al., 1955), γ_0 = 1.5944
From eq. (7-8-8), based on γ_0 = 1.5944, Method 6, C^*_i = 0.7156; error, e = +1.03%
From Figure 7-11.1.4-1, error, e = +1.00% (agreement to the readability of the graph)
Based on Method 3, from Table 7-11.1.2.1-1, ratio of specific heats, γ = 1.4
C^*_i = 0.68473
Error, e = −3.33%
Compared with Method 5, Method 6 reduced the absolute error from 3.33% to 1.03%.

7-11.1.5 Method 7: Ideal Gas, Gas Tables. Most textbooks on thermodynamics and gas dynamics published since 1948 have included gas tables abridged from Keenan and Kaye (1945). These tables enable solutions for isentropic processes to be calculated for ideal gases with the variation of specific heats with temperature taken into account. These tables make it possible to calculate sonic flow more accurately than by Methods 5 and 6, the latter of which will be shown in the example in para. 7-11.1.5.1.

7-11.1.5.1 Example 4, Gas: Air. Gas property data is obtained from Keenan and Kaye (1945). An inlet state is chosen at a sufficiently low pressure to meet the ideal gas requirement quite well and at a high temperature where a large variation in the ratio of specific heats is expected.

Inlet state:

Pressure, P_0 = 10 atm = 1.01325 MPa (146.96 psia)
Temperature, T_0 = 388.9 K (700°R)
Enthalpy, h_0 = 389.745 kJ/kg (167.56 Btu/lbm)
Reduced Pressure, P_{R_0} = 3.446

The first approximation of the sonic state at the throat will be made using the isentropic constant, γ, values from Table 7-11.1.2.1-1.

(SI Units)

$$T^* = T_0(T^*/T_0) = (388.9)(0.83333) = 324.08\,\text{K}$$

(U.S. Customary Units)

$$T^* = T_0(T^*/T_0) = (700)(0.83333) = 583.3^\circ\text{R}$$
$$h^* = 324.384\,\text{kJ/kg}\,(139.46\,\text{Btu/lbm})$$
$$P_{R0}{}^* = 1.8161$$

(SI Units)

$$P^* = P_0(P_R{}^*/P_{R0}) = 1.01325\,MPa\,(1.8161/3.446)$$
$$= 0.5339999\,\text{MPa}$$

(U.S. Customary Units)

$$P^* = P_0(P_R{}^*/P_{R0}) = 146.96\,(1.8161/3.446)$$
$$= 77.4504\,\text{psia}$$

(SI Units)

$$\rho^* = P^*/RT^* = (1\text{E} + 06)(0.5339999)/[(287)(324.08)]$$
$$= 5.74123\,\text{kg/m}^3$$

(U.S. Customary Units)

$$\begin{aligned}\rho^* &= P^*/RT^* = (144)(77.4504)/(53.34)(583.3)\\ &= 0.35850\,\text{lbm/ft}^3\end{aligned}$$

(SI Units)

$$\begin{aligned}V^* &= [2g_c(h_0 - h^*)]^{0.5}\\ &= [(2)(1)(1000)(389.745 - 324.384)]^{0.5}\\ &= 361.555\,\text{m/s}\end{aligned}$$

(U.S. Customary Units)

$$V^* = [2g_c(h_0 - h^*)]^{0.5} = [(2)(32.174)(778.26)(167.56 - 139.46)]^{0.5} = 1186\,\text{ft/sec}$$

(SI Units)

$$q_m/A = \rho V^* = (5.74123)(361.555) = 2075.8\,\text{kg/(s·m}^2)$$

(U.S. Customary Units)

$$q_m/A = \rho V^* = (0.35850)(1186) = 425.2\,\text{lbm/}\left(\text{sec-ft}^2\right)$$

The above calculation is repeated for a range of temperatures in the region of the first approximation of T^* from which the sonic flow state is determined as the point at which maximum flow occurs.

The throat state is established at 324.4 K (584.0°R) corresponding to the maximum mass flow of 2 075.833 kg/(s·m^2) (425.164 lbm/sec-ft^2). This result is in error by −0.12% compared with Sullivan (1989).

Method 7, in which gas tables are used, is similar to Method 4.

7-12 SPECIAL APPLICATIONS

7-12.1 Special Applications of Sonic Flow Nozzles and Venturis

The sonic flowmeter is most commonly used to measure and control the mass flow of a gas or vapor. Special meters with the same name should be mentioned to avoid confusion.

The sonic flow choke has a long history of use as a flow-limiting device. The accuracy with which the mass flow through a choke must be known may vary with the particular application.

The flow through a rupture disk and pressure relief valve are related applications. A mass flow determination under sonic flow conditions may be important, but the accuracy requirement is not as great as for sonic flowmeters.

There is a need to distinguish between sonic flowmeters used for measuring the flow of gases and vapors and sonic flow devices used to measure the discharge of flashing liquids. (These were once called cavitating venturis.) The use of the same names may create some confusion since they operate on different principles. When near-saturated or supercooled liquids enter a nozzle or venturi, they change phase from liquid to vapor (flash), which causes a choked flow condition. These devices share some operational similarities with critical gas flow devices in that the mass flow is nearly linear with the inlet pressure. Liquid sonic flowmeters are used in the nuclear power field (Reshetnikov, Isayev, and Nevolin, 1987).

Another specialized application makes use of the unique characteristics of the sonic flowmeter related to the volumetric flow, which is nearly constant upstream of a sonic flowmeter while the mass flow is varied if certain conditions are met over the operating range. These conditions are as follows:

(a) The stream is nearly an ideal gas (i.e., the variation in the compressibility factor is insignificant).

(b) The discharge coefficient of the meter does not vary significantly over the flow range.

(c) The sonic flow function is constant. This is true for an ideal gas.

(d) The Mach number upstream of the meter is low such that the differences between the static and stagnation properties (pressures and temperatures) of the stream are insignificant.

Based on these assumptions, the volumetric flow upstream of the meter is nearly constant. Real gases and flowmeters will deviate in varying degrees from these conditions.

7-13 REFERENCES

Arnberg, B. T., Britton, C.L., and Seidl, W.F. (1974). "Discharge Coefficient Correlation for Circular-Arc Venturi flowmeters at Critical (Sonic) Flow." Journal of Fluids Engineering, 96(2) (June), 111–123.

Arnberg, B. T., and Ishibashi, M. (2001a). "Discharge Coefficient Equations for Critical-Flow Toroidal-Throat Venturi-Nozzles." The ASME Fluids Engineering Division Summer Meeting. The American Society of Mechanical Engineers.

Arnberg, B. T., and Ishibashi, M. (2001b). "Review of flow nozzle and venturi designs and discharge coefficients." The International Instrumentation Symposium. Instrument Society of America.

Arnberg, B. T., and Seidl, W. F. (2000). "A Comparison of Errors in Four Methods for Determining Critical Flow Functions for Sonic Flow Nozzles and Venturis." The ASME Fluids Engineering Division Summer Meeting. The American Society of Mechanical Engineers.

Aschenbrenner, A. (1983). "The Influence of Humidity on the Flowrate of Air through Critical Flow Nozzles." Proceedings of FLOMEKO (pp. 71–74). International Measurement Conference.

ASME MFC-7–2016. Measurement of Gas Flow by Means of Critical Flow Venturi-Nozzles. The American Society of Mechanical Engineers.

Beale, D. K. (1999). Experimental Measurement of Venturi Discharge Coefficient Including Sensitivity to Geometric and Flow Quality Variables. Sverdrup Technology, Inc.

Bean, H. S., ed. (1971). Fluid Meters: Their Theory and Application (6th ed.). The American Society of Mechanical Engineers.

Brain, T. J. S., and Macdonald, L. M. (1977). "Evaluation of the Performance of Small-Scale Critical Flow Venturi Using the NEL Gravimetric Gas Flow Standard Test Facility." Flow Measurement in the Mid 1970s (pp. 103–125). HMSO.

Brain, T. J. S., and Reid, J. (1978). "Primary Calibration of Critical Flow Venturis in High-Pressure Gas." Flow Measurement of Fluids (pp. 54–64). North Holland Publishing Co.

Brain, T. J. S., and Reid, J. (1981). "An Investigation of the Discharge Coefficient Characteristics and Manufacturing Specification of Toroidal Inlet Critical Flow Venturi-nozzles Proposed as ISO Standard Flowmeters." Proceedings of International Conference on Advances in Flow Measurement Techniques, Paper C1. BHRA Fluid Engineering.

Brennan, J. A., McFaddin, S. E., Sindt, C. F., and Kothari, K. M. (1989). "The Influence of Swirling Flow on Orifice and Turbine Flow-meter Performance." Flow Measurement and Instrumentation, 1(1) (Oct), 5.

Brown, E. F., Hamilton, G.L., and Kwok, D.W. (1985). "A Comparison of Three Critical Flow Venturi Designs." Journal of Fluids Engineering, 107(3), 316–321.

Funaki, T., and Ishibashi, M. (2008). "Effect of Inlet Curvature on the Discharge Coefficients of Critical-Flow Venturi nozzle with a Toroidal Throat in the Laminar-Turbulent Transition." The ASME Fluid Engineering Division Summer Meeting. The American Society of Mechanical Engineers.

Goodenough, G. A. (1920). Principles of Thermodynamics (3rd ed.). Henry Holt and Company.

Hall, I. M. (1962). "Transonic Flow in Two-Dimensional and Axially Symmetric Nozzles." The Quarterly Journal of Mechanics and Applied Mathematics, 15(4) (Nov), 487-508.

Hilsenrath, J., Beckett, C. W., Benedict, W. S., Fano, L., Hoge, H. J., Masi, J. F., Nuttall, R. L., Touloukian Y. S., and Wolley, H. W. (1955). Tables of Thermal Properties of Gases (Circular 564). National Bureau of Standards.

Ishibashi, M. (2003). "Fluid Dynamics in Critical Nozzles Revealed by Measurements." The ASME Fluids Engineering Division Summer Meeting. The American Society of Mechanical Engineers.

Ishibashi, M., Morioka, T., and Arnberg, B.T. (2005). "Effect of Inlet Curvature on the Discharge Coefficients of Toroidal-Throat Critical-Flow Venturi Nozzles (Keynote)." The ASME Fluids Engineering Division Summer Meeting. The American Society of Mechanical Engineers.

Ishibashi, M., and Takamoto, M. (1998). "Discharge Coefficient of Critical Nozzles Machined by Super-Accurate Lathes." Proceedings of the National Conference of Standards Laboratories Workshop and Symposium.

Ishibashi, M., and Takamoto, M. (1999). "Discharge Coefficient of Super-Accurate Critical Nozzle at Pressurized Condition." Proceedings of the 4th International Symposium on Fluid Flow Measurement. Colorado Engineering Experiment Station, Inc.

Ishibashi, M., and Takamoto, M. (2001). "Discharge coefficient of super-accurate critical nozzles accompanied with the boundary layer transition measured by reference super-accurate critical nozzles connected in series." The ASME Fluids Engineering Division Summer Meeting. The American Society of Mechanical Engineers.

IS0 9300:2005. Measurement of gas flow by means of critical flow venturi-nozzles. International Organization for Standardization.

Jacobsen, R. T., Penoncello, S.G., Beyerlein, S.W., Clarke, W.P., and Lemmon, E. (1991). "A thermodynamic property formulation for air." The 11th Symposium on Thermophysical Properties, published in Fluid Phase Equilibria, 79(25) (Nov.), 113–124, 1992.

Johnson, R. C. (1964). "Calculations of Real-Gas Effects in Flow Through Critical-Flow Nozzles." Journal of Basic Engineering, 86(3), 519–526.
Johnson, R. C. (1965). "Real gas effects in critical-flow-through nozzles and tabulated thermodynamic properties." NASA Technical Note D-25655. National Aeronautics and Space Administration.
Karnik, U, Bowles, E. B., Bosio, J., and Caldwell, S. (1996). "North American Inter-Laboratory Flow Measurement Testing Program." Proceedings of North Sea Flow Measurement Workshop. Norwegian Society for Oil and Gas Measurement.
Kastner, L. J., Williams, T. J., and Sowden, R. A. (1964). "Critical Flow Nozzle Meter and Its Application to the Measurement of Mass Flow Rate in Steady and Pulsating Streams of Gas." Journal of Mechanical Engineering Science, 6(1) (Mar.), 88–98.
Keenan, J. H., and Kaye, J. (1948). Gas Tables. Wiley.
Keenan, J. H., and Keyes, F. G. (1959). Thermodynamic Properties of Steam. Wiley.
Lemmon, E., Huber, M., and McLinden, M. (2013). NIST Standard Reference Database 23: Reference Fluid Thermodynamic and Transport Properties Database-REFPROP, Version 9.1, Nat'l Std. Ref. Data Series. National Institute of Standards and Technology.
Murdock, J.W., and Keyser, D.R. (1991a). "Theoretical Basis for Extrapolation of Calibration Data of PTC 6 Throat Tap Nozzles." Journal of Engineering for Gas Turbines and Power, 113(2) (Apr.), 228–232.
Murdock, J. W., and Keyser, D. R. (1991b). "A Method for the Extrapolation of Calibration Data of PTC 6 Throat Tap Nozzles." Journal of Engineering for Gas Turbines and Power, 113(2) (Apr.), 233–239.
Olsen, L. O. (1972). Personal communication, National Bureau of Standards, letter ref. 213.06, to T. Arnberg (January 12).
Reshetnikov, A.V., Isayev, O. A., and Nevolin, M. V. (1987). "An Experimental Unit for Investigating the Discharge of a Flashing Liquid Through Short Channels at Variable Back Pressures." Fluid Mechanics–Soviet Research, 16(5), 61–65.
Shapiro, A. H. (1954). The Dynamics and Thermodynamics of Compressible Flow. The Ronald Press.
Smith, R. E., Jr., and Matz, R. J. (1962). "A Theoretical Method of Determining Discharge Coefficients for Venturis Operating at Critical Flow Conditions." Journal of Basic Engineering, 84(4), 434–445.
Sparks, C. R. (1966). "A Study of Pulsating Effects on Orifice Metering of Compressible Flow." The ASME Flow Measurement Symposium. The American Society of Mechanical Engineers.
Stevens, R. L. (1986). "Development and Calibration of the Boeing 18 kg/s (40 lbm sec) Airflow Calibration Transfer Standard." Proceedings of International Symposium on Fluid Flow Measurement. Colorado Engineering Experiment Station, Inc.
Stratford, B. S. (1964). "The Calculation of the Discharge Coefficient of Profiled Choked Nozzles and the Optimum Profile for Absolute Air Flow Measurement." The Aeronautical Journal, 68(640), 237–245.
Sullivan, D.A. (1981). "Historical Review of Real-Fluid Isentropic Flow Models." Journal of Fluids Engineering, 103(2), 258–267.
Sullivan, D. A. (1989). Personal communication, Fern Engineering Co. to Walter Seidl, Colorado Engineering Experiment Station, Inc.
Thompson, P. A., and Arena, C. C. (1975). "Prediction of the Critical Mass Flow and Related Problems in the Flow of Real Gases." The ASME Joint Fluids Engineering and Lubrication Conference. The American Society of Mechanical Engineers.
Varner, C. E. A. (1970). "Multiple Critical Flow Venturi Air-flowmetering System for Gas Turbine Engines." Journal of Basic Engineering, 92(4), 792–795.
Wendt, G., and von Lavante, E. (2000). "Influence of Surface Roughness on the Flowrate Behavior of Small Critical Venturi Nozzles. Proceedings of the FLOMEKO 2000–IMEKO TC9 Conference.

The following sources were not cited directly but have been consulted in the preparation of this section.

ASME PTC 6-2005. Performance Test Code on Steam Turbines. The American Society of Mechanical Engineers.
ASME Supplement to Power Test Codes, Instruments and Apparatus (1959). "Chapter 4, Flow Measurement by Means of Thin Plate Orifices, Flow Nozzles and Venturi Tubes." The American Society of Mechanical Engineers.
Bean, H. S., ed. (1959a). Fluid Meters: Their Theory and Application (5th ed.). The American Society of Mechanical Engineers.
Bean, H. S. (1959b). "Communications." Proceedings of the Institution of Mechanical Engineers, 173, 36.
Beitler, S. R., and Bean, H. S. (1948). Research on Flow Nozzles. Ohio State University.
Cotton, K. C. (1975). "Coefficient of Discharge for Three Steam Flow Nozzles, Critical Flow." Personal communication to B. T. Arnberg, General Electric Co., Schenectady, NY.
Dudzinski, T. J., Johnson, R.C., and Karuse, L. N. (1969). "Venturi Meter With Separable Diffuser." Journal of Basic Engineering, 91(1) (Mar.), 116–120.

Ishibashi, M., and Takamoto, M. (2000). "Theoretical Discharge Coefficient of a Critical Circular-Arc Nozzle with Laminar Boundary Layer and Its Verification by Measurements Using Super-Accurate Nozzles." Flow Measurement and Instrumentation, 11, 305–313.

Ishibashi, M., Takamoto, M., Nakao, Y., Watanabe, E., Yokoi, Y., and Ina Y. (1998). "Calibration of Critical Nozzles by Critical Nozzles." Proceedings of the 9th International Flow Measurement Conference (pp. 31–36). International Measurement Confederation.

Murdock, J., and Keyser, D. (1986). "NBS Sonic Nozzle Calibrations, NBS-Boulder, NGPLA, and API committee." Personal communication to T. Arnberg.

Olsen, L. O., and Baumgarten, G. (1971). "Gas Flow Measurement by Collection Time and Density in a Constant Volume." Flow: Its Measurement and Control in Science and Industry (pp. 1287–1295). Instrument Society of America.

Paine, C. J. (1966). Determination of ASME Convergent Nozzle Discharge Coefficients by Probe Measurements. United Aircraft Research Laboratories.

Seidl, W. F. (1986). "Primary Calibration of the Boeing 18 kg/s (40 lbm/sec) Airflow Calibration Transfer Standard." Proceedings of International Symposium on Fluid Flow Measurement. Colorado Engineering Experiment Station, Inc.

Smith, R. E., Jr., and Matz, R. J. (1973). "Performance Characteristics of an 8-in.-Diameter ASME Nozzle Operating at Compressible and Incompressible Conditions." Journal of Fluids Engineering, 9, 542–550.

Szaniszlo, A. J. (1974). "Experimental and Analytical Sonic Nozzle Discharge Coefficients for Reynolds Numbers up to 8×10^6." Paper 74-WA/FM-8. Journal of Engineering Power, 97(4), 521–525. The American Society of Mechanical Engineers.

Takamoto, M., Ishibashi, M., Watanabe, N., Aschenbrenner, A., and Caldwell, S. (1994). "Intercomparison Tests of Gas Flow Rate Standards." Bulletin of NRLM (Japan), 43(3), 308–314.

Section 8
Flow Measurement by Velocity Traverse

8-1 NOMENCLATURE

Symbols used in Section 8 are included in Tables 2-3-1 and 8-1-1. For any equation that consists of a combination of symbols with units shown in Tables 2-3-1 and 8-1-1, the user must be careful to apply the proper conversion factors.

8-2 INTRODUCTION

Only circular or rectangular conduits flowing full of gas or liquid are covered by this Section. Pitot tubes, pitot-static tubes, pitometers, and current (propeller) meters measure velocities at given locations in the flow, which are then summed (with weighting factors) or integrated over the whole cross section to obtain the total volumetric flow. These devices, therefore, have similar requirements for installation and flow computations. Several methods for locating traverse measurement stations are detailed.

8-2.1 Flow Computation

Volumetric flow is the integral of velocity over the flow area. As a finite number of velocity measurements are feasible, flow is approximated by numerical integration (summation) of those point velocity measurements using appropriate weighting factors for the area associated with each measurement. Equation (8-2-1) shows the integral and the numerical approximation for pipes. The weighting factors are used to determine the average velocity on a radius.

$$q_v = \int_0^{2\pi} \int_0^R V(r, \Theta)\, d\Theta\, dr \sim \frac{A}{N} \sum_{j=1}^{N} \sum_{i=1}^{n} w_i V_{ij} \tag{8-2-1}$$

For ducts, the same integral and numerical integration are applicable with different variables as shown in eq. (8-2-2).

Weighting factors are required in both the x and y directions for ducts. The weighting factors are dependent only on the number of locations used in each direction.

$$q_v = \int_0^H \int_0^W V(x, y)\, dx\, dy \sim A \sum_{j=1}^{N} \sum_{i=1}^{n} w_i w_j V_{ij} \tag{8-2-2}$$

Several velocity traverse methods are used to compute volumetric flow.

The appropriate weighting factors for each recommended method are shown for pipes in Tables 8-3.1-1 through 8-3.1-4. Measurement locations and weighting factors are used to determine the average velocity associated with each radius.

The measurement locations and weighting factors for each recommended method are shown for ducts in Tables 8-3.2-1 through 8-3.2-3. The measurement locations and weighting factors are used to determine the average velocity associated with a single duct direction such as the width of a rectangular duct. As shown in eq. (8-2-2), the weighting factors for the two directions are multiplied.

8-2.1.1 Pipe Flow Computation. For the Chebychev, log-linear, and equal-area traverse methods for pipe flow described in para. 8-3.1, the measurement locations are chosen so that the weighting factors are all equal (i.e., weighting factor = $1/n$ which, as a constant, may be taken outside the summation) for all of the measurement locations. Therefore, the average of all the velocity measurements may be multiplied by the total area to obtain the volume flow as indicated in

$$q_v = \frac{A}{Nn} \sum_{j=1}^{N} \sum_{i=1}^{n} V_{ij} \tag{8-2-3}$$

where

V_{ij} = observed mean velocity vector parallel to the conduit centerline at the ith sensor location on the jth radius

Table 8-1-1
Symbols Specifically Applied in Section 8 (in Addition to Symbols in Table 2-3-1)

Symbol	Description	Dimensions [Note (1)]	Units	
			SI	U.S. Customary
A	Total area of the conduit	L^2	mm^2	in^2
C_{cal}	Pitot tube coefficient (calibration coefficient)	Dimensionless	Dimensionless	Dimensionless
H	Duct height	L	mm	in.
K_b	Blockage correction coefficient	L^3T^{-1}	m^3/s	ft^3/sec
K_s	Structural blockage coefficient	Dimensionless	Dimensionless	Dimensionless
R	Pipe inside radius	L	mm	in.
r	Radial measurement position	L	mm	in.
S	Frontal area, support structure impeding flow	L^2	mm^2	in^2
n	Number of velocity measurement locations per radius or duct width/height	Dimensionless	Dimensionless	Dimensionless
N	Number of radii or widths/heights used in the numerical calculation	Dimensionless	Dimensionless	Dimensionless
P_{actual}	Corrected static pressure	$ML^{-1}T^{-2}$	Pa	psi
P_{meas}	Observed static pressure	$ML^{-1}T^{-2}$	Pa	psi
P_{stag}	Stagnation pressure	$ML^{-1}T^{-2}$	Pa	psi
P_{static}	Static pressure	$ML^{-1}T^{-2}$	Pa	psi
q_m	Volume flow of each meter	L^3T^{-1}	m^3/s	ft^3/s
V	Mean velocity	LT^{-1}	m/s	ft/sec
W	Duct width	L	mm	in.
w	Weighting factor	Dimensionless	Dimensionless	Dimensionless
Θ	Yaw angle, angle from centerline	...	deg	deg
Subscripts				
i	Index of the sensor location (i = 1 to n)	...	...	...
j	index of the radii (j = 1 to N)	...	...	...

NOTE: (1) Dimensions:
L = length
M = mass
T = time

The Gaussian traverse method requires specific weighting factors for each radial location. Equation (8-2-4) indicates how to calculate the volume flow for the Gaussian traverse method.

$$q_v = \frac{A}{N}\sum_{j=1}^{N}\sum_{i=1}^{n} w_i V_{ij} \tag{8-2-4}$$

where

w_i = weighting factor at the ith sensor location

8-2.1.2 Rectangular Duct Flow Computation. Numerical integration of the flow in conduits of rectangular cross section is two-dimensional using coordinates along the height and width of the duct. The traverse methods recommended are the Gaussian, Chebychev, and area velocity spacings; weighting factors are given in Tables 8-3.2-1 through 8-3.2-3. For the Chebychev and area velocity traverse methods, which are used to compute duct flow described in para. 8-3.2, the weighting factors are equal and eq. (8-2-3) is applicable.

The Gaussian traverse method requires specific weighting factors for each velocity measurement location and the volume flow can be calculated using eq. (8-2-3). There may be different numbers of locations in the two directions to account for the aspect ratio of the duct.

$$q_v = A\sum_{j=1}^{N}\sum_{i=1}^{n} w_i\, w_j V_{i,j} \tag{8-2-5}$$

8-2.1.3 Averaging Time. Sufficient averaging time is required at each sensor location to obtain an accurate mean velocity and reduce the statistical random uncertainty. Plotting the observed velocity profiles is highly recommended to check the degree of asymmetry in the flow profile and whether it is reasonable to expect such a profile in the subject installation.

Sufficient recording time is required at each station at each rate at uniform time intervals to cover at least two complete periods of any acceptable level of flow variations. If periodic flow variations occur, the correct method of averaging is to average the square root of each reading for pitot tubes. Digital pressure transducers have the capability of outputting the square root of the differential pressure such that the reading may be averaged. However, if the average of the pressure readings is used when periodic variation in flow is about 10%, the square root error would add approximately 0.3% to the uncertainty. The outputs of linear devices, such as current meters, may be averaged.

8-2.1.4 Area Measurement. The area of the conduit must be measured. For pipes, measurement of at least four diameters is recommended. For rectangular ducts, four measurements on each axis are required. Any irregularities in the area, such as rounding of corners in ducts, must be evaluated. The uncertainty of the area measurement must be included in the uncertainty of the measured flow.

8-3 TRAVERSE MEASUREMENT LOCATIONS

Various velocity distributions may occur in the field; therefore, velocity measurements at a sufficient number of points are recommended to clearly define the velocity profile without assuming or correcting for boundary layer effects. The measurement locations for each traverse are defined for several techniques in this section.

The four recommended techniques are the Gaussian, Chebychev, log-linear, and area velocity (or equal area for pipe flow) methods. The Gaussian and Chebychev quadrature methods are mathematically based to integrate a polynomial with an order of less than $2n - 1$ (where n = number of measurements) exactly. If the velocity profile may be described by a polynomial these methods should have lower uncertainty than the log-linear and equal-area methods when using the same number of sensors. The converse also holds: equivalent uncertainty can be attained using fewer sensors in the traverse. Sufficient measurement locations are required to evaluate whether the profile is a true polynomial, as polynomials with an order equal to the number of measurement locations will perfectly fit the data but may not reflect the actual velocity distribution. The log-linear method is designed to integrate fully developed velocity profiles that can be described by a linear combination of a logarithmic term and a linear term of the distance from the wall.

The equal-area method is the preferred method in ASME PTC 11. The cross-sectional area of the conduit is divided into equal areas with the measurement location at the centroid of each area. The equal-area method allows measurements at other spacings to better define the velocity distribution and decrease uncertainty. Total flow is the summation of the velocity times the associated subarea.

The equal-area method is less accurate than the Chebychev and Gaussian methods for the same number of measurement locations for some velocity distributions. This may be shown by calculating comparative results using analytic velocity profiles for pipe flow. Schlichting (1968) mathematically describes a fully developed, symmetrical profile that has a definite integral to compare to the numerical integration methods. Both the Chebychev and Gaussian methods have about 0.2% lower deviation from the definite integral of the velocity distribution than the equal-area method does for the same number of points. Deviations from the definite integral for the equal-area method range from +0.75% for three points per radius to +0.3% for seven points. The equal-area method requires an additional measurement location per radius to achieve an uncertainty equal to that of the other two methods.

The log-linear method shows better performance than the equal-area, Chebychev, and Gaussian methods, with deviations ranging from −0.15% to −0.08% for three and five points, respectively. These conclusions are only valid for fully developed flow.

One reason for providing a choice in the traverse pattern is that the sensor locations are different for each, and physical and installation constraints found in the field may dictate the choice of traverse pattern. Five sensors per radius or 10 per diameter should be used in pipes. In small pipes or when the velocity profile and/or installation dimensions as stated in subsection 8-4 are nearly ideal, three stations per radius may suffice. In cases where the installation conditions are much worse than specified in subsection 8-4, more than five sensors per radius are required to achieve acceptable accuracy. Similar numbers of locations in each direction of a rectangular duct are required as for diameters in pipes.

8-3.1 Pipes

Velocities in pipes shall be measured along at least four radii (N), but eight radii are preferred. A typical diametrical pattern is shown in Figure 8-3.1-1 for the equal-area method. The four acceptable methods of numerical integration specify different loci for the measuring stations along each radius referenced to the centerline. Tables 8-3.1-1 through 8-3.1-4 specify these stations along the radii for various numbers (n) per radius with the appropriate weighting factor. More than five locations are recommended for adequate resolution of abnormal or skewed velocity profiles. A reference velocity shall be measured at the center of the area, but this observation is not included in the flow computation methods for pipes. The velocity at the center is always used in the measurement procedures to detect departures from the criteria of velocity profile skewness and unsteadiness, as in para. 8-4(b).

Figure 8-3.1-1
Pipe Velocity Measurement Loci

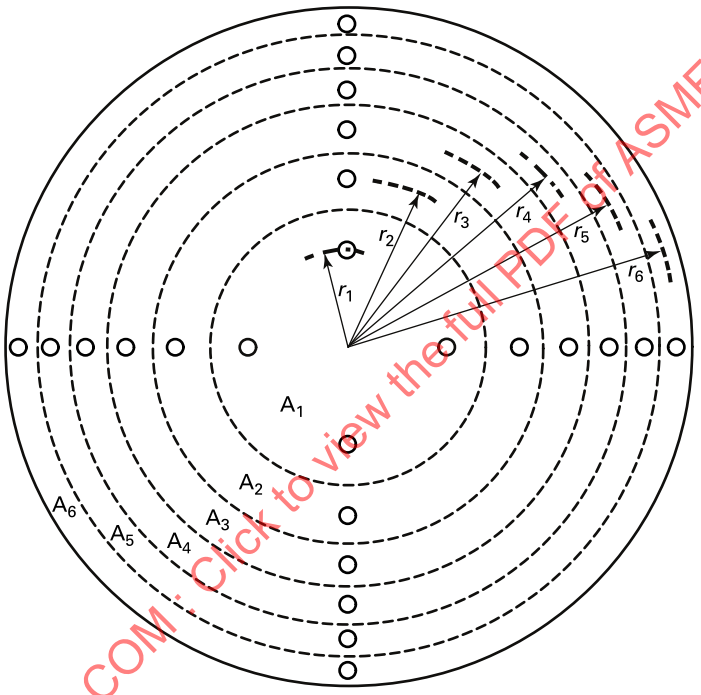

Table 8-3.1-1
Locations and Weighting Factors for Gaussian Method in Pipes

Number per Radius, n	Distance From Centerline, r/R	Weighting Factor, w	Number per Radius, n	Distance From Centerline, r/R	Weighting Factor, w
3	0.21234	0.13966	6 (cont'd)	0.85192	0.27108
	0.59053	0.45848		0.97068	0.14462
	0.91141	0.40186			
			7	0.05626	0.01042
4	0.13976	0.06236		0.18024	0.05482
	0.41641	0.25970		0.35262	0.13276
	0.72316	0.40692		0.54715	0.21426
	0.9429	0.27102		0.73421	0.25478
				0.88532	0.22102
5	0.098535	0.03150		0.97752	0.11194
	0.30454	0.14782			
	0.56203	0.29278	8	0.04464	0.00658
	0.80199	0.33434		0.14437	0.03568
	0.96019	0.19356		0.28682	0.09088
				0.45481	0.1584
6	0.073054	0.01748		0.62807	0.2121
	0.23077	0.08792		0.78569	0.22502
	0.44133	0.19732		0.90868	0.18224
	0.66302	0.28158		0.98222	0.08910

GENERAL NOTE: From Mathematical Tables and Aids to Computation, Volume 11 (1957).

Table 8-3.1-2
Locations and Weighting Factors for Chebychev Method in Pipes

Number per Radius, n	Distance From Centerline, r/R	Weighting Factor, w	Number per Radius, n	Distance From Centerline, r/R	Weighting Factor, w
3	0.3827	$1/3$	6 (cont'd)	0.8434	$1/6$
	0.7071	$1/3$		0.9660	$1/6$
	0.9239	$1/3$			
			7	0.2410	$1/7$
4	0.3203	$1/4$		0.4849	$1/7$
	0.6382	$1/4$		0.5814	$1/7$
	0.7699	$1/4$		0.7071	$1/7$
	0.9473	$1/4$		0.8136	$1/7$
				0.8745	$1/7$
5	0.2891	$1/5$		0.9705	$1/7$
	0.5592	$1/5$			
	0.7071	$1/5$	8	0.2266	$1/8$
	0.8290	$1/5$		0.4513	$1/8$
	0.9572	$1/5$		0.5444	$1/8$
				0.6698	$1/8$
6	0.2586	$1/6$		0.7425	$1/8$
	0.5373	$1/6$		0.8388	$1/8$
	0.6057	$1/6$		0.8924	$1/8$
	0.7958	$1/6$		0.9740	$1/8$

GENERAL NOTE: From Bean (1971).

Table 8-3.1-3
Locations and Weighting Factors for the Log-Linear Method in Pipes

Number per Radius, n	Distance From Centerline, r/R	Weighting Factor, w	Number per Radius, n	Distance From Centerline, r/R	Weighting Factor, w
2	0.914	1/2	4 (cont'd)	0.632	1/4
	0.420	1/2		0.310	1/4
3	0.936	1/3	5	0.962	1/5
	0.730	1/3		0.848	1/5
	0.358	1/3		0.694	1/5
				0.566	1/5
4	0.958	1/4		0.278	1/5
	0.766	1/4			

GENERAL NOTE: From Water Power (1957).

Table 8-3.1-4
Locations and Weighting Factors for the Equal-Area Method in Pipes

Number per Radius, n	Distance From Centerline, r/R	Weighting Factor, w	Number per Radius, n	Distance From Centerline, r/R	Weighting Factor, w
3	0.40825	1/3	5 (cont'd)	0.70711	1/5
	0.70711	1/3		0.83666	1/5
	0.91287	1/3		0.94868	1/5
4	0.35355	1/4	6	0.28868	1/6
	0.61237	1/4		0.50000	1/6
	0.79057	1/4		0.64550	1/6
	0.93541	1/4		0.76376	1/6
				0.86603	1/6
5	0.31623	1/5		0.95743	1/6
	0.54772	1/5			

GENERAL NOTE: Distance from centerline = $(m/2n)^{0.5}$, where m = 1, 3, 5, 7, 9, 11... $(2n - 1)$

Table 8-3.2-1
Locations and Weighting Factors for the Gaussian Method in Rectangular Ducts

Number of Locations, n	Distance From Wall, x/L	Weighting Factor, w	Number of Locations, n	Distance From Wall, x/L	Weighting Factor, w
3	0.11270	0.27778	6 (cont'd)	0.83061	0.18038
	0.50000	0.44444		0.96624	0.08566
	0.88730	0.27778			
			7	0.02544	0.06474
4	0.06943	0.17393		0.12924	0.13986
	0.33001	0.32608		0.29708	0.19092
	0.66999	0.32608		0.50000	0.20898
	0.93057	0.17393		0.70293	0.19092
				0.87077	0.13986
5	0.04691	0.11847		0.97456	0.06474
	0.23077	0.23932			
	0.50000	0.28445	8	0.01986	0.05062
	0.76924	0.23932		0.10167	0.11119
	0.95309	0.11847		0.23724	0.15686
				0.40829	0.18134
6	0.03377	0.08566		0.59172	0.18134
	0.16940	0.18038		0.76277	0.15686
	0.38069	0.23396		0.89834	0.11119
	0.61931	0.23396		0.98015	0.05062

8-3.2 Rectangular Ducts

Velocities in rectangular ducts shall be measured at the loci, n, specified in Tables 8-3.2-1 through 8-3.2-3, depending on the method selected. A typical location pattern is shown in Figure 8-3.2-1 for the Gaussian method. In ducts, the loci are specified from each wall. For odd values of n, the velocity is measured at the center to compute the flow. For even values of n, this central observation shall be monitored to evaluate skewness of the velocity profile and the temporal steadiness of the flow during the period of reading the sensors and/or moving the sensors between measurement stations. At least five measurement loci are recommended on each of five traverse locations, N. More should be used if the flow is expected to be highly skewed or otherwise abnormal. Three sensors per line may be used if the flow profile is expected to be nearly symmetric and smooth with an unchanging sign (i.e., "+" or "−" of its curvature).

When using the area velocity (or equal-area) method, the minimum number of test points is recommended as shown in Figure 8-3.2-2. For measurement planes of rectangular and square cross section, the long dimension of the elemental area shall align with the long dimension of the duct's cross section. The elemental areas should be as geometrically similar to the duct's cross section as possible.

Table 8-3.2-2
Locations and Weighting Factors for Chebychev Method in Rectangular Ducts

Number of Locations, n	Distance From Wall, x/L	Weighting Factor, w
3	0.14645	1/3
	0.50000	1/3
	0.85355	1/3
4	0.10268	1/4
	0.40621	1/4
	0.59380	1/4
	0.89733	1/4
5	0.08375	1/5
	0.31273	1/5
	0.50000	1/5
	0.68727	1/5
	0.91625	1/5
6	0.06688	1/6
	0.28874	1/6
	0.36668	1/6
	0.63332	1/6
	0.71126	1/6
	0.93313	1/6
7	0.05807	1/7
	0.23517	1/7
	0.33805	1/7
	0.50000	1/7
	0.66196	1/7
	0.76483	1/7
	0.94193	1/7
9	0.04421	1/9
	0.19949	1/9
	0.23562	1/9
	0.41605	1/9
	0.50000	1/9
	0.58395	1/9
	0.76438	1/9
	0.80051	1/9
	0.95580	1/9

Table 8-3.2-3
Locations and Weighting Factors for the Equal-Area Velocity Method in Rectangular Ducts

Number of Locations, n	Distance From Wall, x/L	Weighting Factor, w	Number of Locations, n	Distance From Wall, x/L	Weighting Factor, w
3	0.16667	1/3	5 (cont'd)	0.50000	1/5
	0.50000	1/3		0.70000	1/5
	0.83333	1/3		0.90000	1/5
4	0.12500	1/4	6	0.08333	1/6
	0.37500	1/4		0.25000	1/6
	0.62500	1/4		0.41667	1/6
	0.87500	1/4		0.58333	1/6
				0.75000	1/6
5	0.10000	1/5		0.91667	1/6
	0.30000	1/5			

Figure 8-3.2-1
Duct Velocity Measurement Loci for Gaussian Distribution

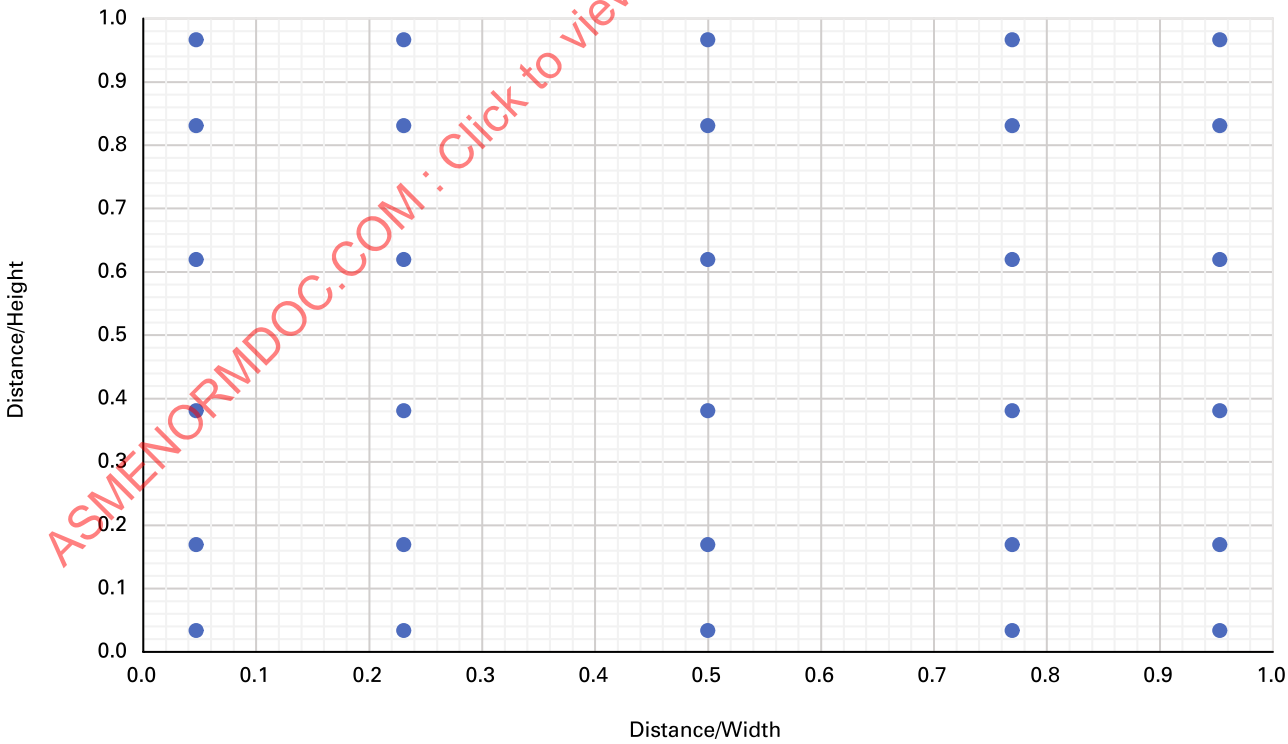

Figure 8-3.2-2
Recommended Number of Measurement Loci for the Equal-Area Method

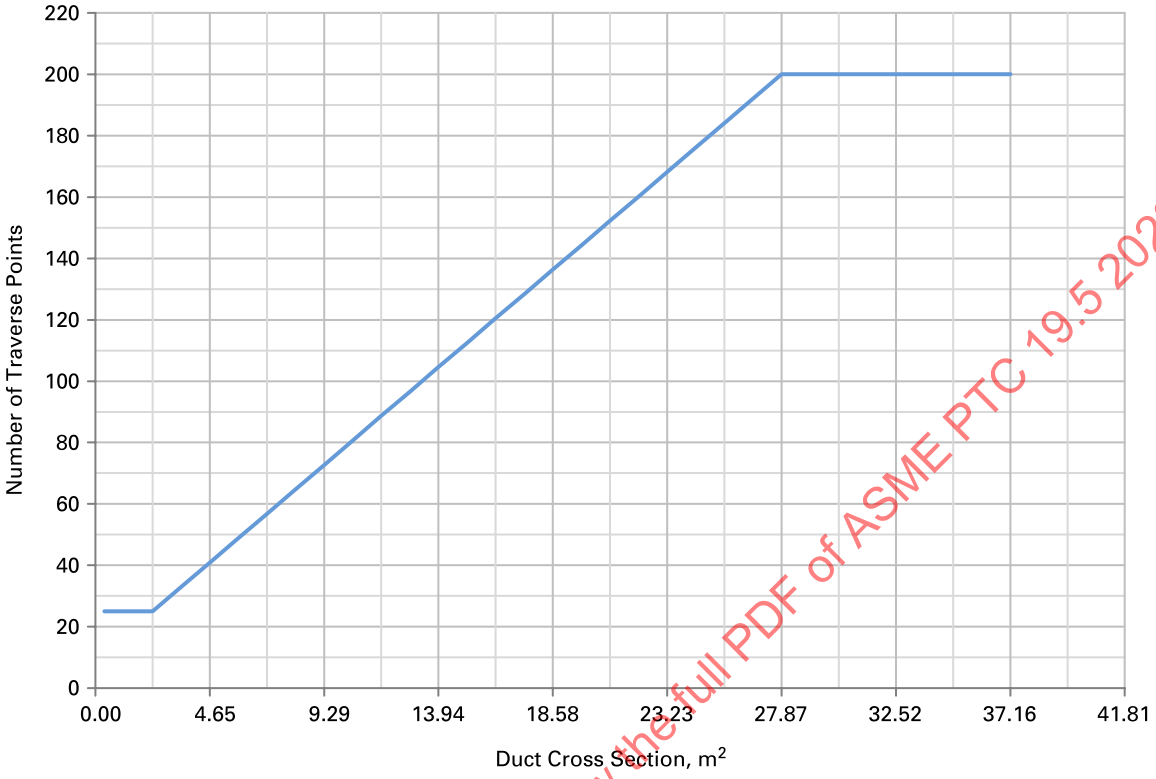

8-4 RECOMMENDED OR REQUIRED LOCATIONS OF MEASUREMENT SECTIONS

The following items are to be considered for the locations for flow measurement by velocity traverse:

(a) The measurement section should be in a straight run of conduit at least 20 diameters downstream and 5 diameters upstream from the nearest bend, change in area, or other flow obstruction.

(b) The mean velocity at the measurement section should be at least 75% of the maximum velocity observed. The velocity distribution should be as close as possible to that of a fully developed, turbulent flow in a straight conduit.

(c) If flow conditioners are required to fulfill the preceding recommendation in (b), they should be placed at least 10 diameters upstream from the measurement section.

(d) If the conduit is of lapped construction, the plane of measurement shall be located in the section of the smaller diameter.

(e) If the measurement section does not fulfill the recommendation in (a) or is in a location where oblique for reverse flows could exist, it is necessary to determine the flow direction using a multiport pitot tube or a directional vane in the case of current meters.

The more uniform the profile, the less important the number of measurement points and the choice of traverse pattern and integration method.

In fully developed flow, the boundary layer is important, and the number of measurement locations must be large enough to assure the boundary layer effect is included. This can mean that many measurement locations are required for the Gaussian and Chebychev methods to account for near-wall effects.

In very large ducts, when allowing for probe-stem droop and the need to avoid duct bracing, the probe tip location may deviate from the ideal. The required location shall not deviate more than 30% of the corresponding dimensions of the elemental area from the ideal location. Likewise, the probe tip may be outside the traverse plane by no more than 30% of the largest elemental area dimension, and then only if the duct area is the same as at the traverse plane. An estimate of the uncertainty due to the location deviation should be made.

8-5 USE AND CALIBRATION REQUIREMENTS FOR SENSORS

8-5.1 Pitot Tubes

Pitot tubes measure the differential pressure corresponding to the dynamic pressure of the flow according to Bernoulli's equation [see eq. (3-4-1)]. Most sensors must be closely aligned with the velocity vector to accurately measure velocity. In swirling flow, the velocity does not parallel the pipe centerline and the sensor must be rotated to correctly measure the velocity. Since the flow is the vector dot product of the velocity and the conduit's area, the direction cosines of the velocity vector so measured must be applied to determine the component of the velocity parallel to the axis of the conduit. It is this component that is used in the numerical integration of the velocities across the conduit area to calculate the total flow in the conduit. Velocity is calculated by

$$V = \cos(\Theta) C_{\text{cal}} \sqrt{\frac{2\, g_c \left(P_{\text{stag}} - P_{\text{static}}\right)}{\rho}} \tag{8-5-1}$$

where

C_{cal} = calibration coefficient
g_C = proportionality constant
P_{stag} = stagnation pressure
P_{static} = static pressure
ρ = density

Pitot-static sensors may be used in liquid or subsonic gas flows (Mach ≤ 0.3).

The sensors must be calibrated in a mutually acceptable laboratory if it is necessary to obtain an accurate coefficient. If the correction for the probe blockage of the flow stream is estimated to exceed one-quarter of the desired test uncertainty, the sensors should be calibrated under conditions duplicating the interference conditions of the test installation.

See Figures 8-5.1-1 and 8-5.1-2.

8-5.1.1 Standard Designs. The only differential pressure pitot probes that do not require calibration are impact tubes and pitot-static tubes of ASME and National Association of Fan Measurement (NAFM) design. Both types are considered primary instruments and need not be calibrated, provided that they are carefully constructed and maintained. Their calibration coefficient is 1.000. The tube should be as thin as feasible to withstand the flowing velocity without vibration. The bent section must be aligned with the velocity using the guide vane. For the impact tube, the static pressure is measured at the wall with one or more piezometers. The impact tube indicates the stagnation pressure of the velocity stream. The uncertainty of the velocity measurement with these designs may be estimated at 0.3% if the angle between the velocity and the axis of the impact (yaw angle) tip is less than 12 deg.

A probe with only yaw-measuring capability can be used only if a preliminary test gives sufficient evidence that the average of absolute values of pitch angle does not exceed 5 deg. A nondirectional probe may be used only where the preliminary test gives sufficient evidence that the average of the absolute values of neither yaw angle nor pitch angle exceeds 5 deg.

8-5.1.2 Typical Pitot-Static Tube Designs. Several other acceptable pitot tube designs may be used as velocity sensors, some of which indicate the direction of the velocity using multiple pressure measurements. Figures 8-5.1.2-1 through 8-5.1.2-3 show pitot-static tubes that require calibration to determine their calibration coefficient. The calibration coefficient, C, corrects the pressure measurement to give the true velocity.

Figures 8-5.1.2-1 through 8-5.1.2-3 depict a probe system that can determine the direction of the velocity vector. Five-hole probes such as those illustrated in Figures 8-5.1.2-1 and 8-5.1.2-2 can determine the two angles (pitch and yaw) necessary to orient the fluid velocity vector in three-dimensional space. Three-hole probes such as the Fechheimer probe shown in Figure 8-5.1.2-3 and the wedge probe can determine only the yaw angle of the velocity vector. In use, the probe is rotated until the pressure difference between the two holes that lie in the plane perpendicular to the probe axis is zero. The angle at which this occurs is measured with a protractor or similar apparatus and interpreted as the yaw angle.

Figure 8-5.1-1
Pitot Tubes Not Requiring Calibration

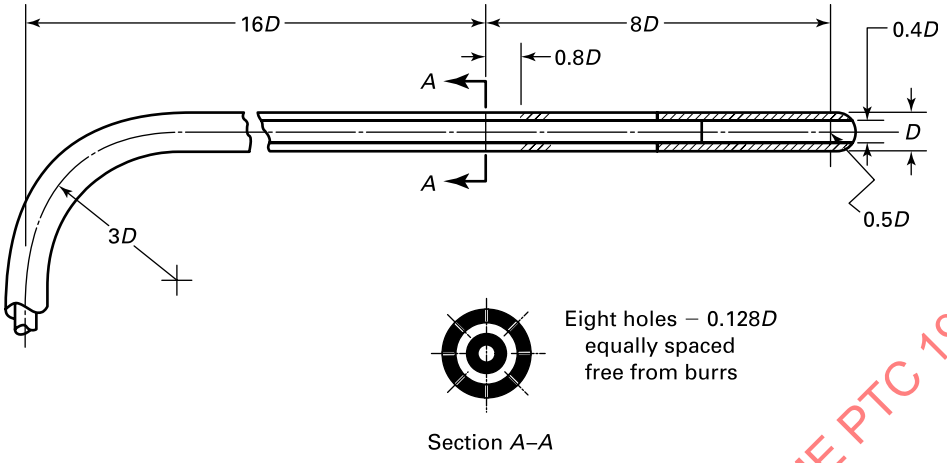

(a) NAFM and ASME

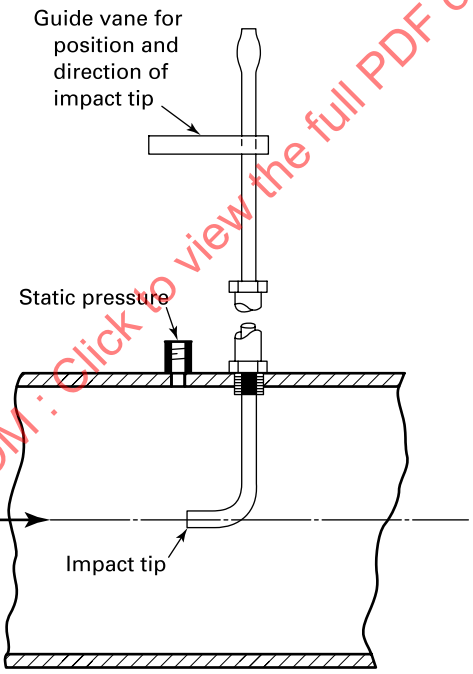

(b) A Type of Basic Pitot Tube or Impact Tube

GENERAL NOTES:
(a) Two designs of pitot-static tubes are shown in this figure.
(b) Values of diameters between $^{3}/_{16}$ in and $^{5}/_{16}$ in. are suitable.
(c) Calibration coefficient = 1.000

Figure 8-5.1-2
Pitot Tubes Needing Calibration But Acceptable

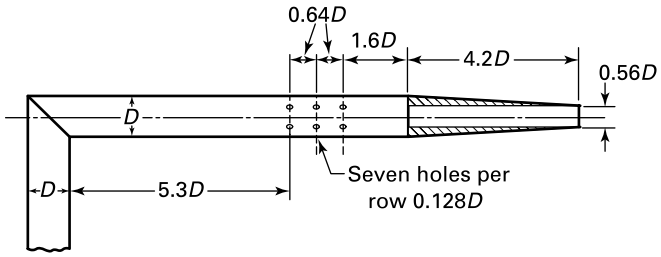

N.P.L. (Taper)

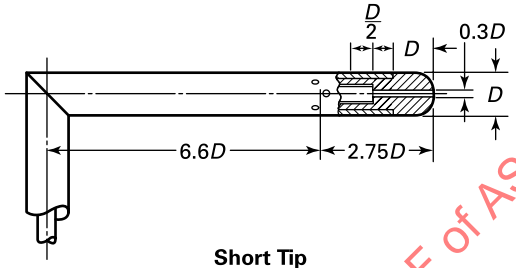

Short Tip

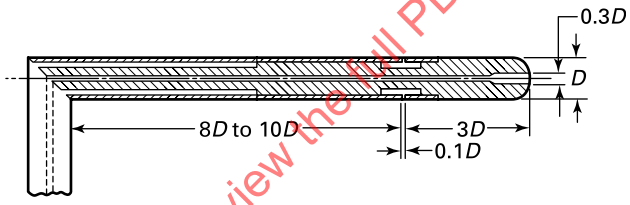

Prandtl

Figure 8-5.1.2-1
Wedge-Type Five-Hole Probe Installation Schematic

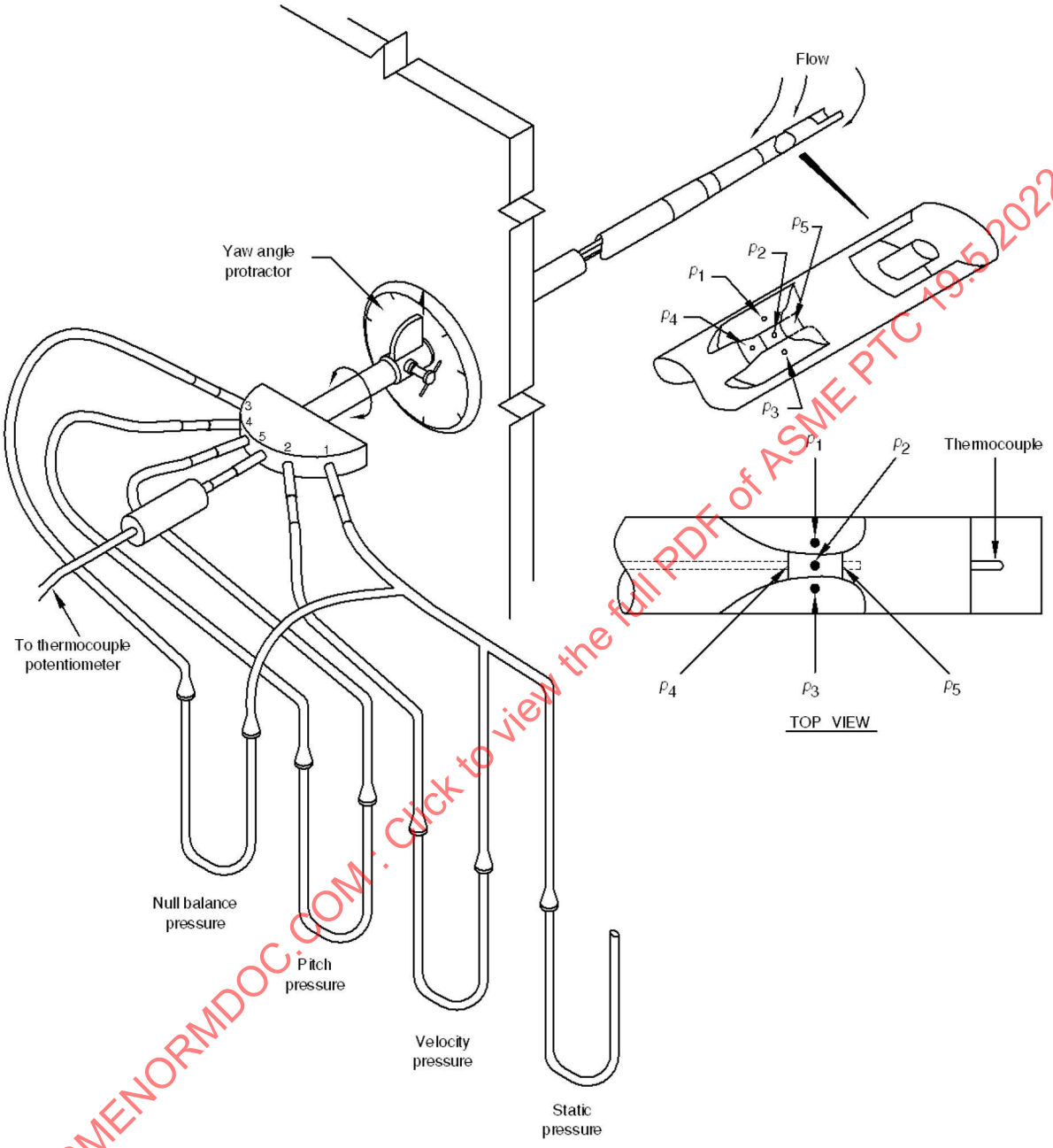

Figure 8-5.1.2-2
Five-Hole Probe Designs

(a) Spherical Type

(b) Wedge Type

Figure 8-5.1.2-3
The Fechheimer Probe Installation

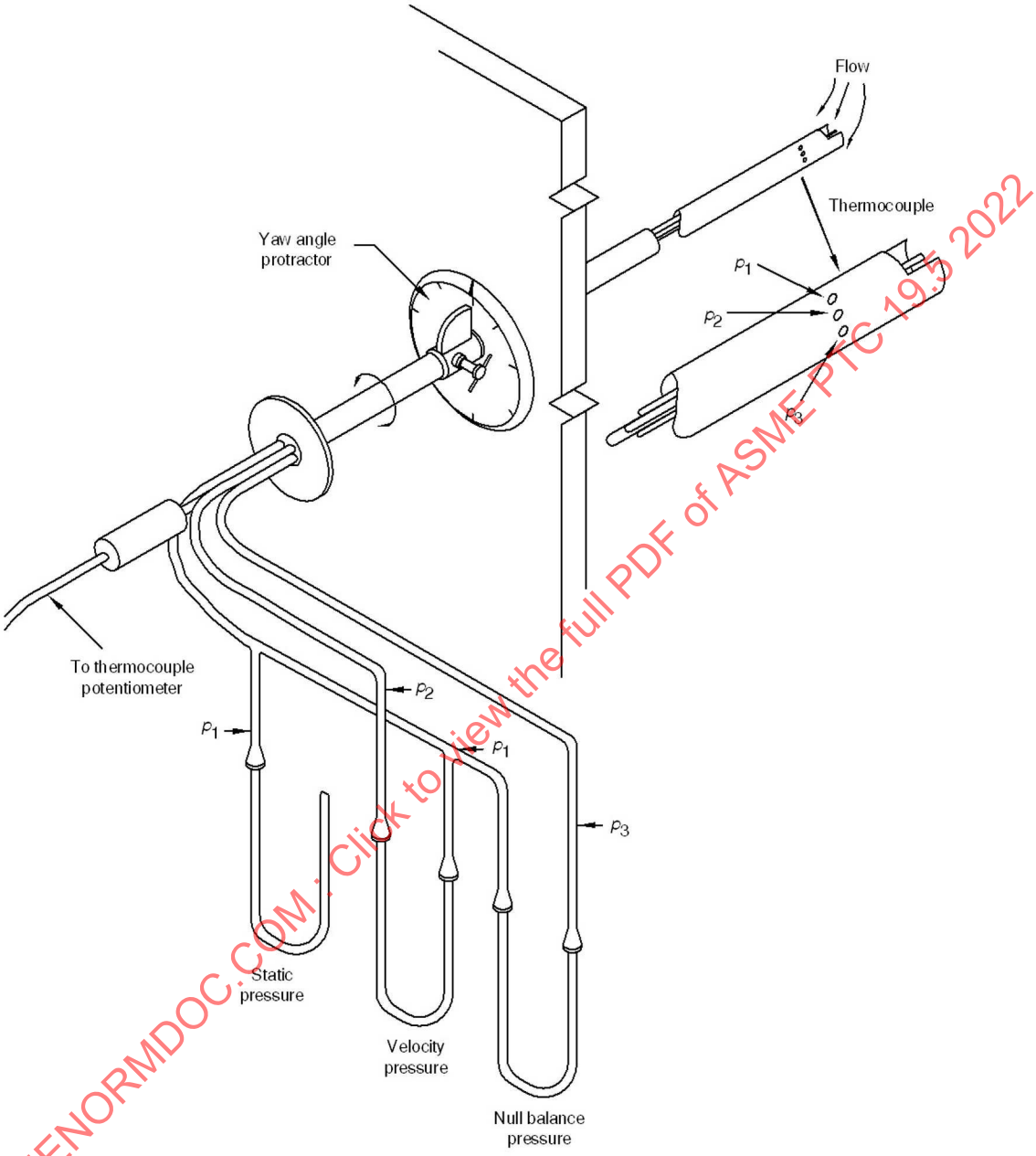

Five-hole probes have one pressure tap farthest upstream (in the center of the array of holes), which senses the stagnation pressure, and four downstream holes distributed around the center. The probe is rotated until the pressure difference between the two holes that lie in the plane perpendicular to the probe axis is determined to be zero. The angle at which this occurs is measured with a protractor or similar apparatus and interpreted as the yaw angle. The pressure difference between the remaining pair of holes, aligned along the axis of the probe, is used to determine the pitch angle from a calibration curve. Calibration is also required to determine the true stagnation pressure from the center hole and the static pressure from the yaw holes. The component of the velocity normal to the plane of the duct cross-sectional area is determined from the cosines of the measured pitch and yaw angles.

Some five-hole probes, mounted to be movable in the pitch and yaw directions, have one pressure tap farthest upstream, which senses the stagnation pressure, and four downstream holes, which are located where the static pressure will be sensed. When both pairs of static pressure taps are nulled (i.e., the differential pressure between opposing pairs of downstream pressure taps is zero) by manipulating the orientation of the probe, then the probe is aligned with the velocity vector, and the stagnation pressure is sensed by the upstream tap. The differential pressures sensed between the probe and each of the downstream taps should be equal and measure the velocity vector via Bernoulli's equation. The component of the velocity normal to the plane of the cross-sectional area is determined from the cosines of the pitch and yaw angles measured by the apparatus shown in Figures 8-5.1.2-1 through 8-5.1.2-3.

8-5.1.3 Calibration Procedures. Probe calibration may be carried out in a free-stream nozzle jet or a closed wind (or water) tunnel. In either case, the blockage caused by the probe shall be less than 5% of the cross-sectional area. Preferably, the probe blockage should be as small as possible. The flow should be adjusted to produce equally spaced calibration points over the range of velocities that the probe is expected to measure. For two- and three-hole probes in air (gas), a minimum of eight points between the range of 9.144 m/s (30 ft/sec) and 30.48 m/s (100 ft/sec) nominal velocity is required. For five-hole probes in air (gas), calibration points are required at a minimum of three points, typically 12.192 m/s (40 ft/sec), 21.336 m/s (70 ft/sec), and 30.48 m/s (100 ft/sec) nominal velocity. The calibration reference may be a standard pitot-static tube (preferred) or a previously calibrated reference probe of another type. The blockage by the reference probe should be as small as possible, and in no case shall the blockage of the reference probe exceed 5% of the cross-sectional area.

The reference probe and test probe shall each be mounted so that each can be placed in the stream alternately, and their positions in the stream shall be the same and firmly held. Alternatively, the test probe and the reference probe can be placed side by side if it can be shown that there is no difference in flow conditions between the two locations, the total blockage by both probes does not exceed 5%, and there is no interference between the test probe and reference probe.

8-5.2 Calibration of Current and Propeller Meters

8-5.2.1 Design Requirements. Axial flow current meters shall be used. The bearing arrangement must minimize the ingress of water and water-borne solids that may cause a change in bearing friction and, thus, the meter calibration. Water temperature can affect the calibration. Meters specifically designed to respond only to the velocity in the meter axis are preferred. Typical blade tip diameters should be between 50 mm (2 in.) and 100 mm (4 in.). The meters shall be mounted with their axes parallel to the conduit axis. The mounting shall not allow deflection or vibration of the meters.

8-5.2.2 Calibration. Current or propeller meters shall be calibrated in a towing tank or free stream with the same mounting that will be used for the test. Where the meters are closely spaced, the calibration shall include the effects of the adjacent meters. Unless sufficient experience with the meter design indicates the meter responds only to the velocity component in the meter axis direction, the calibration shall include data on oblique flow up to 10 deg off the meter axis. The calibration curve may not be extrapolated. These meters shall be inspected before and after the test. Any blade deformation or defect found subsequent to the calibration may require recalibration of the meter if requested by either party to the test.

8-6 FLOW MEASUREMENT BY PITOT RAKE

A pitot rake is a battery of impact tubes arranged along two or three pipe diameters as shown in Figures 8-6-1 through 8-6-3. Measurement by pitot rake has been the primary flow measurement method for ASME performance tests over other recommended traverse methods. It is valid for fully developed velocity distributions with little or no swirl.

Figure 8-6-1
Insertion Type Pitot Rake

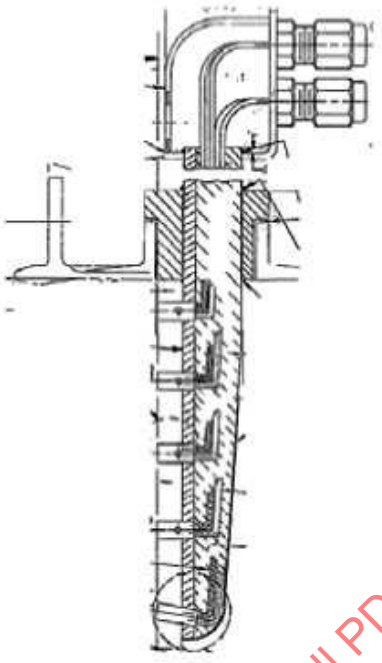

Figure 8-6-2
Pitot Rake

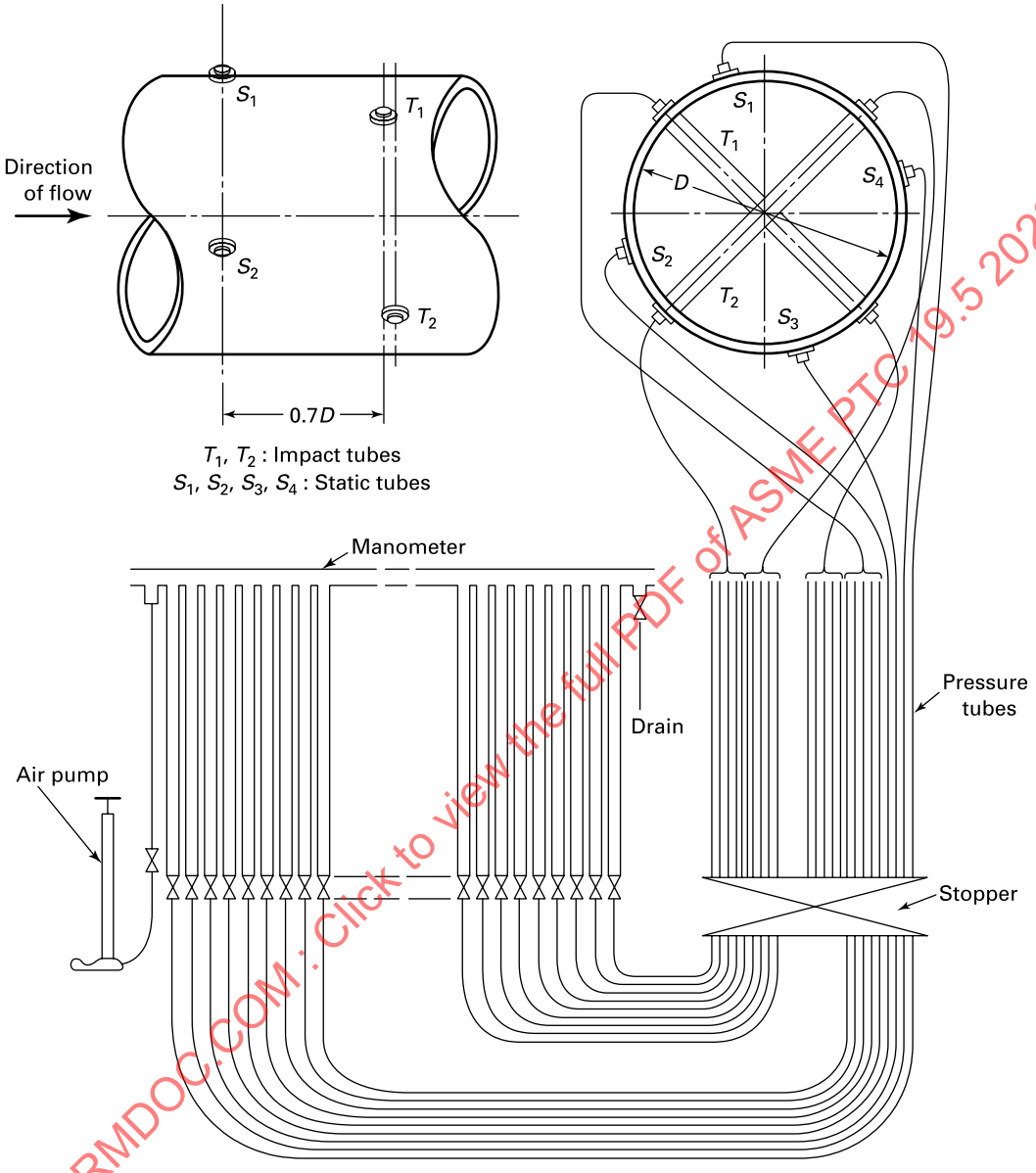

Arrangement of the Pitot Rack Apparatus

Figure 8-6-3
Impact Pressure Tube Rake

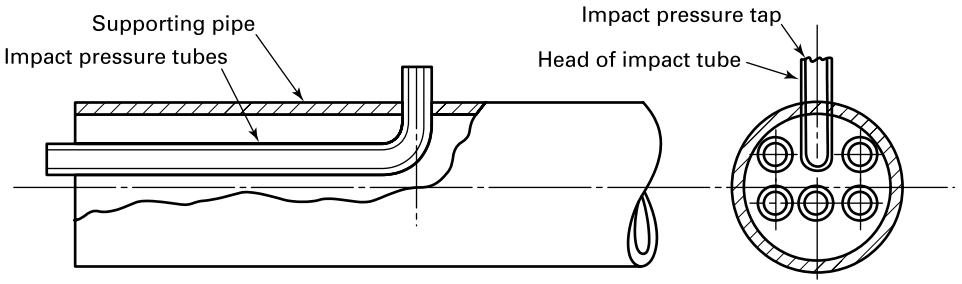

The radial spacing of the total pressure holes is specified in Tables 8-3.1-1 through 8-3.1-4, corresponding to the numerical integration method selected for the test. All total pressure openings are to be coplanar. Four static pressure taps should be installed in the conduit's wall in the same plane as the total pressure taps, if possible. If located upstream of the total pressure taps, a correction for the pipe friction pressure loss shall be made to the data and the blockage correction altered, as described in para. 8-8.1. In liquid flows, no static tap shall be located in either the top of a round pipe (because air bubbles may enter the sensing lines) or the bottom (because of the likelihood of particles clogging these sensing lines). A reference total pressure measurement shall be made at the center to satisfy paras. 8-4(b) and 8-7.3. Each static and total pressure tap is connected separately to a calibrated transducer or by using a switching method.

Typical pitot-static rake designs used in performance testing are shown in Figures 8-6-1 through 8-6-3.

8-7 GENERAL REQUIREMENTS

8-7.1 Pressure-Sensing Lines

Pressure-sensing lines shall be of noncorrosive material. For pressure measurement using manometers, sensing lines should have an inside diameter of 6 mm (¼ in.). For measurements using transducers in place of manometers, sensing lines of 3 mm (⅛ in.) are acceptable. These lines must be free from leaks and shall be installed to avoid air entrapment in the connections. The lines shall be protected from thermal sources such as direct sunlight, exhaust air from heat exchangers, or drafts.

8-7.2 Required Pressure Measurement Uncertainty

To maintain overall uncertainty, the pressure transducers shall have an uncertainty of less than 0.3%. ASME PTC 19.2 describes the application of pressure transducers and shall be used for reference. Their uncertainties shall be evaluated according to ASME PTC 19.1.

8-7.3 Velocity Traverse — Moveable Sensor

In pipes, flow measurement by pitot traverse is typically conducted by moving one sensor to the radial locations specified in Tables 8-3.1-1 through 8-3.1-4. Multiple sensors on different radii may be used. In rectangular conduits with the current meters method, multiple sensors across one dimension may be traversed across the second dimension. Using this method, the flow must remain steady throughout the period required to complete the traverse. The steadiness of the flow shall be monitored by a fixed sensor in the center of the conduit. An additional uncertainty accrues due to the observation period; this added uncertainty shall be estimated as a random uncertainty using the flow variation data from the fixed sensor during the period of the velocity traverse.

8-8 FLOW COMPUTATION CORRECTIONS

All corrections in subsection 8-8 shall be included (e.g., calibration coefficient and blockage or stem and mutual interference corrections).

8-8.1 Blockage Correction for Static Taps Upstream of Pitot Tubes

The pitot tube's support structure must be stiff enough that the effect of its vibration on all flow velocity measurements is negligible. The presence of this supporting structure causes a reduction in the observed static pressures without changing the total pressure. The observed flow measurement must be corrected [reduced according to eq. (8-8-1)] to account for this blockage.

$$\Delta P_{\text{actual}} = \left(1 - 0.7K_s\frac{S}{A}\right)\Delta P_{\text{meas}} \tag{8-8-1}$$

where

A = conduit flow area
K_s = structural blockage coefficient
ΔP_{actual} = corrected static pressure
ΔP_{meas} = observed static pressure
S = the frontal area of the support structure

In eq. (8-8-1), the factor 0.7 has an uncertainty of 0.05.

The blockage factor, K_s, is calculated using the following:

$$K_s = 1.0226 - 0.9984\,x\,\frac{x}{\sqrt{A}} - 0.8723\left(\frac{x}{\sqrt{A}}\right)^2 + 1.223\left(\frac{x}{\sqrt{A}}\right)^3 \tag{8-8-2}$$

where

x = the axial distance between the static pressure taps and the supporting structure

8-8.2 Blockage Correction for Current and Propeller Meters

A blockage correction, K_b, caused by the installation of the measurement system shall be applied to the flow calculation. The traverse array of meters reduces the flow area in the measurement section, which increases the measured flow velocities. The flow measurement must be corrected using eq. (8-8-3), in which S_m is the total area of meters in the direction of flow and q_m is the volume flow of each meter.

$$K_b = q_m\left[1 - 0.125\left(\frac{S}{A}\right) - 0.03\sum\frac{S_m}{A}\right] \tag{8-8-3}$$

8-9 UNCERTAINTY ANALYSIS

An uncertainty analysis must be conducted after the test is completed. As per ASME PTC 19.1, systematic uncertainties are estimated from experience and literature. Random uncertainties are estimated from the data standard deviations. Uncertainties for each of these elementary uncertainty sources are combined by the root sum square (RSS) method. Flow measurement uncertainty is comprised of area, velocity meter calibration, data acquisition, data reduction, and flow stability. Typical elementary error sources for these parameters include

(a) flow area measurement
(b) sensor calibration
(c) data acquisition
  (1) sensor reading
  (2) turbulence fluctuation
  (3) velocity direction
  (4) sensor alignment
  (5) temperature or density effects
(d) data reduction
  (1) integration
  (2) wall effects
  (3) blockage correction
(e) Flow Stability

The sensor output may be either a differential pressure in the case of pitot tubes or a pulse output in the case of current meters. These individual elementary error sources must be considered in both the calibration and the data acquisition. Data acquisition uncertainty includes sensor output, velocity direction, alignment of the sensor, averaging of turbulent fluctuations, and any effects of temperature or density on the sensor output. The data reduction uncertainty includes integration of the velocity distribution uncertainty considering the uniformity of the profile and wall effects and deleterious conditions such as reverse flow, wall effects, and blockage corrections. Flow may vary over the measurement period, which may introduce a systematic uncertainty.

A sample uncertainty estimate is shown in Table 8-9-1. All sensitivity factors are equal to 1 in the example. This example includes typical systematic and random uncertainties, each at a confidence interval of 68% (1 standard deviation).

8-10 REFERENCES

Bean, H. S., ed. (1971). Fluid Meters: Their Theory and Application (6th ed.). The American Society of Mechanical Engineers.

Mathematical Tables and Other Aids to Computation, Volume 11 (1957). National Research Council.

Schlichting, H. (1968). Boundary-layer Theory (6th ed.). McGraw-Hill.

Water Power (London) (1957). 9(6) (Jun.), 226.

The following sources of fluid and material data were not cited directly but have been consulted in the preparation of this section.

Abramowitz, M., and Stegun, I., eds. [1983 (1964)]. Handbook of Mathematical Functions with Formulas, Graphs, and Mathematical Tables. Dover Publications.

Gerald, C. F., and Wheatley, P. O. (1989). Applied Numerical Analysis (4th ed.). Addison Wesley Publishing Co.

Haynes, W. M., Lide, D. R., and Bruno, T. J. (2016). CRC Handbook of Chemistry and Physics: A Ready-reference Book of Chemical and Physical Data. CRC Press.

Keyser, D. R. (1978). "Laser Flow Measurement." Paper 77-WA/FM-2. The American Society of Mechanical Engineers..

Table 8-9-1
Sample Uncertainty Estimate

Elementary Error Source	Systematic Standard Uncertainty	Random Standard Uncertainty
Area	0.10%	0.00%
Sensor calibration	0.18%	0.39%
Data acquisition	0.18%	0.55%
Data reduction	0.79%	0.00%
Flow stability	0.00%	0.395%
Root sum square	0.835%	0.781%
Combined standard uncertainty	1.14% [Note (1)]	
Expanded uncertainty	2.28% [Note (2)]	

NOTES:

(1) The combined standard uncertainty is calculated from the root sum square (RSS) combination of the systematic and random uncertainties as follows:

$$\text{combined standard uncertainty, } u = \sqrt{(0.835\%)^2 + (0.781\%)^2} = 1.14\%$$

(2) The expanded uncertainty is at the 95% confidence interval (2 times the combined standard uncertainty):

$$\text{expanded uncertainty, } U = 2u = 2 \times 1.14\% = 2.28\%$$

Section 9
Ultrasonic Flowmeters

9-1 SCOPE

This Section applies to ultrasonic flowmeters that base their operation on the measurement of transit times of acoustic signals crossing the flow path of a moving fluid. This Section is only concerned with the use of such meters to measure the volumetric flow of a fluid exhibiting homogenous acoustic properties flowing in a completely filled and closed conduit.

This Section does not cover ultrasonic flowmeters that derive volumetric flow measurement from the deviation, Doppler scattering, or statistical correlation of acoustic signals. Some parts of this Section may apply to other transit-time-based meter types (e.g., phase-shift and sing-around, including clamp-on transducer meters) but this Section was not specifically written to include them.

9-2 PURPOSE

This Section provides

(a) a description of the operating principles employed by the ultrasonic flowmeters covered in this Section
(b) a description of typical applications and accuracies achieved
(c) a description of error sources and performance verification procedures
(d) a common set of terminology, symbols, definitions, and specifications

9-3 DEFINITIONS AND SYMBOLS

Terminology and symbols used in this Section, except for those defined below, are in accordance with ASME PTC 2.

9-3.1 Terminology

acoustic path: the path that the acoustic signals follow as they propagate through the measurement section between the transducer pairs.

axial flow velocity: the average component of the fluid velocity that is parallel to the measurement section axis (walls) over a cross-sectional area of the measurement section that is perpendicular to the measurement section axis (intended direction of flow).

dry calibration: calibration of the flowmeter without using transfer flow rate measurement standards. Calibration consists of an exact determination of pipeline diameter, path lengths, angles, and locations in the pipeline cross section. This process does not determine a meter factor, leaving the potential for large uncertainties and therefore is not a true calibration. Accurate measurements during dry calibration are critical for accurate flow measurement.

measurement section: the section of conduit in which the volumetric flow rate is sensed by the acoustic signals. The measurement section is bounded at both ends by planes perpendicular to the axis of the section and located at the extreme upstream and downstream transducer positions.

nonrefractive system: an ultrasonic flowmeter in which the acoustic path crosses the solid/fluid interface between the transducer and the fluid it is in contact with at a right angle.

refractive system: an ultrasonic flowmeter in which the acoustic path crosses the solid/fluid interface between the transducer and the fluid it is in contact with at other than a right angle.

secondary flow: flow with streamlines that are not parallel to the measurement section axis (conduit walls). Fluid flow with secondary flow components may commonly be referred to as “cross-flow” (perpendicular) or “swirl” (tangential).

transducer: the combination of the transducer element and passive materials.

transducer element: an active component that produces either acoustic output in response to an electric stimulus and/or an electric output in response to an acoustic stimulus.

Table 9-3.2-1
Symbols Specifically Applied in Section 9 (in Addition to Symbols in Table 2-3-1)

Symbol	Description	Dimensions [Note (1)]	Units	
			SI	U.S. Customary
A	Average cross-sectional area of the measurement section	L^2	mm	in.
c	Speed of sound	LT^{-1}	m/s	ft/sec
c_p	Sound speed in the intervening material	LT^{-1}	m/s	ft/sec
l_a	Length of intervening material at transducer a	L	mm	in.
l_b	Length of intervening material at transducer b	L	mm	in.
l_0	Distance between transducers or intervening material in the measurement pair	L	mm	in.
n	Number of acoustic paths	Dimensionless	...	...
S_V	Velocity profile correction factor	Dimensionless	...	...
t	Transit time	T	s	sec
V_{ax}	Average axial flow velocity along acoustic path	LT^{-1}	m/s	ft/sec
$\overline{V}_{ax}$	Average axial flow velocity over the entire cross-sectional area	LT^{-1}	m/s	ft/sec
W_i	Weighting factor for acoustic path, i, that depends on measurement section geometry and acoustic path location	Dimensionless	...	...
θ	Angle of transducers to measurement section axis	Dimensionless	deg	deg
ϕ	Incident angle	Dimensionless	deg	deg
ϕ_P	Refracted angle	Dimensionless	deg	deg
Subscript	**Description**			
ab	From transducer a to transducer b	...	...	...
ba	From transducer b to transducer a	...	...	...
i	Path number	...	...	...
0	Average, conditions at rest	...	...	...
1	Upstream flow conditions	...	...	...
2	Downstream flow conditions	...	...	...

NOTE: (1) Dimensions:
L = length
T = time

transit time: the time required for an acoustic signal to traverse an acoustic path.

velocity profile correction factor, S_V: a meter- and application-specific, dimensionless factor used to adjust the meter measurement output (meter factor) to account for several meter or process characteristics. Velocity profile adjustments may be required to improve meter accuracy based on actual measured or estimated flow data.

9-3.2 Symbols

Symbols used in Section 9 are included in Tables 2-3-1 and 9-3.2-1. For any equation that consists of a combination of symbols with units shown in Tables 2-3-1 and 9-3.2-1, the user must be sure to apply the proper conversion factors.

9-4 APPLICATIONS

Differential transit-time acoustic flowmeters are able to provide accurate bidirectional measurements over a wide range of process conditions with minimal pressure loss. This type of ultrasonic meter is typically available as a factory-built spool piece with integral transducer mounts in the 25 mm to 3 000 mm (1 in. to 120 in.) diameter range or, for larger flow conduits, as field-installed transducers in 900 mm (36 in.) and larger sizes.

There are meters that offer a low-cost measurement solution where accuracy is less important, such as in smaller pipes for water, wastewater, and industrial flow rate measurement. When process conditions are well controlled, a properly calibrated single-path meter can offer high accuracy and high repeatability. Some ultrasonic meters use multiple measuring paths within the metering section and are used for high measurement accuracy for acceptance testing of pumps and turbines and in custody-transfer applications.

Ultrasonic meters typically accommodate fluid conditions in the −40°C to 180°C (−40°F to 355°F) range with maximum pressure ratings around 150 bar (2,175 psi). Special constructions of ultrasonic meters are designed to accommodate fluid temperatures as low as −200°C (−330°F) and as high as 600°C (1,110°F), while others are rated for fluid pressures up to 1 500 bar (21,755 psi). With no flow obstructions, no moving parts, and a full-bore metal pipe measurement section, ultrasonic meters provide a durable measurement with long-term stability for a wide range of applications and process conditions.

9-4.1 Liquid Flow Measurement

Ultrasonic meters are adept at measuring a wide variety of single-phase, clean liquids in a variety of conditions. Liquid should contain at most 2% gas content and 5% solid content, by volume, to ensure an accurate and reliable measurement. Liquids typically must have a viscosity of less than 100 cSt. However, there are special ultrasonic meters that can measure fluids with viscosity of up to 1 000 cSt. Transit-time ultrasonic meters are commonly able to achieve liquid flow measurement uncertainty of between 0.3% and 1%.

9-4.2 Gas Flow Measurement

Ultrasonic flowmeters are able to measure dry gas flows for gas with densities from 1 kg/m^3 to 150 kg/m^3 (0.06 lbm/ft^3 to 9.36 lbm/ft^3), with some designs able to handle measurement of gas densities from 0.2 kg/m^3 to 250 kg/m^3 (0.01 lbm/ft^3 to 15.6 lbm/ft^3). Some ultrasonic flowmeters can measure wet gas or steam flows. Most ultrasonic flowmeters have the ability to calculate gas flows at standard reference conditions and specified fuel properties when input from an external pressure and temperature sensor is added. For a performance test or more accurate determination of fuel flow, this flow needs to be corrected for the actual fuel properties during the performance test.

Basic ultrasonic flowmeters are able to measure gas flows with an uncertainty of close to 1.5%, while some designs are able to achieve linearity of 0.1% or better, allowing for a measurement uncertainty of 0.3% or lower. These provide the accuracy and repeatability required for natural gas custody transfer points, pipeline measurement, and equipment testing.

Transit-time ultrasonic meters are also ideally suited to measure steam flow rates, providing great accuracy and long-term stability with minimal required maintenance. Mass flow measurements of fluids with known properties are also possible with many meters that provide inputs for external temperature and pressure readings.

9-5 FLOWMETER DESCRIPTION

The transit-time ultrasonic flowmeter described in this Section is a complete system composed of the primary device, consisting of the measurement section with one or more pairs of transducers, and the secondary device, which contains the electronic equipment necessary to operate the transducers, take measurements, process the data, and display, transmit, or record results.

9-5.1 Primary Device (Sensor)

The primary device consists of a spool piece and the acoustic transducers. The measurement section may be a single piece produced by the meter manufacturer or an existing section of conduit into which transducers are installed in the field. The measurement section contains the fluid under pressure and enables a secure and stable installation for the transducers at the appropriate locations, distances, and angle to the flow. The transducers create and detect the acoustic signal used to measure fluid flow.

9-5.1.1 Measurement Section. The section of conduit in which the volumetric flow is sensed by the acoustic signals is called the measurement section. This section is bounded at both ends by planes perpendicular to the axis of the section located at the extreme upstream and downstream transducer positions. The measurement section is usually circular. Although it may be square, rectangular, elliptical, or some other shape, it must provide geometrically stable installation points for the transducers and a predictable flow profile to achieve an accurate measurement.

9-5.1.2 Transducers. Transducers are responsible for the creation and detection of the acoustic signal used to measure fluid flow and are always installed in and work in pairs, each alternating between transmitting and receiving acoustic signals from the other. Each pair of transducers defines an acoustic path that is oriented at an angle to the axial flow direction in which acoustic signals are transmitted along in both directions. Transducers may be factory mounted or field mounted by clamping, threading, or bonding. Transducers may be wetted by the fluid or have a barrier (intervening) material separating them from the fluid being measured. Transducers may be flush-mounted, recessed, or may protrude

Figure 9-5.1.3-1
Common Acoustic Path Configurations

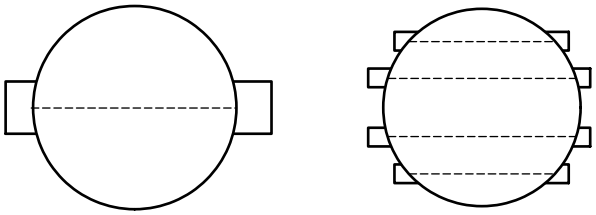

(a) Diametric (b) Chordal

into the flow stream, as shown in Figures 9-6.1.2.5-1, 9-6.1.2.6-1, and 9-6.1.2.7-1. Some nonwetted transducers can be removed while the line is in service.

9-5.1.3 Acoustic Paths. There may be one or more acoustic paths in the measurement section, each having a pair of transduc,ers. Common arrangements are diametric and chordal, as shown in Figure 9-5.1.3-1. Paragraph 9-6.1.1 offers a discussion of how the number of acoustic paths affects installed meter accuracy.

9-5.2 Secondary Device (Electronics)

The secondary device consists of the electronic equipment required to operate the transducers, make the measurements, process the measured data, display or record the results, and transmit information.

The secondary device, in addition to calculating the flow rate from measured transit times, should be capable of rejecting spurious signals, noise, etc. The measured flow may be the result of a single measurement or an average of many individual measurements.

9-5.2.1 Displays and Outputs. Most meters have several outputs available, either as standard features or as optional additions to the equipment. Displays may be analog or digital and show flow, integrated flow volume, and/or direction. Signal outputs usually include one or more of the following: current, voltage, digital, and a pulse rate proportional to flow. These outputs may or may not be electronically isolated. flowmeter outputs may also include alarms and diagnostic aids.

9-5.2.2 Self-Test and Diagnostics. The secondary device should also be capable of completing self-test and diagnostic functions and inform the user by display or output if there are any suspected problems with the primary device, transducers, transducer circuits, secondary device electronics, flow conditions, device configurations, and/or measured values. The diagnostic tests should include transmitter output power, receiver sensitivity, and timing accuracy as a minimum.

9-5.3 Operating Principles

9-5.3.1 Introduction. The volumetric flow rate of a fluid flowing in a completely filled and closed conduit is defined as the average velocity (averaged over a cross section) multiplied by the area of the cross section. Thus, by measuring the velocity profile to determine the average velocity of a fluid along one or more acoustic paths and then applying a weighting factor and combining those measurements, it is possible to calculate the volumetric flow of the fluid through the conduit. The average flow speed in the axial direction along each acoustic path is determined by comparing the transit times of the acoustic signal in the upstream and downstream direction. The theory behind these concepts is described in para. 9-5.3.2.

9-5.3.2 Path Flow Velocity. The path flow velocity refers to the velocity of the moving fluid that passes through the acoustic signal path. The path flow velocity is determined by the geometry and orientation of the transducers and the difference in time required for the acoustic signal to travel from the downstream transducer to the upstream transducer versus the time required to travel from the upstream transducer to the downstream transducer. Since the orientation and distance between the two transducers do not change, the difference in the transit times is directly related to the velocity of the moving fluid. This is the primary measurement of a time differential ultrasonic meter. See Figure 9-5.3.2-1 for basic common geometry of an ultrasonic flowmeter transducers and acoustic path.

The process for calculating the path flow velocity is illustrated in eqs. (9-5-1) through (9-5-9) for a simplified situation where the flow profile is fully developed and $(V_{ax}/c)^2 \ll 1$.

Figure 9-5.3.2-1
Wetted Recessed Transducer Configuration

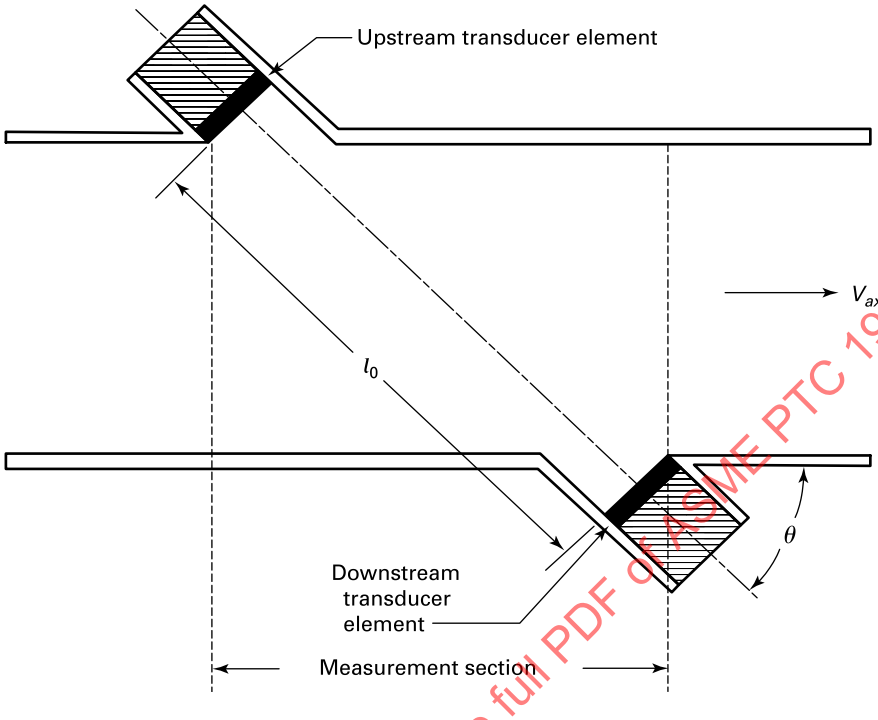

The time, t, for the acoustic signal to travel from one transducer to the other is measured by the meter's electronics and is equal to distance traveled divided by velocity and can be described as shown in eqs. (9-5-1) and (9-5-2).

$$\text{downstream: } t_{ab} = \frac{l_0}{c_{ab} + V_{ax}\cos(\theta)} \tag{9-5-1}$$

$$\text{upstream: } t_{ba} = \frac{l_0}{c_{ba} - V_{ax}\cos(\theta)} \tag{9-5-2}$$

where

c_{ab} = speed of sound of acoustic signal traveling from transducer a to transducer b
c_{ba} = speed of sound of acoustic signal traveling from transducer b to transducer a
l_0 = distance between transducers or intervening material in the measurement pair
t_{ab} = time of acoustic signal to travel from transducer a to transducer b
t_{ba} = time of acoustic signal to travel from transducer b to transducer a
V_{ax} = average axial flow velocity along acoustic path
θ = angle of transducers to measurement section axis

Ultrasonic meters require a homogeneous fluid with a stable speed of sound value. This means that $c_{ab} = c_{ba} = c$. Substituting into eqs. (9-5-1) and (9-5-2) and solving for c results in the following:

$$\text{downstream: } c = \frac{l_0}{t_{ab}} - V_{ax}\cos(\theta) \tag{9-5-3}$$

$$\text{upstream: } c = \frac{l_0}{t_{ba}} + V_{ax}\cos(\theta) \tag{9-5-4}$$

The upstream and downstream measurements are taken within fractions of a second of one another. This ensures the two measurements are taken quickly enough that both occur during identical flow conditions. The speed of sound, c, and the fluid velocity, V_{ax}, are unlikely to have changed in the short interval between upstream and downstream measurements and eqs.(9-5-3) and (9-5-4) are equal to one another. Combining both equations and solving for V_{ax} results in the following equations:

$$\frac{l_0}{t_{ab}} - V_{ax}\cos(\theta) = \frac{l_0}{t_{ba}} + V_{ax}\cos(\theta) \tag{9-5-5}$$

$$\frac{l_0}{t_{ab}} - \frac{l_0}{t_{ba}} = 2V_{ax}\cos(\theta) \tag{9-5-6}$$

$$\frac{l_0}{2\cos(\theta)}\left(\frac{1}{t_{ab}} - \frac{1}{t_{ba}}\right) = V_{ax} \tag{9-5-7}$$

$$V_{ax} = \frac{l_0}{2\cos(\theta)}\left(\frac{t_{ba} - t_{ab}}{t_{ab}t_{ba}}\right) \tag{9-5-8}$$

$$V_{ax} = \frac{l_0}{2\cos(\theta)}\left(\frac{\Delta t}{t_{ab}t_{ba}}\right) \tag{9-5-9}$$

where

$\Delta t = t_{ba} - t_{ab}$

As can be noted from the equations, the value of V_{ax} is equal to the averaged axial fluid velocity along the acoustic path. The value is determined by the average velocity of both the upstream and downstream measurements but is also an average of the fluid velocity along the acoustic path itself. For example, a fully developed flow profile has a higher fluid velocity in the center of the conduit and has slower velocity closer to the conduit walls. The resulting flow velocity measurement is an average of the flow velocity at each point along the acoustic path.

The meter uses this flow speed value in a series of calculations involving scaling factors to extrapolate the average flow speed of the fluid over the entire cross-sectional area of the measurement section.

9-5.3.3 Average Fluid Velocity. The average fluid velocity passing through the measurement section (entire cross-sectional area) is determined by applying multiple factors based on the geometry of the flow section, the locations and number of acoustic paths, and the average axial flow velocity along each acoustic path as determined in para. 9-5.3.2.

$$\overline{V}_{ax} = \frac{1}{n}S_V\sum_{i=1}^{n} W_i V_{ax_i} \tag{9-5-10}$$

where V_{ax_i} is derived similarly to eq. (9-5-9) except completed for each individual acoustic path and is equal to

$$V_{ax_i} = \frac{l_{0_i}}{2\cos(\theta_i)}\left(\frac{\Delta t_i}{t_{ab_i}t_{ba_i}}\right) \tag{9-5-11}$$

9-5.3.4 Volumetric Flow Rate. Once the average axial flow velocity along an acoustic path has been found, the volumetric flow can be calculated from the following equation:

$$q_v = S_V A \sum_{i=1}^{n} W_i V_{ax_i}$$

or

$$q_v = A \times \overline{V}_{ax}$$

where

A = average cross-sectional area of the measurement section

n = the number of acoustic paths
S_V = velocity profile correction factor
$\overline{V}_{ax}$ = average axial flow velocity over the entire cross-sectional area
V_{ax_i} = average axial flow velocity along acoustic path i
W_i = a weighting factor for acoustic path i that depends on measurement section geometry and acoustic path location (dimensionless)

Note that increasing n can reduce the sensitivity of S_V to flow profile variations.

9-5.3.5 Speed of Sound. When the fluid in the measuring section of the meter is at rest, the speed of sound of that fluid can be measured directly by dividing the acoustic path length by the measured transit time since the V_{ax} term of eqs. (9-5-1) and (9-5-2) is zero. More importantly, the speed of sound of a flowing fluid can be determined by substituting the average axial flow velocity from eq. (9-5-9) into eqs. (9-5-1) and (9-5-2). The speed of sound measurement can be used for several different purposes including identifying changes in fluid properties, composition, phase transitions, product change indication, and mixture concentrations among other uses. Comparing speed of sound measurements over time for a steady process is a great indication that the meter is continuing to function properly. Comparing speed of sound measurements of individual acoustic paths of a multipath meter can help diagnose a faulty acoustic circuit as well as a variety of other conditions including fouling, sediment, secondary flows, or product separation.

9-5.3.6 Single Path. For a single acoustic path meter intersecting the measurement section axis, the calculation of the volumetric flow rate is simplified by the fact that the weighting factor is equal to one and is simply the average axial velocity measured times the cross-sectional area of the measurement section. Single path meters offer good measurement accuracy when properly calibrated and used in well-controlled processes. Particular attention should be paid to ensure that the fluid has a fully developed turbulent flow profile. It shall also be ensured that the flow conduit is completely filled.

9-5.3.7 Multipath. Multipath meters are able to measure the flow profile in greater detail and can therefore offer much greater measurement accuracy than the single path meters. To calculate the volumetric flow rate for a multipath flowmeter, a weighting factor needs to be applied to each acoustic path average axial velocity measurement to determine the average axial velocity over the entire cross-sectional area. The weighting factor, W_i, is based upon several factors, including measurement section geometry, number of acoustic paths, and the acoustic path locations, that affect how much each path's axial velocity measurement contributes to the overall average axial flow velocity over the entire cross-sectional area.

9-5.4 Acoustic Signal

The transducers create the acoustic signal at a fixed frequency; however, that frequency varies depending upon the application. Gases are typically measured at a frequency in the range of 50 kHz to 600 kHz, while a liquid is typically best measured with a signal in the 500 kHz to 2 MHz range. The manufacturer should be consulted to determine the best frequency for a specific application.

9-5.5 Measurement Circuitry

The measuring circuit for an ultrasonic flowmeter is illustrated in Figure 9-5.5-1. Inaccuracies due to variances in measurement circuits for each of the acoustic paths and each measurement direction, upstream and downstream, are avoided by using a single measurement circuit and switching the path and direction. This system ensures that all individual transit time measurements are equivalent and any variabilities in the measurement circuit are canceled out.

9-6 PERFORMANCE-AFFECTING CHARACTERISTICS

Acoustic transit time flow rate measurement has potential operational limits. These should be investigated for each application. Limitation sources can originate from meter characteristics, flow characteristics, or installation effects. Each should be investigated completely when choosing a measurement solution for each application.

9-6.1 Meter Characteristics

There are many possible configurations of differential time-based ultrasonic meters and they can vary by manufacturer. Many of the available options can be tailored to provide the best measurement solution for a specific application. This section discusses the most commonly available options, but a manufacturer should be consulted before making a final selection.

Figure 9-5.5-1
Acoustic Flow Measuring System Block Diagram

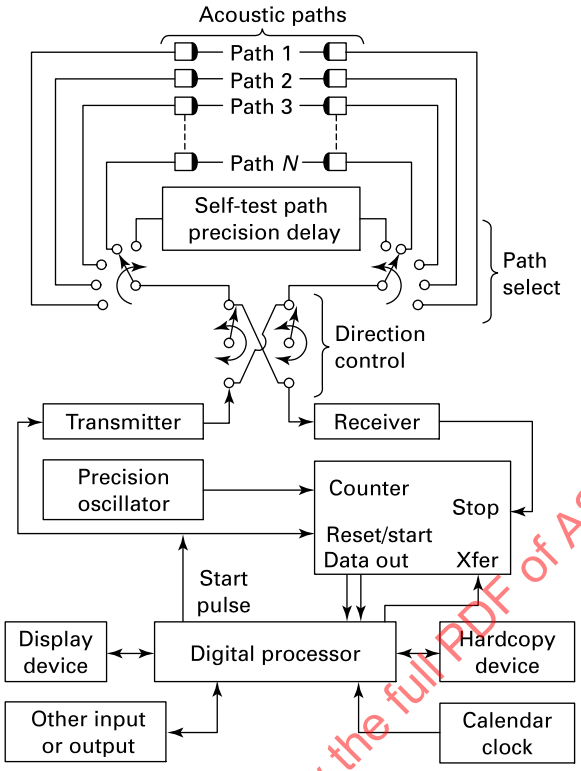

9-6.1.1 Acoustic Paths. The number and orientation of acoustic paths in a meter have a significant impact on the meter's performance, including measurement uncertainty, versatility, sensitivity to contamination and poor flow conditions, as well as on meter diagnostics, as outlined in paras. 9-6.1.1.1 through 9-6.1.1.3.

9-6.1.1.1 Single Path. A single acoustic path flowmeter is a basic version of an ultrasonic meter. It is an economical measurement solution for applications where accuracy is less important and where process conditions are well controlled. Single path meters use a single acoustic path, almost always across the horizontal diameter of the measuring section and intersecting the measurement section axis. See Figure 9-5.1.3-1 for an illustration of a diametric meter configuration. Because the meter is only able to measure the axial velocity of the fluid across the diameter, the flow profile must be uniform, fully developed, and in a known flow regime, which is typically turbulent. This is required so that the correlation factors that are applied can closely approximate the flow across the entire cross section. Flows in the transitional regime must be avoided since they can create errors as large as 35%.

9-6.1.1.2 Multipath. Multiple acoustic paths have several advantages over single path meters. Multipath meters take advantage of having several measurements across the flow profile to develop a more accurate estimation of the axial flow velocity over the entire cross-sectional area. As the number of flow paths increases, the measurement becomes more accurate and less susceptible to variations in the flow profile and other flow variations. This increases the ability of the flowmeter's electronics to determine and compensate for flow variations that affect the volumetric flow rate calculations. The placement of the acoustic paths can be critical in obtaining a good understanding of the flow profile and can vary depending upon the application. Figure 9-8.4-1 illustrates the differences in flow profiles and their relation to acoustic path locations.

9-6.1.1.3 Reflective Path. Reflective path flowmeters can offer better averaging of flow velocity along the acoustic path and better resilience to swirl. They also offer increased diagnostic functions from the same number of transducer pairs by reflecting the acoustic signal off the internal surface of the flow conduit one or more times as it transits from one transducer to the other (see Figure 9-6.1.1.3-1). This allows each acoustic signal to cross the flow path multiple times as it travels from one transducer to the other. This provides for better averaging, lower susceptibility to secondary flows, and

Figure 9-6.1.1.3-1
Reflective Path Transducer Configuration

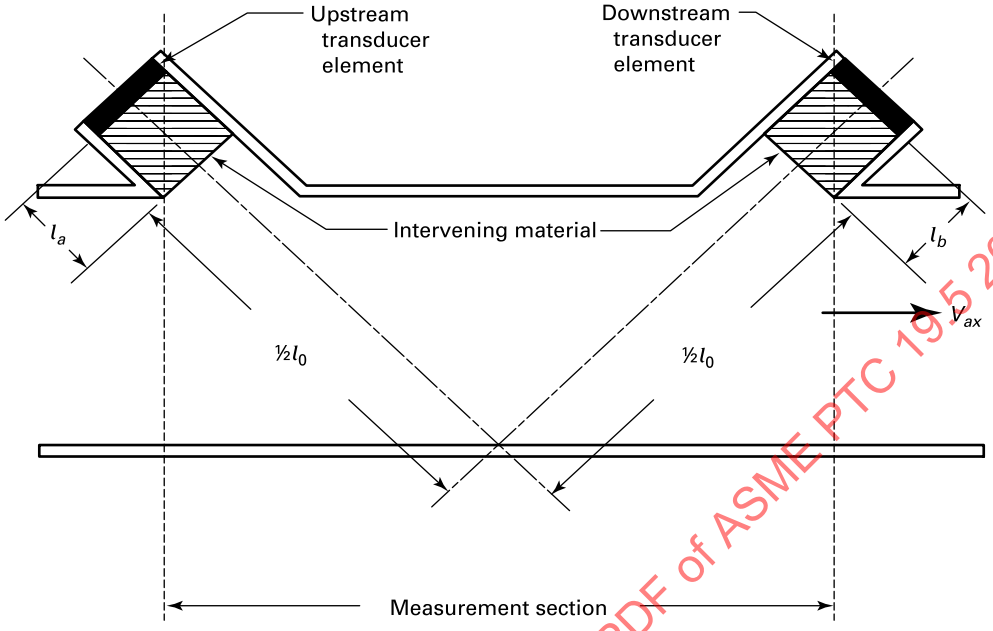

reduced Reynolds number influence. Lower resolution is also required for the transit time measurement. However, a reflected path acoustic signal does not undergo a perfect reflection, and some energy from the acoustic signal is lost into the conduit wall at each reflection. As a consequence, the transducers require more power and may necessitate greater meter electronics sensitivity or significant filtering to ensure reliable sensing and measurement. Reflective paths are more susceptible to influence due to contamination and scaling, particularly in the area of the reflection point that might inhibit reflection. Fluid contamination can have an increased impact on signal strength at the receiving transducer since the same acoustic signal is exposed to any contamination on multiple passes through the fluid. The manufacturer should be consulted, and care should be taken with reflected path meters if these conditions exist. More advanced meters can include a reflective path for the specific purpose of monitoring for contamination, scaling, or gas and condensation buildup inside the meter. This diagnostic feature can alert the user that cleaning may be required.

9-6.1.2 Transducer Considerations

9-6.1.2.1 Distance and Angle. When manufactured as a complete assembly, an ultrasonic meter will have little variation in transducer distance and angle. For field-installed devices, the transducer installation and alignment are important and must be held stable to ensure long-term measurement accuracy. Small changes in the distance between the two transducers or a variation in the actual versus the measured distance between them can have a significant effect on accuracy. The transducer angle must also be measured accurately and programmed into the meter electronics to ensure the calculation of axial velocity is completed correctly. The manufacturer should be consulted for optimizing the transducer distance and angle for field-installed units based on the application.

9-6.1.2.2 Location in Pipe. The physical location of the transducers in the conduit is also a crucial measurement in determining the correct profile and weighting factors that are applied to each path's measurement. The location of the acoustic path is also important to provide the best possible estimation of the flow profile, which varies based on the number of paths and the application. This is illustrated in Figure 9-8.4-1, which shows the relation between flow profiles and acoustic path locations.

9-6.1.2.3 Contamination Buildup. Contamination buildup in the pipe should be monitored and removed as regular maintenance on the meter. Contamination can cause increased uncertainties through several different modes. Most common is a buildup on the transducer, potentially slowing, scattering, and weakening the acoustic signal. Slowed signals may be filtered out if they do not arrive at the other transducer in a manufacturer-determined time window, while scattered or weakened signals may not be strong enough to trigger a reading by the receiving transducer.

In more severe instances of contamination buildup, the resulting change in the cross-sectional area of the metering section can affect the accuracy of the flow rate calculation, which assumes that the flow is passing through an unobstructed conduit. The measurement section should be cleaned regularly for applications where contamination buildup is a concern.

9-6.1.2.4 Transducer Construction and Fluid Interface. Transducer construction can vary between manufacturers and applications. The velocity calculations of wetted transducers are straight forward since the transducer is in direct contact with the fluid [see Figure 9-5.3.2-1 and eq. (9-5-9)]. However, wetted transducers have no protection from aggressive and/or high temperature fluids, and they cannot be replaced while the system is pressurized. To protect the transducer from potentially harmful effects of the fluid, an intervening material between the transducer and the fluid is used. The addition of the intervening material affects the calculation of the transit time due to the added distance to the acoustic path (transducer to transducer) and the different speed of sound of the intervening material as shown in the following equations.

$$t_{ab} = \frac{l_0}{c_0 + V_{ax}\cos(\theta)} + \frac{l_a}{c_a} + \frac{l_b}{c_b} \tag{9-6-1}$$

or

$$t_{ab} = \frac{l_0}{c_0 + V_{ax}\cos(\theta)} + t_a + t_b$$

The transit time of the acoustic signals through both intervening materials a and b is represented by $t_o = t_a + t_b$, a function of temperature. Replacing $t_a + t_b$ with t_0 and combining eqs. (9-6-1) and (9-5-9) results in the following:

$$v_{ax_i} = \frac{l_{0_i}}{2\cos(\theta_i)}\left[\frac{\Delta t_i}{\left(t_{ab_i} - t_{0i}\right)\left(t_{ba_i} - t_{0i}\right)}\right] \tag{9-6-2}$$

NOTE: The values of length, speed of sound, and consequently the time for the acoustic signal to travel through the intervening material are temperature dependent and should be taken into account when determining values other than the axial flow velocity, V_{ax}. The above equations pertain to the calculation for a single acoustic path; for multipath meters, these calculations should be repeated with specific path values for each variable.

There are several common transducer configurations using intervening materials outlined in paras. 9-6.1.2.5 through 9-6.1.2.9.

9-6.1.2.5 Recessed Transducers. Recessed transducers are the most common configuration for transducers (see Figure 9-6.1.2.5-1). They are recessed from the inner wall of the measurement section, thus allowing for a perpendicular fluid interface to the transducer/intervening material and providing a more reliable flow calculation. Recessed transducers do not obstruct the flow through the measurement section, which reduces pressure drop and flow disturbances while also enabling the use of inspection gauges. When properly designed, the open recess of this transducer geometry will flush itself of any contamination or alternate phase product; however, the manufacturer should be consulted when heavy contamination buildup is possible.

Where condensation is a concern for gases, recessed transducers should not be oriented vertically. This can lead to the accumulation of condensate in the bottom transducer recess, which will adversely affect the acoustic signal due to the difference in speed of sound of a liquid versus a gas as well as cause a change in angle of the transducer/fluid interface. Likewise, liquid flows with entrained gas or cavitation concerns should not have transducers oriented vertically on top of a metering section to prevent gas accumulation and the same detrimental effects on the measurement accuracy. More advanced meters may offer a vertical acoustic path that can assist in determining the flow profile; however, this additional acoustic path's primary function is to provide diagnostic feedback to detect any contamination buildup in the meter and alert the user.

9-6.1.2.6 Protruding Transducers. Protruding transducers, like recessed transducers, allow both upstream and downstream transducer surfaces to be perpendicular to the acoustic path (see Figure 9-6.1.2.6-1) and protect the transducers with intervening material. However, protruding transducers do extend into the metering section, so it is no longer a smooth bore, and have the potential to create some disturbances to the flow profile that may affect downstream devices. Due to their geometry, protruding transducers should not be oriented in the 6 or 12 o'clock position to avoid the potential accumulation of gas or condensate.

Figure 9-6.1.2.5-1
Recessed Transducer Configuration

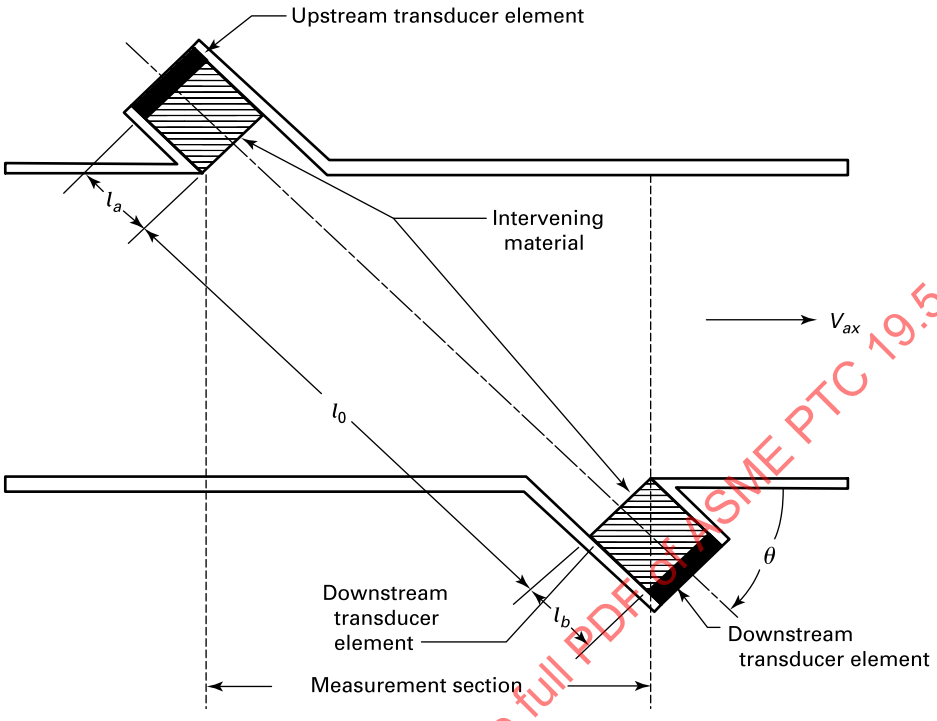

Figure 9-6.1.2.6-1
Protruding Transducer Configuration

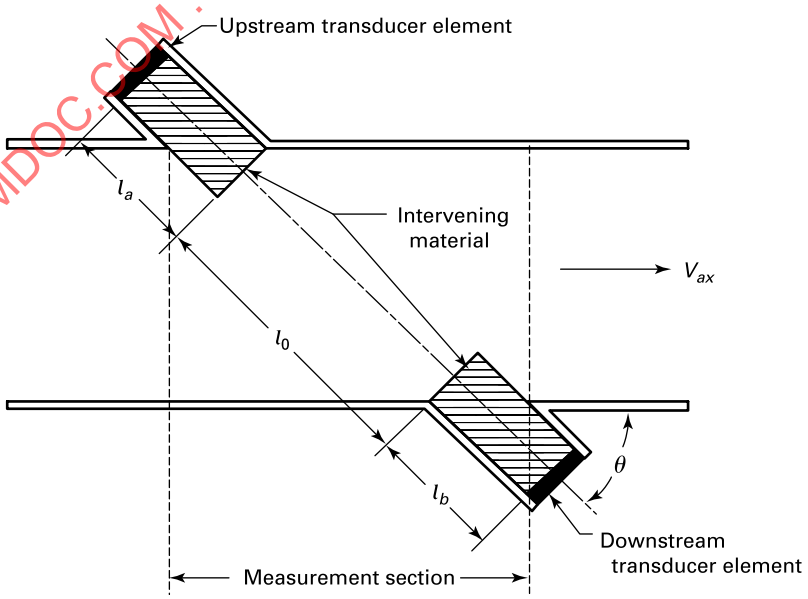

Figure 9-6.1.2.7-1
Flush Transducer Configuration

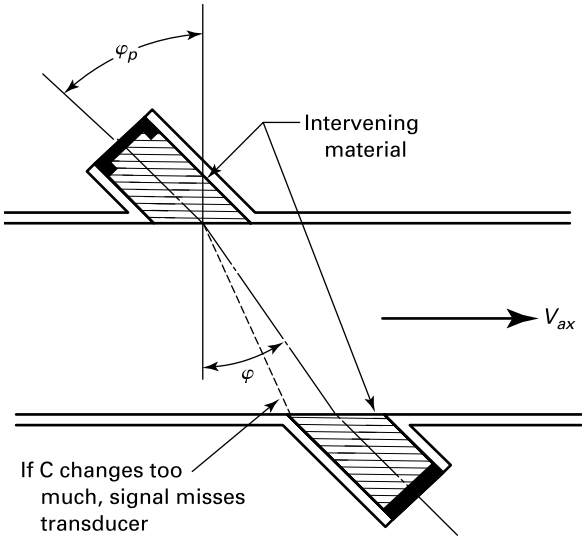

9-6.1.2.7 Flush Transducers and Nonperpendicular Interface. Paragraphs 9-6.1.2.5 and 9-6.1.2.6 assume the intervening material in contact with the fluid is perpendicular to the acoustic path and that the acoustic signal is propagated normal to the transducer/fluid interface (see Figures 9-6.1.2.5-1 and 9-5.3.2-1). Flush mounted transducers, however, require that the acoustic signals enter and leave the fluid along a path that is not normal to the transducer's solid/fluid interface. For example, the intervening material could be flush with the inside surface of the conduit as in Figure 9-6.1.2.7-1. This further complicates the acoustic analysis since corrections for the refraction of the acoustic signals at the solid/fluid interface must also be introduced. This refraction takes place according to Snell's Law, i.e.,

$$\sin\frac{\varphi}{c} = \sin\frac{\varphi_p}{c_p} \tag{9-6-3}$$

where

c = sound speed in the fluid
c_p = sound speed in the intervening material
ϕ = incident angle
ϕ_P = refracted angle

As a consequence, l_0 and t_0 in eq. (9-6-2) now become functions of the sound speeds (c, c_p), and, in general, of the temperature, pressure, and composition of the process fluid and intervening materials.

9-6.1.2.8 Signal Conduction (Through Wall). Because the acoustic signal of an ultrasonic meter is at very low power, care must be taken in the design of ultrasonic transducers and intervening material to ensure that as much of the energy in the acoustic signal is transferred into the fluid as possible. The most common and largest loss of acoustic signal energy is into the pipe wall of the measuring section, where it can travel quickly to other transducers causing noise and the potential for triggering on the conducted signal instead of the signal passed through the fluid. This can be mitigated by isolating the transducers and intervening material to prevent signal loss and by increased filtering of the signal into the meter's electronics. Since the speed of sound in the metal pipe is much greater than that of a fluid, the conducted signal will always arrive before the actual signal, making it easy to filter out.

9-6.1.2.9 Extended Transducers (Waveguides). Extended transducers, or waveguides, are commonly seen in high-temperature applications. The waveguide transducer configuration is shown in Figure 9-6.1.2.9-1. By moving the electronic components of the ultrasonic transducers away from the process, the waveguides are able to thermally decouple the transducers from the process while still delivering a focused ultrasonic signal to the fluid interface. Extended transducers are generally used for process temperatures above the 200°C to 250°C (392°F to 482°F) range of standard designs and can be used for process temperatures as high as 620°C (1,148°F). The transit time proportion in the extended

Figure 9-6.1.2.9-1
Waveguide Transducer Configuration

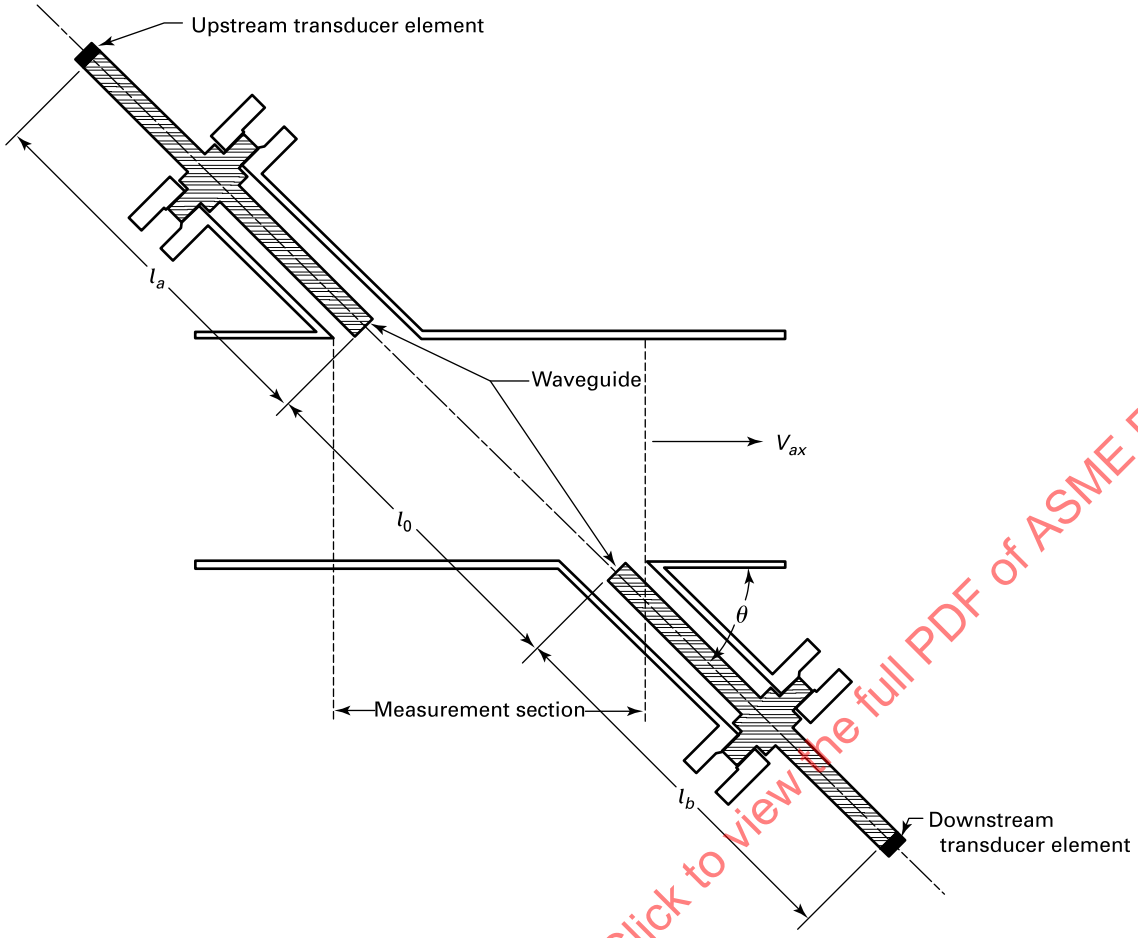

transducer can be relatively large in relation to the transit time proportion in the fluid. Variations in the transit time caused by the change of the temperature profile within the waveguide should be corrected in the secondary device.

9-6.1.2.10 Wiring. The transducers are connected to the electronics (secondary device) by shielded cables. The cable lengths between the secondary and primary devices are an important consideration because longer cables may introduce timing delays and signal losses. The timing delays can change the calibration factor if not accounted for. Signal losses, when combined with path length (spreading loss) and acoustic attenuation in the fluid, can reduce the signal strength to the point where the meter will not operate properly. Cable specifications and maximum lengths are usually defined by the manufacturer.

9-6.2 Flow Characteristics

Differential travel-time ultrasonic meters are well suited for a wide range of flow measurement applications. However, there are some limitations in the technology that are described in paras. 9-6.2.1 and 9-6.2.2.

9-6.2.1 Flow Speed. While acoustic transmission will not be affected by low velocities, the differential transit time may be so small that the system is incapable of measuring it within the required accuracy. The zero offset may also become unacceptably large. This is particularly true in smaller conduits and is highly dependent on the design of the transducers and transit-time measurement electronics. In addition, secondary flows may develop under low velocity conditions. Secondary flows will also reduce flow measurement accuracy and should be avoided by ensuring sufficient straight pipe length or a flow straightener is installed upstream of the meter.

Figure 9-6.2.2-1
Cross-Beam Transducer Configuration

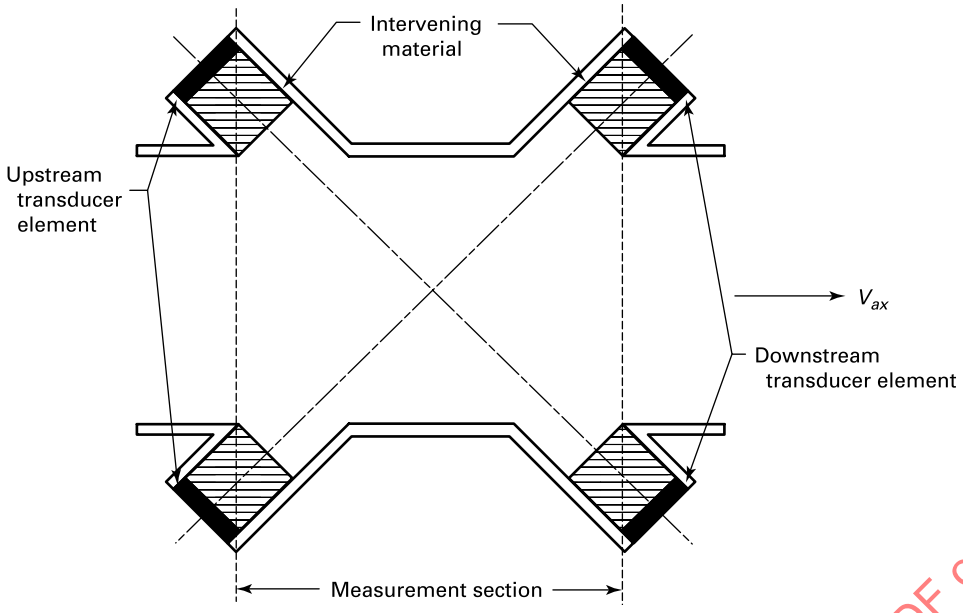

High fluid velocity combined with low pressure can cause local cavitation around piping joints or the transducers, generating noise and introducing entrained gas in the acoustic path that can disrupt the acoustic signal. Increased back pressure is recommended to reduce cavitation.

9-6.2.2 Secondary Flow. Secondary flow can produce an error in the determination of V_{ax} since it is normally assumed in the calculations that all flow is in the axial direction. Secondary flow is a result of flow perturbations occurring upstream or downstream of the measurement section from devices such as elbows, valves, and pumps. Secondary flow may result in an error in determining the transit time, which ultimately affects the calculation of V_{ax}.

The most effective way to reduce the uncertainty caused by secondary flow is to avoid installations where severe secondary flow exists or to use additional, suitably placed acoustic paths. Reduction of secondary flow may require long upstream straight runs of pipe, depending on the nature of the secondary flow source and the accuracy required. (See para. 9-6.3 on installation effects for general guidelines.) Secondary flow uncertainties can also be reduced by using an appropriate acoustic path orientation or by computing line velocities on multiple crossed chordal acoustic paths, as shown in Figure 9-6.2.2-1, and averaging the resultant measured velocities.

9-6.2.3 Flow Temperature. Typical ultrasonic flowmeters are easily able to accommodate temperatures in the range of −40°C to 180°C (−40°F to 355°F). Special designs may be required to accommodate extreme temperature service. Ultrasonic flowmeters, particularly in custody transfer applications of liquefied gas, are capable of operating in the cryogenic range of −200°C (−330°F) with no effect on accuracy. Other meter designs for high temperature applications such as steam are capable of temperatures of well over 500°C (930°F).

Processes with large fluctuations in temperature during operation can have an increased uncertainty since many of the variables, like the speed of sound, path length, density, and cross-sectional area, can be dependent upon temperature. Some meter designs have the ability to compensate for changes in temperature and should be considered in processes with large changes in temperature.

9-6.2.4 Viscosity. Fluid viscosity is a limiting media characteristic for ultrasonic flowmeters due to the damping of the acoustic signal in high viscosity fluids. Common meter designs are typically limited to fluids in the range of 0.1 cSt to 100 cSt. Special constructions have the ability to measure fluids with viscosity of up to 1 000 cSt.

9-6.2.5 Contamination. Ultrasonic flowmeters require a homogenous fluid but are capable of handling limited amounts of contamination. Processes where contamination is likely require special attention to prevent loss of measurement accuracy and/or ability. The primary concern with contamination is that the acoustic signal is scattered or blocked

by contaminant particles and does not reach the receiving transducer leading to a loss of measurement ability. Contamination most often leads to a loss of measurement capability and not a loss of measurement accuracy.

9-6.2.5.1 Entrained Gas or Suspended Solids in Liquid Flow. Large quantities of entrained gas bubbles or solids suspended in a liquid flow will cause the acoustic signal to reflect and refract. As a result, the scattered acoustic signal may be too weak to be detected by the receiving transducer. The source of the air or other gases could be localized cavitation in the upstream piping or upstream pumps or turbines; or obstructions such as partially closed valves; or cavitation in fast moving liquids. This cavitation can create sufficient attenuation in the acoustic signals to prevent operation. Gas bubbles in liquid flow should be limited to less than 2% by volume and solid particles should be limited to less than 5% by volume.

9-6.2.5.2 Entrained Solids and Liquids in Gas Flow. Gas flow measurement can also be impacted by liquid loading or solids suspended in the gas flow stream. In large quantities, these will cause the acoustic signal to reflect and refract. As a result, the scattered acoustic signal may be too weak to be detected by the receiving transducer. Larger solid particles and large amounts of liquid can fall to the bottom of the measuring section, thus reducing the cross-sectional area for the gas flow until they are flushed out. This condition will introduce some additional uncertainty in the flow measurement and should be avoided. The source of the liquid could be contaminants or upstream pumps or compressors. Solid particles should be limited to less than 5% by volume.

9-6.2.5.3 Contamination, Condensate, Sources of Fouling. Contamination will not affect the measurement accuracy of a well-designed meter, but the meter will not operate when contaminate levels exceed allowable levels. There are several options to consider when operation is required under adverse conditions. In particular, it may be possible to operate at a lower acoustic frequency, which is less susceptible to attenuation from entrained air and sediment. It may also be possible to locate the meter away from the source of entrained air or at a location with higher pressure. Alternatively, a smaller diameter measurement section or larger path angle could be used to reduce path lengths and, consequently, total acoustic attenuation.

9-6.2.5.4 Variance in Speed of Sound. The speed of sound in the fluid and in any intervening materials along the acoustic path varies with composition, temperature, and pressure. Depending on a particular ultrasonic flowmeter's design, l_0 and t_0 [see eq. (9-6-2)] can be affected. In nearly all cases, the errors caused by sound speed variations in the fluid are negligible for a properly implemented, nonrefractive, wetted transducer system. Changes in the speed of sound in the intervening material may, however, require compensation for nonwetted transducer systems.

In refractive systems, changes in the speed of sound in intervening materials and the fluid affect the acoustic path length and angle. While it is possible to compensate for these effects, large changes in the speed of sound in the fluid may refract the beam to the extent that it misses the opposite transducer. The manufacturer should be consulted for an acceptable range for the speed of sound in a particular fluid to prevent this possibility.

9-6.2.6 Multiple Fluids (Nonsimultaneous). The manufacturer should be consulted if an application requires measuring multiple fluids with widely differing acoustic properties. A large change in acoustic properties can cause excessive signal loss due to acoustic attenuation or angular variations in refractive or nonparallel transducer interfaces. It may require multiple primary devices (spool pieces) to provide reliable measurement for fluids with widely differing acoustic properties.

9-6.2.7 Density for Gas Flows. Special attention should be paid to the density of gaseous fluids. Sound and the acoustic signal cannot be transmitted in a vacuum and are also severely attenuated or lost in low density fluids, thus resulting in a minimum density requirement for gas flows. Increasing the gas pressure is the easiest method of increasing the gas density; if this is not possible, then the meter manufacturer should be consulted for guidance on the requirements for specific gases and process conditions.

9-6.2.8 Nonmeasured Interface Effects on Cross-Sectional Area. Accumulation of a substance other than the intended fluid in the measurement section can affect the accuracy of the volumetric flow rate calculation performed by the meter electronics. Consideration should be given to any process in which any gas or liquids may collect in the meter. For example, condensation from a gas flow that builds up in the bottom of a measuring section will not be evident to the meter until the condensate level reaches the first acoustic path and the acoustic signal is disrupted. Until the liquid reaches this height, the meter is calculating the volumetric flow rate using the measured gas velocity while assuming that the gas is flowing through the entire cross-sectional area. For a single-beam meter, that means that the measured flow rate can be nearly double the actual flow rate before the acoustic path is blocked.

9-6.2.9 System Noise. Because ultrasonic meters operate using acoustic signals, they can potentially be susceptible to noise in a piping system. Even though ultrasonic meters use a high frequency that attenuates rapidly, reducing the possibility of an interfering signal, the potential for noise interference still exists and should be considered.

Sources of acoustic noise may result from upstream obstructions, mechanical vibration, exposed sharp edges, other ultrasonic meters in close proximity, or another part of the system. Gas flows are most susceptible to system noise; sharp edges in a pipe system, like a partially open valve, can easily generate noise in the same 100 kHz range as the transducers for this application. This is easily solved with a straight and smooth inlet section.

Another consideration for system design is the electrical interference between meters with cables in close proximity, such as when they run long distances in conduit or in a cable tray.

9-6.3 Installation Considerations

Many of the error sources listed in subsection 9-8 can be reduced or eliminated by proper installation. Sources of error and installation problems the user should address during the design phase of a project are described in paras. 9-6.3.1 through 9-6.3.7.

9-6.3.1 Flow Profiles and Secondary Flow. Sufficient lengths of straight pipe or other flow straightening devices should be installed upstream of an ultrasonic meter to ensure a uniform flow profile. See para. 9-8.6 for a discussion on the potential effects of flow profile variations and uncertainty. The manufacturer's recommendations for required inlet straight pipe lengths should be consulted.

Secondary flows can affect the transit time of the acoustic signal, thus affecting the fluid velocity calculation and the flow measurement, and should be avoided wherever possible. Ultrasonic meters should be installed away from pumps, tees, bends, and other equipment that can cause disturbances or secondary flows.

In the absence of manufacturer's recommended straight pipe lengths, there shall be by default a minimum of 20 nominal pipe diameters upstream and 5 downstream. If a flow conditioner is placed upstream of the metering section, there shall be by default a minimum of 10 nominal pipe diameters of straight pipe length upstream and 3 lengths downstream.

9-6.3.2 Meter Location. Ultrasonic meters should be installed in piping systems where they will not collect entrained gas, condensate, or solid particles and away from pumps and other equipment that can cause interference noise or turbulent or secondary flows. Ultrasonic meters should be installed upstream of any potential sources of fluid contamination. Sufficient lengths of straight pipe or other flow straightening devices should be installed upstream of an ultrasonic meter to ensure a uniform flow profile. The manufacturer's guidelines for meter installation location shall be consulted.

9-6.3.3 Meter Orientation. The measuring principle of an ultrasonic meter is bidirectional, which allows the meter to measure flow in either direction. However, if the meter was lab calibrated, it should be installed in the same orientation as it was installed in the laboratory test setup to ensure the meter will perform to its calibrated uncertainty. Ultrasonic flowmeters should be installed in a piping arrangement that prevents the collection of gas bubbles, condensate, or other contaminates around the transducer cavities or allows for their self-flushing.

9-6.3.4 Temperature, Pressure, Viscosity, and Loading Fluctuations. Ultrasonic flowmeters are able to measure fluids over a wide range of temperatures, pressures, and viscosities. To ensure accurate measurement, rapid fluctuations in these characteristics should be avoided. Rapid changes in temperature can have immediate effects on the fluid density, speed of sound, and composition, while changes to dimensional properties of the meter may be slower to react, causing the potential for increased uncertainty. Some ultrasonic meters are able to compensate for the dimensional effects of temperature changes ensuring continued measurement accuracy.

9-6.3.5 Multiphase or Multiple Fluids. Ultrasonic meters generally require a homogenous fluid to ensure accurate flow measurement. If the fluid is not homogeneous, special attention should be paid. When using an ultrasonic meter in applications with a multiphase fluid or with multiple fluid mixtures, the phase/fluid interface can disrupt the acoustic signal in the same manner as gas bubbles, solid particles, and other contamination. Efforts should be made to remove and prevent different phases from entering the measurement section.

In flows with significant amounts of an additional phase or fluid, the interface between the two may act as a reflective surface that can scatter and weaken the acoustic signal. If possible, orient the meter so that the acoustic paths do not cross a fluid interface, or ensure that fluids are completely mixed before entering the meter to help mitigate this risk.

In a stratified flow, different fluids may be moving at different velocities that will negatively affect the volumetric flow calculation.

Finally, attention should be paid to the differences in the speed of sound of different fluids or fluid phases. Where a multipurpose conduit may have different fluids with speed of sound in a similar range, the change in the measured speed of sound can be used to identify the fluid change. However, for vastly different fluid speeds of sound, the transducer frequency can become ineffective and the ability to measure flow can be lost.

9-6.3.6 Contamination. Ultrasonic flowmeters should be installed upstream of any sources of contamination, intentional or otherwise, to avoid introducing bubbles, solids, multiple fluids, or other potential sources of contamination that may disrupt the acoustic signal. Soluble additives may be added far enough upstream to ensure complete mixing/dissolving of the material before it reaches the meter.

9-6.3.7 Scale and Erosion. Flow profile changes and dimensional changes in the measurement section, including those caused by corrosion, erosion, or material buildup, directly affect meter performance and should be considered in the selection, location, and orientation of a meter. The measurement section should be inspected periodically to determine if the cross-sectional area or meter factors determined during calibration remain valid.

Any part of an ultrasonic meter in contact with the fluid is typically constructed of robust materials. Erosion is not typically a concern. However, the manufacturer should be consulted if an aggressive fluid is going to be used.

Scale buildup can affect the measurement accuracy by changing the cross-sectional area of the metering section in a way that is not detectable by the meter, affecting the volumetric flow rate calculations. Scale buildup directly on the transducers or intervening material can affect the performance of the meter by attenuating, refracting, and/or changing the speed of the acoustic signal. Scale on the transducers may not be immediately evident in the performance of the meter; the measurement section and the transducers should be inspected often if scaling is likely for the fluid and process conditions.

Some ultrasonic meters offer diagnostic functions that indicate contamination, bottom sediments, scaling, and secondary flow. At installations where high accuracies are required or that are prone to these effects, the diagnostic functions can be used to check the meter integrity.

9-7 CALIBRATION

Installation considerations and the required accuracy usually determine the methods of calibration. There are four principal methods of meter factor determination

(a) factory calibration
(b) laboratory calibration
(c) field calibration
(d) analytical procedures (dry calibration)

The first three can be used to verify meter performance.

9-7.1 Purpose

Calibration of ultrasonic flowmeters reduces errors resulting from uncertainties in path length and angle, cross section, and path location. Velocity profile errors can be corrected with in situ calibration or by properly simulated laboratory calibrations.

There remains an uncertainty in the flow measurement that results from uncertainty of the calibration equipment and procedures. To reduce calibration uncertainty, calibration should be conducted according to national (ANSI) or international (ISO) standards.

9-7.2 Factory Calibration

All ultrasonic flowmeters are provided by the manufacturer with a basic calibration that is used to determine the meter factor, S_v, and ensure that the meter meets the stated accuracy in its technical documents. The basic factory calibration can involve flow testing at as few as two flow rates and is usually completed using water for liquid flowmeters and air for gas meters. The meter manufacturer should be consulted for specific details of the basic factory calibration, but most offer a more thorough calibration with additional or specific flow rates upon request. Increasing the number of data points increases the range of flow rates with known uncertainty, and additional data points at the same flow rate allow the repeatability of the meter to be determined. Standard factory calibrations can yield uncertainty values as low as 1% for gas flows and 0.3% for liquid flows.

9-7.3 Laboratory Calibration

Laboratory calibrations should be conducted at facilities where the procedures are in accordance with national (ANSI) or international (ISO) standards.

Generally, the calibration tests should be run using water that is free from entrained air or solid particles. Calibration tests should be conducted using flows that are free from non-axisymmetric flow and pulsation and by using sufficient lengths of straight pipe upstream and downstream of the measurement section and, if necessary, by installing upstream flow conditioners.

If the laboratory calibration is designed to model the field application, one of the advantages of multiple-path acoustic flowmeters is that they can measure the actual velocity profile (to the extent possible with the number of paths installed). This can increase the confidence in the expected field accuracy by comparison of the velocity profiles achieved in the field with the laboratory data. The extent to which the above conditions have been achieved can be determined by noting the sensitivity of the meter factor to rotation and translation of the primary device.

A statistically significant number of 30 sec to 100 sec runs (usually 10 to 20 runs) should be made over a range of flows. Flowmeter accuracy, within the uncertainty of the laboratory standards, should be determined by the combined random and systematic uncertainties in the measurement of the volumetric flow following the methods of ASME PTC 19.1.

Special calibration tests can also be performed for those cases where piping in the final installation can produce an asymmetric flow or where other flow irregularities are suspected. These will require appropriate modeling of upstream and downstream piping.

Laboratory calibrations, particularly for custody transfer applications, can yield meter uncertainties of as low as 1% for gas flows and 0.3% for liquid flows.

9-7.4 Field Calibration

Field calibrations have an advantage in that true operating conditions are encountered, but it can be difficult to obtain reference flow measurements depending on the process application and the availability of accurate reference flow measurement equipment. These field calibration methods are less accurate than an original factory calibration and considerably less accurate than a laboratory calibrated meter.

9-7.5 Dry Calibration

Analytical procedures, commonly referred to as dry calibrations, are another available technique for field installations in large line sizes [>3 000 mm (>118.11 in.) in diameter] where a laboratory calibration is not practical. These procedures require precise physical measurements (such as acoustic path length, transducer angles, path locations, intervening material, and cross-sectional area) as well as instructions and data supplied by the manufacturer. Dry calibrations are not true calibrations since no meter factor, S_V, is determined, but they provide the necessary physical dimensions needed for the meter to make an uncalibrated flow rate measurement. These physical measurements and their contributions to the overall flowmeter uncertainty are discussed in Section 9-8. The uncertainty in the meter performance should reflect uncertainties associated with these procedures.

9-7.6 Calibration Considerations

Whether calibrating a meter at a laboratory or in the manufacturer's lab, there are several test setup and configuration parameters of which the user should be aware. The test shall be conducted with a secondary device and transmitter configuration that reflects the end use configuration. This will minimize configuration-induced measurement errors in the final installation.

9-7.6.1 Calibration Equipment Uncertainty. The uncertainty of the calibration test setup must be determined and included in the overall measurement uncertainty. To achieve a useful measurement uncertainty level, the calibration should conform to best practices outlined in ASME PTC 19.1.

9-7.6.2 Replicating Installation Conditions. The installation of the meter in the calibration test setup should be as close as possible to the actual field installation conditions. Inlet sections and any flow disturbances upstream of the meter in the final installation should be replicated in the test setup. Where possible, fluid and flow conditions should mimic field conditions as closely as possible.

9-7.7 Measurement Uncertainty

Ultrasonic flowmeters are available with varying flow uncertainties that can range from 0.3% to 1.5% for gases and from 0.1% to 1.0% for liquids under ideal conditions. There are two categories of parameters that influence the overall uncertainty of an ultrasonic meter's measurement. The first is the determination of primary calibration factor, and the second is the contribution to measurement uncertainty by secondary effects.

Primary calibration factors for an ultrasonic meter are the linear calibration factor and the zero value. When a meter is manufactured, a unique calibration factor is determined through the manufacturer's calibration. The process for evaluating the overall calibration uncertainty should be in accordance with the general practices outlined in ASME PTC 19.1. In addition to determining a calibration factor, the manufacturer must determine a zero value during the calibration process. Although the zero value cannot be improved during calibration, its stability or random uncertainty contribution at lower flows can be determined during the calibration process. A meter with flow points outside the lower end of the

flow range (10% of flow or less) may have an incorrect zero or an unstable sensor. Uncertainty in low-flow measurement will primarily be affected by the stability of the zero for that meter type.

Secondary effects on measurement uncertainty are typically the result of changes in fluid properties, which include changes in temperature and pressure that can affect the speed of sound through the fluid and intervening materials, changes to the density or viscosity, additional contamination, or changes in flow velocity resulting in a flow regime change. These changes in fluid properties will also influence the zero value. The greatest effect occurs when the operating temperature of the meter is different from the temperature at which the zero is determined and the meter is being operated at low flows.

9-8 ERROR SOURCES AND THEIR REDUCTION

Possible error sources of ultrasonic flowmeters covered by this Section are described herein. Although these additional sources of error may be insignificant in some cases, they should all be addressed in detail when analyzing the uncertainties for a particular flowmeter; ASME PTC 19.1 shall be used to estimate the overall uncertainty of the overall flow measurement process. ASME PTC 18 also contains criteria for flow measurement in large pipes as well as uncertainty estimation methods. The manufacturer should be consulted if any of the topics discussed in paras. 9-8.1 through 9-8.9 are relevant to an individual application.

9-8.1 Axial Velocity Measurement Uncertainty

Axial velocity errors are estimated uncertainties in the determination of V_{ax} along an acoustic path and are described in paras. 9-8.1.1, 9-8.1.2, and 9-8.1.3. [See eqs. (9-5-9) and (9-6-2).]

9-8.1.1 Acoustic Path Length and Angle. The determination of axial flow velocity, V_{ax}, is based on the acoustic path length, l_0, and angle, θ. The error in V_{ax} is in direct proportion to the uncertainty in the acoustic path length and angle. Acoustic path length and angle errors are systematic errors caused by inaccuracies in the initial measurements. The errors vary if there are dimensional changes in the measurement section. In the case of refractive systems, changes in the index of refraction of the materials in the acoustic path by, for example, temperature variations can cause changes in the path length and angle (see Figure 9-5.3.2-1).

Errors in the acoustic path length or angle for nonrefractive systems can be reduced by accurate geometric and acoustic measurements. For flowmeters in which sound energy undergoes refraction, errors in acoustic path length or angle can be reduced by design and/or compensation based on knowledge of the speed of sound in the fluid and intervening materials.

Changes in acoustic path length and angle can be caused by significant temperature or pressure changes and external loading of the meter section. The installation location should be chosen to minimize these effects. In certain applications, changes in acoustic path length and angle that result from temperature or pressure-induced pipe deformation can be compensated for in both the refractive and the nonrefractive systems.

Using crossed paths is particularly useful in field-installed systems. This offers an important advantage where it is difficult to accurately determine the location of the centerline of the pipe to the required degree of accuracy. An example of this would be where the pipe is out-of-round or tapered. It is relatively simple to accurately determine the angle between the crossed paths, even when there is a relatively large uncertainty in the orientation of the acoustic paths relative to the true centerline of the pipe. Thus, errors in V_{ax} caused by the unknown path angles cancel because the angle between the paths is accurately known (see Figure 9-6.2.2-1).

9-8.1.2 Transducer Flow Disturbance. Transducer protrusion into the pipeline, as shown in Figure 9-6.1.2.6-1, can cause two types of errors. The protruding transducer cannot measure a true average velocity all the way along the path because the flow between the transducer and pipe wall will be missed. Because this is usually the lowest velocity in the pipe, the effect of not including this in the line velocity average will be to overestimate this average. On the other hand, the flow streamlines in the vicinity of the transducer tend to increase the angle between the local velocity vector and the transducer, on both upstream and downstream transducers, causing the path velocity estimate to be low. There is also a wake downstream of the upstream transducer. Fortunately, these two effects are in the opposite direction and are not usually important in pipes larger than about 1.2 m (4 ft) in diameter. For smaller size pipes, where relatively large transducers are used or where accuracy requirements are very high, it can be necessary to determine the effect of transducer protrusion experimentally or use a non-protruding transducer design as shown in Figure 9-6.1.2.5-1 or Figure 9-6.1.2.7-1.

9-8.1.3 Transit Time Measurement Errors. Uncertainties in the transit time measurements result from limits in the internal timing accuracy and resolution and lead to a corresponding uncertainty in V_{ax}. Errors in the measurement of transit time can be reduced by the use of stable and accurate high-frequency transducers and by averaging many

individual transit time measurements. Transit time measurements of slow flow speeds require the most resolution from the timing circuit and are the most likely to be susceptible to this type of error.

Transit-time measurement errors from differences between upstream-to-downstream and downstream-to-upstream electronic signal paths can be reduced by using the same detection electronics and transmitter for both.

9-8.2 Signal Detection

Acoustic transit time measurements may be affected by inconsistencies in recognition of the received acoustic signal, which are caused by variations in received signal level or waveform and noise.

Variations in received signal level or waveform can occur as the acoustic properties of the fluid in the measurement section change due to excessive amounts of entrained air, suspended solids, temperature, or pressure or as transducer fouling occurs. These variations may result in uncertainty in determining the transit time, thus causing uncertainty in V_{ax}. The receiving circuits should be designed to prevent use of these distorted signals for the flow rate measurement.

Noise can affect the accuracy of the transit time measurement. Noise sources can be either electrical or acoustic and either external or self-generated. Generally, externally generated electronic or acoustic noise is random with respect to the received signal and can be attenuated by increasing the signal-to-noise ratio of the transmitted signal level.

However, in many cases the most troublesome noise is self-generated acoustic noise. Particularly in refractive systems, the acoustic noise can be synchronized to the received signal and is, therefore, much harder to compensate for in the secondary device. This noise comes from energy being coupled directly into the pipe wall and then to the opposite transducer. The noise generally increases as the level of the transmitted signal increases. The signal-to-noise ratio, in these cases, can be improved by acoustically isolating the transducers from the measurement section by application of damping materials.

9-8.3 Computation and Integration

There is a small error associated with the computations made by the electronic circuits due to the finite limits in processing precision. However, this error will normally be negligible. Computation errors due to electronic malfunction can be reduced by using built-in self-checking features in the processor.

Integration error is the error in the flow measurement that occurs in the computation of the flow from V_{ax}, A, S, and W_i.

9-8.4 Velocity Profile Uncertainties

As part of the meter's internal computation of V_{ax}, assumptions about the flow profile must be made. As seen in Figure 9-8.4-1, there can be a significant difference in the flow profile moving through the measuring section, leading to potential errors in assumptions used to calculate V_{ax}. This error may affect both the linearity and the value of the flow measurement. This is particularly true for single-path meters, where there is potential for as much as a 35% error in flow rate if the meter applies the wrong flow profile characteristics. The single-path ultrasonic meters should not be used in flows that are in the transition zone between laminar and turbulent regimes. Increasing the number of acoustic paths provides the meter with a clearer picture of the flow profile, reducing the amount of assumptions required for a flow rate calculation. The use of a meter with five acoustic paths, as shown at the bottom of Figure 9-8.4-1, enables the determination of the flow regime based on the values of the five individual measurement points, as well as detection and consideration for irregular flow profiles.

Velocity profile variations can be caused by changes in flow rate (both transient and steady state), wall roughness, temperature, viscosity and viscosity change due to temperature, upstream or downstream hydraulic conditions, and transducer projections or cavities. Sufficiently long, straight upstream piping and the absence of upstream and downstream hydraulic effects help to ensure a fully developed and uniform flow profile, reducing the risks of added uncertainty due to flow profile variations.

There is usually a difference between the actual velocity profile and that assumed in the flowmeter's computations. Since most flowmeter computations assume a fully developed velocity profile, errors can be reduced by placing the measurement section as far as possible from bends, valves, tees, transitions, and so on (see para. 9-6.3). These errors can be reduced by using a more accurate model of the actual velocity profile or, in general, by increasing the number of acoustic paths so that the meter is not required to make as many assumptions about the flow profile. Even when the meter section is located 50 or more diameters from an upstream obstruction, there will almost always be a swirl or spiral component to the flow. Therefore, to minimize errors produced by any swirl, the path placement should be symmetrical to the centerline.

Figure 9-8.4-1
Laminar (Blue) and Turbulent (Red) Flow Velocity Profiles and 1-, 2-, 3-, and 5-Beam Acoustic Patch Diagrams

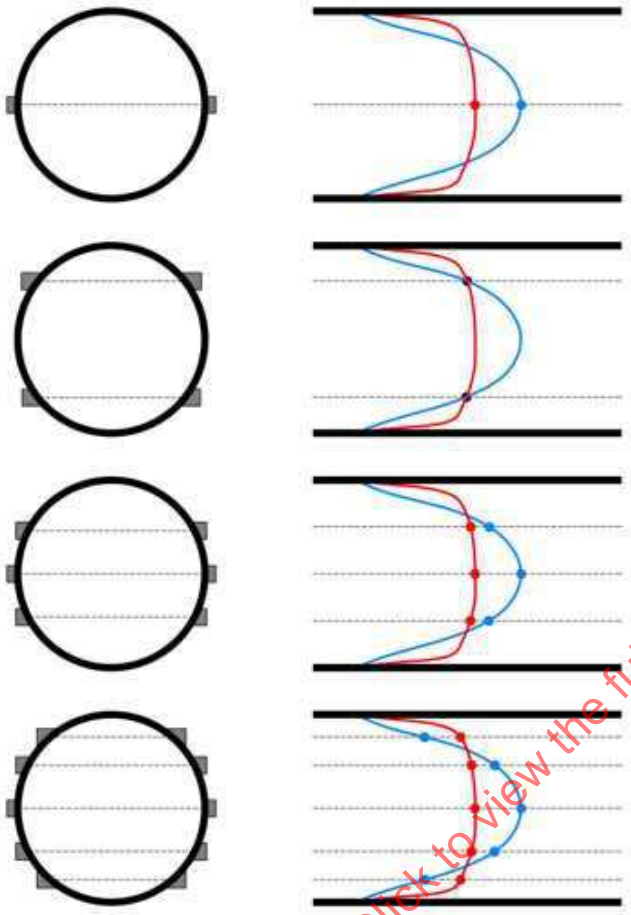

9-8.5 Cross Section Dimensional Errors

Error in the assumed cross-sectional area of the measurement section causes an error in the flow calculations. This error may be from irregular shape, such as out-of-roundness, or by changes from the initial shape caused by temperature, pressure, structural loading, or the formation of deposits or growths, such as algae, in the measurement section. Usually, it is caused by combinations of the preceding conditions.

Cross section dimensional errors can be reduced by choosing a measurement section that has constant dimensions along its length and can be measured accurately. Measurement section dimensional stability is important because changes resulting from corrosion, material buildup, or loss of protective coatings will affect meter accuracy and can require recalibration. Furthermore, it is important that the pipeline not be distorted by mechanical stress (for example, from the pipeline being buried). Also, if temperatures or pressures are expected to be substantially different from reference conditions, it may be necessary to adjust the measured dimensions to compensate for dimensional changes that occur under operating conditions.

In circular pipes, dimensional errors can be reduced by minimizing the effects of out-of-roundness through averaging of radius (not diameter) measurements made at the upstream, middle, and downstream ends of the measurement section.

The measurement section should be inspected periodically to determine if the dimensions have changed and, if so, the meter factor, S_v, should be adjusted appropriately. It is important to remember that the flow rate measured is linearly proportional to the cross-sectional area.

9-8.6 Acoustic Path Location

The acoustic path location is an important contributor to overall flowmeter accuracy. The uncertainty in the position of the acoustic path can cause errors through improper assignment of a weighting factor, W_i, and by causing unnecessary sensitivity of V_{ax} to the velocity profile through nonoptimum placement of transducers.

Errors in acoustic path location can be reduced by accurately determining the acoustic path location for systems in which the transducers are assembled in the field.

9-8.7 Upstream and Downstream Flow Disturbances

Flow disturbances in close proximity to the measuring section of an ultrasonic meter can create uncertainties in the measurement value by distorting the flow profile and creating secondary flows that are not perceived along the acoustic paths. Because the meter makes assumptions that the flow is uniformly developed across the entire cross-sectional area, distortion or asymmetry in the flow profile will result in an additional uncertainty as described in para. 9-8.4. The manufacturer should be consulted for the minimum straight pipe length requirements to avoid flow disturbances.

9-8.8 Proximity to Other Meters

If meters are too close together they may interfere acoustically. This seldom happens in practice because the high frequencies used are attenuated rapidly. However, there can be electrical interference between meters with output cables in close proximity, such as when they run long distances in conduit or in a cable tray. These problems can usually be overcome with proper system and software design and the use of shielded cables.

9-8.9 Equipment Degradation

Performance errors may arise from fouling or physical degradation of the equipment. Equipment design should accommodate changes in component values and process conditions. The equipment should indicate when degradation of flowmeter performance occurs. The probability of error can be reduced considerably by including suitable self-test or diagnostic circuits in the equipment.

While most modern ultrasonic flowmeters automatically monitor meter performance, periodic checks comparing each path's speed of sound measurement to one another and over a historical trend can be a useful tool in identifying potential problems or diagnosing the health of the meter. Consult the manufacturer for appropriate procedures.

Section 10
Tracer Method for Measuring Water Flow

10-1 NOMENCLATURE

Symbols used in Section 10 are included in Tables 2-3-1 and 10-1-1. For any equation that consists of a combination of symbols with units shown in Tables 2-3-1 and 10-1-1, the user must be sure to apply the proper conversion factors.

10-2 INTRODUCTION

This Section covers the measurement of water flow in closed conduits using a tracer dilution method. Fluorescent dyes such as rhodamine B, rhodamine WT, and fluorescein are typically used as tracers. Rhodamine WT was developed specifically as a water tracer and is generally preferred for water flow measurement. Measuring tracer dilution using the constant rate injection method is the only method included in this Supplement.

Dilution techniques offer the following advantages:

(a) independence of geometric or hydraulic quantities (size of pipe)
(b) portable measurement equipment that can be used where other methods are difficult or inappropriate
(c) minimal invasiveness; equipment performance can be measured in situ
(d) the ability to measure large flows [up to 170 m^3/s (6,000 ft^3/sec)] in any conduit size

10-2.1 Applicability

Radioactive tracers are applicable in nuclear power plants where licensing requirements for possession and handling of radioactive materials are standard. The materials should be short-lived to eliminate long-term contamination and exposure problems and the measured concentrations must be corrected for decay to a base reference time. Refer to ASME PTC 6 for further details on the safe and proper use of radioactive tracers.

10-3 CONSTANT RATE INJECTION METHOD

The constant rate injection method begins with the injection of a tracer into a flow at a known constant rate. A sample is taken after the complete mixing of the tracer into the flow. The flow is then measured by determining the tracer concentration of the downstream sample. The dilution method is based on the conservation of mass and the control volume shown in Figure 10-5-1.

The governing equation is

$$q_{v1}C_{m1} + q_vC_{m0} = (q_v + q_{v1})C_{m2} \tag{10-3-1}$$

where

C_{m0} = background mass concentration
C_{m1} = injection mass concentration
C_{m2} = mixed mass concentration
q_v = flow to be measured
q_{v1} = flow of tracer injected

C_{m1} is typically much greater than C_{m2}, sometimes by a factor of 10^7; therefore, eq. (10-3-1) may be simplified to

$$q_v = \frac{q_{v1}C_{m1}}{(C_{m2} - C_{m0})} \tag{10-3-2}$$

Table 10-1-1
Symbols Specifically Applied in Section 10 (in Addition to Symbols in Table 2-3-1)

C_m	Mass concentration	ML^{-3}	kg/m^3	lbm/ft^3
D	Diameter of conduit	L	m	in.
L_m	Length of measuring section (mixing length)	L	m	in.
L_m/D	Mixing distance	Dimensionless	Dimensionless	Dimensionless
F	Fluorescence	Dimensionless	Dimensionless	Dimensionless
n	Fluorescence exponent	$1/\theta$	1/°C	1/°F
x	Maximum percentage variation in concentration across the conduit	Dimensionless	...	...
q_v	Volumetric flow	L^3T^{-1}	m^3/s	ft^3/sec
λ	Resistance of the conduit (friction factor)	Dimensionless	Dimensionless	Dimensionless

GENERAL NOTE: Dimensions:
L = length
M = mass
T = time
θ = thermodynamic temperature

To use this technique, the following conditions must be satisfied:
(a) Sufficient mixing length must exist between injection and sampling points.
(b) The tracer must be injected at a known, constant, and measured rate.
(c) The tracer must have homogeneous concentrations at both injection and sampling points.
(d) The background of the tracer (or other fluorescence) in the measurement stream must be considered in the uncertainty analysis if it is not negligible.
(e) No tracer shall be lost to withdrawal between injection and sampling points.
(f) The observed property of the tracer used in measurement must vary in a known quantitative manner with tracer concentration, and the effect of any chemical reducing agent(s) in the flow stream must be considered in the uncertainty analysis.

10-4 TRACER SELECTION

There are numerous nonradioactive tracers used in water flow studies. These include sodium chloride, rhodamine B, rhodamine WT, and fluorescein. For a material to be used as a water tracer, it must
(a) mix easily with water
(b) require minimal modifications to the system piping for injection and sampling
(c) be detectable at a concentration lower than the highest permissible concentration considering toxicity, corrosion, etc.
(d) not be used in flow-containing substances that mimic the tracer, and background levels must be negligible or constant and measured
(e) be accurately measured at expected concentrations
(f) not react with water flowing in the conduit or with any other substance with which it can react and affect the flow measurement
(g) have low-absorption tendencies (to help prevent the loss of tracer via adherence to suspended and bed materials or absorption by such materials)

10-5 MIXING LENGTH AND MIXING DISTANCE

The mixing length, L_m, is defined as the length of conduit between the injection and sampling points (see Figure 10-5-1). If the mixing length includes fluid losses, the measurement results are valid only if it is possible to show that the mixture is homogenous upstream of the loss zone. The mixing distance, L_m/D, is defined as the shortest distance in which the maximum variation in tracer concentration, across the conduit's cross section, is less than a predetermined value.

10-5.1 Experimental Derivation of Mixing Length

Values of mixing completeness versus mixing distance obtained experimentally for a central injection in an unobstructed straight circular conduit and three other injection configurations are shown in Figure 10-5.1-1.

Figure 10-5-1
Schematic Control Volume

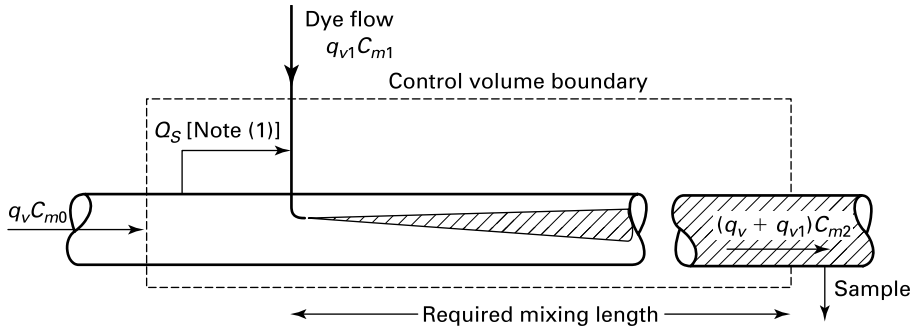

GENERAL NOTE: Used with permission from ASCE.

NOTE: (1) Secondary transport flow, if required.

Figure 10-5.1-1
Experimental Results

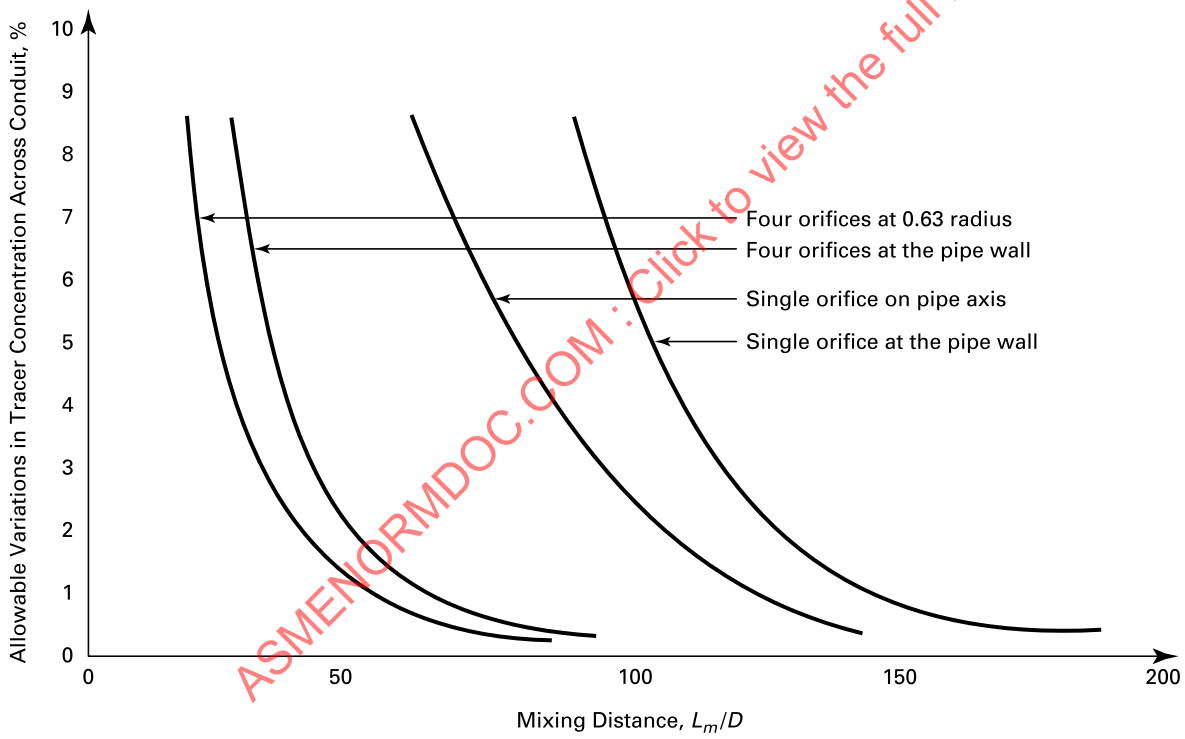

10-5.2 Methods of Reducing the Mixing Distance

Several techniques may be used to reduce the mixing distance. These include ring injection, multiple-orifice injectors, pumps and turbines, and piping bends, valves, or other obstructions in the conduit.

10-5.2.1 Ring Injection. Uniform injection over a ring installed within a conduit, with a radius of 0.63 of the conduit radius, reduces the mixing distance to about one-third of that achieved with a central (axial) injection. See Figure 10-5.1-1.

10-5.2.2 Multiple-Orifice Injectors. When the tracer is injected equally through several orifices spaced across the conduit, the mixing distance can be reduced compared to that associated with a central injector. An example of the reduction in mixing distance that can be achieved using four injectors, equally spaced around the wall of a conduit with a radius of 0.63, is shown in Figure 10-5.1-1.

10-5.2.3 Pumps and Turbines. Injecting the tracer upstream of a pump can effect a considerable reduction in mixing distance. Information on mixed-flow pumps indicates that this type of pump can reduce the mixing distance by about 100 diameters.

10-5.2.4 Bends, Valves, and Other Obstructions. Obstructions in the conduit introduce additional turbulence, which tends to reduce the mixing distance. Quantitative information on these types of mixing promoters is not available, but measuring sections that include these devices are preferred.

10-5.3 Experimental Checking

It is sometimes possible to check experimentally the homogeneity of the mixture in conduits. In practice, this evaluation consists of

(a) checking at the time of the measurement that the mixture is homogeneous by taking samples from at least two points of the measurement cross section.

(b) sampling at another cross section further downstream to determine if any systematic difference between the mean concentrations at the two measurement cross sections occurs. This method also permits verification that the injected tracer was not absorbed in the mixing length either by entrained products in the liquid or by the conduit's walls.

(c) evaluating the stability of concentration of the tracer as indicated during the sampling period as described in para. 10-8.3.

10-6 PROCEDURE

10-6.1 Preparation of the Injection Solution

It is essential for the injected solution to be homogeneous. The homogeneity of the solution can be obtained by vigorous mixing, or by means of a mechanical stirrer, or by a closed-circuit pump. The injection solution should be prepared in a container separate from the supply container using water that was filtered using an appropriate procedure. However, if mixing is carried out in the supply container, the latter shall have sufficient capacity so that it is not necessary to add liquid or tracer during the injection. The solution shall be taken from above the bottom of the container, and every precaution shall be taken to prevent undissolved particles of the tracer from being carried into the injected solution. If the injection is of long duration, provisions shall be made to avoid variation of the solution's concentration with time (e.g., by evaporation under the influence of ambient temperature).

10-6.2 Injection of the Concentrated Solution

The concentrated solution shall be injected into the conduit at a constant rate and for a sufficient time to ensure a constant concentration at the measurement cross section and sufficient averaging time to reduce the random uncertainty of the measurement's mean value. Several devices may be used for the injection of the concentrated solution. For all devices, it must be possible to check that

(a) the injection system is always free from leaks

(b) the injection rate is constant over the duration of the injection

Typically, a variable displacement piston pump with a high pulse rate is used with a constant inlet head to achieve a low injected flow uncertainty.

Any entrained impurities in the solution shall be eliminated because they could partly or totally block the injection circuits.

10-6.3 Measurement of Injected Flow

The accuracy with which the injected flow can be measured depends on the measuring instruments used. The accuracy of the device shall be considered in the estimation of the total uncertainty of flow measurement. Various measuring devices can be used provided they comply with one of the following requirements:

(a) They satisfy a principle directly involved in the definition of the quantity of flow based on the measurement of the basic quantities of mass, length, and time.

(b) They are calibrated in the conditions of use by measuring basic quantities involved in the flow definition (e.g., calibrated capacity method, weighing method).

(c) They are installed and used in conformity with the requirements of a Standard, making it possible to calculate the accuracy obtained.

10-6.4 Samples

Samples shall be taken

(a) from the conduit to verify that the background concentration of tracer in the flow system is constant

(b) from the conduit to determine the tracer concentration in the measuring cross section, to check that the tracer concentration is homogeneous in the sampling cross section, and to check the concentration level

(c) from the injected solution to check the homogeneity of the tracer concentration

(d) from the injected solution to compare the concentration of tracer in the injected solution with the concentration of tracer in the samples taken from the conduit

10-7 FLUOROMETRIC METHOD OF ANALYSIS

Fluorescent substances are those which, when illuminated, emit radiation having wavelengths longer than those of the incident light. Fluorometric analysis is based on comparing, with a fluorometer, the fluorescence obtained from samples of known dilution ratios (control solutions). This is the most widely used tracer technique for water flow measurement and is also called the dye-dilution method. With the dye-dilution method, a fluorescent dye is injected at a known constant rate, and downstream samples are taken in accordance with guidelines given in this Section. A fluorometer is used to measure the downstream concentration of dye in the sample. Equation (10-3-2) is then used to calculate the flow of water in the conduit.

10-7.1 Fluorometer Description

The fluorometer operates by directing a beam of light at a select wavelength that causes the tracer in the sample to fluoresce. This wavelength is determined by a color filter placed over the light source. A second filter is used to absorb the transmitted beam and pass only the fluorescent light. The intensity of the light is linearly proportional to the concentration of tracer in the sample.

10-7.2 Factors Affecting Fluorescence

Several factors can affect the fluorescence of the sample, including temperature, pH, tracer quenching, and air bubbles in the sample stream. Some of these factors have a significant effect. Cooler temperatures typically increase the fluorescence. For example, a 1°C (1.8°F) decrease in temperature raises the fluorescence by 2.6% in some dyes. Likewise, a 1°C (1.8°F) increase in temperature can lower the fluorescence by 2.6%. It is recommended that the fluorometer be acclimated and calibrated to the temperature of the water being measured to within 1°C (1.8°F). Temperature correction curves must be used when measurements are taken at varying temperatures. Correction equations have been developed for various dyes and are given in eq. (10-7-1) and Table 10-7.2-1.

Table 10-7.2-1
Temperature Exponents for Tracer Dyes

Dye	n, 1/°C (1/°F)
Rhodamine WT	−0.0267 (−0.01483)
Pontacyl pink	−0.0285 (−0.01583)
Fluorescein	−0.0036 (−0.0020)
Acid yellow 7	−0.00462 (−0.00257)

$$F_s = F\exp[n(T - T_s)] \quad (10\text{-}7\text{-}1)$$

where

F = fluorescence reading at measured temperature
F_s = fluorescence at calibration temperature, T
T = temperature of sample
T_s = calibration temperature

If the water flow to be measured is highly acidic, a decrease in fluorescence may be observed. However, one of the most commonly used dyes, rhodamine WT, is stable in the pH range of 5 to 10. Fluorescence may also be affected by other chemicals in the measurement stream, which act by

(a) absorbing the exciting light
(b) absorbing the light emitted by the tracer
(c) reducing the excited state energy
(d) chemically altering the fluorescent compound

Air bubbles in the sample tend to scatter the exciting light within the fluorometer measurement chamber. As a result, the instrument will indicate higher than actual fluorescent intensity. This effect can be minimized by using higher dye concentrations.

10-7.3 Fluorometer Calibration

The signal generated by the fluorometer is proportional to the fluorescent intensity of the sample. Therefore, the development of a calibration curve is necessary to relate fluorescence to tracer concentration. This is accomplished by creating a set of known concentration standards. The standards are produced by diluting the stock, or injected concentration, C_{m1}, by a precise amount. Normally, a series of dilution standards are selected to bracket the expected test concentration, C_{m2}. A linear relationship exists for concentrations up to 0.5 ppm (parts per million) of rhodamine WT. Examples of typical calibration curves are shown in Figure 10-7.3-1. Only calibrations in the linear range should be used; the two curves on the right are unacceptable. It is recommended that a calibration be performed before and after each series of flow tests to verify the stability of the fluorometer.

10-8 FLOW TEST SETUP

Although various testing setups and methods can be used, the basic theory and guidelines outlined in this Section should be followed. Paragraphs 10-8.1 through 10-8.3 give an example of a typical testing setup and procedure for flow measurement in a closed conduit.

10-8.1 Tracer Injection Setup

The tracer injection system is shown in Figure 10-8.1-1. The injection rate, q_{v1}, is measured by timing the delivery of a precise volume of tracer dye from a calibrated burette. A metering pump delivers the dye to a mixing chamber where a small amount of water is added to carry the dye to the injection point in the conduit.

Other methods of injection include using a calibrated injection pump or a weighing scale to measure injection rate on a mass per time basis.

Figure 10-7.3-1
Example Calibration Curves

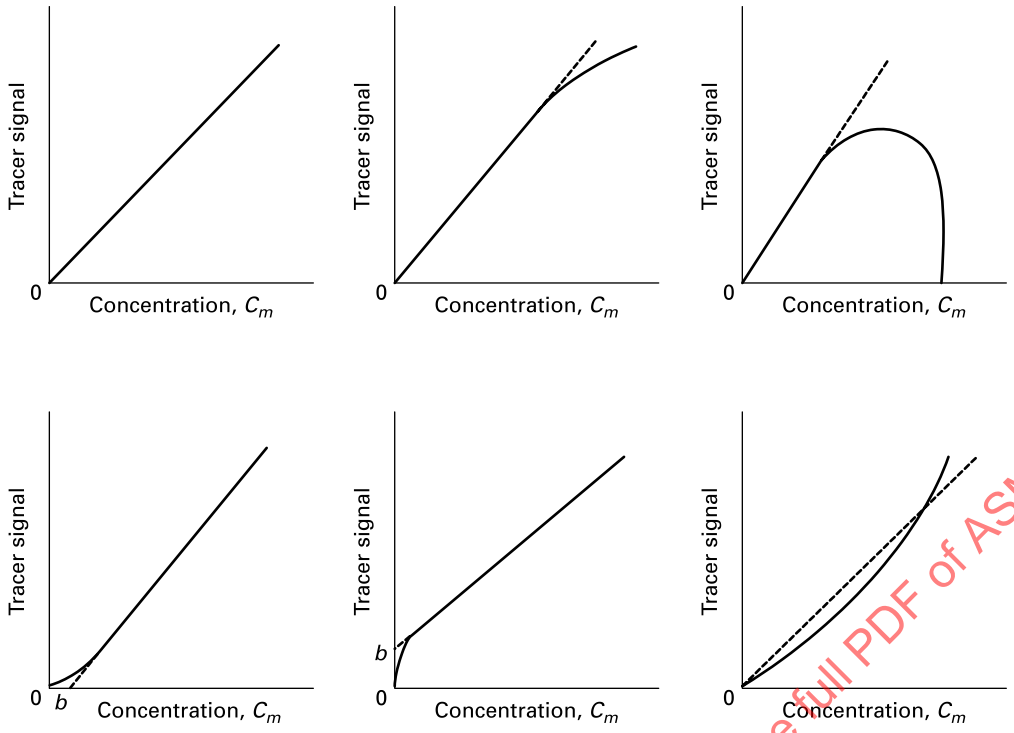

GENERAL NOTE: Adapted from Wilson (1986).

Figure 10-8.1-1
Tracer Injection Schematic

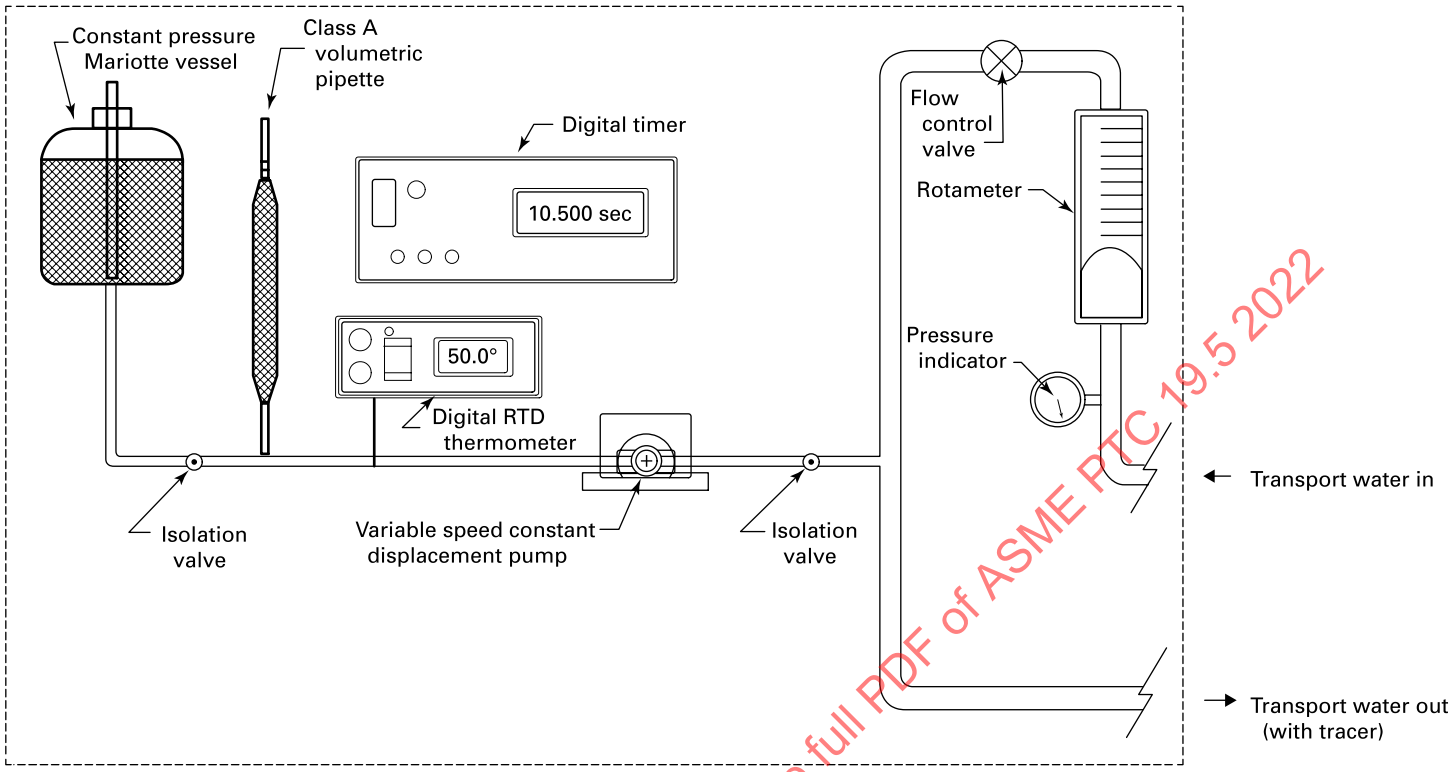

10-8.2 Sampling Methods

The downstream sampling system for real-time flow-through analysis is shown in Figure 10-8.2-1. The continuous sample first passes through a chamber to separate air bubbles from the sample stream. The sample then passes through the fluorometer and the fluorescent intensity is recorded.

The sample temperature is measured within the fluorometer so that correction factors can be applied. The sample stream can be discharged into a drain or returned to the conduit.

10-8.3 Flow-Through Tracer Flow Signal

A typical flow test will take between 10 min and 20 min. If a plot is constructed of dye concentration versus time, a trend similar to Figure 10-8.3-1 should be observed.

An average signal is recorded during the plateau period of the concentration curve. This value is corrected for temperature and the background of tracer in the stream. The concentration, C_2, is determined from the previously established calibration curve.

Figure 10-8.2-1
Sampling System

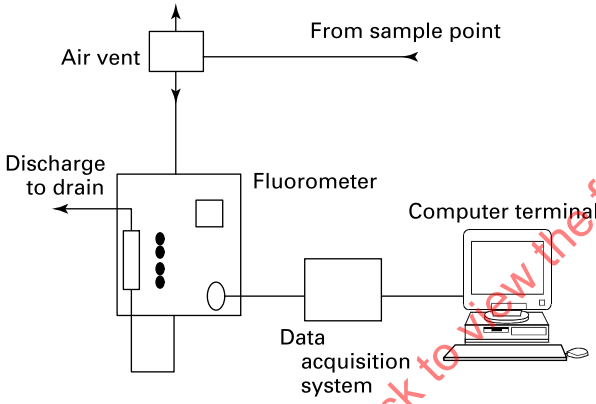

Figure 10-8.3-1
Fluorometer Signal Versus Time

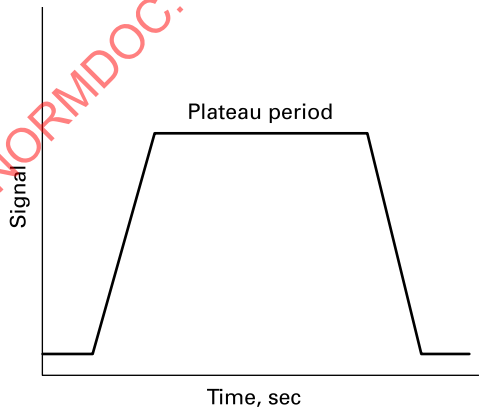

10-9 UNCERTAINTY

The determination of flow in a conduit by tracer methods is subject to uncertainties related either to systematic errors in the measuring apparatus or the measuring process used or to random error obtained by variations in the flow system or the measuring equipment.

10-9.1 Systematic Errors

In the measurement of flow with tracers, a type of systematic error can exist in which the direction may be defined but the magnitude cannot be estimated. Phenomena related to the dissolution removal or precipitation of tracer from the water results in the loss or transformation of the injected tracer and subsequently this type of error. In some cases, the injected tracer may react with the water in the conduit or with other substances between the injection and sampling points. When using dilution methods, the systematic error caused by such reactions leads to an overestimation of the flow due to loss of tracer. This overestimation can be reduced to insignificance by selection of a suitable nonreactive tracer and the use of appropriate injection, detection, sampling, and analysis.

10-9.2 Example of Uncertainty Analysis — Fluorescent Tracer

Elementary error sources in the tracer method include the injected flow, concentration measurement, mixing, and tracer losses. Tracer loss can be caused by reaction of the tracer or physical loss from the flow before full mixing occurs. With proper care and technique, this error source may be eliminated and will not contribute to overall uncertainty. If fluorometer calibration samples are constructed with the tracer to be injected, its absolute concentration does not contribute to overall uncertainty.

Injected flow may be measured by volumetric or gravimetric methods that carry elementary error sources, including time and volume or weight. Since mass concentration of tracer is required, density differences between the injected tracer and the calibration samples must be considered when estimating the uncertainty in the injected flow.

Tracer concentration is usually measured using a fluorometer acting as a comparator. The fluorometer must be calibrated before and after the measurements by using concentration samples constructed by the serial dilution technique with the injection solution and water being tested. Before and after calibrations are used to indicate any changes in water quality affecting the concentration measurement as well as to document the stability of the fluorometer. The concentration measurement includes the elementary error sources due to the preparation of the calibration solutions, calibration curves, and data acquisition. Differences in temperature of the sample from that of the calibration solutions shall be mathematically corrected and considered when estimating the uncertainty.

Table 10-9.2-1 includes typical values for the elementary error sources and assumes no tracer loss and no changes of water quality during the test. This example includes typical systematic and random standard uncertainties, each at a confidence interval of 68% (1 standard deviation).

Table 10-9.2-1
Typical Uncertainties Using a Fluorescent Tracer

Elementary Error Source	Systematic Standard Uncertainty	Random Standard Uncertainty
Injected flow	0.54%	0.34%
Fluorometer calibration	0.25%	0.26%
Concentration measurement	0.65%	0.34%
Mixing	0.55%	0.00%
Tracer loss	0.00%	0.00%
Root sum square	1.039%	0.547%
Combined standard uncertainty	**1.17%** [Note (1)]	
Expanded uncertainty	**2.34%** [Note (2)]	

NOTES:

(1) The combined standard uncertainty is calculated from the root sum square (RSS) combination of the systematic and random uncertainties as follows:

$$\text{combined standard uncertainty, } u = \sqrt{(1.039\%)^2 + (0.547\%)^2} = 1.17\%$$

(2) The expanded uncertainty is at the 95% confidence interval (2 times the combined standard uncertainty).

$$\text{expanded uncertainty, } U = 2u = 2 \times 1.17\% = 2.35\%$$

10-10 REFERENCE

Wilson, J. F., Jr., Cobb, E. D., Kilpatrick, F. A. (1984). "Fluorometric procedures for dye tracing. [Contains glossary]." Open File Report 84–234. U.S. Geological Survey.

The following sources were not cited directly but have been consulted in the preparation of this section.

Field Measurements. Alden Research Laboratory.
ISO 2975/I:1974. Measurement of water flow in closed conduits, tracer methods — Part I: General. International Organization for Standardization.
ISO 2975/II:1975. Measurement of water flow in closed conduits, tracer methods — Part II: Constant rate injection method using nonradioactive tracers. International Organization for Standardization.
Nystrom, J. B., and Hecker, G. E. (1987). "Tracer Dilution Flow Measurement Application to Short Penstock Length." Water Power '87. American Society of Civil Engineers.
Smart, P. L., and Laidlaw, I. M. S. (1977). "An evaluation of some fluorescent dyes for water tracing." Water Resources Research, 13(1), 15–33.

Section 11
Vortex Shedding Meters

11-1 NOMENCLATURE

Symbols used in Section 11 are included in Tables 2-3-1 and 11-1-1. For any equation that consists of a combination of symbols with units shown in Tables 2-3-1 and 11-1-1, the user must be sure to apply the proper conversion factors.

11-2 PRINCIPLE OF MEASUREMENT

Vortex meters are flow measurement devices that use the phenomena of vortex shedding from a bluff body to measure the volumetric flow of a fluid in a pipe. When a bluff body is placed in a pipe in which fluid is flowing, a boundary layer forms and grows along the surface of the bluff body. Due to insufficient momentum and an adverse pressure gradient, separation occurs and an inherently unstable shear layer is formed. This shear layer rolls up into vortices that shed alternately from the sides of the body and propagate downstream. This series of vortices is called a von Karman-like vortex sheet (see Figure 11-2-1). The frequency at which vortices are shed is directly proportional to the fluid velocity. Since the shedding process is repeatable, it can be used to measure flow.

Sensors are used to detect the shedding vortices to convert the pressure or velocity variations associated with the vortices into electrical signals. One shedding cycle corresponds to the generation of two vortices: one from one side of the bluff body, followed by another from the bluff body's other side. The electrical signal generated by a flowmeter's vortex sensor varies at the shedding frequency, f, one cycle of which corresponds to the shedding of a pair of vortices. The Strouhal number, St, relates the frequency, f, of generated vortices, the bluff body characteristic dimension, d, and the fluid velocity, V.

$$\mathrm{St} = f \times d/V \tag{11-2-1}$$

For certain bluff shapes, the Strouhal number remains essentially constant within a large range of Reynolds numbers. This means that the Strouhal number is independent of density, pressure, viscosity, and other physical parameters. Given this behavior, the flow velocity is directly proportional to the frequency at which the vortices are being shed. By taking into

Table 11-1-1
Symbols Specifically Applied in Section 11 (in Addition to Symbols in Table 2-3-1)

Symbol	Description	Dimensions [Note (1)]	Units	
			SI	U.S. Customary
d	Width of bluff body perpendicular to the flow	L	m	ft
f	Frequency	T^{-1}	Hz	1/sec
K	K-factor	L^{-3}	m^{-3}	ft^{-3}
St	Strouhal number	Dimensionless	Dimensionless	Dimensionless
V	Average fluid velocity	LT^{-1}	m/s	ft/sec
q_v	Volumetric flow rate	L^3T^{-1}	L/s	gal/min
α	Thermal expansion coefficient	θ^{-1}	1/°C	1/°F
ρ_f	Density at flowing conditions	ML^{-3}	kg/m^3	lbm/ft^3
ρ_b	Density at base conditions	ML^{-3}	kg/m^3	lbm/ft^3

NOTE: (1) Dimensions:
L = length
M = mass
T = time
θ = thermodynamic temperature

Figure 11-2-1
Vortex Formation

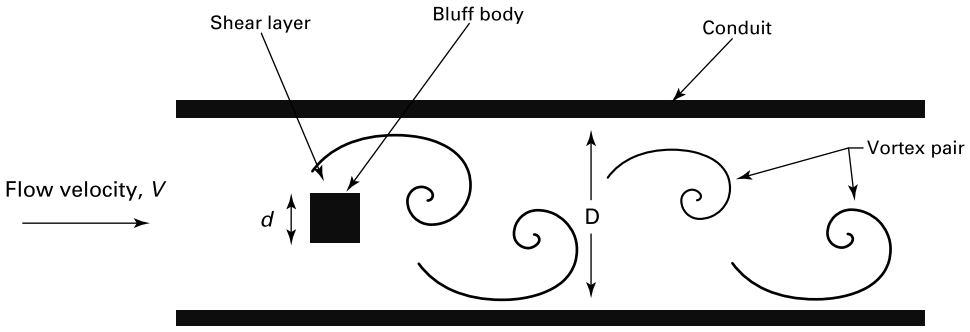

account constant meter geometry, the Strouhal number can be converted to a K-factor, K, and the volumetric flow can be calculated from this K-factor.

$$q_v = f/K \tag{11-2-2}$$

When the density at flowing temperature and pressure is known, the mass flow, q_m [see eq. (11-2-3)], and the volumetric flow at base conditions, i.e., the standard volume flow, q_v [see eq. (11-2-4)], can be determined.

$$q_m = \rho_f \times (f/K) \tag{11-2-3}$$

$$q_v = (\rho_f/\rho_b) \times f/K \tag{11-2-4}$$

For application of these equations, the user shall follow subsections 11-3 and 11-4.

11-3 FLOWMETER DESCRIPTIONS

11-3.1 Physical Components

The vortex shedding flowmeter consists of two elements, the flow tube and the transmitter.

11-3.2 Flow Tube

The flow tube is made up of the meter's body, the bluff bodies, and the sensor.

The meter's body is typically available in two styles

(a) a flanged version that bolts directly to the flanges on the pipeline

(b) a wafer version that is clamped between two adjacent pipeline flanges via bolts

The bluff body is the shedding element positioned in the cross section of the meter body. Its shape and dimensions and the ratio of the frontal area in relation to the open area in the meter body cross section influence the linearity of the K-factor. Figure 11-2-1 shows the bluff body as having a square cross section, but that is not intended to imply a preferred shape.

The sensor detects the shedding vortices (see subsection 11-5). Sensor technology and location vary with each flowmeter's design. The most common methods used in sensing the vortices include piezoelectric-based pressure or force sensors, capacitive sensors, and acoustic-style sensors.

11-3.3 Transmitter

The electronic transmitter processes the raw input frequency signals and provides usable output signals. This output can be analog 4-20mA analog output, pulse output, or a digital output such as HART (Highway Addressable Remote Transducer), Foundation Fieldbus, etc.

11-3.4 Equipment Markings

Meters shall be marked by the manufacturer to identify the manufacturer, serial number, pressure rating, allowable temperature range, mean K-factor or meter factor, and hazardous location certification, if any. The direction of flow shall be indicated by the manufacturer permanently on the meter's body.

11-4 APPLICATION CONSIDERATIONS

Primary considerations in vortex meter measurement are sizing, flow influences, and safety.

11-4.1 Sizing

The meter should be sized according to the desired flow range rather than the nominal pipe size. Proper vortex meter sizing is critical to ensure measurement accuracy and commonly results in the measurement section diameter being smaller than the nominal line pipe size. The flowmeter's size shall be selected such that the expected flows fall between the maximum and minimum flows that provide the required uncertainty.

11-4.1.1 Maximum Flow. The maximum flow for a vortex meter can be determined by the structural limits of the meter, the pressure drop at the shedder bar, or the maximum "accurate" velocity specified by the vendor.

Meter manufacturers provide a series of upper velocity limits. Manufacturers may specify an upper velocity limit as a function of fluid density. This is usually for structural integrity relating to the maximum stress caused by vortex shedding that the sensor or meter body is able to withstand. For liquid flows, the maximum flow limit is generally set for pressure drop. Pressure loss increases with flow; as a result, the meter has a maximum velocity due to cavitation for any given pressure. Also, most meters have a maximum velocity for which an analog current output may be obtained.

11-4.1.2 Minimum Flow. The minimum volumetric flow is determined by the manufacturer's recommended limits. The manufacturer specifies recommended measurement limits based on the minimum measurable and minimum "accurate" flows. Minimum measurable flow can be useful for start-up operations or when having a less accurate indication of flow is useful. Minimum "accurate" flow is useful for testing where accuracy is important. The transmitter provides a means of configuring a low-flow cutoff for the output of the meter based on these recommendations or other specific applicable requirements. See para. 11-4.1.2.3.

Manufacturers generally provide sizing programs or published equations to calculate the minimum measurable flow and minimum "accurate" flows.

11-4.1.2.1 Minimum Measurable Flow. The minimum measurable flow, V_{min}, is the rate at which the force exerted on the sensor is too small to generate a signal strong enough for the meter to reliably differentiate between the flowing signal and noise. This limit is a function of the fluid's momentum and therefore is described by the following equation, where C is a manufacturer-specified value:

$$q_{v,min} = \frac{\sqrt{C}}{\rho} \tag{11-3-1}$$

Generally, this equation will yield values around 0.3048 m/s (1 ft/sec) in liquid and 3.048 m/s (10 ft/sec) in gases. The range of values in gases will be higher due to the wider range of densities seen in gas flows as compared to liquids.

11-4.1.2.2 Minimum "Accurate" Flow. The minimum "accurate" flow is the lowest flow at which the meter reads at the specified accuracy. This is generally expressed in terms of Reynolds number. Generally, the minimum accurate flow will be near Re = 20,000. A specific meter's design and size may have accuracy limits above or below that number. Manufacturers may have recommendations for use of the meter at lower Reynolds numbers.

11-4.1.2.3 Low-Flow Cutoff. The meter will have a low flow cut off (LFC). This is a configurable parameter that defines the velocity, or volumetric flow, below which the meter will read zero regardless of the actual flow in the pipe. This value is generally configured to be at or above the minimum measurable flow. It can also be programmed to the minimum accurate flow or, in a high-noise environment, to a higher flow that increases noise rejection. The meter manufacturer's literature should be consulted for the method by which the LFC is programmed.

11-4.2 Process Influences

A number of flowing process influences can affect measurement of temperature, pressure, density, and composition, etc. (see paras. 11-4.2.1 through 11-4.2.4).

11-4.2.1 Process Effect of Thermal Expansion on the Meter. Measurement accuracy is directly related to K-factor uncertainty. Flowing temperatures that differ significantly from those during calibration can affect the geometry of the flow tube and hence the K-factor of the meter. When the bluff body and the meter body are made of the same material, the change in K-factor for a given change in temperature is estimated by

$$K = K_0[1–3\alpha(T_f – T_0)] \tag{11-3-2}$$

where

K = flowing K-factor
K_0 = K-factor at calibration
T_0 = temperature during calibration
T_f = flowing temperature
α = linear thermal expansion coefficient of the meter's material

Pipe-pressure effects on the K-factor by expansion are generally negligible, except in high-pressure applications. The manufacturer should be consulted for information and relevant correction procedures for temperature and pressure effects.

11-4.2.2 Process Effect on Range. The range of a vortex meter generally depends on the K-factor, fluid density, and Reynolds number. From a practical viewpoint, the K-factor, as described above, depends only on the flowing temperature. The fluid density depends on its temperature and pressure. The Reynolds number is a function of geometry, fluid density, and fluid viscosity, and hence depends on temperature and pressure. The manufacturer should be consulted for specific information regarding these effects.

11-4.2.3 Flow. The fluid stream should be steady or slowly varying. Pulsations in flow or pressure may affect flow measurement.

11-4.2.4 Flashing and Cavitation. Localized reduction of pressure occurs when the fluid velocity is increased by the reduced cross section around the bluff body of the meter. In liquids, this can lead to flashing and cavitation. Operation of the meter under conditions of flashing or cavitation, or both, is beyond the scope of this Standard.

NOTE: Flashing and cavitation can lead to measurement errors, structural damage, or both.

To avoid flashing and cavitation in low vapor-pressure fluids, the downstream pressure after recovery must be equal to or greater than $P_{d\min}$ of eq. (11-4-3) or eq. (11-4-4).

In the absence of manufacturer's recommendations, the numerical value of the minimum back pressure at the outlet of the meter can be calculated by eq. (11-4-3) or eq. (11-4-4), whichever is less. This calculated back pressure has proven to be adequate for most applications, and it could be conservative for some applications.

$$P_{d\min} = 2.8 \times \Delta P + 1.25 \times P_{\text{vap}} \tag{11-4-3}$$

or

$$P_{d\min} = (3 + P_{\text{vap}}) \text{ in bar} \tag{11-4-4}$$

where

P_{dmin} = minimum allowable downstream pressure after recovery
P_{vap} = vapor pressure of the liquid at the flowing temperature
ΔP = pressure drop through the meter at the maximum operating flow

Equation (11-4-3) is useful for all units of measure, though the comparison to eq. (11-4-4) requires a unit conversion for a meaningful comparison.

11-4.3 Safety

11-4.3.1 Mechanical. Since vortex flowmeters are an integral part of the process piping (in-line instrumentation), it is essential that the instrument be designed and manufactured to meet or exceed industry standards for piping codes. Requirements for specific location, piping codes, material traceability, cleaning requirements, nondestructive evaluation, etc., shall be the responsibility of the user.

11-4.3.2 Electrical. The water tightness and hazardous area certification shall be suitable for the intended location.

11-5 INSTALLATION

Adjacent piping, fluid-flow disturbances, flowmeter orientation, and location can affect flowmeter performance. The manufacturer's installation instructions shall be consulted regarding installation. Paragraphs 11-5.1 through 11-5.4 discuss some of the factors to consider.

11-5.1 Adjacent Piping

A vortex meter is sensitive to distorted velocity profiles and swirl, including those caused by changes in pipe size or schedule and by flow through pipe fittings, valves, and other process instrumentation or control elements. Procedures for eliminating these effects are as follows:

(a) The diameter of the adjacent pipe should be the same nominal diameter as the flowmeter. Internal pipe diameter should be the same as that of the pipe used in calibration unless appropriate corrections are applied. Some meters have pipe diameter corrections built into their software.

(b) The flowmeter shall be mounted concentric with the pipe according to the manufacturer's recommendations.

(c) Gaskets shall not protrude inside the pipe since they can also shed vortices. Flush or recessed gaskets are required.

(d) The flowmeter should be mounted with straight runs of pipe upstream and downstream. The straight runs shall be free of changes in pipe size or schedule, and of pipe fittings, valves, and other internal obstructions. The minimum lengths of straight pipe required to obtain the specified accuracy at operating conditions differ depending on the flowmeter's construction and the nature of the piping configuration. When there is an unavoidable upstream disturbance, the manufacturers may be able to provide an expected calibration shift for each particular upstream disturbance.

(e) If more than one pipe section is used within the minimum length of straight pipe, the joined pipe should be straight, with minimal misalignment. Welding rings should be avoided within the required number of straight pipe lengths.

(f) The required length of straight pipe may be reduced through the use of an appropriate flow conditioner; otherwise, one must accept higher uncertainties. The manufacturer should be consulted regarding the use of flow conditioners and their effect on meter's uncertainty. This includes the type of flow conditioner, its sizing, and its location relative to the flowmeter (see subsection 11-7).

(g) The location of additional process measurement devices external to the meter (e.g., those that measure pressure, temperature, or density) can adversely affect the performance of a vortex flowmeter and should be located downstream from the flowmeter.

(h) To satisfy the minimum measurable flow requirement, a meter size smaller than the pipe size may have to be used. Pipe reducers may be used upstream and downstream to install such flowmeters. When pipe reducers are installed without sufficient downstream straight lengths of pipe, adjustment of the K-factor and/or to the uncertainty shall be required. (See Table 11-7.3-1 for guidance.)

(i) In some applications, it may be desirable to inspect or clean the flowmeter periodically. If a bypass is installed to facilitate this, the fittings shall be ahead of the upstream straight length of pipe or flow conditioner and beyond the downstream straight section.

(j) When a particular meter installation is expected to deviate from the manufacturer's recommendations, the user may desire to perform in situ calibration.

11-5.2 Flowmeter Orientation

Flowmeters should be installed with the orientation recommended by the manufacturer. Proper orientation of the flowmeter in the pipe may depend on the nature of the fluid. The orientation of the meter should take into consideration the temperature of the stream being measured and its effect on the transmitter.

In liquid flow measurement, the pipe must be flowing full. One way to ensure this is to install the meter in a vertical pipe with the flow upward. Review liquid flowmeter locations during design and avoid installations in horizontal lines located at the highest point in the piping, unless assured that the line will remain full of liquid at all times.

11-5.3 Flowmeter Location

11-5.3.1 Proper Support. The flowmeter shall be supported to reduce any effects of vibration and pipe stress. Good piping support is important to good vortex meter operation.

11-5.3.2 Noise and Interference. Common mode electrical noise can interfere with the measurement. RFI, electromagnetic interference (EMI), improper grounding (earthing), and insufficient signal shielding can also interfere with the measurement. In some cases, it might not be possible to check the noise in the output signal with no flow. The manufacturer should be contacted for advice if it is suspected that any of these noise levels is high enough to cause an error.

Figure 11-5.5-1
Locations of Pressure and Temperature Measurements

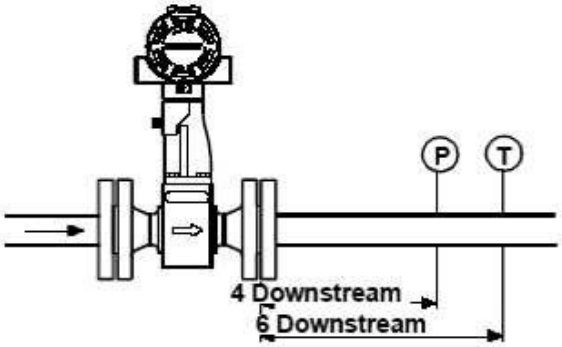

11-5.3.3 Bypass. In applications where the process cannot be shut down for maintenance, a bypass may be installed. In some cases, a meter can be purchased with an online replaceable sensor. In these cases, a bypass might not be required.

11-5.4 New Installations

For new installations, the pipeline shall be cleaned to remove any collection of welding beads, rust particles, or other pipeline debris. The flowmeter should be removed for cleaning.

11-5.5 Complementary Measurements

For gas or steam flows where mass flow is the desired quantity to be measured, pressure and temperature will need to be measured to calculate density and mass flow [see eq. (11-2-3)]. Pressure and temperature should be measured downstream of the meter. The pressure should be measured between 3 and 5 diameters downstream, and the temperature sensor 2 diameters downstream of the pressure to ensure that there is no influence from the temperature probe on the pressure measurement. See Figure 11-5.5-1 for the locations of pressure and temperature measurements.

11-6 OPERATION

Flowmeters shall be operated within the manufacturer's recommended operating limits to achieve the stated uncertainty and normal service life.

The manufacturer's recommended startup procedures should be followed to avoid damage to the bluff bodies or sensor (s) by over-range, water hammer, etc.

11-7 CALIBRATION AND UNCERTAINTY

The meter manufacturer shall calibrate the meter to determine the meter's mean K-factor. This mean K-factor shall be marked on the meter. The manufacturer shall provide expected meter uncertainty under stated reference conditions as well as a certificate of calibration. This process should be in keeping with the practices outlined in ASME PTC 19.1.

11-7.1 Calibration Methods

The mean K-factor is established by flow calibration with a suitable fluid. All calibrations should be performed according to acceptable standards. For gas flows, the reference flow measurement device is usually a transfer device, a volumetric tank with pressure and temperature corrections, or critical flow nozzles. For liquid flows, transfer, weighing, or a volumetric technique is used. See Figure 11-7.1-1.

Vortex meter calibrations are characterized by the shedding cycles per unit volume. This value is independent of fluid type, provided the Reynolds number is above the minimum set by the manufacturer. A great deal of data and historical use supports the use of vortex meters and gas and steam applications using K-factors generated with water calibrations. Calibrating a vortex flowmeter with gas will lead to additional uncertainty because the density calculation adds to the overall uncertainty and has to be taken into account for the vortex flowmeter. For reduced uncertainty, a vortex flowmeter should be calibrated with liquid. See subsection 11-8.

Figure 11-7.1-1
Illustration of a K-Factor Curve

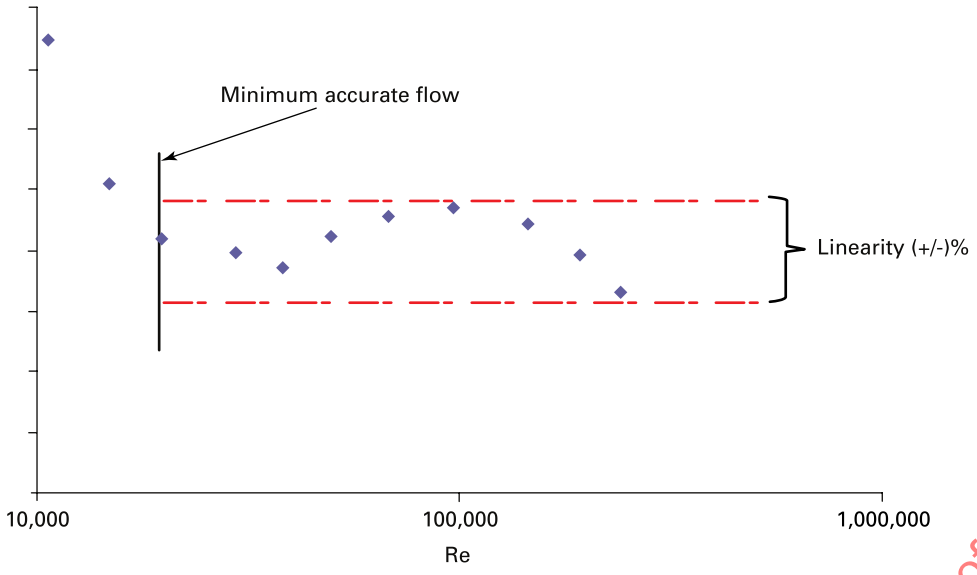

11-7.2 Mean K-Factor Calculation and Uncertainty

Calibration data should be provided that includes calibration fluid, flow rate, Reynolds number, K-factor, and deviation from mean K-factor for each calibration point. A K-factor for each flow is calculated. From these, the mean K-factor is calculated as follows.

The mean K-factor, K_{mean}, is typically defined by

$$K_{mean} = \frac{K_{max} + K_{min}}{2} \quad (11\text{-}7\text{-}1)$$

where

K_{max} = the maximum K-factor over a designated range
K_{min} = the minimum K-factor over the designated range

Typical systematic uncertainties for gas flows are 1% and for liquid flows, 0.75%. These values may vary across the spectrum of manufacturers.

After calibration, the K-factor shall not be changed unless a new calibration is conducted.

The meter may also be lab calibrated per Mandatory Appendix I.

11-7.3 Installation Influence on Uncertainty

All commercially available vortex meters use proprietary shedder bar and sensor designs. For this reason, the additional uncertainty from installations where the flow profile is not fully developed turbulent flow may be different for each design of meter. Consequently, users should check with manufacturers to determine the impact of piping on any particular design of vortex meter. Table 11-7.3-1 lists a minimum recommended upstream length from a disturbance to ensure less than 0.5% additional uncertainty due to installation issues.

Some vendors may provide more precise guidance for their particular geometry of shedder bar and sensor. Guidance of this sort should only be used with that particular type of meter. Testing with different types of shedder bar designs with the same disturbance, the same fluid, and the same Reynolds number show variations in the added uncertainty of several percent. It may be possible to use certain meter designs with upstream distances shorter than those shown in Table 11-7.3-1; if data exists showing that the meter design has a lower additional uncertainty, then that data should take precedence over Table 11-7.3-1. In many cases, a flow conditioner will significantly decrease the impact of upstream disturbances. Meter manufacturers should be consulted about the impact of flow conditioners.

Table 11-7.3-1
Recommended Distance From Disturbance for Less Than 0.5% Increase in Uncertainty

Location on Pipe Assembly	Distance, in Pipe Diameter, *D*, Required for Less Than 0.5% Impact
Single elbow	17
Double elbow in plane	12
Double elbow out of plane	43
Reducer	14
Expander	16
Gate valve 100% open	5
Gate valve 50% closed	16

Generally, there should be at least 40 pipe diameters, or 40*D*, of straight run located upstream of a meter to have no impact from piping disturbances. However, requirements may differ by manufacturer. In some cases, a meter may need more upstream length than that. In cases where data are not available from the manufacturer, and the meter is used with less than the recommended 40*D* upstream pipe length but greater than the value in Table 11-7.3-1, add 0.5% to the uncertainty. If the upstream pipe lengths are less than those listed in Table 11-7.3-1 and data are not available from the manufacturer, or from independent testing, add 2.0% to the uncertainty.

11-7.4 Measurement Uncertainty Examples

Uncertainty values may vary by manufacturer *K*-factor, but users should get the necessary data to verify the uncertainty. Other factors that can affect uncertainty include the fluid temperature, fluid pressure, and, in the case of analog output, the output type being monitored. This Section presents how some of these factors contribute to overall measurement uncertainty for volumetric and mass flow measurements.

For digital vortex meters using an analog output, an additional uncertainty that is a function of the analog span is added to the uncertainty. This is generally in the range of 0.025% of span. For example, the total measurement uncertainty for a 40 mm (1½ in.) vortex meter measuring water in a pipe with 40*D* of straight pipe upstream of the meter at 1.577 L/s (25 gal/min) with a K-factor uncertainty of 0.75% and a 4-20mA upper range value for the analog output of 6.30902 L/s (100 gal/min) would be summarized as shown in Table 11-7.4-1.

Tables 11-7.4-1 through 11-7.4-3 show the systematic uncertainties at 95% confidence level. During a test run, the random standard uncertainty must be determined, multiplied by the Student's *t* value (typically 2 for a test run), and combined with the systematic uncertainty by root sum square to determine the expanded uncertainty (the overall uncertainty at 95% confidence level).

For some applications, it may be impossible to get the recommended upstream straight pipe length. An example is a case where there is an elbow upstream of the meter at 20*D* and the manufacturer states that the uncertainty is increased by 0.30%. Using the same application data as above with the reduced upstream pipe length, the calculation of uncertainty is shown in Table 11-7.4-2.

For applications where mass flow of a gas or super-heated steam is required and pressure and temperature measurements are available to calculate fluid density, the uncertainty will be the root sum square of the uncertainty of the vortex meter, pressure sensor, and temperature sensor. As an example, using uncertainties of 1% for the flowmeter, 0.05% for the pressure, and 0.1% for temperature, the overall measurement uncertainty is shown in Table 11-7.4-3.

While values for each installation will vary, the uncertainty of the vortex meter will most often be the dominant portion of the uncertainty calculation. The analog output, if used, would be added into the vortex meter uncertainty in the manner shown in the previous example.

Table 11-7.4-1
Vortex Measurement Uncertainty Example

Component	Systematic Uncertainty
Vortex meter K-factor uncertainty	0.75%
Analog uncertainty = 0.025% × 6.30902 L/s / 1.577 L/s = 0.10%	0.10%
Root sum square total volumetric flow systematic uncertainty	**0.76%**

Table 11-7.4-2
Vortex Measurement Uncertainty Example With Installation Uncertainty

Component	Systematic Uncertainty
Vortex meter K-factor uncertainty plus installation uncertainty (0.3%) due to elbow (0.75% + 0.3% = 1.05%)	1.05%
Analog uncertainty = 0.025% × 6.30902 L/s / 1.577 L/s = 0.10%	0.10%
Root sum square volumetric flow systematic uncertainty	**1.055%**

Table 11-7.4-3
Vortex Measurement Uncertainty Example With Vortex Meter, Pressure Sensor, and Temperature Sensor Uncertainties

Component	Systematic Uncertainty
Vortex meter uncertainty	1.00%
Pressure sensor	0.05%
Temperature sensor	0.10%
Root sum square mass flow systematic uncertainty	**1.01%**

11-8 REFERENCES

The following sources were not cited directly but have been consulted in the preparation of this section.

Aguilera Mena, J. J. (2018). "Vortex flowmeters: Transferability of water-based calibration results to liquids, gases and steam applications." The 10th International Symposium on Fluid Flow Measurement. Colorado Engineering Experiment Station, Inc.

ASME MFC-6–2013. Measurement of Fluid Flow in Pipes Using Vortex Flowmeters. The American Society of Mechanical Engineers.

Emerson Electric (2018). Rosemount 8800 Vortex Installation Effects. Technical Data Sheet 00816-0100-3250.

Takamoto, M., Utsumi, H., Watanabe, N., and Terao, Y. (1993). "Installation effects on vortex shedding flowmeters." Flow Measurement and Instrumentation, 4(4), 277–285.

Section 12
Mechanical Meters

12-1 NOMENCLATURE

Symbols used in Section 12 are included in Tables 2-3-1 and 12-1-1. For any equation that consists of a combination of symbols with units shown in Tables 2-3-1 and 12-1-1, the user must be sure to apply the proper conversion factors.

12-2 INTRODUCTION

This Section addresses the operation and proper use of turbine meters and positive displacement flowmeters. Most of the operating conditions, precautions, and recommendations in this Section apply equally to both types of meters. Therefore, the subsections discussing positive displacement meters are limited to presenting the exceptions and differences in their use relative to turbine meters.

Table 12-1-1
Symbols Specifically Applied in Section 12 (in Addition to Symbols in Table 2-3-1)

Symbol	Description	Dimensions [Note (1)]	Units	
			SI	U. S. Customary
f	Meter frequency	T^{-1}	Hz	1/sec
K_f	Calibration constant for flowmeter	L^{-3}	m^{-3}	ft^{-3}
L	Calibration linearity envelope	Dimensionless	%	%
L_c	Characteristic length of the meter	L	m	ft
ΔP_m	Meter pressure loss	$ML^{-1}T^{-2}$	Pa	psi
q_v	Volumetric flow	L^3T^{-1}	m^3/s	ft^3/sec
Ro	Roshko number	Dimensionless	Dimensionless	Dimensionless
U	Uncertainty	Dimensionless	%	%
V_d	Displacement volume	L^3	m^3	ft^3
U_f/f	Uncertainty of the frequency counter	Dimensionless	%	%
U_{K_f}	Uncertainty of lab calibration	Dimensionless	%	%
U_{lab}	Flow calibration lab uncertainty	Dimensionless	%	%
U_{q_v}/q_v	Total actual volumetric flow rate uncertainty	Dimensionless	%	%
σ_p	Standard deviation of two points to define linearity envelope	Dimensionless	%	%
θ	Angle of inclination	...	deg	deg
ϕ	Viscosity pressure drop factor	Dimensionless	Dimensionless	Dimensionless
Ω	Angular velocity	T^{-1}	rad/s	1/sec
ρ_b	Reference fluid density	ML^{-3}	kg/m^3	lbm/ft^3
ρ_f	Fluid density	ML^{-3}	kg/m^3	lbm/ft^3
Subscript				
f	Fluid properties			
v	Volumetric property			

NOTE: (1) Dimensions:
L = length
M = mass
T = time
θ = thermodynamic temperature

All mechanical meters used in performance testing must be calibrated in a mutually agreed-upon laboratory that uses standard measuring instruments traceable to national standards. These calibrations should be performed using the fluid, operating conditions, and piping arrangements matching, as closely as practical, the performance test conditions. If flow straighteners or other flow-conditioning devices are needed in the test, they should be included in the meter piping run when the calibration is performed.

12-3 TURBINE METERS

Turbine flowmeters contain a turbine wheel (or rotor) that rotates with a speed proportional to the flow through the meter. These meters produce an electrical frequency (pulse train) related to the rotor revolutions, often tied to the passing of individual blades on the rotor; to achieve greater resolution. Flow is commonly measured by the frequency of the pulse train. Totalized flow may be determined by counting pulses. Turbine meters should be operated within the flow range and operating conditions specified by the manufacturer to achieve the desired accuracy and normal life. Turbine meters are subject to premature wear and damage by over speeding the turbine wheel and by debris in the flow.

12-3.1 Meter Design Data and Construction Details

The information provided with the meter should include the manufacturer's name or mark, the meter serial number, the maximum operating pressure, and the maximum and minimum flow capacities. The meter calibration factor must also be included. The calibration factor may be pulses per volume for pulse output signals or volume per rotation (or count) for totalizing outputs. The meter should be designed to withstand occasionally running 20% above the maximum flow (within the temperatures and pressures for which it is rated) for at least 30 min without damage or significant change in its calibration curve.

Turbine meters can be used to measure both liquid and gas flows, providing the following four criteria are met:

(a) The range of Reynolds numbers of the calibration data covers the intended performance test requirements.

(b) The Mach number of the flow is less than 0.2.

(c) The turbine wheel friction is negligible, as determined by the spin test in para. 12-6.4(c).

(d) The test fluid is compatible with the meter section material.

The construction of a meter with a removable meter mechanism shall be such that the performance characteristics of the meter are maintained after interchanging the mechanism and/or repeated mounting and dismounting of the same mechanism. The design and method of replacement of a removable mechanism shall ensure that the construction of the meter is maintained. Each removable mechanism shall have a unique serial number marked on it, and any removable meter mechanism shall be capable of being sealed against unauthorized interference.

Turbine meters are available with single and dual rotor designs. For the dual rotor designs, the first rotor (main rotor) is used for the flow measurement and the second rotor (sense rotor) is used for diagnostics. The sense rotor has a different blade pitch, which causes it to spin at a slower speed compared to the main rotor. The sense rotor can be compared to the main rotor at a given flow to determine if the two rotors differ significantly from the initial calibration. If the outputs from the two rotors do not correlate, this is an indication of a mechanical issue with the turbine meter that warrants further investigation.

12-4 TURBINE METER SIGNAL TRANSDUCERS AND INDICATORS

The meter may require an ancillary counter or timer if the output signal is an electrical pulse, or the meter may have an integral display that indicates volumetric total or rate of flow. The totalizing register shall have sufficient number of digits to display a throughput equal to at least 2,000 hr of operation at the maximum flow while maintaining the minimum resolution desired. When the only output of the meter is a mechanical counter, the readout shall enable the meter to be calibrated with the required accuracy at the minimum flow in a reasonably short time. The smallest division or the least significant digit of the counter (or a test element) should be smaller than the minimum hourly flow divided by 400. Provision shall be made for covering and sealing the free ends on any extra output shafts when they are not being used; the direction of rotation shall be marked on the shaft or an adjacent point on the meter. The pulse output is converted electronically to read flow or totalize volume.

The volume per pulse or its inverse must be defined by calibration.

12-5 CALIBRATION

An individual calibration of each meter shall be made. The results of this calibration shall be available together with a statement of conditions under which the calibration took place.

12-5.1 Meter Factor

Meter factor, K_f, is determined by the manufacturer and confirmed by calibration. During calibration, meter pulses are recorded by totalizing the number along with the total gallons collected through the meter or by measuring the frequency of the pulse output versus flow through the meter.

The rotation rate of the rotor is affected by viscous forces and drag forces. Reynolds number, Re, or Roshko number, Ro, characterize the performance of turbine meters for ranges of viscosity and density when operated in the turbulent regime.

$$\mathrm{Ro} = \frac{f{L_c}^2}{\nu} \tag{12-5-1}$$

where

L_c = characteristic length of the meter

The pulse per volume factor, K_f, or its inverse shall be plotted versus flow, Reynolds number, or Roshko number (Cuthbert and Beck., 1999; Hochreiter, 1958; Lee and Karlby, 1960; Mattingly, 1992; Pope et al., 2012; Pope, Wright, and Sheckels, 2012b; Wright et al., 2012; AGA, 2006). In use, the meter-indicated flow is calculated using the meter factor derived from the calibration. For cases where viscosity and density do not vary from the calibration properties and a constant meter factor provides sufficient uncertainty, meter factor may be plotted versus flow or Reynolds number.

In applications where best uncertainty is desired, Ro is preferable to Re since Ro does not include the flow while Re requires an iterative process to obtain a low uncertainty meter factor. By using Ro for the meter calibration curve, the frequency readout and the kinematic viscosity are all that are needed to determine the flow from the K_f value.

For meters with display-only output, similar display-based data are collected during calibration and the meter is adjusted electrically or mechanically, or both, during calibration.

The Reynolds and Roshko numbers perform adequately only in turbulent flow regimes. In laminar flow regimes, calibration shall be performed with the viscosity and density that will be used.

12-5.1.1 Calibration Data The calibration data shall include

(a) for each calibration run of pulse-output meters
- *(1)* number of pulses collected (gated)
- *(2)* the average output frequency
- *(3)* duration
- *(4)* volume of collected calibration fluid
- *(5)* average rate of flow (laboratory)

(b) for each run of display-only mechanical meters
- *(1)* initial meter reading
- *(2)* final meter reading
- *(3)* duration
- *(4)* volume of collected calibration fluid
- *(5)* average rate of flow (laboratory)

(c) the indicated (meter) flow versus actual (laboratory) flow between the $q_{v,\min}$ and $q_{v,\max}$ of the flowmeter. The following is a suggested calibration flow rate range: $q_{v,\min}$, $0.01q_{v,\max}$, $0.25q_{v,\max}$, $0.40q_{v,\max}$, and $0.70q_{v,\max}$ and $q_{v,\max}$

(d) the name and the location of the calibration facility

(e) the method of calibration (gravimetric, bell prover, sonic nozzles, secondary standard)

(f) the estimated calibration uncertainty using ASME PTC 19.1

(g) the characteristics (pressure, temperature, viscosity) of the test fluid

(h) the position of the meter (horizontal, vertical — flow up, vertical — flow down)

(i) the piping geometry upstream and downstream from the meter along with the location of any flow-conditioning devices

12-5.1.2 Calibration Conditions. The preferred calibration is one that is performed at conditions as close as possible to the conditions under which the meter will operate. Special consideration should be given to the fluid used for the calibration to ensure that it is representative of the fluid that will be used in the field. Density and viscosity are known to affect turbine meters and matching the operating values should be considered when choosing a calibration facility. The facility at which the calibration is performed shall provide primary standards of mass, length, time, and temperature.

To achieve the specified performance, the mounting position of the meter shall be stated. The following positions shall be stated and considered:

(a) horizontal

(b) vertical — flow up

(c) vertical — flow down

Where a mechanical output and/or mechanical counter is used, the different possible positions of these devices shall be taken into consideration when specifying the meter position.

12-5.2 Temperature Range

The meter shall have a stated operating fluid, range of fluid temperature, and ambient temperature.

12-5.3 Pressure Loss

Pressure loss data for the meter shall be provided.

The pressure loss of a turbine meter is determined by the energy required for driving the meter mechanism, the losses due to the internal passage friction, and changes in flow velocity and direction. The pressure loss is measured between a point one-pipe diameter upstream and a point six-pipe diameters downstream of the meter in piping of the same size as the meter. Care should be taken in selection and manufacture of the pressure tap locations to ensure that flow pattern distortions do not affect the pressure readings. Refer to subsections 4-7 and 5-4 for recommendations regarding the construction of pressure taps.

The pressure loss follows the turbulent flow loss relationship (except at very low flow rates).

$$\Delta P_m \propto \rho_f q_v f^2 \tag{12-5-2}$$

12-5.4 Installation Conditions

Consideration shall be given to such items as the straight lengths of pipe upstream and/or downstream of the meter and/or the type and location of flow conditioner required. Where practical, the piping geometry at the inlet and outlet to the flowmeter and the location of the flow conditioner should match between the flow calibration and the field installation. Paragraph 12-7.2 provides guidance on a recommended piping configuration with a flow conditioner for turbine meter installations.

12-5.5 Mechanically Driven External Equipment

Loading of an output shaft that drives instrumentation other than the normal mechanical counter can affect the meter output. This effect is largest for small flows and low gas densities. Therefore, the meter specifications shall state the maximum torque that may be applied to the output shaft, the effect of this torque on the meter performance for different densities, and the range of flow for which this statement is valid.

12-5.6 Temperature and Pressure Effects

Changes in meter performance can occur when the operating temperature and pressure are very different from the calibration conditions. These changes may be caused by changes in dimensions, bearing friction, or other physical phenomena in the meter fluid (density and viscosity). Sufficient back pressure is required in liquid flow to prevent cavitation. The manufacturer should provide a cavitation index to allow determination of minimum back pressure.

12-6 RECOMMENDATIONS FOR USE

12-6.1 Start-up Recommendation

Before placing a meter installation in service, particularly on new lines or lines that have been repaired, the line should be cleaned to remove any collection of welding beads, rust accumulation, and other pipeline debris. The meter mechanism should be removed during all hydrostatic testing and similar line-cleaning operations to prevent damage to the measuring element.

Foreign substances in a pipeline can cause serious damage to turbine meters. Strainers are recommended when the presence of damaging foreign material in the gas stream can be anticipated. Strainer should be sized so that at maximum flow there is a minimum pressure drop and installed so that there is no excessive flow distortion. A greater degree of meter protection can be accomplished through the use of a dry-type or separator-type filter installed upstream of the meter inlet

piping. It is recommended that the differential pressure across a filter be monitored to maintain it in good condition to prevent flow distortion.

12-6.2 Over-Range Protection

Turbine meters can usually withstand a gradual over-ranging without causing internal damage other than accelerated wear. However, extreme velocity encountered during pressurizing, venting, or purging can cause severe damage from sudden turbine wheel overspeeding.

As with most flowmeters, line flow and pressure should be increased slowly and in a controlled manner. Shock loading by opening valves quickly can result in turbine wheel damage. In high-pressure applications, the installation of a small bypass line around the meter can be used to safely pressurize the meter to its operating pressure.

In those installations where adequate pressure is available, either a critical flow orifice or sonic (choked-flow) venturi nozzle may be installed to help protect the meter turbine wheel from over speeding. The restriction should be installed in the piping downstream of the meter and sized to limit the meter loading to approximately 20% above its $q_{v,\max}$. Generally, a critical flow orifice will result in a 50% pressure loss and a sonic venturi nozzle will result in a 5% to 20% pressure loss.

12-6.3 Bypass

If interruption of the fluid cannot be tolerated, a bypass should be installed so that the meter can be removed for maintenance.

12-6.4 Maintenance and Inspection Frequency

In addition to sound design and installation procedure, turbine meter accuracy depends on good maintenance practice and frequent inspection. The meter inspection period depends on the fluid condition. Meters used in dirty fluids will require more frequent attention than those used with clean fluids, and inspection periods should reflect this.

12-6.5 Other Installation Considerations

In addition to the recommendations in paras. 12-6.1 through 12-6.4, the following steps shall be taken during installation to avoid errors:

(a) Install the meter and meter piping so as to reduce strain on the meter from pipeline stresses.

(b) Use care to ensure a concentric alignment of the pipe connections with the meter inlet and outlet connections.

(c) Prevent gasket and/or weld bead protrusion into the pipe bore, which could disturb the flow pattern.

(d) In gas flow cases where a considerable quantity of liquid is expected, consideration should be given to installing a separator upstream of the meter. Flow distortion by the separator should be considered during the piping design and meter calibration.

12-6.6 Accessories Installation

Accessory devices used for converting indicated volume to standard conditions or for recording operating parameters should be installed properly and the connections made as follows:

(a) Temperature Measurement. Since upstream disturbances should be kept to a minimum, the recommended location for a thermowell is downstream of the turbine wheel. It should be located 5 pipe diameters from the turbine wheel and upstream of any outlet valve or flow restriction. The thermowell should be installed to ensure that the temperature measured is not influenced by heat transfer from the piping and well attachment.

(b) Pressure Measurement. For gas flow applications, at least one pressure tap shall be provided on the meter to enable measurement of the static pressure at the turbine wheel of the meter at flowing conditions. The connection of the pressure tapping shall be marked P_m. If more than one P_m tap is provided, the difference in pressure readings shall not exceed 100 Pa (0.015 psi) at maximum flow rate with air at a density of 1.2 kg/m^3 (0.7 lbm/ft^3). The pressure tap marked P_m on the meter body should be used as the pressure-sensing point for recording or integrating instruments.

(c) Density Measurement. For liquid applications, the conditions of the fluid in the density meter should represent the conditions in the turbine wheel over the operating rates of the meter. Consideration should be given to the possibility of unmetered fluid when using purged density meters. Density meters installed in the piping should be installed downstream of the turbine wheel.

For gas applications, the density is generally calculated using an equation of state along with the measured pressure, temperature, and gas composition. Since the turbine meter measures volumes at metering conditions, the density of the metered fluids may be applied to convert the indicated volume to a volume at conditions or to mass flow when the conditions are constant.

12-7 PIPING INSTALLATION AND DISTURBANCES

The following paragraphs provide guidance for evaluating flow disturbances that may affect meter performance and standardized tests to assess the effects of such disturbances. During calibration and in actual use, the meter should be installed such that the conditions that are described in paras. 12-7.1 and 12-7.2 are mitigated through the use of straight upstream piping and a flow conditioner. Section 6 provides a recommended upstream piping configuration including the location of a flow conditioner. For gas applications, American Gas Association Report No. 7 (2006) also provides recommendations for upstream straight piping lengths and the location of a flow conditioner.

12-7.1 Swirl Effect

Swirl entering a turbine meter can influence its reading. Swirl in the direction of turbine rotation may increase the turbine wheel speed, whereas a swirl in the opposite direction may decrease the turbine wheel speed. For high-accuracy flow measurement, such a swirl effect must be reduced to an acceptable level by installation of upstream flow conditioning.

12-7.2 Velocity Profile Effect

Turbine meters are designed to have a uniform velocity profile at the meter inlet. In general, a nonuniform velocity profile results in a higher turbine wheel speed than that produced by a uniform velocity profile. For high-accuracy flow measurement, the velocity profile at the turbine wheel should be conditioned by proper installation of upstream flow conditioning.

12-8 EXAMPLE OF FLOW MEASUREMENT BY TURBINE METER WITH NATURAL GAS

12-8.1 Meter Flow

Volumetric flow through a turbine meter with pulse output is

$$q_v = \frac{f}{K_f} \tag{12-8-1}$$

where

q_v = meter volumetric flow
f = flowmeter output frequency
K_f = calibration constant for flowmeter from laboratory calibration

The uncertainty of K_f is calculated as

$$U_{K_f} = U_{\text{lab}} + \sqrt{L^2 + 4\sigma_p^2} \tag{12-8-2}$$

where

L = linearity envelope of calibration; the linearity envelope brackets the range of lab-determined calibration constants, K_f, and is expressed as a percentage (%); the linearity envelope can vary depending on meter type, but is typically in the range of 0.5% to 1%
U_{lab} = flow calibration laboratory uncertainty, %; laboratory estimates are typically 0.25% for gas flow
σ_p = standard deviation of two data points used to define linearity envelope; 0.05% is assumed

If the laboratory calibration is done at the actual operating conditions (temperature, pressure, viscosity) and includes the operating mass flow or Reynolds number range, the uncertainty of the derived q_v may be reduced to essentially that of the laboratory uncertainty.

Most gas flow calibrations are done at either atmospheric or low pressure, ignoring pressure effects, or at relatively low flow rates relative to operational conditions and at the expected operating pressure. Ideally, the calibration should be conducted with a fluid that closely matches the operating conditions (pressure, temperature, viscosity, density).

It is assumed in this analysis that the calibration was performed at operational line pressure and flow(s).

Hence, the uncertainty of calibration is calculated from eq. (12-8-3) as follows:

$$U_{K_f} = 0.25 + \left(0.5^2 + 4 \times 0.05^2\right)^{0.5} = 0.76\% \tag{12-8-3}$$

Total actual volumetric flow rate uncertainty (actual m^3/h or similar units) is calculated as follows:

$$\frac{U_{q_v}}{q_v} = \left[\left(\frac{U_{k_f}}{K}\right)^2 + \left(\frac{U_f}{f}\right)^2 + \left(\frac{U_{\text{calibration shift}}}{\text{shift}}\right)^2\right]^{0.5} \tag{12-8-4}$$

where

U_f/f = the uncertainty of the frequency counter in fraction units, which is usually 0.002 or 0.2%

The calibration shift is assumed to be at maximum 0.3%. Hence, over the operating range of flow

$$\frac{U_{q_v}}{q_v} = \left[(0.0076)^2 + (0.002)^2 + (0.0030)^2\right]^{0.5} = 0.0084 = 0.84\% \tag{12-8-5}$$

12-8.2 Normalizing Meter Flows

Metered fuel flow rate is often in units of mass flow or "normal" volumetric flow, e.g., m^3/h [or standard ft^3/min (SCFM) in U.S. Customary units] when used to determine the thermal heat input term in calculating heat rate or efficiency. Fuel heating values are usually in units of energy/mass.

To convert actual m^3/h (ACMH) to the units of normal m^3/h (NCMH)

$$q_{v,\text{ACMH}} = \left(\frac{\rho_f}{\rho_b}\right) q_{v,\text{NCMH}} \tag{12-8-6}$$

where

ρ_b = a reference density, usually the gas density at 101.325 kPa (14.696 psia) and 15°C (59°F); however, other base conditions are sometimes used, and care must be taken in being consistent (note that this is a constant)

ρ_f = density of the flowing fluid [see para. 12-6.6(c)]

Note that the term $\rho_f \times q_{\text{ACMH}}$ is mass flow rate units from fundamental principles (mass = density × volume).

For the gas industry, the ratio of the actual density to a base density is used for applications or calculations requiring density or mass flow rates. Thus, the units in this calculation are normal m^3/h, but it is mass flow rate that is being determined from the product of the measured volume flow rate and the actual density of the flowing fluid.

It is important to realize this when comparing uncertainty levels of various meters on the market. If uncertainty is determined strictly for ACMH but NCMH is needed, then the additional error incurred from the density term of the flowing fluid must be considered.

12-8.3 Systematic Uncertainty Calculation of Flow in Units of Normalized Flow

The uncertainty in the determination of fuel gas density was shown in subsection 4-13 as 0.33% under steady state conditions.

Thus, in units of NCMH or other normal volume flow units, the steady state uncertainty in the determination of gas fuel flow with a turbine meter is as follows:

$$\frac{U_{q_v,\text{SCFH}}}{q_{v,\text{SCFH}}} = \left(0.84^2 + 0.33^2\right)^{0.5} = 0.90\% \tag{12-8-7}$$

12-8.4 Specific Range of Flow

If only a particular range of flow is of interest, then the linearity within that range of flow is probably lower for a properly sized meter. Enough data must be taken over the smaller range during calibration to ensure adequate precision for determining the linearity. Under those circumstances, over a smaller range of flows, the uncertainty is lower.

12-9 RANDOM UNCERTAINTY DUE TO TIME VARIANCE OF DATA

The post-test uncertainty analysis must consider variance of data due to unsteady conditions.

The random standard uncertainty is multiplied by the Student's t value (typically 2 for a data set) and combined with the systematic uncertainty by root sum square to determine the expanded uncertainty (the overall measurement uncertainty at 95% confidence level).

See ASME PTC 19.1 for examples of complete uncertainty analyses, including random errors introduced by time variance of data. Reference is made to PTC 19.1 for the details of post-test uncertainty analysis requirements for adding the effects of the time variance of data to the random uncertainty component.

12-10 FIELD CHECKS

Several field checks can be used to determine if significant damage has occurred that would adversely affect accuracy of the meter. These conditions would require immediate correction.

(a) General. The most commonly applied field checks are visual inspection and a spin time test. Meters in operation can often provide information through their generated noise and vibrations. Severe vibration usually indicates damage that has unbalanced the turbine wheel and can lead to complete meter failure. Turbine wheel rubbing and poor bearings can often be heard at relatively low flows, when such noises are not masked by normal flow noise.

(b) Visual Inspection. The turbine wheel should be visually inspected for missing blades, accumulation of solids, erosion, or other damage that would affect the turbine wheel balance and the blade configuration. Meter internals should be checked to ensure there is no accumulation of debris. Flow passageways, drains, breather holes, and lubrication systems should also be checked to ensure there is no accumulation of debris.

(c) Spin Time Test. The spin time test determines the relative level of the mechanical friction present in the meter. If the mechanical friction has not significantly changed and if the meter internals are clean and show no damage, there should be no change in accuracy. If the mechanical friction has increased, this can indicate that the accuracy of the meter at low flow has degraded. Typical spin times for a meter can be provided by the manufacturer on request.

The spin time test must be conducted in a draft-free area with the measuring mechanism in its normal operating position. The turbine wheel is rotated at a reasonable speed with a minimum speed of approximately one-twentieth of rated speed corresponding to that at $q_{v,\max}$ and is timed from the initial motion until the turbine wheel stops. Spin tests should be repeated at least three times and the average time should be taken. The usual cause for a decrease in spin time is increased shaft-bearing friction. There are other causes of mechanical friction that affect spin time, such as heavily lubricated bearings, low ambient temperature, drafts, and attached accessories.

Other methods of conducting a spin time test are permitted as long as the method is specified.

The spin time test may not be applicable for all types of turbine meters. The manufacturer of the turbine meter should be consulted to determine if the spin test is relevant for the specific model.

(d) Other Checks. Meters equipped with pulse generators at the turbine wheel can assist in detection of the loss of a blade on the wheel. This can be accomplished by observing the output pulse pattern or comparing the pulse output from the turbine wheel pulse generator to a pulse generator on a follower disc connected to the turbine wheel shaft.

A pulse generator activated by the turbine wheel blading, or at any other location in the drive train between the turbine wheel and the meter index, can be used in conjunction with a pulse generator on the index to determine the integrity of the drive train. The ratio of a low-frequency pulse from the index to a high-frequency pulse generated from any location down the drive train should be a constant regardless of rate.

Certain volume conversion devices attached to turbine meters also indicate volumes at flowing conditions. The change in the registered volume on the conversion device should equal the change in registered volume on the mechanical index of the turbine meter over the same period.

12-11 POSITIVE DISPLACEMENT METERS

The general approach presented in this subsection should work with many designs of positive displacement meters (wobble plate, rotating piston, rotating vanes, gear, or impeller). All of these meters, which are also called volumeters, measure flow by channeling it through discrete passages of known volumes and counting the volumes. Typical designs in use are shown in Figure 12-11-1.

In the case of the common wobble plate (or nutating disk) meter, the fluid flows into the lower right port and around the chamber, either above or below the disk, and out the top left port. In the process, the disk drives a gear train that serves to convert the number of meter displacement volumes into the desired engineering units. There is a diaphragm between the top and bottom of the chamber that causes the fluid to flow around the meter, in one side of the diaphragm and out the other. This diaphragm also prevents the disk from rotating so that its motion is precession without spin.

The metering action of the sliding vane meter, rotating vane meter, and gear-type meter are illustrated in Figure 12-11-1 with arrows showing the flow path.

Figure 12-11-1
Positive Displacement Volumeters

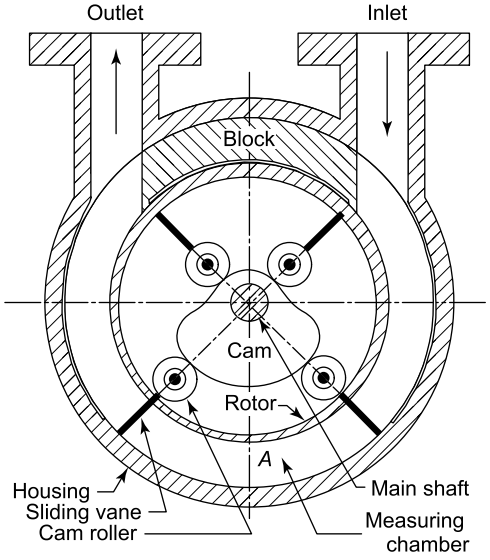

(a) Metering Chamber of a Sliding Vane Meter

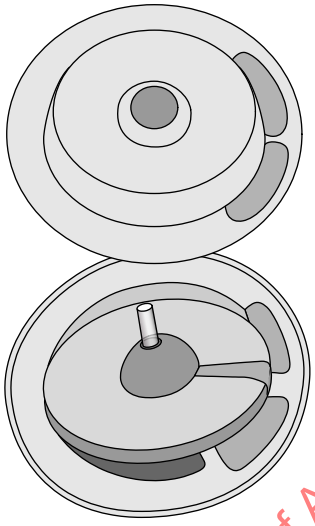

(b) Measuring Chamber and Disk

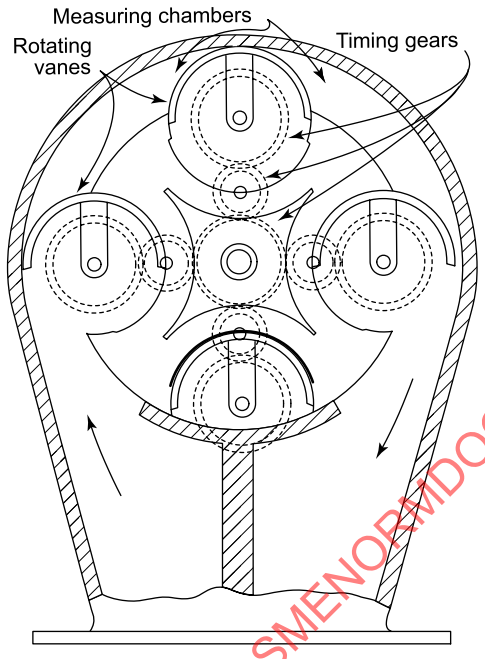

(c) Schematic Representation of the Operating Features of a Rotating Vane Meter

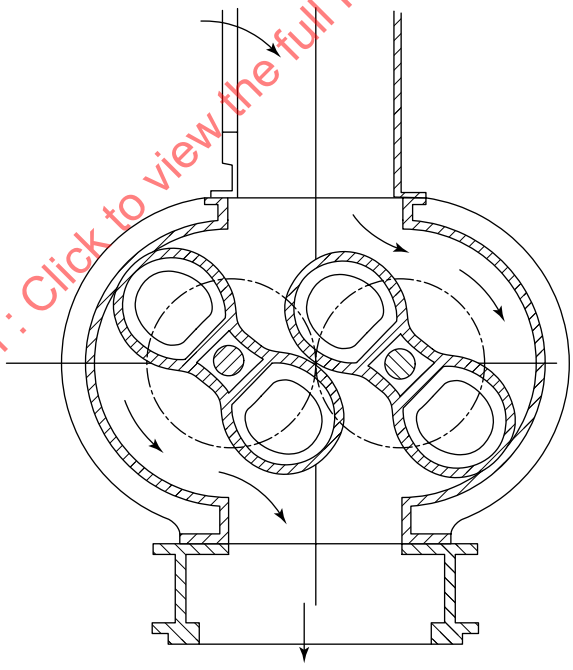

(d) Cross Section Through a Gear-Type Meter [Note (1)]

NOTE: (1) The gears in this illustration have two "teeth" or lobes.

12-11.1 Positive Displacement Meter Performance

If all of the seals in the meter were perfect, the only errors in flow measurement that these meters would exhibit would be those due to the inaccuracies of the measurement of the meter displacement volume and the fluid properties and to the accuracy of the calibration laboratory. Obviously, the seals cannot be perfect. Clearances allow a small portion of the flow to slip by uncounted.

Dimensional analysis using Buckingham's pi theorem (AGA 2006) has shown that two dimensionless groups describe the meter performance. The first is the meter's volumetric efficiency, in which $q_{v_{act}}$ is the actual number of meter displacement volumes counted before conversion to engineering units by the gear train and readout device.

$$\eta_v = \frac{q_{v_{ind}}}{q_{v_{act}}} \tag{12-11-1}$$

The second consists of a viscosity pressure drop factor related to the speed of the meter's moving parts.

$$\phi = \frac{\mu\Omega}{\delta P} \tag{12-11-2}$$

where

δP = incremental change in pressure
μ = dynamic, or absolute, viscosity
ϕ = viscosity pressure drop factor
Ω = angular velocity

Generally, pressure drop increases relative to the meter speed and the volumetric efficiency increases with increasing absolute viscosity, but not in a directly proportional or linear way. The maximum volumetric efficiency usually occurs in the middle of the range of the viscosity pressure drop factor [see eq. (12-11-2)].

12-11.2 Calibration Requirements

Positive displacement meters should be calibrated using the same fluid at the same temperature as is expected in their intended performance test environment or service. Unlike turbine meters, these machines are relatively insensitive to piping installations and otherwise poor flow conditions; in fact, they are more of a flow disturbance than practically anything else upstream or down in plant piping. If the calibration laboratory does not have the identical fluid, the next best procedure is to calibrate the meter in a similar fluid over the same range of viscosity expected in service. This recommendation implies duplicating the absolute viscosity of the two fluids as described in para. 12-11.3. It has been reported (AGA 2006) that temperature effects, apart from influence on viscosity, were negligible relative to the accuracy of the meter. Under most uses, an uncertainty of 0.5% to 1% can be expected from such a calibrated meter. These meters should be calibrated periodically because mechanical wear enlarges the internal clearances in the meter, which degrades the volumetric efficiency and, therefore, changes the meter factor or registration.

12-11.3 Interpolation of Calibration Data

Positive displacement meters are typically used within the calibration data envelope but may require interpolation of the calibration data to the service condition of the meter as explained herein.

The following procedure should be used to predict the meter calibration for fluid conditions different from those of the actual calibration, based on U.S. Navy test data (Keyser 1973):

(a) Obtain a current calibration as closely matching the range of viscosity pressure drop factor [see eq. (12-11-2)] as possible. The calibration procedure must include measuring the pressure drop across the meter. Whenever possible, two calibrations should be performed: one at high viscosity and one at low viscosity. Then interpolation can be used to predict the meter calibration under service conditions.

The multiplicative factor of the gear train ratio can be changed to bring the viscosity pressure drop factor closer to unity over the new range of use, so this factor must be removed for the dimensional analysis. The precise volume of the meter is not required; the statistical mean value normally found for that size and make of meter will suffice.

(b) Find the point of minimum meter error (relative maximum of the volumetric efficiency). This is the point that will be interpolated to the new operating conditions.

Figure 12-11.3-1
Method of Interpolation of Positive Displacement Meter Performance From Calibration Data to Other Fluid Viscosity and Operating Conditions

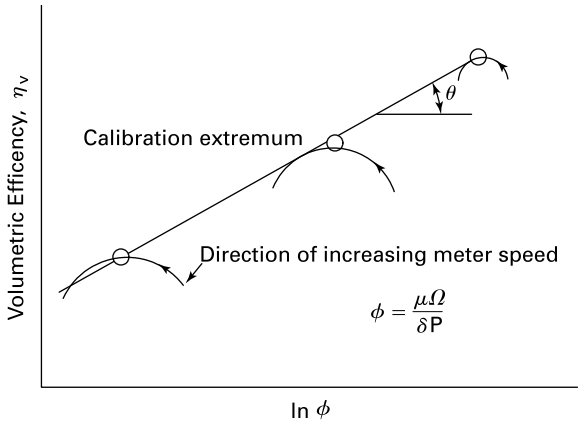

(c) Calculate the angle of inclination, the line along which the maximum efficiency is to move. This is done best by drawing a line between the maxima of two different calibrations with the given meter on a plot of efficiency versus viscosity pressure drop factor, as shown in Figure 12-11.3-1. Alternatively, it can be estimated from the meter displacement volume using eq. (12-11-3).

$$\theta(\text{deg}) = -12.35 - 11.42 \ln V_d \tag{12-11-3}$$

(d) Calculate the predicted maximum volumetric efficiency. To calculate the viscosity pressure drop factor [see eq. (12-11-2)] at the new operating conditions, assume that the maximum efficiency occurs at the same ratio of δ_p/Ω. Then the shift in the locus of the maximum efficiency along the line shown in Figure 12-11.3-1 is

$$\delta(\eta_{\max}) = 0.01467 \tan\theta[\ln(\mu/\mu_{\text{cal}})] \tag{12-11-4}$$

In other words, this shift of maximum efficiency is proportional to the logarithm of the ratio of viscosities.

(e) Draw the predicted calibration curve. The predicted volumetric efficiency must be transformed, using the gear ratio, to either percentage registration or its reciprocal, the meter factor, whichever is intended for use. This latter value should be plotted versus the indicated flow. If the change in viscosity from the calibration conditions is not too great, the same shape of curve can be used as in the original calibration. Since the meter calibration curves normally are nearly constant, this assumption results in negligible additional error.

12-12 REFERENCES

AGA Report No. 7. (2006). "Measurement of Natural Gas by Turbine Meter." American Gas Association.

Cuthbert, M. R., and Beck, S. B. M. (1999). "A nondimensional method to increase the accuracy of turbine flowmeters." Proceedings of the Institution of Mechanical Engineers, Part E: Journal of Process Mechanical Engineering, 213(2), 121–126.

Hochreiter, H. M. (1958). "Dimensionless Correlation of Coefficients of Turbine-Type Flowmeters." Transactions of the American Society of Mechanical Engineers, 80(7) (Oct.)1363–1366.

Keyser, D. R. (1973). "The Calibration Correlation Function for Positive Displacement Liquid Meters." Journal of Fluids Engineering, 95, 180.

Lee, W. F. Z., and Karlby, H. (1960). "A study of viscosity effect and its compensation on turbine-type flowmeters." Journal of Fluids Engineering, 82(3), 717–725.

Mattingly, G. E. (1992). "The characterization of a Piston Displacement-Type Flowmeter Calibration Facility and the Calibration and Use of Pulsed Output Type Flowmeters." Journal of Research of the National Institute of Standards and Technology, 97(5), 509–531.

Pope, J. G., Wright, J. D., Johnson, A. N., and Moldover, M. R. (2012a). "Extended Lee Model for the Turbine Meter and Calibrations with Surrogate Fluids." Flow Measurement and Instrumentation, 24, 71–82.

Pope, J. G., Wright, J. D., and Sheckels, S. D. (2012). "Tests of the Extended Lee Model Using Three Different Turbine Meters." The 8th International Symposium on Fluid Flow Measurement. Colorado Engineering Experiment Station, Inc.

Wright, J. D., Johnson, A., Kline, G., Crowley, C., Pope, J., Bean, V., John, K., Latsko, J.Pfeffer, D., Winchester, J., et al. (2012). "A Comparison of 12 US Liquid Hydrocarbon Flow Standards and the Transition to Safer Calibration Liquids." Cal Lab: The International Journal of Metrology, 19(2), 30–38.

Section 13
Coriolis Mass Flowmeters

13-1 DEFINITIONS AND NOMENCLATURE

13-1.1 Definitions

drive coil: the coil that is actively energized to establish the oscillation of the flow tubes.

drive current: the current supplied to the drive coil. This current may also be represented as a percentage of total current allowable.

downstream sensor coil (DSC): a passive magnet and coil set used to measure flow tube oscillations downstream of the drive coil. Also known as *downstream pickoff coil* or *pickup coil* in industry.

flow calibration factor (FCF): the ratio of mass flow per unit time expressed in units of grams/second/microsecond or as a nondimensional factor.

measuring tube(s): single or multiple sets of tubes, which contain the fluid being measured, that are oscillated by the drive coils and make up the measurement section of the device.

resistance thermal device (RTD): a device used to measure tube and/or sensor housing temperature to compensate for the influence of thermal expansion as well as the changes in modulus of elasticity on the mass flow and density calculations.

sensor case: an enclosure surrounding the measuring tubes that protects the internal components and will contain fluid leakage resulting from a tube failure. Some Coriolis sensor cases provide secondary containment. Also known as *sensor housing*.

NOTE: Some sensor designs have pressure-rated secondary enclosures. The manufacturer should be consulted for pressure containment rating.

upstream sensor coil (USC): a passive magnet and coil set used to measure flow tube oscillations upstream of the drive coil. Also known as *upstream pickoff coil* or *pickup coil* in industry.

zero offset: the value of Δt_z (see para. 13-1.2) captured in a no-flow condition and stored in the transmitter.

zero stability: the base variation of the flow signal expressed in mass flow units.

13-1.2 Nomenclature

Symbols used in this Section are included in Tables 2-3-1 and 13-1.2-1. For any equation that consists of a combination of symbols with units shown in Tables 2-3-1 and 13-1.2-1, the user must be sure to apply the proper conversion factors.

13-2 INTRODUCTION

Coriolis flowmeters can measure liquids, gases, and slurries within acceptable ranges of fluid temperature and pressure. Coriolis mass flow sensors have a fluid-conveying tube or tubes that are oscillated at a resonant frequency, thereby generating a rotating reference frame. The flow of the fluid in the oscillating tube results in the development of Coriolis forces along the length of the tube. The Coriolis forces, perpendicular to the direction of flow, resist and accelerate the motion along the length of the tube causing a delay of its basic motion. Coriolis flowmeters provide measurement of mass flow and density. The continuously measured density and mass flow rate are used to calculate the volumetric flow rate.

13-2.1 Sensor Physical Properties

Coriolis flowmeters operate by oscillating a single or multiple set of tubes through which fluid is flowing. The tubes may be straight or have a curved geometry, each providing benefits to best suit different flow applications. The oscillation of the tube(s) is analogous to a simple spring-mass system. The natural frequency, f, of the Coriolis sensor is derived from

Table 13-1.2-1
Symbols Specifically Applied in Section 13 (in Addition to Symbols in Table 2-3-1)

Symbol	Description	Dimensions [Note (1)]	Units	
			SI	U.S. Customary
C_s	Flow tube stiffness	MT^{-2}	N/m	lbf/ft, lbf/in.
f	Natural frequency	T^{-1}	Hz	1/sec
FCF	Flow calibration factor	MT^{-2}	g/s/μs	lbm/s/μs
m_f	Fluid mass	M	kg	lbm
m_t	Tube mass	M	kg	lbm
P_T	Test pressure	$ML^{-1}T^{-2}$	Pa	psi
q_m	Mass flow rate	MT^{-1}	g/s	lbm/sec
T_C	Coriolis flowmeter temperature output	θ	°C	°F
Δt	Time difference between the left and right pickoff coil signals	T	μs	μsec
Δt_z	Time difference between the left and right pickoff coil signals at no flow	T	μs	μsec

NOTE: (1) Dimensions:
L = length
M = mass
T = time
θ = thermodynamic temperature

tube stiffness, C_s, tube mass, m_t, and fluid mass, m_f. Natural frequency is linearly related to the square root of the ratio of sensor stiffness to mass.

$$f = \sqrt{\frac{C_s}{m_t + m_f}} \tag{13-2-1}$$

During operation, the tube mass and stiffness values remain constant (ignoring any potential long-term effects like scale, erosion, corrosion, material fatigue, or hardening), creating a direct correlation between changes in the mass of the fluid and any changes in the natural frequency of the system. Since the volume of fluid contained in the meter also remains constant, the changes in natural frequency are directly related to fluid density. This allows the Coriolis flowmeter to provide a fluid density measurement and makes it possible to calculate a volumetric flow rate.

The oscillation of the flow tube(s) creates a rotating reference frame for the fluid to pass through. When there is no flow through the meter, the flow tube oscillations are symmetric. However, once the fluid is flowing through the rotating reference frame of the flow tubes, its inertia generates the Coriolis force, which creates an asymmetric deflection of the flow tube upstream and downstream of the drive coil. The greater the mass flow rate through the meter, the larger the asymmetries in flow tube oscillations at the pickoff coils become. A Coriolis flowmeter measures the deflection of the flow tubes at a point upstream and downstream from the driving coil and compares the time difference, or phase shift, in their sine wave signals to determine the mass of the fluid passing through the meter. As the fluid flow increases, the asymmetries in the flow tube oscillations become greater, creating a larger phase shift between the sine wave signals of the two sensors.

Due to variation in manufacturing, all Coriolis flowmeters have a zero offset. This is the Δt or phase shift observed during zero flow conditions. This zero-offset value must be captured during calibration and is usually verified or captured again in the final installation. These zero offsets must be subtracted from the total flow signal by the transmitter to correctly calculate flow. This calculation is shown in eq. (13-2-2).

Mass flow is determined by the following equation:

$$q_m = (\Delta t - \Delta t_z) \times \text{FCF} \tag{13-2-2}$$

Figure 13-3.1-1
Typical Mechanical Arrangement

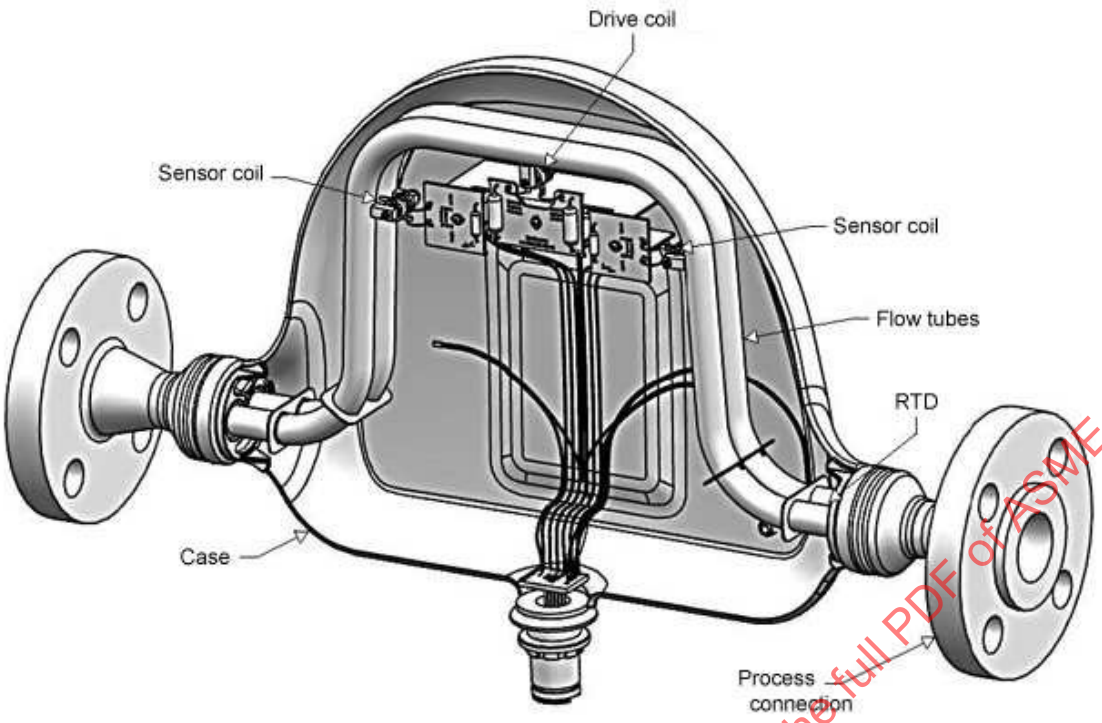

GENERAL NOTE: Courtesy of Emerson Electric.

where

FCF = flow calibration factor, g/s/μs (lbm/sec/μsec)
q_m = mass flow, g/s (lbm/sec)
Δt = time difference between coil signals, μs
Δt_z = time difference between coil signals at a no flow condition, μs

NOTE: Some manufacturers use nondimensional factors for the variables shown above.

13-3 METER CONSTRUCTION

Coriolis flowmeters consist of two components, the meter body or sensor (primary) and the transmitter or electronics (secondary).

13-3.1 Primary Device

The primary device of the Coriolis flowmeter is the mechanical sensor (see Figure 13-3.1-1). It consists of flow tubes, sensor coils and magnets, driver coil and magnet, process connections, a resistance temperature detector (RTD), and case or housing.

Coriolis flowmeters employ a single or multiple oscillating flow tubes. The geometry of the flow tubes varies and can be straight or have a curved design similar to the one shown in Figure 13-3.1-1. The primary device or sensor is installed in the process line, so the user measures the entire flow stream. During operation, the drive coil is energized periodically, pushing or pulling the flow tube(s) in an oscillating manner. Energizing the drive coil causes the flow tubes to oscillate at their natural frequency (see Figure 13-3.1-2). Once process fluid is flowing through the oscillating tube (the rotating reference frame), the Coriolis force is generated.

Figure 13-3.1-2
Oscillating Flow Tubes

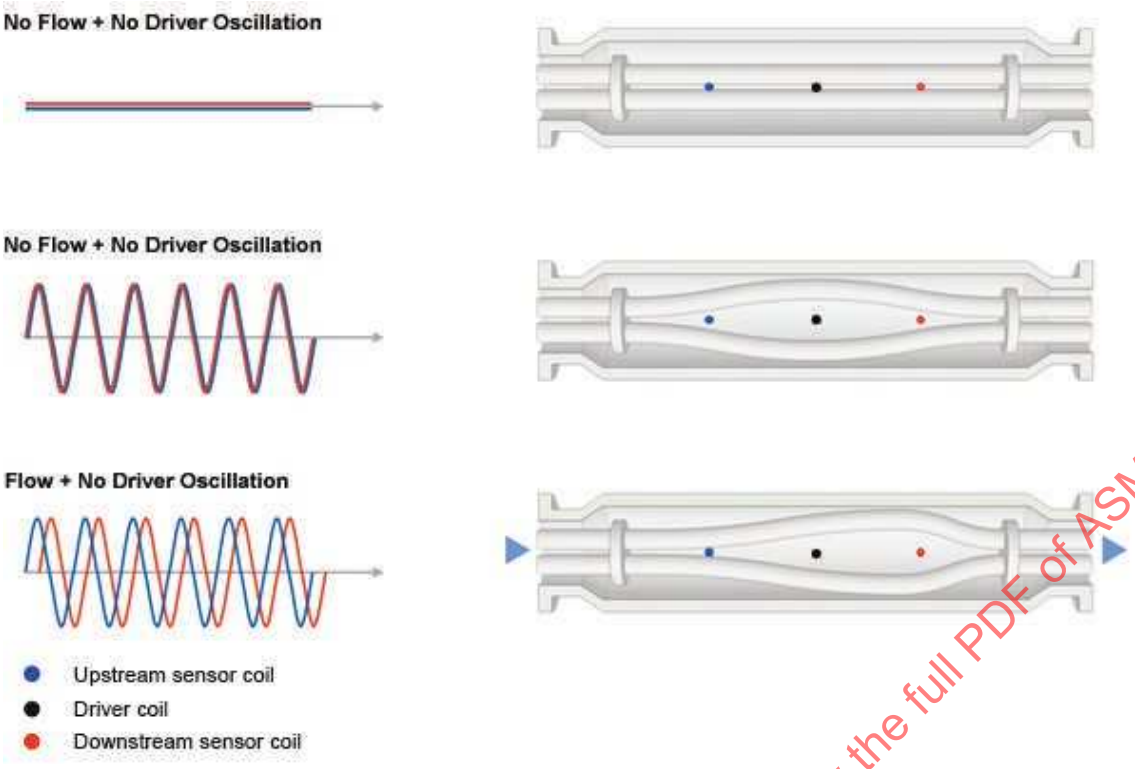

GENERAL NOTE: Courtesy of KROHNE, Inc.

The Coriolis force creates the asymmetric distortion of the tube set described in para. 13-3.2. The flow tube response is measured by the sensor coil(s) and magnet sets. These are passive coils mounted on the flow tube, with the magnets mounted on either an adjoining tube or the meter body. The magnets pass through the coils as the tube is oscillating, creating the measurement signal. The time difference, Δt, used to calculate mass flow is measured from these signals.

The RTD is used to measure the tube's temperature. This measurement is used by the transmitter (secondary device) and is discussed in para. 13-3.2.

13-3.2 Secondary Device

The secondary device consists of the electronics that energize the drive coil(s), causing the tubes to oscillate at their natural frequency, as well as the hardware to provide the corresponding data output. Figure 13-3.2-1 is an image of a typical transmitter that would be installed on a mass flowmeter.

Additionally, the secondary device determines temperature by using a RTD mounted on the sensor tube. The RTD circuit transmits a current to the RTD and, by monitoring the voltage output, can indicate the tube surface temperature and compensate for the temperature effect on flow tube response. Temperature variation changes the stiffness of the flow tubes and influences the measurement. A Coriolis meter uses the RTD to automatically compensate for these changes without intervention.

Figure 13-3.2-1
Electronic Transmitter

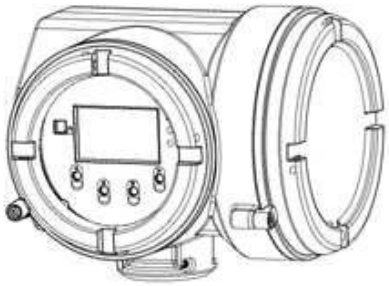

GENERAL NOTE: Courtesy of Emerson Electric.

13-4 CALIBRATION AND UNCERTAINTY

13-4.1 Calibration

The calibration factor is the linear relationship of mass flow to time delay. Depending on the Coriolis manufacturer, periodic calibration may be recommended. Some manufacturers have *in situ* verification systems capable of performing verification without disruption of the flowing process. Secondary effects, such as pressure and temperature, can affect the calibration factor and zeroing and are discussed in para. 13-4.2

Meter calibration will be directly affected by anomalies such as pitting, corrosion, erosion, cracks, alloy decomposition, and fatigue. If any of these conditions are known to exist, the meter must be recalibrated or replaced. Normal tube oscillation should not induce fatigue stress that affects the calibration. Coriolis meters can be calibrated in the field but typically at a higher uncertainty than in a factory or accredited laboratory. A field calibration can be conducted with another flowmeter, usually Coriolis, in a portable test rig that is plumbed into the user's system. Manufacturer-provided in-field verification tools should be used as an alternative or complement to field calibrations where possible. Using field verification tools can prolong calibration intervals and reduce the risk of systematic faults associated with recurring lab calibrations (removal, shipping, and reinstallation).

13-4.2 Lab Calibration and Testing Considerations

There are several test setup and configuration parameters the user should be aware of when calibrating a meter either at the manufacturer or in a commercial laboratory. Laboratory calibration configurations should reflect the end-use configuration to reduce measurement errors incurred upon final installation.

13-4.2.1 Testing Fluid. Coriolis meters work on a very wide variety of fluids. They can be calibrated or verified on fluids ranging from natural gas to crude oil. Typically, Coriolis meters are calibrated with water, and the user determines if a secondary verification or calibration on an alternate fluid is required. The water calibration is transferable to other fluids, and manufacturers should provide documentation supporting this transferability. The Coriolis principle works equally well on this wide range of fluids, but regulatory or contractual obligations may require verification/calibration on a fluid closer to the application. Some considerations when testing on various fluids are addressed in paras. 13-4.2.1.1 through 13-4.2.1.3.2.

13-4.2.1.1 Water. Most manufacturers will calibrate using air and water to determine the primary calibration coefficients (both mass and density). A laboratory water calibration is typically at low pressure [under 350 kPa (50 psi)] and stable temperature conditions and compares meter performance to traceable mass and density references. Many Coriolis meters have a mass flow uncertainty specification of 0.1% as delivered from the factory. The required application uncertainty should be considered when selecting a lab for water flow testing.

13-4.2.1.2 Oils (Hydrocarbons). Testing laboratories that provide oil or other hydrocarbon calibrations on Coriolis meters will use products that include mineral oil, diesel or kerosene (light hydrocarbons), and sometimes crude oil or fuel oil (heavy hydrocarbons). This can be a challenging measurement because the labs often employ volumetric technologies to measure these fluids (i.e., ball or piston provers or a volumetric flowmeter used as a transfer standard). The Coriolis meter provides a real-time actual volume flow rate output but, because the Coriolis meter calculates volume flow rate

Table 13-4.2.1.3.1-1
Impact of Meter Tube Gas Velocity on Performance

Mach Number [Note (1)]	Performance Expectation
Ma ≤ 0.2	Ideal performance — pressure drop suitable to most applications
0.2 ≤ Ma ≤ 0.3	Acceptable performance — sensors typically meet spec, but degradation in repeatability may be observed. The range of acceptable performance of a meter is dependent on the meter design, and the manufacturer should be consulted. Pressure drop may exceed requirements for some applications.
Ma ≥ 0.3	Not recommended — repeatability and bias issues are highly likely. Pressure drop becomes excessive and nonlinear as rate increases.

NOTE: (1) The Mach number is equal to the meter tube gas velocity divided by the speed of sound.

output based on continuously measured density and mass, the density of the liquid hydrocarbon passing through the meter needs to be stable relative to the measurement reference. Large temperature differences between the measuring points of reference and the Coriolis meter under test indicate relatively large differing fluid properties (e.g., density). Greater than expected uncertainties will be observed if the system does not have sufficient fluid temperature and density stability. There should be no greater than a 3°C (5.4°F) difference between the fluid temperature at the meter and the fluid temperature at the measurement reference. These same considerations apply when testing the Coriolis meter in mass and converting the volumetric flow rate output of the reference flow rate to mass with a sampled density.

Heavier hydrocarbons are prone to entrained gas, which impacts both the Coriolis measurement and the volumetric reference. If testing on heavier hydrocarbons is required, the fluid temperature may have to be elevated to drive air out of the solution. Although temperature and density stability are more challenging at elevated temperatures, the requirement is the same as previously described. If the user or laboratory has concerns about entrained air during testing, the drive current output of the Coriolis meter should be monitored. The drive current will rise quickly with small amounts of entrained air. The drive current is a useful diagnostic tool.

13-4.2.1.3 Gas. As mentioned above, the water calibration of Coriolis meters can be transferred to gas applications. It is important to note that Coriolis meters are not recommended for actual volume measurement of gases. Coriolis meters calculate actual volume from measured density and mass flow. Although the density measurement of Coriolis meters works well on liquids, it can have a large uncertainty on gasses. This is because Coriolis meters do not have enough sensitivity to measure gas density. As a result, Coriolis meters should only be configured for mass or standard volume (fixed reference density) output when measuring gasses.

Most gas laboratories offer either natural gas or air calibrations. Both fluids work equally well for testing Coriolis meters, but there are test setup considerations as listed in paras. 13-4.2.1.3.1 and 13-4.2.1.3.2.

13-4.2.1.3.1 Gas Velocity. Although most gas flow testing of Coriolis meters is specified in mass rate, flow tube velocity needs to be considered. Excessive velocity in the flow tubes will create excessive pressure drop as well as induce measurement performance issues.

Because gas testing pressures and densities vary widely, the velocity realized in the flow tube for a given mass rate also varies. The velocity in the flow tube drops by roughly half every time the pressure doubles. Higher pressures and lower gas velocity will yield the best measurement with Coriolis meters. Table 13-4.2.1.3.1-1 shows guidelines for tube velocity and impacts to performance. These velocities are relative to the speed of sound (Mach number) of the gas used during the test. The Mach number serves as a normalized indicator for gas flow velocities regardless of the gas being used. Calculating velocity of the gas in the meter tube will require input from the manufacturer on tube diameter and knowledge of the gas's speed of sound (see Table 13-4.2.1.3.1-1).

13-4.2.1.3.2 Gas Test Pressure. Coriolis meters need sufficient mass flowing through them to perform a useful measurement. Higher pressure gases have higher densities and provide higher mass flow rates for any given volumetric flow rate. The test pressure directly impacts what mass flow rates can be reasonably tested, and higher pressures are always preferable. Since lower pressure gases have lower densities, high velocities in the flow tubes are required to achieve meaningful mass rates. Excessive gas velocity in the flow tubes can contribute to measurement issues as mentioned in para. 13-4.2.1.3.1. See Table 13-4.2.1.3.2-1 for gas pressures and recommendations for applications and testing.

Table 13-4.2.1.3.2-1
Measurement Recommendations for Different Gas Test Pressures

Test Pressure	Measurement Recommendation
P_T < 700 kPa (100 psi)	Not recommended — Coriolis meters can be used in applications below 700 kPa (100 psi), but accuracy can be greatly reduced. Consult manufacturer for specific sizing information.
700 kPa (100 psi) ≤ P_T ≤ 1 700 kPa (250 psi)	Recommended — suitable pressure range for Coriolis meters. Evaluation of fluid velocity still required.
1 700 kPa (250 psi) ≤ P_T ≤ 8 270 kPa (1,200 psi)	Ideal — this pressure range will provide the greatest flow range capability. Evaluation of fluid velocity still required, but velocity-induced issues are less likely.
8 270 kPa (1 200 psi) < P_T	Coriolis meters work well in applications above 8 270 kPa (1 200 psi), but few laboratories are capable of testing at pressures this high.

13-4.2.2 Test Setup and Configuration. Coriolis meters are highly configurable to suit a wide variety of applications. However, misunderstood or incorrect setup can have significant impact on performance. Test laboratories should provide a record of the as-calibrated configuration condition as part of their report. A list of guidelines for both performance testing and application sizing considerations is provided in paras. 13-4.2.2.1 through 13-4.2.2.6 along with flow rate and data collection times.

13-4.2.2.1 Nominal Flow Rate. Nominal flow rate is the ideal liquid flow rate for a given meter size. At this rate, the pressure drop with water is typically 99.9 kPa (14.5 psi). Liquid flow testing should be based on this rate.

13-4.2.2.2 Maximum Flow Rate. The recommended maximum that can flow through the meter is determined by taking pressure drop and cavitation (or structural damage) into consideration. Pressure drop at the maximum flow rate can range from 2 times to 4 times the nominal flow rate, depending on meter design. Using or testing a meter at maximum flow rate is not desirable due to the significant increase in energy required to flow through the meter. At rates at or above nominal, cavitation may occur if the downstream pressure is 140 kPa (20 psi) or less. This can be remedied by creating more back pressure (through closure of a valve), or by increasing inlet pressure, or both. Cavitation will impact meter performance and can damage the sensor tubes if it is sustained over long periods.

13-4.2.2.3 Minimum Flow Rate. Most Coriolis meters are within standard specification at 10:1 turn down; in some situations, 20:1 turn down might be an acceptable range for flow testing. These ratios are greatly reduced in gas applications due to velocity constraints (see para. 13-4.2.1). However, large turn down impacts accuracy (see para. 13-4.2) and must be fully understood before conducting a test.

13-4.2.2.4 Test Data Collection Time. Data collection time is the duration of the measurement in a testing system (i.e., the batch or flowing period) for a given condition that is used to calculate uncertainty. Totalization time must be sufficient to achieve the desired uncertainty levels. If pulse output is used, the total pulses must meet uncertainty requirements.

(a) Example 1. A flow test is conducted on a Coriolis meter collecting data for 1 hr at 30-sec intervals, and the mass flow uncertainty calculated on the 1 hr aggregate results meets the criteria listed in Table 13-4.2.2.4-1. The uncertainty and associated statistics are based on the 1 hr results and not the 30-sec samples.

(b) Example 2. A flow test is conducted on a Coriolis meter for 20 sec (i.e., flowing to a weigh scale tank), and the mass flow uncertainty calculated on this 20-sec measurement does not meet the criteria listed in Table 13-4.2.2.4-1.

Some test requirements may demand short measurement batches and that special procedures be employed, such as multiple test points to reduce uncertainty in those cases. Although flow rate and lab capability may limit collection times, best practices should be adhered to when possible. Table 13-4.2.2.4-1 lists the best practices for liquid and gas testing.

Table 13-4.2.2.4-1
Best Practices for Liquid and Gas Testing Data Collection Time

	Collection Time, s	
Testing Medium	Minimum	Recommended
Liquid	30	60
Gas	90	120

13-4.2.2.5 Output Configuration

13-4.2.2.5.1 Flow. Coriolis meters can be configured to measure flow in either mass or volumetric units, depending on the application requirements. Paragraph 13-4.2.1 covers some considerations for testing in volume units. A Coriolis meter is a rate of flow-type device, and evaluation of the flow output with minimum damping will appear noisy. This noise band may be up to 2% of the average flow reading. Although this noisy behavior exists on the flow signal, the meter is measuring correctly. This output noise can be reduced by increasing the flow damping parameter in the transmitter. This function will average the flow signal over longer periods, smoothing the output. Increasing the flow damping parameter will decrease flow output response time and should be evaluated against the application requirements.

13-4.2.2.5.2 Frequency Output. A Coriolis meter is a synthesized pulse device. The transmitter synthesizes a frequency or pulse output based on the current value of the measured parameter. Because the frequency output is not limited by mechanical operation, it is also highly configurable. Most Coriolis transmitters are capable of 0 Hz to 10,000 Hz output scaling. The transmitter frequency output can be configured based on units/pulse, pulses/unit, or frequency equal to flow rate. The highest frequency output should be used without over-ranging the output. This will provide the greatest resolution and ensure additional uncertainties are not being induced due to lack of pulse resolution. In a test environment, the frequency output should be configured so that at minimum 10,000 pulses are recorded for each data point.

13-4.2.2.6 Meter Zeroing. Due to asymmetries in manufacturing, Coriolis meters have some measurable flow reading at zero flow. This flow rate offset reading must be captured in the transmitter in order to properly calculate mass flow as discussed in para. 13-2.1. The process of zeroing should be conducted in stable conditions by experienced personnel. Conducting unneeded zero calibrations, or zero calibrations in unstable conditions, can make the measurement worse. Although many manufacturers have their own recommendations to assist in zeroing Coriolis meters, the guidelines below are best practices for all Coriolis meters. For instances where these guidelines cannot be adhered to, the zero established in the factory calibration should be used.

(a) Temperature Stability. The Coriolis meter temperature output, T_C, should be monitored prior to zeroing the meter. The following criteria should be met for conducting a zero calibration:

(1) $T_C \leq 5°C$ (9°F) difference between fluid temperature and Coriolis temperature

(2) $T_C \leq 1.5°C$ (2.7°F) variation of the Coriolis temperature during the zero calibration

(b) No Flow State. In order to properly conduct a zero calibration, a known no flow state must be created in the meter. This is best accomplished by closing upstream and downstream isolation valves. Closing a single downstream isolation valve is also suitable if upstream and downstream isolation is not possible. The flow output of the Coriolis meter shall be monitored prior to executing the zero procedure. This can be accomplished through diagnostic parameters or through the primary mass output. If the primary mass output is used, the low flow, or mass flow, cutoff and damping will have to be temporarily set to zero and the flow direction will need to be set to bidirectional flow. Consult the manufacturer for which flow parameter to monitor prior to zeroing. The selected parameter should be monitored to ensure that no flow is present and then zero calibration can take place.

(c) Zero Value. The units of the zero parameter vary by manufacturer. This parameter may be displayed in flow units, time units, or percent. The "goodness" of a specific zero value will depend on manufacturer and specific model. Although this value is model specific, the robustness of the zero process conducted can still be evaluated. This requires process conditions that allow for multiple zero calibrations in a row.

(1) Trending. Multiple zero values trending in one direction (i.e., increasingly negative) may indicate a leak in the block valves. Flows in the meter section can also be caused by pressure differentials in the system. Localized flows can be created when the pressures equalize. Trending the zero value may also indicate a transient temperature condition (i.e., the meter is slowly equalizing to ambient when fluid is warmer than ambient). The leaks may need to be repaired, or additional purging time may be required to stabilize temperature.

(2) Instability. Normally, zero values will alternate around a central point in sinusoidal fashion. If the values collected are highly varied, then there may a system problem. In a liquid system, this could be trapped air in the meter or partially full tubes. This will cause an imbalanced condition and yield poor zeros or fail the zero calibration entirely. This is also true when liquid is present in the tubes in a gas system. Block valve leaks can also manifest themselves as instability in the zero values because not all leaks flow at a predictable rate. If none of these issues are present, the manufacturer may need to be consulted for further diagnosis.

13-4.2.3 Measurement Uncertainty. Coriolis flowmeters are available with varying, specified mass-flow uncertainties and can range between 0.35% (gas) to 0.1% (liquid) under ideal conditions. There are two categories of parameters that influence the overall uncertainty of a Coriolis meter's measurement. The first is the determination of primary calibration

Figure 13-4.2.3-1
Typical Calibration Curve With Uncertainty Bands (2σ Limits Shown)

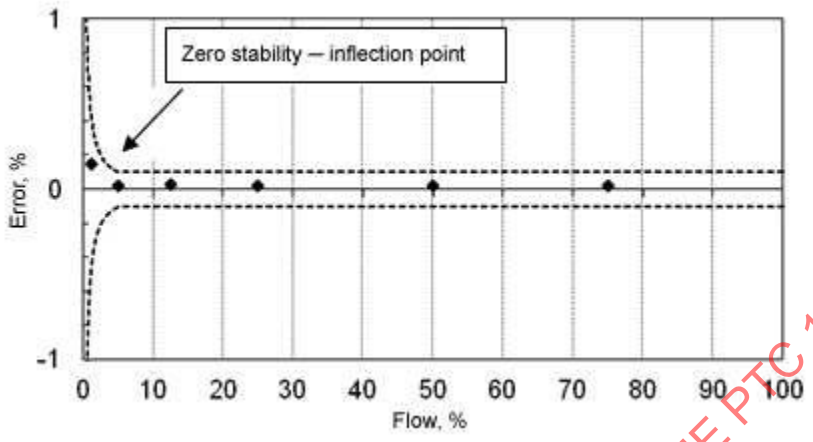

factor, and the second is the contribution to measurement uncertainty by secondary effects. Detailed uncertainty evaluations of a Coriolis meter with different line temperature and pressure impacts are shown in subsection 13-6.

Primary calibration factors for a Coriolis meter are the linear calibration factor and the zero value. When a meter is manufactured, a unique calibration factor is determined through the manufacturer's calibration (calibration systems accredited to ISO/IEC 17025 are preferred). The process for evaluating the overall calibration uncertainty should be in accordance with the general practices outlined in ASME PTC 19.1. In addition to the calibration factor, the manufacturer must determine a zero value during the calibration process. Although the zero value is typically captured again in the final customer's installation, evaluation of the zero value during calibration is necessary. As flow is decreased and there is a subsequent reduction in primary flow signal, zero stability has an increasing influence on the flow calculation. This is often quantified by the manufacturer's zero-stability specification and can be seen on the typical trumpet curve provided on the calibration documentation (see Figure 13-4.2.3-1). Although the zero value cannot be improved during calibration, its stability or random uncertainty contribution at lower flows can be measured during the calibration process. A meter with flow points outside the lower portions of the trumpet curve (10% of flow or less) may have an incorrect zero, or the sensor is unstable. Uncertainty in low flow measurement will be dictated by the stability of the zero for that meter type.

Secondary effects on measurement uncertainty are also typically quantified by the manufacturer. Most Coriolis meters automatically compensate for changes in fluid temperature that affect overall performance, but changes in fluid temperature will also influence the zero value. This difference has the greatest effect if the operating temperature of the meter is different from the temperature at which the zero is determined and the meter is being operated at low flows. In order to understand the impact of temperature-related effects, flow performance must be evaluated against the operating flow and the manufacturer's process temperature effect specification. See examples in subsection 13-6 for additional information.

Process pressure can also contribute to measurement uncertainty. In cases where a Coriolis sensor is affected by pressure, a systematic negative uncertainty can be observed with higher line pressures. The effect of pressure, and whether it will influence the measurement for a given meter, should be documented in the manufacturer's literature. See para. 13-4.3.2 for additional information on temperature and pressure influences.

13-4.3 Fluid Properties Affecting Meter Performance

13-4.3.1 Density. The Coriolis flowmeter measures both mass flow and density independently. The density of fluid is measured from the frequency of oscillations of the sensor (tube period) and not Δt, or phase shift, measurement (mass flow). Because density and mass flow measurements are measured independently, fluid density has no impact on the mass flow measurement. However, variation in fluid density will impact the volumetric output as volume is calculated from the measured mass flow and density.

13-4.3.2 Fluid Temperature and Pressure. The effects of temperature and pressure vary depending on geometry and construction of the meter. Temperature can affect temperature-dependent properties of the tubing material and cause changes to material sensitivity or stiffness as well as damping. Thermal expansion or pressure forces can cause increased

Figure 13-4.3.2.1-1
Temperature Effect on Zero (2σ Limits Shown)

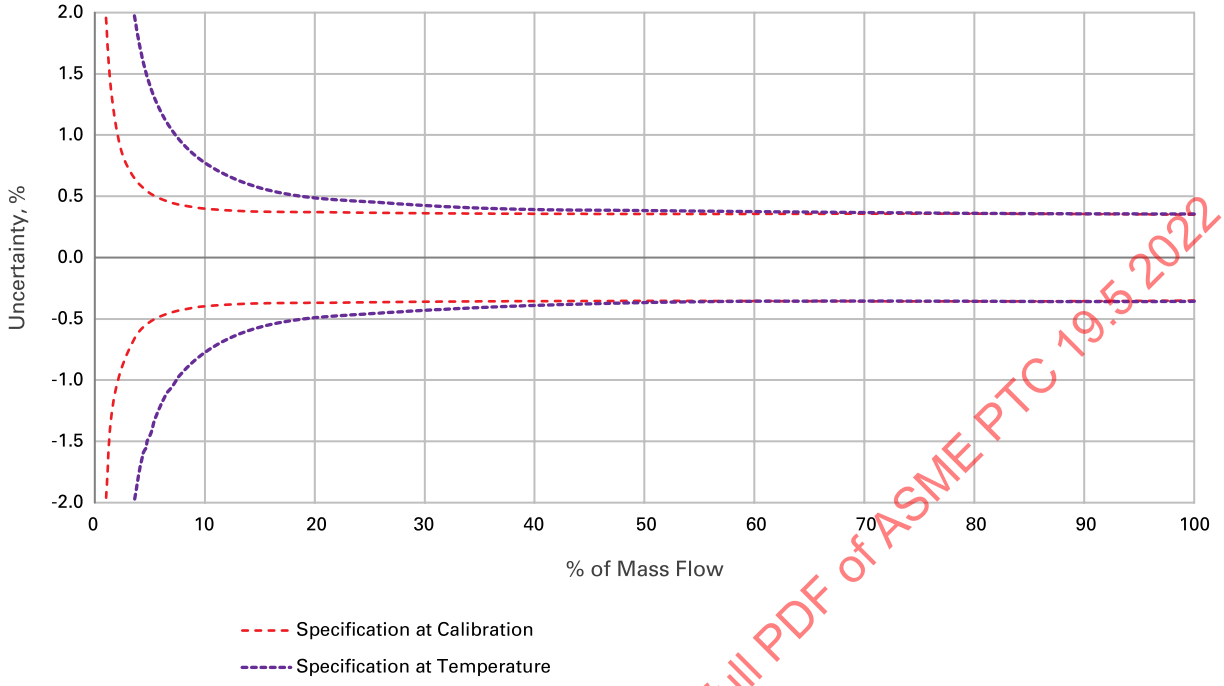

tube stresses and area changes. Temperature effects tend to be higher in straight tube meters when compared to bent tube meters because of their inability to flex and accommodate some expansion. The Coriolis flowmeter electronics should compensate for temperature variations, as described earlier in this paragraph. These type of temperature effects are linear, and associated compensation is also linear. Coriolis meters also have a temperature-related zero shift that must be properly adjusted in the field or accounted for in uncertainty calculation.

Pressure shifts can also result in measurement uncertainty. As pressure inside the flow tubes increases, the forces acting on the tube increase, creating stress in the tube walls that acts to stiffen the tubes, changing their response. Changes in pressure tend to have a greater effect on bent tube meters when compared to straight tubes, as the increased pressure acts to make the tubes rounder and the tubes try to straighten. Since the tubes are constrained by the meter's construction, they cannot fully realize this new shape, and subsequently stiffen. Stiffening of the tube can cause a Coriolis meter to underread relative to true mass flow. Not all Coriolis meters will display this pressure effect, but those that do will require compensation. Compensation is typically implemented when the operating pressure is at least 700 kPa (100 psi) greater than the calibration pressure.

Examples of how pressure and temperature can impact performance are described in paras. 13-4.3.2.1 and 13-4.3.2.2. For both high-temperature and high-pressure applications, consult the manufacturer.

13-4.3.2.1 Elevated Temperature Example. Coriolis manufacturers shall automatically compensate the flow signal for temperature-related span effects. Automatic compensation built into the Coriolis sensor requires no user interaction. Coriolis meters also have a temperature-related zero drift. This is only a concern if the meter is being operated at a temperature other than the temperature at which it was zeroed. To compensate for temperature effects relating to zero drift, the meter must be zeroed at the process temperature. The magnitude of this zero drift is meter-design specific and should be provided in the manufacturer's specifications.

Figure 13-4.3.2.1-1 is a performance curve example of a Coriolis meter that employs automatic span compensation, operates at 60°C (140°F), and was zeroed at 20°C (68°F). In the example, there are two specification lines. The dashed line (specification at calibration) represents the standard specification for this particular model and would be the specification if the meter were zeroed at operating temperature. The solid line (specification at temperature) represents the specification in the process conditions described above with a 40°C (72°F) difference between zeroing and operating temperature. The specification at temperature illustrates the maximum possible drift that may be observed for this meter in these conditions. The meter may not actually drift to this degree, but this is the new specification for the Coriolis meter

Figure 13-4.3.2.2-1
Pressure Effect on Span (2σ Limits Shown)

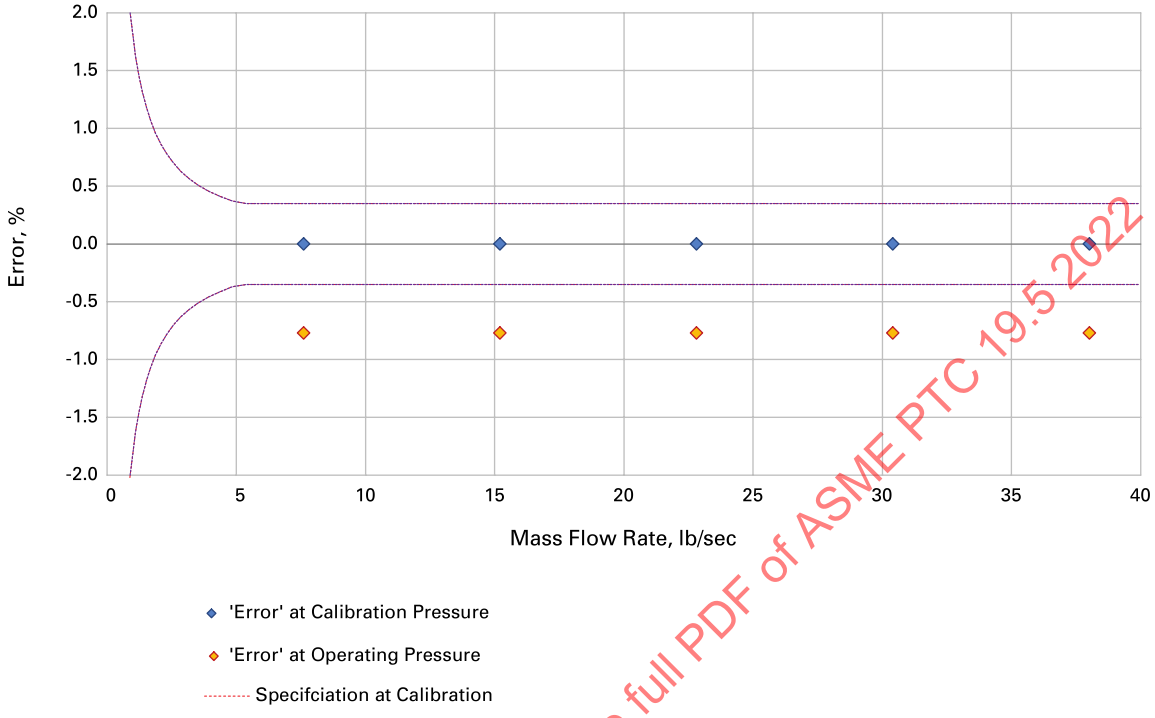

in the process condition. As the example illustrates, this is less of a concern as flow rate increases but could impact lower flow performance.

13-4.3.2.2 Elevated Pressure Example. Not all Coriolis meters require pressure compensation. Some designs do not have a pressure effect, and many meters are operated close enough to the calibration pressure that compensation is not needed. For meters that do have a pressure effect and are operated at a pressure that is 700 kPa (100 psi) or greater from the calibration pressure, pressure compensation should be considered. Pressure compensation can typically be implemented in one of two ways. The compensation can be a

(a) fixed value entered into the transmitter, or

(b) dynamic compensation that is based on live line pressure

For instances where line pressure is relatively stable [up to ±207 kPa (±30 psi) variation], fixed pressure compensation is suitable. In systems where larger pressure variation is present, dynamic pressure compensation should be used. With dynamic pressure compensation, a live pressure value is fed into the Coriolis transmitter via a digital protocol or an analog output from a pressure transmitter. This value is then used in real-time pressure compensation calculations.

Pressure effect on Coriolis meters creates a systematic span uncertainty, which can easily be observed in a high-pressure testing laboratory. Figure 13-4.3.2.2-1 is a performance curve example of a Coriolis meter that has a pressure effect [−0.00023% of rate/kPa (−0.0016 % of rate/psi)] tested at 3 447 kPa gauge (500 psig) on natural gas and no compensation is implemented. This 0.75% difference between the original water calibration (uncertainty at calibration pressure) and the high-pressure gas calibration (uncertainty at operating pressure) is the systematic span uncertainty induced by the stiffening of the tubes at elevated pressure.

Some shift in zero value may be observed between a zero captured at ambient and a zero captured at high pressure [≥700 kPa (≥100 psi)]. A Coriolis meter should not shift more than the stated zero stability of the sensor when changing from one pressure to another. If the sensor is to be operated at elevated pressure, it is best practice to zero at the operating pressure.

13-4.3.3 Viscosity. Coriolis flowmeter measurements can be affected by changes in viscosity, particularly with high viscosity liquids operated at low Reynolds numbers. The manufacturer should be consulted as to what compensation techniques are appropriate when measuring high-viscosity liquids. Gas applications are not impacted by viscosity, regardless of design.

13-5 APPLICATION CONSIDERATIONS

It is essential for the user of the flowmeter to clearly define and understand the flowing fluid, process conditions, and requirements of the application to determine a suitable flowmeter. The useable range, or turn down, of a Coriolis meter will be determined by both pressure drop and stability of the zero.

In applications where maximum flow must be achieved, the pressure drop of the Coriolis meter should be evaluated. In applications where little pressure drop can be tolerated, using a Coriolis meter with straight-tube geometry or a meter larger than the nominal pipe size may be desirable.

However, increasing the size of the Coriolis meter will increase (worsen) the overall zero stability of the sensor. This in turn moves the inflection point of the meter's specification curve (see Figure 13-4.2.3-1) higher in flow compared to a smaller meter. This increase in uncertainty at low flow may be acceptable, depending on the application requirements. Also, use of a large meter will result in the measured flow being at a lower percent of full scale, so the overall zero stability has a large impact on the measured flow.

Conversely, if optimum low-flow performance is required for a given application, the smallest meter possible should be used.

13-5.1 Materials of Construction

The user must define the fluid and ambient conditions of the application so that a suitable meter can be selected. This selection should be driven by the flowing material and the external environment.

13-5.1.1 Pressure. Pressure ratings of the Coriolis flowmeter will depend on the application and manufacturer. Most sensor designs are equipped with a process connection that may inform a specific range of available pressure ratings. The tube pressure rating within the meter will be dependent on manufacturer, design, and material. A primary containment pressure rating for the measurement tube(s) and process connections of 9,990 kPa (1,450 psi) is common. Some manufacturers offer high-pressure designs as well as pressure ratings on the sensor housing as a means of secondary containment in the event of a tube failure. Manufacturers can also provide rupture discs on the case or housing for high-pressure applications where a tube failure would create excessive pressure inside the case.

13-5.1.2 Pressure Loss. Unrecoverable pressure loss induced by a Coriolis meter varies by design and manufacturer. Coriolis meters are commonly sized around a nominal flow that equates to 99.9 kPa (14.5 psi) of pressure loss, but some specialty designs do not follow this convention. Pressure loss at higher rates may be beyond the application requirements, and a larger meter should be considered. Consult manufacturer's sizing recommendations to ensure an appropriate size has been selected.

Figure 13-5.1.2-1 shows pressure loss versus rate. This is a sample of various meter designs, manufacturers, and line sizes.

13-5.1.3 Temperature Rating. The flowmeter's temperature range is specific to material and manufacturer. A temperature range of −200°C to 200°C (−328°F to 392°F) is commonly available from most manufacturers, and high temperature Coriolis meters rated up to 350°C (662°F) are also available. Most Coriolis meters' electronics systems will accommodate for the modulus of elasticity-related performance shifts for the entire operating range of the sensor. However, the Coriolis meter must be zeroed at line temperature to achieve lowest possible measurement uncertainty.

13-5.2 Installation

The manufacturer installation guidelines should be followed when installing a Coriolis flowmeter and its electronics. The considerations in paras. 13-5.2.1 through 13-5.2.3 may help in defining these requirements.

13-5.2.1 Electrical Grounding. The manufacturer should provide grounding recommendations, instructions, and hardware to protect the sensor and the electronics. A Coriolis meter is typically designed to work with a process connection bolted into a pipeline, and this typically serves as the primary ground. Improper grounding can cause performance issues such as excessive zero drift.

13-5.2.2 Piping Requirements. The piping is a function of the specific meter's design. Manufacturers design Coriolis meters to national and international standards such as ASME B31.3 and ASME B31.1 and will have obtained various approvals and certifications that drive the facility's requirements. The piping alignment should conform to standard piping practices. During installation, sensor piping should be adequately supported by pipe clamps on either side of the meter to ensure a sturdy installation and minimize the transfer of any static or dynamic forces from the piping system to the meter. Block valves should be upstream and downstream of the meter to facilitate zeroing of the Coriolis flowmeter.

Figure 13-5.1.2-1
Pressure Drop Versus Mass Flow

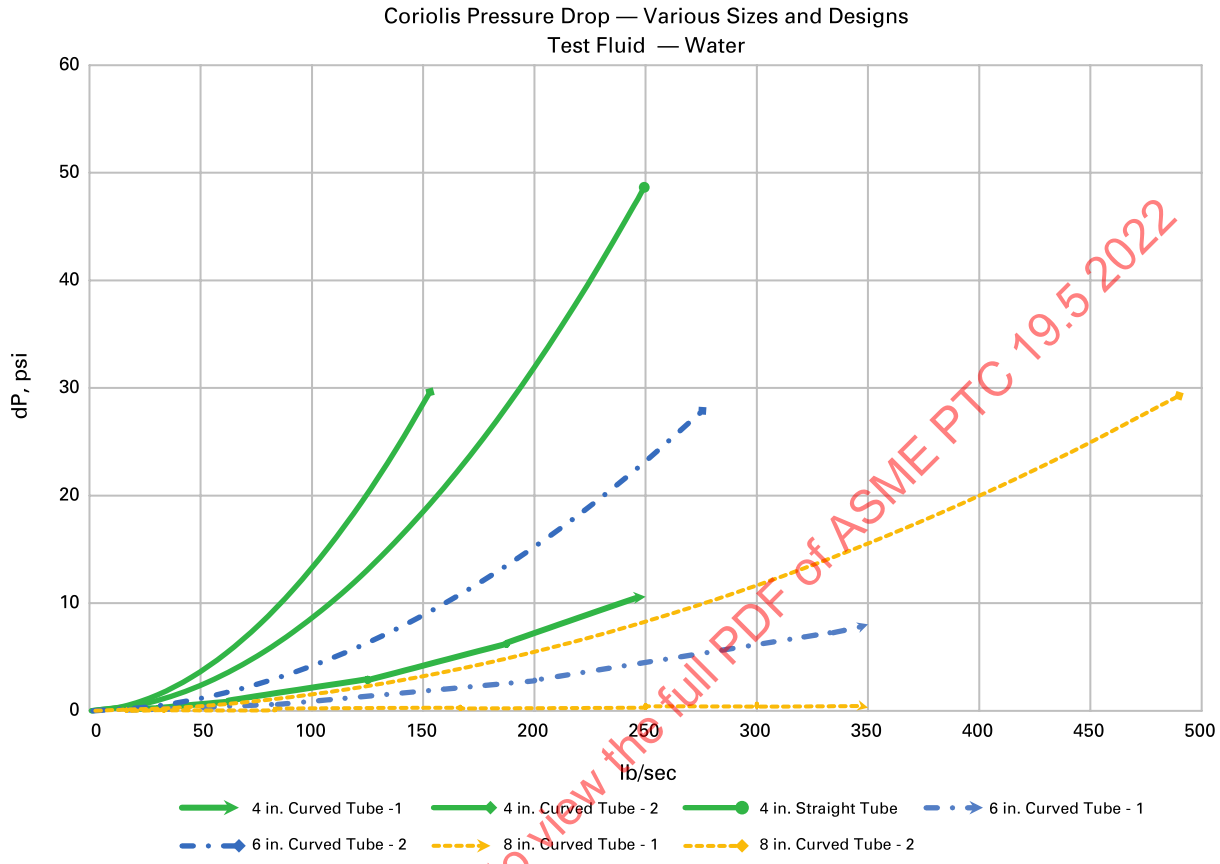

13-5.2.3 Flow Conditioning. Because Coriolis meters do not rely on a specific flow distribution to function properly, flow conditioning is not required. Coriolis meters are highly tolerant of elbows, tees, and other various piping configurations on both the inlet and the outlet.

Although flow conditioning is not required for Coriolis meters, there are still installation considerations that must be taken into account for optimum performance. Improper system arrangement, poor assembly, and some process connections will impact performance. The guidelines in paras. 13-5.2.3.1 through 13-5.2.4 provide best practice recommendations.

13-5.2.3.1 Flow Control Valves. A flow control valve should be located downstream of the Coriolis meter. When the control valve is located upstream, it can reduce line pressure before the meter and cause cavitation in the flow tubes. A large pressure drop across an upstream valve can also generate significant flow noise that will impact the overall measurement.

13-5.2.3.2 Pipe Assembly and Gasket Alignment. Poorly assembled pipe work can create cavities that create air traps that degrade liquid flow measurement. Gaskets that are improperly installed or damaged such that they are "hanging" in the flow can create flow noise that interferes with measurement. This is primarily a concern in gas flow applications but should be avoided in liquid flow as well.

13-5.2.3.3 Process Connections. Coriolis meters are compatible with nearly all process connections. However, connections such as ring type joint (RTJ) flanges require special consideration. RTJ flanges create an annular cavity between the flange faces. This gap between flange faces can create broad flow noise at higher gas velocities. It is less of a concern in liquid flows, but particulates can still accumulate in this cavity. If RTJ or similar flanges are used, then a gasket/seal ring with an interior filled to the diameter of the pipe bore should be employed.

13-5.2.4 Tube Orientation. For curved tube Coriolis meters, orientation of the tubes must be considered for the application. Generally, the tubes are mounted downward for liquid applications (to ensure they remain full), and upward for gas applications (to ensure no liquid is trapped). In applications where draining is required, a vertical mount, or 'flag,' position should be used. Other orientations can also be used successfully, but the manufacturer should be consulted for the specific application. Straight-tube Coriolis meters are less susceptible to trapping gas or liquid; however, attention should be paid to the connected piping configuration to ensure the meter does not contain any trapped fluids.

Special attention should be paid when a Coriolis meter with multiple flow tubes is used with a multiphase fluid in a horizontal pipe run to prevent the phases from separating and passing through different flow tubes. This would create a difference in densities between the flow tubes and alter their response from one another, introducing uncertainty in the flow measurement.

13-6 FIELD UNCERTAINTY EXAMPLES

The examples in this subsection provide an estimated uncertainty of a Coriolis meter used in natural gas and in liquid condensate flow measurement applications. These estimates are performed at maximum and minimum flow rate conditions to demonstrate the impacts of zero stability on flow rate, zero-related temperature drift, and the pressure effect on span.

13-6.1 Example 1

(a) In this example, the Coriolis flowmeter is used to measure natural gas fuel feed to a power generation turbine. The fuel gas is unheated, and the flowmeter has been zeroed at the operating temperature. Dynamic pressure compensation is enabled. Table 13-6.1-1 shows the analysis for maximum flow rate; Table 13-6.1-2 shows the analysis for minimum flow rate.

(b) Flowmeter Information and Operating Conditions

(1) 150 mm (6 in.) U-tube Coriolis meter
(2) Pulse output
(3) Natural gas — unheated
(4) Operating pressure = 3 500 kPa gauge (500 psig)
(5) Operating maximum flow = 16.5 kg/s (38 lbm/sec)
(6) Operating minimum flow = 3.5 kg/s (8 lbm/sec)
(7) Zero stability = 0.0183 kg/s (0.042 lbm/sec)
(8) Base uncertainty for gas measurement = 0.35%
(9) Pressure effect on span = −0.00023%/kPa (−0.0016%/psi)
(10) Pressure effect residual uncertainty = 0.000015%/kPa (0.0001%/psi)
(11) Environmental temperature effect (zero drift) = ±0.0003% of maximum flow per °C
(12) Rated maximum liquid flow = 391.9 kg/s (900 lbm/sec)
(13) Calibration pressure (water) = 138 kPa gauge (20 psig)
(14) Operating temperature = 26.7°C (80°F)
(15) Flowmeter zeroing temperature = 26.7°C (80°F)

13-6.2 Example 2

(a) In this example, the flowmeter is used for a natural gas fuel feed onto a power generation turbine. The fuel gas is heated and the flowmeter has not been zeroed at the operating temperature. Dynamic pressure compensation is enabled. Table 13-6.2-1 shows the analysis for maximum flow rate; Table 13-6.2-2 shows the analysis for minimum flow rate.

(b) Flowmeter Information and Operating Conditions

(1) 150 mm (6 in.) U-tube Coriolis meter
(2) Pulse output
(3) Natural gas — heated
(4) Operating pressure = 3 500 kPa gauge (500 psig)
(5) Operating maximum flow = 16.5 kg/s (38 lbm/sec)
(6) Operating minimum flow = 3.5 kg/s (8 lbm/sec)
(7) Zero stability = 0.0183 kg/s (0.042 lbm/sec)
(8) Base uncertainty for gas measurement = 0.35%
(9) Pressure effect on span = −0.00023%/kPa (−0.0016%/psi)
(10) Pressure effect residual uncertainty = 0.000015%/kPa (0.0001%/psi)

(11) Environmental temperature effect (zero drift) = ±0.0003% of maximum flow per °C
(12) Rated maximum liquid flow = 391.9 kg/s (900 lbm/sec)
(13) Calibration pressure (water) = 138 kPa gauge (20 psig)
(14) Operating temperature = 144.4°C (292°F)
(15) Flowmeter zeroing temperature = 26.7°C (80°F)

Table 13-6.1-1
Example 1 — Analysis of Unheated Natural Gas Applications at Maximum Flow Rate

Source of Uncertainty	Calculation to Achieve Systematic Uncertainty	Systematic Uncertainty Contribution (k = 2)	Note
Flowmeter base specification (spec.)	Base uncertainty for gas measurement = 0.35%	Spec = 0.35%	Water calibration transferred to gas manufacturer's specification.
Zero stability contribution (Z.S.) including environmental temperature effect (E.E.)	Z.S. without temp. effect = 0.0183 kg/s Additional contribution to Z.S. from the environmental specification (E.S.): $\left(\frac{\text{E.E.}}{100}\right)(\text{rated max. flow})(\text{max. operating temp.} - \text{sensor zeroing temp.}) = \text{E.S.}$ $\left(\frac{0.0003\%}{100}\right)\left(\frac{391.9\ \text{kg}}{\text{s}}\right)(26.7°\text{C} - 26.7°\text{C}) = 0\ \text{kg/s}$ E.S. = 0 kg/s Systematic uncertainty contribution due to Z.S. at 16.5 kg/s: $\frac{\text{Z.S. w/o temp. effect} + \text{E.S.}}{\text{operating max. flow}} * 100 = \text{Z.S.}$ $\frac{0.0183\ \text{kg/s} + 0\ \text{kg/s}}{16.5\ \text{kg/s}} * 100 = 0.11\%$	Z.S. = 0.11%	Because the meter was zeroed at operating temperature, there is no change to overall zero stability due to temperature induced drift.
Pressure effect (P.E.)	Span effect (S.E.) without pressure component: (P.E. on span) (operating press. − calibration press.) = S.E. −0.00023%/kPa*(3500 kPa − 138 kPa) = −0.77% S.E. = −0.77% Pressure compensation residual uncertainty at 3 500 kPa (P.E.): (P.E. residual uncertainty) (operating press.) = P.E. $0.000015\frac{\%}{\text{kPa}} * 3\,500\ \text{kPa} = 0.05\%$	P.E. = 0.05%	With the implementation of dynamic pressure compensation, only the residual uncertainty of the pressure compensation needs to be included.
Systematic uncertainty at 95% confidence level (root-sum-square)	$\sqrt{\text{spec.}^2 + \text{Z.S}^2 + \text{P.E.}^2} = \text{systematic uncertainty}$ $\sqrt{0.35^2 + 0.11^2 + 0.05^2} = 0.37\%$		The resulting systematic uncertainty in Example 1 is 0.37%.

Table 13-6.1-2
Example 1 — Analysis of Unheated Natural Gas Application at Minimum Flow Rate

Source of Uncertainty	Calculation to Achieve Systematic Uncertainty	Systematic Uncertainty Contribution (k = 2)	Note
Flowmeter base specification (spec.)	Base uncertainty for gas measurement = 0.35%	Spec = 0.35%	Water calibration transferred to gas manufacturer's specification.
Zero stability (Z.S.) contribution including environmental temperature effect (E.E.)	Z.S. without temp. effect = 0.0183 kg/s Additional contribution to Z.S. from the environmental specification (E.S.): $\left(\frac{\text{E.E.}}{100}\right)(\text{rated max. flow})(\text{max. operating temp.} - \text{sensor zeroing temp.}) = \text{E.S.}$ $\left(\frac{0.0003\%}{100}\right)\left(\frac{391.9\,\text{kg}}{\text{s}}\right)(26.7°C - 26.7°C) = 0\,\text{kg/s}.$ E.S. = 0 kg/s Systematic uncertainty contribution due to Z.S. at 3.5 kg/s: $\frac{\text{Z.S. w/o temp. effect} + \text{E.S.}}{\text{operating min. flow}} * 100 = \text{Z.S.}$ $\frac{0.0183\text{kg}/\text{s} + 0\,\text{kg/s}}{3.5\,\text{kg/s}} * 100 = 0.52\%$	Z.S. = 0.52%	Because the meter was zeroed at operating temperature, there is no change to overall zero stability due to temperature induced drift.
Pressure effect (P.E.)	Span effect (S.E.) without pressure component: (P.E. on Span) (operating press. − calibration press.) = S.E. $-0.00023\frac{\%}{\text{kPa}} * (3\,500\,\text{kPa} - 138\,\text{kPa}) = -0.77\%$ S.E. = −0.77% Pressure compensation residual uncertainty at 3 500 kPa (P.E.): (P.E. residual uncertainty) (operating press.) = P.E. $0.000015\frac{\%}{\text{kPa}} * 3\,500\,\text{kPa} = 0.05\%$	P.E. = 0.05%	With the implementation of dynamic pressure compensation, only the residual uncertainty of the pressure compensation needs to be included.
Systematic uncertainty at 95% confidence level (root-sum-square)	$\sqrt{\text{spec.}^2 + \text{Z.S}^2 + \text{P.E.}^2} = \text{systematic uncertainty}$ $\sqrt{0.35^2 + 0.52^2 + 0.05^2} = 0.63\%$		The resulting systematic uncertainty in Example 1 is 0.63%.

Table 13-6.2-1
Example 2 — Analysis of Heated Natural Gas Applications at Maximum Flow Rate

Source of Uncertainty	Calculation to Achieve Systematic Uncertainty	Systematic Uncertainty Contribution (k = 2)	Note
Flowmeter base specification (spec.)	Base uncertainty for gas measurement = 0.35%	Spec = 0.35%	Water calibration transferred to gas manufacturer's specification.
Zero stability (Z.S.) contribution including environmental temperature effect (E.E.)	Z.S. without temp. effect = 0.0183 kg/s Additional contribution to zero stability from the environmental specification (E.S.): $\left(\frac{\text{E.E.}}{100}\right)(\text{rated max. flow})(\text{max. operating temp.} - \text{sensor zeroing temp.}) = \text{E.S.}$ $\left(\frac{0.0003\%}{100}\right)(391.9\,\text{kg/s})(144.4°\text{C} - 26.7°\text{C}) = 0.13814\,\text{kg/s}$ E.S. = 0.1384 kg/s Total uncertainty contribution due to Z.S. at 16.5 kg/s: $\frac{\text{Z.S. w/o temp. effect} + \text{E.S.}}{\text{operating max. flow}} * 100 = \text{Z.S.}$ $\frac{0.0183\,\text{kg/s} + 0.1381\,\text{kg/s}}{16.5\,\text{kg/s}} * 100 = 0.95\%$	Z.S. = 0.95%	Because the meter was zeroed at a temperature lower than operating temperature, the temperature induced drift of zero has been included in the overall zero stability.
Pressure effect (P.E.)	Span effect (S.E.) without pressure component: (P.E. on span) (operating press. – calibration press.) = S.E. $-0.00023\frac{\%}{\text{kPa}} * (3\,500\,\text{kPa} - 138\,\text{kPa}) = -0.77\%$ S.E. = − 0.77% Pressure compensation residual uncertainty at 3 500 kPa (P.E.): (P.E. residual uncertainty) (operating press.) = P.E. $0.000015\frac{\%}{\text{kPa}} * 3\,500\,\text{kPa} = 0.05\%$	P.E. = 0.05%	With the implementation of dynamic pressure compensation, only the residual uncertainty of pressure compensation needs to be included.
Systematic uncertainty at 95% confidence level (root-sum-square)	$\sqrt{\text{spec.}^2 + \text{Z.S}^2 + \text{P.E.}^2} = \text{systematic uncertainty}$ $\sqrt{0.35^2 + 0.95^2 + 0.05^2} = 1.01\%$		The systematic uncertainty for Example 2 is 1.01%.

Table 13-6.2-2
Example 2 — Analysis of Heated Natural Gas Applications at Minimum Flow Rate

Source of Uncertainty	Calculation to Achieve Systematic Uncertainty	Systematic Uncertainty Contribution (k = 2)	Note
Flowmeter base specification (spec.)	Base uncertainty for gas measurement = 0.35%	Spec = 0.35%	Water calibration transferred to gas manufacturer's specification.
Zero stability (Z.S.) contribution including environmental temperature effect (E.E.)	Z.S. without temp. effect = 0.0183 kg/s Additional contribution to zero stability from the environmental specification (E.S.): $\left(\frac{\text{E.E.}}{100}\right)(\text{rated max. flow})(\text{max. operating temp.} - \text{sensor zeroing temp.}) = \text{E.S.}$ $\left(\frac{0.0003\%}{100}\right)(391.9\,\text{kg/s})(144.4°\text{C} - 26.7°\text{C}) = 0.1384\,\text{kg/s}.$ E.S. = 0.1384 kg/s Total uncertainty contribution due to Z.S. at 3.5 kg/s: $\frac{\text{Z.S. w/o temp. effect} + \text{E.S.}}{\text{operating min. flow}} * 100 = \text{Z.S.}$ $\frac{0.0183\,\text{kg/s} + 0.1381\,\text{kg/s}}{3.5\,\text{kg/s}} * 100 = 4.5\%$	Z.S. = 4.5%	Because the meter was zeroed at a temperature lower than operating temperature, the temperature induced drift of zero has been included in the overall zero stability.
Pressure effect (P.E.)	Systematic uncertainty (S.U.) without pressure compensation: (P.E. on span) (operating press. − calibration press.) = S.U. $-0.00023\frac{\%}{\text{kPa}} * (3\,500\,\text{kPa} - 138\,\text{kPa}) = -0.77\%$ S.U. = −0.77% Pressure compensation residual uncertainty at 3 500 kPa (P.E.): $(\text{P.E. residual uncertainty})(\text{operating press.}) = \text{P.E.}$ $0.000015\frac{\%}{\text{kPa}} * 3\,500\,\text{kPa} = 0.05\%$	P.E. = 0.05%	With the implementation of dynamic pressure compensation, only the residual uncertainty of pressure compensation needs to be included.
Systematic uncertainty at 95% confidence level (root-sum-square)	$\sqrt{\text{spec.}^2 + \text{Z.S.}^2 + \text{P.E.}^2} = \text{systematic uncertainty}$ $\sqrt{0.35^2 + 4.5^2 + 0.05^2} = 4.5\%$		The systematic uncertainty for Example 2 is 4.5%.

13-6.3 Example 3

(a) In this example, the flowmeter is used for liquid condensate flow in a fossil fuel steam power generation plant. The condensate is at an elevated temperature, and the flowmeter has been zeroed at the operating temperature. Fixed pressure compensation is enabled. Table 13-6.3-1 shows the analysis of liquid condensate application with the flowmeter zeroed.

(b) Flowmeter Information and Operating Conditions

(1) 200 mm (8 in.) U-tube Coriolis meter
(2) Pulse output
(3) Liquid condensate flow
(4) Operating pressure = 2 400 kPa gauge (350 psig)
(5) Operating flow = 1 270 058 kg/h (2,800,000 lbm/hr)
(6) Zero stability = 136.1 kg/h (300 lbm/hr)
(7) Base uncertainty for liquid measurement = 0.1%
(8) Pressure effect on span = −0.00015%/kPa (−0.001%/psi)
(9) Pressure effect residual uncertainty = 0.0001%/psi
(10) Environmental temperature effect (zero drift) = ±0.0003% of maximum flow per °C
(11) Rated maximum liquid flow = 2 558 261 kg/s (5,640,000 lbm/hr)
(12) Calibration pressure (water) = 138 kPa gauge (20 psig)
(13) Operating temperature = 148°C (300°F)
(14) Flowmeter zeroing temperature = 148°C (300°F)

Table 13-6.3-1
Example 3 — Analysis of Liquid Condensate Application With Flowmeter Zeroed

Source	Specification	Systematic Uncertainty Contribution (k = 2)	Note
Flowmeter base specification (spec.)	Base uncertainty for gas measurement = 0.1%	Spec = 0.1%	Base liquid specification
Zero stability (Z.S.) contribution including environmental temperature effect (E.E.)	Z.S. without temp. effect = 136.1 kg/h Additional contribution to Z.S. from the environmental specification (E.S.): $\left(\frac{\text{E.E.}}{100}\right)(\text{rated max. flow})(\text{max. operating temp.} - \text{sensor zeroing temp.}) = \text{E.S.}$ $\left(\frac{0.0003\frac{\%}{°\text{C}}}{100}\right)\left(2\,558\,261\frac{\text{kg}}{\text{h}}\right)(148.9°\text{C} - 148.9°\text{C}) = 0\,\text{kg/h}$ E.S. =0 kg/h Systematic uncertainty contribution due to Z.S. at 1 270 058 kg/h: $\frac{\text{Z.S. w/o temp. effect} + \text{E.S.}}{\text{operating min. flow}} * 100 = \text{Z.S.}$ $\frac{136.1\,\text{kg/h} + 0}{1\,270\,058\,\text{kg/h}}\text{kg/h} * 100 = 0.01\%$	Z.S. = 0.01%	Because the meter was zeroed at operating temperature, there is no change to overall zero stability due to temperature induced drift.
Pressure effect (P.E.)	Systematic uncertainty (S.U.) without pressure compensation: (P.E. on span) (operating press. − calibration press.) = S.U. $-0.00015\frac{\%}{\text{kPa}} * (2400\,\text{kPa} - 138\,\text{kPa}) = -0.34\%$ S.U. = 0.34% Pressure compensation residual uncertainty at 2 400 kPa (P.E.): (P.E. residual uncertainty) (operating press.) = P.E. $0.000015\frac{\%}{\text{kPa}} * 2\,400\,\text{kPa} = 0.36\%$ P.E. = 0.036%	P.E. = 0.035%	With a fixed pressure compensation, and a relatively stable line pressure, only the residual uncertainty of the pressure compensation needs to be included.
Systematic uncertainty at 95% confidence level (root-sum-square)	$\sqrt{\text{spec.}^2 + \text{Z.S}^2 + \text{P.E.}^2} = \text{systematic uncertainty}$ $\sqrt{0.1^2 + 0.01^2 + 0.036^2} = 0.11\%$		The systematic uncertainty for Example 3 is 0.11%.

13-6.4 Example 4

(a) In this example, the flowmeter is used for liquid condensate flow in a fossil fuel steam power generation plant. The condensate is at an elevated temperature, and the flowmeter has not been zeroed at the operating temperature. Fixed pressure compensation is enabled. Table 13-6.4-1 shows the analysis of liquid condensate application with the flowmeter zeroed.

(b) Flowmeter and Operating Conditions

(1) 200 mm (8 in.) U-tube Coriolis meter
(2) Pulse output
(3) Condensate flow
(4) Operating pressure = 2 400 kPa (350 psig)
(5) Operating flow = 1 270 058 kg/h (2,800,000 lbm/hr)
(6) Zero stability = 136.1 kg/h (300 lbm/hr)
(7) Base uncertainty for liquid measurement = 0.1%
(8) Pressure effect on span = −0.00015%/kPa (−0.001%/psi)
(9) Pressure effect residual uncertainty = 0.000015%/kPa (0.0001%/psi)
(10) Environmental temperature effect (zero drift) = ±0.0003% of maximum flow per °C
(11) Rated maximum liquid flow = 2 558 261 kg/h (5,640,000 lbm/hr)
(12) Calibration pressure (water) = 138 kPa gauge (20 psig)
(13) Operating temperature = 148.9°C (300°F)
(14) Flowmeter zeroing temperature = 26.7°C (80°F)